

University of Alberta

New Aspects of Nazarov Reaction: Additive Effects, Gold Catalysis and Application Toward the
Synthesis of Taxinine

by

Shaon Joy

A thesis submitted to the Faculty of Graduate Studies and Research
in partial fulfillment of the requirements for the degree of

Doctor of Philosophy

Department of Chemistry

©Shaon Joy

Fall 2013

Edmonton, Alberta

Permission is hereby granted to the University of Alberta Libraries to reproduce single copies of this thesis and to lend or sell such copies for private, scholarly or scientific research purposes only. Where the thesis is converted to, or otherwise made available in digital form, the University of Alberta will advise potential users of the thesis of these terms.

The author reserves all other publication and other rights in association with the copyright in the thesis and, except as herein before provided, neither the thesis nor any substantial portion thereof may be printed or otherwise reproduced in any material form whatsoever without the author's prior written permission.

Abstract

Methods involving efficient and stereoselective carbon-carbon bond formation enable chemists to synthesize bioactive natural products and drugs. The Nazarov reaction is a versatile tool for the construction of functionalized cyclopentenones. This 4π -electrocyclization provides easy and efficient access to multi-substituted cyclopentenones with excellent stereocontrol at two contiguous ring carbons and opportunities to link to additional bond-forming events.

Typically, the Nazarov cyclization involves 1,4-pentadien-3-ones. However, development of unconventional initiation protocols to access the key pentadienyl cation in the Nazarov reaction has gained considerable popularity over the past decade. Chapter 1 describes the recent activity in the area of alternate activation protocols for Nazarov cyclization. One rapidly expanding area of homogeneous gold catalysis is the Au(I) catalyzed rearrangements of propargylic carboxylates, leading to domino reaction sequences. Chapter 2 discusses the synthesis of bridged bicyclic enynyl acetates and their use as dienone surrogates. The compounds undergo a [3,3]-rearrangement followed by a 4π -electrocyclization under Au(I) catalysis to form cyclopentenones in a regioselective fashion.

Chapter 3 recounts our comprehensive investigation on the effects of additives in the silicon-directed Nazarov cyclization. We have found that the presence of hydroxylic additives can lead to facile and clean cyclizations of β -silyl substituted dienones. Successful cyclization of some lightly substituted

dienones have been reported, which are otherwise highly unreactive under standard conditions.

In chapter 4 our continued efforts toward the synthesis of taxinine are reported. The completion of the synthesis requires a six-membered ring annulation method to a previously established bicyclo[5.3.1]undecene core. Our attempts at the six-membered ring annulation involving a late-stage C-H insertion via metal-carbenoid chemistry has been presented. Some novel reactivities of the late-stage intermediates have also been explored.

Prion diseases are a group of infectious neurodegenerative disorders that affect both humans and animals. They are invariably fatal due to the lack of proper treatment or cure. Current research relies heavily on the hypothesis that prion pathogenesis coincides with the cellular prion protein (PrP^{C}) undergoing conformational change to the β -sheet enriched isoform PrP^{Sc} . Chapter 5 elaborates our efforts in the development of multivalent PrP^{Sc} binding compounds. Three classes of compounds were synthesized and tested for anti-prion activity.

Acknowledgement

First and foremost I would like to thank my supervisor Dr. Frederick West. His mentorship over the years has been highly inspiring, and I have learned a lot from him about what it takes to be a good chemist. I am indebted to him for his guidance all along my graduate work, specially with respect to thesis writing, and for his support when it came to postdoctoral fellowship applications.

I would like to express my gratitude toward the members of my supervisory committee, especially Dr. D. Clive and Dr. Todd Lowary for their support and valuable suggestions during my graduate years.

I would also like to thank various members of the staff at the Department of Chemistry, especially Mr. Michael Ferguson. His assistance was crucial to the progress of my various projects.

I extend a lot of appreciation to the members of my research group and other friends in the Department of Chemistry for their valuable discussions on chemistry, as well as for their friendship.

Lastly, I would like to thank my family for always being there to support me over the last few years. Thank you for being so patient and optimistic all the time. I would also like to thank Souvik for all his love and support and constant encouragement.

Table of Contents

Chapter 1

1. Unconventional Substrates for Nazarov Cyclization ¹	1
1.1 Alternative Activation Strategy	1
1.1.1. Activation through diketones	2
1.1.2. Activation through Cross-conjugated Trienes	6
1.1.3. Activation Through Linearly Conjugated Trienes	7
1.1.4. Activation Through Conjugated Dienals	8
1.1.5. Electrophilic Activation of Oxygenated Vinyl Allenes	10
1.1.6. Brønsted Acid Activation of Vinyl Allenes	11
1.1.7. Dihalocyclopropane Nazarov Reaction	12
1.2 Generation of Pentadienyl Cation Through Activation of Alkyne .	12
1.2.1. Nazarov Cyclization via Divinylmetallocarbene Formation Under Gold Catalysis	13
1.2.2. Generation of Vinylcarbenoid Species via Other Transition Metal Catalysis.....	17
1.2.3. Activation of Enynes by Transition Metals Toward Nazarov- Type Cyclizations.....	18
1.2.4. Lewis Acid Mediated Intermolecular Generation of the Pentadienyl Cationic Species	20
1.3 <i>In situ</i> Generation of Allenyl Vinyl Ketone	22
1.4 Imino Nazarov and Aza Nazarov Cyclizations.....	24

1.5 Cyclization of Pentadienyl Carbocation Generated Through Dehydration.....	31
1.6 Piancatelli Reaction	33
1.7 Conclusion	36
1.8 References.....	37

Chapter 2

2. Bridged Bicyclic Enynyl Acetates in a Highly Efficient Domino [3,3]-Propargylic Shift/ Nazarov Cyclization/[1,5]-Hydride Shift Pathway Catalyzed by Au(I)	42
2.1 Au(I) Mediated Activation of Alkynes	42
2.2 Propargylic Esters in Gold Catalysis	43
2.2.1. Examples of Gold Catalyzed [3,3]-Rearrangement of Propargylic Esters and Further Evolution of the Vinyl Gold Species.....	44
2.3 Gold Catalyzed Domino Reactions of Enynyl Carboxylates Involving Nazarov Cyclization as the Key Step	46
2.4 Results and Discussions	48
2.4.1. Synthesis of Starting Material.....	52
2.4.2. Domino [3,3]-Rearrangement/Nazarov Cyclization and [1,5]-Hydride Shift of Enynyl Acetates	56
2.4.3. Au(I) Catalyzed Reactions of Cyclopropyl Substituted Enynyl Acetates	60
2.5 Conclusion	64

2.6 Future Plans	65
2.7 Experimental	66
2.7.1. General Information	66
2.7.2. Synthesis and Characterization of Compounds	67
2.8 References	80

Chapter 3

3. Additive Effects in Silicon-Directed Nazarov Cyclization	84
3.1 Silicon-Directed Nazarov Cyclization	84
3.2 Diastereoselective Silicon-Directed Nazarov Cyclizations	87
3.2.1. Torquoselectivity Induced through Tetrahedral Chirality ...	88
3.2.2. Silicon as a Traceless Auxiliary	88
3.2.3. Diastereoselective Nazarov Cyclization of Strained Bridged Bicycles	89
3.3 Additive Effect in Silicon-Directed Nazarov Cyclization	90
3.3.1. Synthesis of the Divinyl Ketone Precursors	92
3.3.2. Optimization of the Reaction Conditions	95
3.3.3. Effect of Additive on the Cyclization of Acyclic Divinyl Ketones	96
3.4 Conclusion	106
3.5 Future Plans	106
3.6 Experimental	109
3.6.1. General Information	109

3.6.2. Synthesis and Characterization of Compounds	110
3.7 References	117

Chapter 4

4. Some Interesting Novel Reactivities of Advanced Intermediates Towards the Chemical Synthesis of Taxinine	121
4.1 Biological Significance of Taxinine and its Synthetic Challenges	121
4.2 Enantiospecific Synthesis of the AB-Ring Substructure of Taxinine by the Banwell Group	123
4.3 West Group's Efforts Toward the Total Synthesis of Taxinine ...	126
4.3.1. The First Generation Approach to Taxinine (Giese)	126
4.3.2. The Second Generation Approach to Taxinine (Mazzola) .	130
4.3.3. The Third Generation Approach to Taxinine (Benson)	135
4.3.4. The Fourth Generation Approach to Taxinine (Benson, Nakanishi, Joy).....	139
4.4. Results and Discussion	144
4.4.1. Alternative Attempts at C-Ring Formation (Nakanishi, Joy)	144
4.4.2. Further Attempts at Early Stage C-3 Functionalization of the Taxane Skeleton (Joy)	149
4.5 Conclusion	163
4.6 Future Plans	165
4.7 Experimental	167
4.7.1. General Information	167

4.7.2. Experimental Procedures and Characterization of Compounds	168
4.8 References	181

Chapter 5

5. Prion Inhibition with Multivalent PrP ^{Sc} Binding Compounds	186
5.1 Prions and Transmissible Spongiform Encephalopathies	186
5.1.1. Prion Replication Models	187
5.1.2. Transmissible Spongiform Encephalopathies (TSEs)	188
5.2 Challenges and Recent Progress in Prion Research	190
5.3 Results and Discussions	194
5.3.1. Planning and Synthesis of Multivalent PrP ^{Sc} Binding Molecules	196
5.3.2. Synthesis of Anti-Prion Compounds: Attachment of Chloroquinoline and Acridine Linkers to the Scaffolding Units	199
5.4 Biological Studies on the Anti-Prion Compounds	205
5.4.1. Cytotoxicity of Monomeric Units and their Respective Scaffolding Compounds	205
5.4.2. Ability of Chloroquinoline and Acridine Fragments to Clear PrP ^{Sc} In Vitro	206
5.4.3. Effect of Novel Congo Red Derivative on PrP ^{Sc} Propagation in Cultured Cells	207

5.4.4. Tetraporphyrin Tetracarboxylic Acid Scaffolding Compounds as Antiprion Agents.....	208
5.4.5. Enhanced Antiprion Activity of Trimesic Acid-Based Chloroquinoline Scaffolds.	208
5.4.6. Ability of 17b and 17c to Eradicate PrP ^{Sc} of a Different Prion Strain	209
5.5 Rationale for the Anti-Prion Activity of Various Scaffolded Compounds	210
5.5.1. Antiprion Activity of Compounds	210
5.5.2. Role of Cell Type and Prion Strain in Antiprion Activity .	211
5.5.3. PrP ^{Sc} Enhancing Compounds	212
5.6 Conclusion	213
5.7 Future Plans	213
5.8 Experimental	214
5.8.1. General Information	214
5.8.2. Synthesis and Characterization of Compounds	215
5.9 References	218

Appendices

Appendix I (Selected NMR Spectra)	225
Chapter 2	225
Appendix II (Selected NMR Spectra).....	246
Chapter 3	246
Appendix III (Selected NMR Spectra)	269

Chapter 4	269
Appendix IV (Selected NMR Spectra)	285
Chapter 5	285

List of Tables

Chapter 1

Chapter 2

Table 2.1 Sonogoshira Coupling of Bridged Bicyclic Enol Triflates and Propargylic Alcohol 53

Table 2.2 Preparation of C-5 Substituted Bridged Bicyclic Enynyl Acetates via Sonogoshira Coupling 55

Table 2.3 (PPh₃)AuCl/AgSbF₆ Catalyzed Formation of Fused Cyclopentenones 58

Chapter 3

Table 3.1 Preparation of the Bridged Bicyclic Divinyl Ketones 94

Table 3.2 Effect of Additive and FeCl₃ Stoichiometry 96

Table 3.3 Silicon-Directed Nazarov Cyclization of Simple Acyclic and Cyclic Divinyl Ketones with MeOH as Additive 100

Table 3.4 Cyclization with Brønsted Acid Catalysts 105

Chapter 4

Chapter 5

<i>Table 5.1</i> Synthesis of N-(7-chloroquinolin-4-yl)-alkyl-diamine adducts 16a-f	200
<i>Table 5.2</i> Preparation of Trivalent Anti-Prion Compounds 17a-d using Trimesic Acid as the Scaffold.....	202
<i>Table 5.3</i> Anti-Prion Activity of Independent Chloroquinoline Moieties	207
<i>Table 5.4</i> Efficient Clearance of PrP ^{Sc} with Trimesic Acid Scaffolds for Treated-SMB Cells	209

List of Figures

Chapter 1

Chapter 2

<i>Figure 2.1</i> The A-B-C Ring System of a Representative Member of the Taxane Family	50
<i>Figure 2.2</i> Relative Stereochemical Assignment of 21d Based on 2D TROESY Correlations	59

Chapter 3

Chapter 4

<i>Figure 4.1</i> Representative Examples of the Members of the Taxane Family	122
<i>Figure 4.2</i> Late Stage C-H Insertion Intermediate	139
<i>Figure 4.3</i> Rationale for the Stereoselective Reduction of the Diketone 45 and Relative Stereochemical Assignment of Diacetate 51	146
<i>Figure 4.4</i> Structural Assignment of Compound 62 Based on HMBC Correlations	155

Chapter 5

<i>Figure 5.1</i> Pyridine Dicarbonitrile Scaffold for Dose Dependant Prion Inhibition.....	193
<i>Figure 5.2</i> Pyridine Dicarbonitrile Scaffolds with Enhanced Potency ...	194
<i>Figure 5.3</i> Diketopiperazines as Prion Replication Inhibitors.....	194
<i>Figure 5.4</i> Quinacrine: A Potent Anti-Prion Compound.....	195
<i>Figure 5.5</i> Structures of the Selected Multivalent Scaffolds	197
<i>Figure 5.6</i> Structures of the Chosen Diamine Linkers	198
<i>Figure 5.7</i> The Chosen Monomeric Binding Units	198
<i>Figure 5.8</i> Acridine Based Diamine Linkers	201
<i>Figure 5.9</i> Tetravalent Anti-Prion Compounds 18a-i Using Tetraporphyrin as the Scaffold.....	204
<i>Figure 5.10</i> The 3,3' Dicarboxy Analog of Congo Red as an Anti-Prion Compound.....	204
<i>Figure 5.11</i> Chloroquine as an Anti-Prion Compound.....	206
<i>Figure 5.12</i> Cyanine dye Cy5 as a Fluorophore	214

List of Schemes

Chapter 1

<i>Scheme 1.1</i> The Nazarov Cyclization	2
<i>Scheme 1.2</i> Nazarov Cyclization of α -Diketone 5 Using Yb(OTf) ₃	3
<i>Scheme 1.3</i> Conjugate Addition Initiated Nazarov Cyclization	4
<i>Scheme 1.4</i> Domino Cyclization of Dienyl Diketone 12 Initiated by 1,6-Conjugate Addition	5
<i>Scheme 1.5</i> Organocatalytic Asymmetric Nazarov Cyclization of Diketoesters 17	6
<i>Scheme 1.6</i> Neutral Pd(0) Catalyzed Cyclization of Diketoester	6
<i>Scheme 1.7</i> Vinylogous Nazarov Cyclization of Cross-Conjugated Trienes	7
<i>Scheme 1.8</i> Triflic Acid Mediated Cyclization of Cross-Conjugated Triene 20	7
<i>Scheme 1.9</i> Nazarov Cyclization of Electron-rich Trienes to form Fused Cyclopentenones	8
<i>Scheme 1.10</i> Iso-Nazarov Cyclization of Dienals.....	9
<i>Scheme 1.11</i> Reductive Oxy-Nazarov Cyclization	10
<i>Scheme 1.12</i> Oxidative Nazarov Cyclization of Vinyl Allene 37	11
<i>Scheme 1.13</i> Brønsted Acid Mediated Cyclization of Vinyl Allene 41 ...	11
<i>Scheme 1.14</i> Silver Assisted Electrocyclization of Vinyl Dihalocyclopropanes.....	12
<i>Scheme 1.15</i> Au(I) Catalyzed Domino Cyclization of Propargylated Indoles.....	14

<i>Scheme 1.16</i> Au(I)-Catalyzed Domino Cyclization to Form 2-indol-3-ylbenzofulvenes	15
<i>Scheme 1.17</i> Au(I) Catalyzed Domino Cyclization of Enynes involving [3,3]-Rearrangement and Nazarov Cyclization	16
<i>Scheme 1.18</i> Formation of Indenes Under Platinum or Ruthenium Catalysis	17
<i>Scheme 1.19</i> One-Pot Domino Cyclization of Oxiranyl Propargylic Ester 72	18
<i>Scheme 1.20</i> Metal Catalyzed Domino Cyclizations of Enynes	19
<i>Scheme 1.21</i> Heteroenyne Metathesis of 1,3-Enynyl Carbonyls 83	20
<i>Scheme 1.22</i> FeCl ₃ Catalyzed Cyclization of Diynes 86 in Presence of Aldehyde-Acetal 87	21
<i>Scheme 1.23</i> Brønsted Acid Catalyzed Formation of Hydroazulenes 96 or 97	22
<i>Scheme 1.24</i> Synthesis and Cyclization of Allenyl Vinyl Ketones	23
<i>Scheme 1.25</i> Nazarov Cyclization of Alkoxy Allenes and Alkoxy Cumulenes.....	23
<i>Scheme 1.26</i> Nazarov Cyclization of an <i>In Situ</i> Generated Allenyl Vinyl Ketone	24
<i>Scheme 1.27</i> An Imino Nazarov Cyclization to Form α -Aminocyclopentenones 115	25
<i>Scheme 1.28</i> Au(I) Catalyzed Imino Nazarov Cyclization of Propargyl Tosylates	26
<i>Scheme 1.29</i> Au(I) Catalyzed Imino Nazarov Cyclization of α -Aryl Allenamides	27
<i>Scheme 1.30</i> Aza Nazarov Cyclization of Hydrazones to Form Pyrroles	28

<i>Scheme 1.31</i> Synthesis of Pyrroles Under Superelectrophilic Conditions via an Aza Nazarov Reaction Cascade	29
<i>Scheme 1.32</i> Aza Nazarov Cyclization of 2-Azapentadienone 140 under Superelectrophilic Conditions.....	30
<i>Scheme 1.33</i> Formation of 2,3-Dihydro-1 <i>H</i> -Pyrrolizines 146 via Au(I) Catalyzed Tandem Cyclization of Azidoenynes 143	31
<i>Scheme 1.34</i> Synthesis of Benzofulvenes via Nazarov Cyclization of Divinyl Alcohol Following a Dehydrative Protocol	32
<i>Scheme 1.35</i> Dehydrative Nazarov Cyclization of Divinyl Alcohols.....	33
<i>Scheme 1.36</i> The Piancatelli Reaction	34
<i>Scheme 1.37</i> Piancatelli Reactions in Presence of Mild Lewis Acids	35
<i>Scheme 1.38</i> Intramolecular Aza-Piancatelli Reaction of 2-Furylcarbinols 168	36

Chapter 2

<i>Scheme 2.1</i> Gold Activation of Alkynes	43
<i>Scheme 2.2</i> Two Possible Pathways of Rearrangements of Propargylic Esters under Gold Activation.....	44
<i>Scheme 2.3</i> First Report of Acetoxyallene Formation in AuCl ₃ Catalyzed Reaction of Propargylic Acetates.....	44
<i>Scheme 2.4</i> Au(I) Catalyzed Formation of Tetracyclic Cyclobutanes.....	45
<i>Scheme 2.5</i> Formation of Substituted Indenes via Au(I)-Catalyzed [3,3]-Rearrangement and Electrophilic Aromatic Substitution	46

<i>Scheme 2.6</i> Synthesis of Bicyclo[3.1.0]hexenes from Propargylic Acetates with a Tethered C-C Double Bond	46
<i>Scheme 2.7</i> A Tandem Au(I)-Catalyzed Nazarov Cyclization/Cyclopropanation of Gold Carbenoid to Form Polycyclic Products.....	48
<i>Scheme 2.8</i> Au(I)-Catalyzed Tandem Iso-Nazarov/Nazarov Cyclization to Form Bicyclo[3.3.0]octene	48
<i>Scheme 2.9</i> Silicon-Directed Nazarov Cyclization of Bridged Bicyclo[3.2.1]octadiene Substrate	49
<i>Scheme 2.10</i> Preparation of the Bicyclo[3.2.1]octene Dienone.....	50
<i>Scheme 2.11</i> Difficulties in Installation of a Tetra-Substituted Olefin in a Highly Functionalized Cyclopentenone Framework	51
<i>Scheme 2.12</i> Proposed Reaction Pathway for the Conversion of Bridged Bicyclic Enynyl Acetates to Cyclopentenones	51
<i>Scheme 2.13</i> Proposed Pathway for the Preparation of Bridged Bicyclic Enynyl Acetates	52
<i>Scheme 2.14</i> Preparation of the Propargyl Acetate 19	54
<i>Scheme 2.15</i> Au(I)-Catalyzed Domino Cyclization of Camphor-Derived Enynyl Acetate	56
<i>Scheme 2.16</i> Proposed Mechanistic Pathway for the Formation of Cyclopentenones 20 and 21	60
<i>Scheme 2.17</i> Au(I)-Catalyzed Cyclopropyl Ring Opening to Form Substituted Cyclopentenes	61
<i>Scheme 2.18</i> Rh(I)-Catalyzed Domino Cycloisomerization/Carbonylation of Cyclopropyl Propargylic Esters.....	61
<i>Scheme 2.19</i> A Proposed Reaction Pathway for Domino Cyclization of Cyclopropyl Enynyl Ester.....	62
<i>Scheme 2.20</i> Synthesis of Cyclopropyl Enynyl Acetates	63

<i>Scheme 2.21</i> Au(I)-Catalyzed Domino Cyclization of Cyclopropyl Substituted Propargyl Acetates	64
<i>Scheme 2.22</i> Enynyl Acetates with Substituted Cyclopropyl Unit	65
Cyclopentenones 20 and 21	60

Chapter 3

<i>Scheme 3.1</i> Nazarov Cyclization of a Divinyl Ketone.....	85
<i>Scheme 3.2</i> Silicon-Directed Nazarov Cyclization	86
<i>Scheme 3.3</i> Effect of Substitution on the Silicon-Directed Nazarov Cyclization	86
<i>Scheme 3.4</i> Torquoselectivity in Nazarov Cyclization	87
<i>Scheme 3.5</i> Diastereoselective Nazarov Cyclization: Steric Effect on Torquoselectivity	88
<i>Scheme 3.6</i> Stereoelectronic Control of Torquoselectivity through an Allylsilane Moiety	89
<i>Scheme 3.7</i> Diastereoselective Nazarov Cyclization of Bridged Bicyclic Dienones	90
<i>Scheme 3.8</i> Effect of Water as an Additive on the Diastereoselective Nazarov Cyclization of Bicyclo[3.2.1]octadienone	92
<i>Scheme 3.9</i> Preparation of β -Silyl Divinyl Ketones	93
<i>Scheme 3.10</i> Consumption of the Reactive Dienolate Through Michael Addition Pathway.....	97
<i>Scheme 3.11</i> Mechanistic Rationale for the Formation of the Unusual Product 11h	99

<i>Scheme 3.12</i> Silicon-Directed Nazarov Cyclization of a Furan-Substituted Divinyl Ketone 7j	102
<i>Scheme 3.13</i> Attempted Silicon-directed Nazarov Cyclization on Cyclic Dienones	102
<i>Scheme 3.14</i> Nazarov Cyclization of Strained Bridged Bicyclic Dienones	103
<i>Scheme 3.15</i> Cyclization in Presence of CD ₃ OD	104
<i>Scheme 3.16</i> Homo-Nazarov Cyclization	107
<i>Scheme 3.17</i> A Possible Silicon-Directed Homo-Nazarov Cyclization .	107
<i>Scheme 3.18</i> Attempt at the Formation of Substituted Cyclopropane	107
<i>Scheme 3.19</i> Corey-Chaykovsky Cyclopropanation of Furanyl Divinyl Ketone	108
<i>Scheme 3.20</i> Possible Pathway to an Interrupted Silicon-Directed Nazarov Cyclization	109

Chapter 4

<i>Scheme 4.1</i> Anionic Oxy-Cope Rearrangement to Construct the AB-Ring System of Taxinine.....	124
<i>Scheme 4.2</i> Formation of the Allylic Alcohol 8 via Thermal Grob Fragmentation	125
<i>Scheme 4.3</i> Taxinine C-Ring Annulation Attempts Through Aldol Reaction	126
<i>Scheme 4.4</i> Retrosynthetic Analysis of Taxinine in the First Generation Approach.....	127

<i>Scheme 4.5</i> Nazarov Cyclization to Form the Fused Cyclopentenone 19	128
<i>Scheme 4.6</i> Preparation of the Tetrasubstituted Olefin 21 via Selenoxide Elimination.....	129
<i>Scheme 4.7</i> Oxidative Cleavage of 21 to Access the Tricyclic Core of the Taxane Skeleton.....	130
<i>Scheme 4.8</i> Retrosynthetic Scheme for Mazzola's Route	131
<i>Scheme 4.9</i> Silicon-Directed Nazarov Cyclization of a Bridged Bicyclic Dienone 28 and Methylation to Install the Quaternary Stereocenter of 29	132
<i>Scheme 4.10</i> Elaboration of Ketone 29 to the AB-Bicyclic Core of Taxinine	134
<i>Scheme 4.11</i> Attempts to Form the Tricyclic Core of the Taxane Skeleton	135
<i>Scheme 4.12</i> Retrosynthetic Approach to Taxinine: The Third Generation Approach.....	136
<i>Scheme 4.13</i> Functionalization of the C3 Position of 28 with Isopropenyl Group	137
<i>Scheme 4.14</i> Vinylation of the Enone 28 and Attempted α -Selenylation	138
<i>Scheme 4.15</i> Generation of the Siloxy Diene 40 from α , β -Unsaturated Ketone 29	138
<i>Scheme 4.16</i> Effect of Additive on the Nazarov Cyclization Step	140
<i>Scheme 4.17</i> Preparation of the Diketone Intermediate 45	142
<i>Scheme 4.18</i> Conversion of the Diketone 45 to β -Keto ester 48	143
<i>Scheme 4.19</i> Conversion of 48 to a β -Keto Diazo ester 49 and Attempt at Intramolecular C-H Insertion	144

<i>Scheme 4.20</i> Elaboration of the Diketone 45 to the Carboxylic Acid 54	145
<i>Scheme 4.21</i> Synthesis of Diazoketone 55 and Attempts at C-Ring Formation	147
<i>Scheme 4.22</i> An Alternate Approach to C3 Functionalization	148
<i>Scheme 4.23</i> Attempts at the Synthesis of the Diazo Ester 59 and Its Further Elaboration	149
<i>Scheme 4.24</i> Wender's Route to the Late Stage C-Ring Annulation Using a C3 Tether	150
<i>Scheme 4.25</i> Holton's Strategy for the Construction of the C-Ring	151
<i>Scheme 4.26</i> Late Stage C-Ring Annulation Strategy Of the Holton Group Toward the Total Synthesis of Taxusin	151
<i>Scheme 4.27</i> Formation of a Diene Byproduct 61 Under DIBAL-H Reduction of Cyclopentenone 31	153
<i>Scheme 4.28</i> π -Facial Selectivity in the Diels-Alder Reactions of Isodicyclopentadienes	154
<i>Scheme 4.29</i> A Surprising Reactivity of the Isodicyclopentadiene 61 in Presence of Ethyl Glyoxalate as Dienophile.....	155
<i>Scheme 4.30</i> A Plausible Mechanism for the Formation of the Adduct 62	155
<i>Scheme 4.31</i> Diels-Alder Reactions of Isodicyclopentadiene 63 with DMAD and Maleic Anhydride as Dienophiles.....	157
<i>Scheme 4.32</i> Attempts at the Synthesis of Cyclopentenone 71	158
<i>Scheme 4.33</i> Alternate Attempt at Cyclopentenone 74 Formation.....	159
<i>Scheme 4.34</i> Volhardt's Protocol for the Synthesis of Camphor-Based Diene	160
<i>Scheme 4.35</i> Au(I) mediated Tandem Cyclization for the Synthesis of Cyclopentenones	161

<i>Scheme 4.36</i> Conversion of the Cyclopentenones to the Isodicyclopentadienes Under DIBAL-H Mediated Conditions	161
<i>Scheme 4.37</i> Diels-Alder Reactions of Isodicyclopentadiene 78	162
<i>Scheme 4.38</i> Au(I) Catalyzed Cyclization of C5-Substituted Enynyl Acetates	163
<i>Scheme 4.39</i> Accessing the Six-Membered C-Ring Via an Early Stage C3 Functionalization.....	166
<i>Scheme 4.40</i> A Late Stage C3 Functionalization Through Barton Reaction	166
<i>Scheme 4.41</i> Accessing the C3 Enolate via Conformational Change of the Eight-Membered B-ring	167

Chapter 5

List of Standard Abbreviations

Ac	acetyl
Ar	aryl
app	apparent
aq	aqueous
BOM	benzyloxymethyl ether
Bn	benzyl
br	broad (spectral)
<i>i</i> -Bu	<i>iso</i> -butyl
<i>n</i> -Bu	butyl
<i>t</i> -Bu	<i>tert</i> -butyl
Bz	benzoyl
°C	degrees Celsius
Calcd	calculated
CSA	(1- <i>S</i>)-camphorsulphonic acid
cat.	Indicates that the reagent is used in catalytic amount
d	day(s); doublet (spectral)
D	deuterium; dimensional
DABCO	1,4-diazabicyclo[2.2.2]octane
dba	dibenzylideneacetone
DBU	1,8-diazabicyclo[5.4.0]undec-7-ene
DCC	<i>N,N'</i> -dicyclohexyl carbodiimide
DCE	dichloroethane

DCM	dichloromethane
dd	doublet of doublets (spectral)
ddd	doublet of doublets of doublets (spectral)
Δ	indicates that the reaction was heated
DDQ	2,3-dichloro-5,6-dicyano-1,4-benzoquinone
DEA	diethyl amine
DEPT	distortionless enhancement by polarization transfer (spectral)
DIBAL-H	diisobutylaluminium hydride
DIPA	diisopropylamine
DMAD	dimethyl acetylenedicarboxylate
DMAP	4-(<i>N,N</i> -dimethylamino)pyridine
DMDO	dimethyldioxirane
DMF	<i>N,N'</i> -dimethylformamide
DMP	Dess-Martin periodinone
dr	diastereomeric ratio
dt	doublet of triplets (spectral)
Dy	dysprosium
EC ₅₀	equiv
EDA	ethyl diazoacetate
EDC	1-ethyl-3-(3-dimethylaminopropyl)carbodiimide
ee	enantiomeric excess
EI	electron impact (mass spectrometry)
equiv	equivalents

ESI	electrospray ionization
Et	ethyl
EtOAc	ethyl acetate
FCC	flash column chromatography
g	grams(s)
h	hour(s)
HFIP	1,1,1,3,3,3-hexafluoroisopropanol
HMBC	heteronuclear multiple bond correlation (spectral)
HMDS	1,1,1,3,3,3-hexamethyldisilazane
HMPA	hexamethylphosphoramide
HMQC	heteronuclear multiple quantum correlation (spectral)
HOBt	1-hydroxybenzotriazole
HSQC	heteronuclear single quantum correlation (spectral)
HRMS	high resolution mass spectrum
Hz	Hertz
IBX	<i>o</i> -iodobenzoic acid
IC ₅₀	half maximal inhibitory concentration
<i>i</i> -Pr	<i>iso</i> -propyl
IPr	1,3-bis(diisopropylphenyl)imidazole-2-ylidene
IR	infrared (spectroscopy)
<i>J</i>	coupling constant (NMR)
<i>K</i> _D	dissociation constant
L	an unspecified ligand

LDA	Lithium diisopropylamine
L-Selectride	lithium tri- <i>sec</i> -butylborohydride
LTMP	lithium tetramethylpiperidide
M	moles per liter
m	multiplet (spectral)
m/z	mass to charge ratio (mass spectrometry)
M ⁺	molecular ion
<i>m</i> -CPBA	<i>m</i> -chloroperoxybenzoic acid
Me	methyl
MEM	β-methoxyethoxymethyl
mg	milligrams
MHz	megahertz
min	minute(s)
mL	milliliter
mmol	millimoles(s)
MOM	methoxy methyl
mol	mole(s)
m.p.	melting point
MS	molecular sieves
N	gram equivalent weight per liter
<i>n</i> -Pr	propyl
NMO	<i>N</i> -methylmorpholine- <i>N</i> -oxide
NMR	nuclear magnetic resonance

nOe	nuclear Overhauser effect
Nu	nucleophile
Ph	phenyl
PMA	phosphomolybdic acid
PMB	4-methoxybenzyl
PPA	polyphosphoric acid
ppm	parts per million
pyr	pyridine
q	quartet
R _f	retention factor (chromatography)
RML	Rocky Mountain Laboratory
rt	room temperature
s	singlet (spectral); second(s)
t	triplet (spectral)
TBAF	tetra- <i>n</i> -butyl ammonium fluoride
TBDPS	<i>tert</i> -butyldiphenylsilyl
TBS	<i>tert</i> -butyldimethylsilyl
Tce	2,2,2-trichloroethyl
temp	temperature
TES	triethylsilyl
TFA	trifluoroacetic acid
Tf	trifluoromethanesulfonyl
TFE	2,2,2-trifluoroethanol

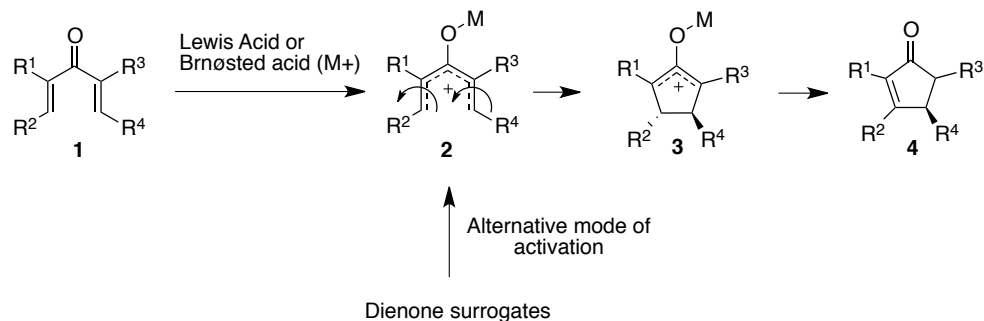
THF	tetrahydrofuran
TIPS	triisopropylsilyl
TLC	thin layer chromatography
TMS	trimethylsilyl
TPAP	tetra- <i>n</i> -propylammonium perruthenate
TROESY	transverse rotating-frame Overhauser enhancement spectroscopy
Troc	2,2,2-trichloroethyl carbonate
Ts	tosyl; <i>p</i> -toluenesulfonyl
triflimide	bis(trifluoromethanesulfonyl)amide
UV	ultra-violet

Chapter 1

Unconventional Substrates for Nazarov Cyclization¹

1.1 Alternative Activation Strategy

The abundance of five-membered carbocycles in natural products and other bioactive compounds has provided a major impetus for the development of efficient methods for their construction. The Nazarov cyclization has been increasingly refined to meet this need since its discovery in 1941.² In its traditional format, the Nazarov reaction proceeds via activation of a 4π -cross-conjugated dienone **1** with strong Lewis or Brønsted acid, followed by conrotatory electrocyclization of the resulting pentadienyl cation **2** (Scheme 1.1).³ The oxallylcationic intermediate **3** formed after electrocyclization undergoes elimination followed by tautomerization to give the cyclopentenone **4**. The Nazarov reaction is an excellent protocol, which occurs with predictable stereochemistry to construct cyclopentenones.⁴ Catalytic and/or asymmetric versions of the reaction have been developed.^{4b} A considerable amount of work has also been dedicated to the capture of the cationic species **3** through different bond forming processes to add to the complexity of the Nazarov-derived product.



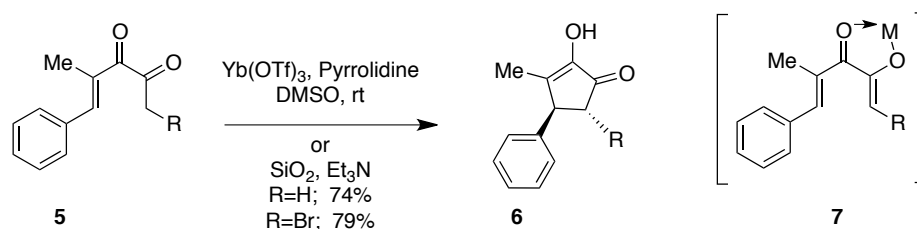
Scheme 1.1 The Nazarov Cyclization.

However, some possible applications are precluded by limitations in substitution pattern or reagent compatibility with the dienone precursors. Dienones require activation of the carbonyl with strong Lewis or Brønsted acids for cyclization, which is a major disadvantage for both catalysis and reaction scope. Catalytic Nazarov reactions are often limited to highly polarized dienone substrates, which hamper the reaction scope greatly. Product inhibition is often a crucial problem of this reaction with dienone precursors. As both the starting material and the product are ketones, a catalyst needs to bind preferably to the dienone than the cyclopentenone product. This often leads to the use of stoichiometric amount of catalyst and slow reaction rates. As a result, there has been a considerable recent activity directed toward the development of alternative routes to generate the key pentadienyl cation **2**. Unconventional substrate development has been of key focus to expand the application of this popular cyclopentannulation strategy.⁵ A key advantage to the development of alternate activation strategies is the potential to use activating agents other than strong acids.

1.1.1. Activation through Diketones

α -Diketones can act as potential pentadienyl cation precursors via tandem enolization/carbonyl activation. The pentadienyl cation can be formed via an

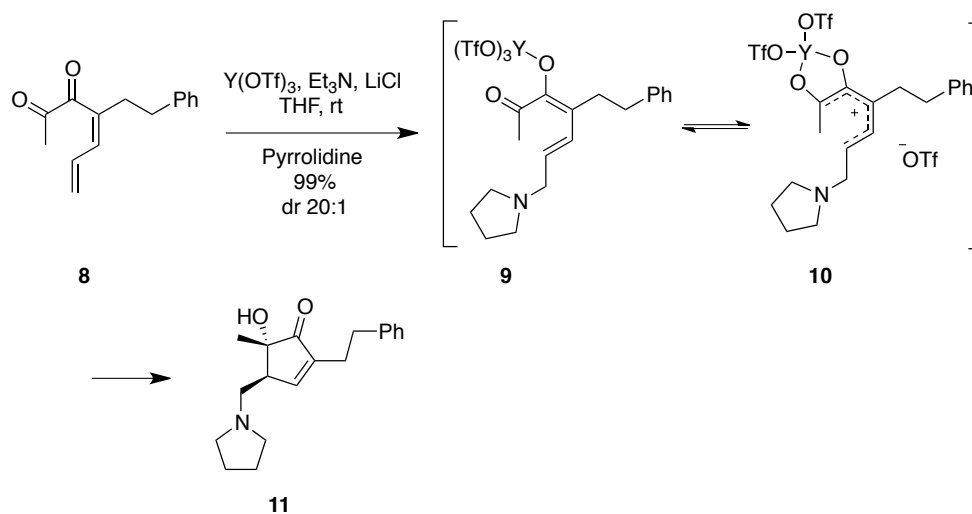
initial enol ether formation in presence of Lewis acid followed by activation of the carbonyl as seen in case of dienones. The formation of enol-ether is presumed to lower the activation barrier for the electrocyclic ring closure because of its electron donating ability. α -Hydroxycyclopentenones were first reported to be formed from enediones in 1965, through a Nazarov type cyclization of a chelated metalloenolate intermediate.⁶ Later, the Tius group demonstrated the cyclization of diketones **5** using $\text{Yb}(\text{OTf})_3$ and pyrrolidine, producing diosphenols **6** in good yield (Scheme 1.2).⁷ Intramolecular Michael addition of the metalloenolate derived from **5** is ruled out due to poor orbital overlap (a *5-endo-trig* ring closure disfavored by Baldwin's rules).⁸ Instead, 4π -electrocyclization of the internally chelated metalloenolate **7** analogous to the Nazarov cyclization could better account for the stereospecific formation of **6**.



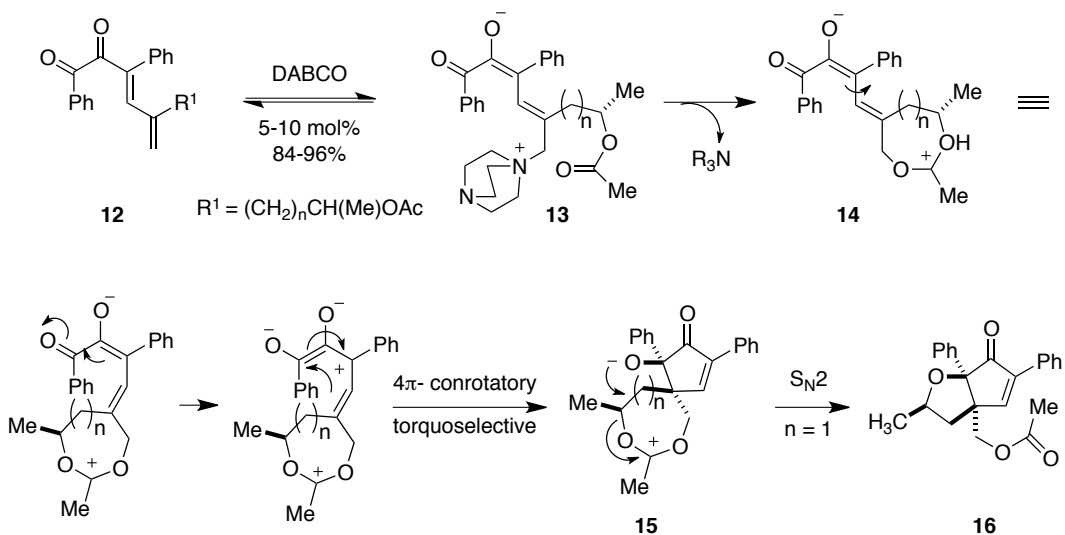
Scheme 1.2 Nazarov Cyclization of α -Diketone **5** Using $\text{Yb}(\text{OTf})_3$.

On the other hand, the Frontier group found that treatment of dienyl diketone **8** with $\text{Y}(\text{OTf})_3$ provided α -hydroxycyclopentenone **11** with incorporation of the pyrrolidine moiety in the cyclopentenone product (Scheme 1.3).⁹ Lewis acid promoted conjugate addition of the pyrrolidine to the diketone is proposed to form the dienolate **9**. A pentadienyl cation **10** could then be generated through activation of the keto-carbonyl moiety, which undergoes a Nazarov type cyclization to provide the α -hydroxycyclopentenone **11**. A dramatic change in reaction outcome was observed for the dienone substrate **12** having an acetate tether in presence of DABCO as the basic additive (Scheme 1.4).¹⁰ The initial mechanistic steps were proposed to be similar to the previous one,

involving a 1,6-conjugate addition of DABCO to the dienyl diketone **12**, producing the zwitterionic intermediate **13**. Now, in presence of the acetate tether, the allylic quaternary ammonium group is displaced by the pendant acetate in an intramolecular S_N2 fashion to produce the cyclic zwitterion **14**. The acetoxonium stereocenter subsequently controls the torquoselectivity of the electrocyclization process, forming the spirocyclic zwitterion **15**. Finally, the domino cyclization sequence is concluded with an intramolecular ether formation in **16**.

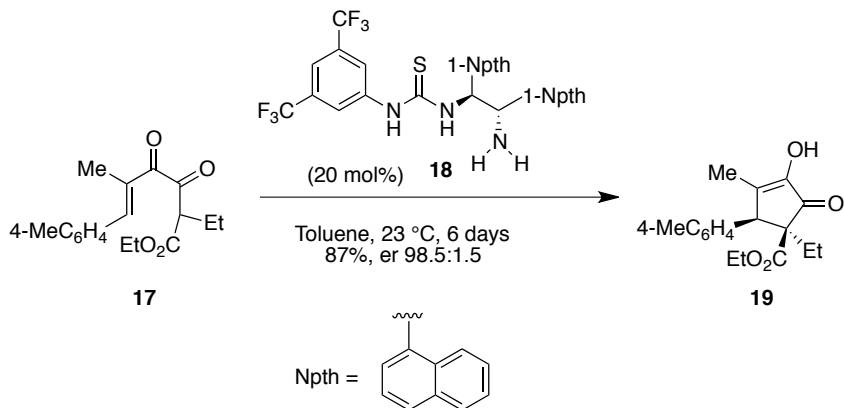


Scheme 1.3 Conjugate Addition Initiated Nazarov Cyclization.

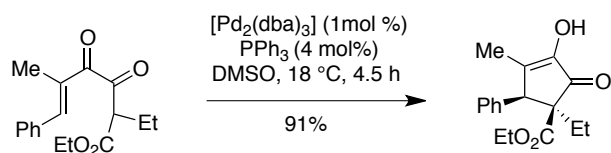


Scheme 1.4 Domino Cyclization of Dienyl Diketone **12** Initiated by 1,6-Conjugate Addition.

Nazarov reaction of enolic diketoesters **17** to provide highly functionalized cyclopentenones **19** in moderate to good yields with enantiomeric ratios that range from 90:10 to 98.5:1.5 has been reported (Scheme 1.5).¹¹ A key advantage of this transformation is that two contiguous stereogenic centers, one of which is a quaternary stereogenic center, could be readily installed. The fact that catalyst **18** lacking a basic amine group, was not an effective compound highlighted the cooperative activity between acidic thiourea and basic primary amine moieties residing in the catalyst. However, this protocol was restricted to substrates having aryl groups at C6. A branched substituent at C2 was not tolerated under these conditions. The organocatalytic process was slow, which is attributed to product inhibition of the catalyst, due to binding with the diketone and product through similar keto-enol forms. An effective solution was found to circumvent these limitations through neutral Pd(0) catalysis (Scheme 1.6).¹² The reaction proceeds to completion within a few hours in good to excellent yields under strictly neutral conditions. An initial asymmetric version of this protocol has also shown some promise.



Scheme 1.5 Organocatalytic Asymmetric Nazarov Cyclization of Diketoesters **17**.

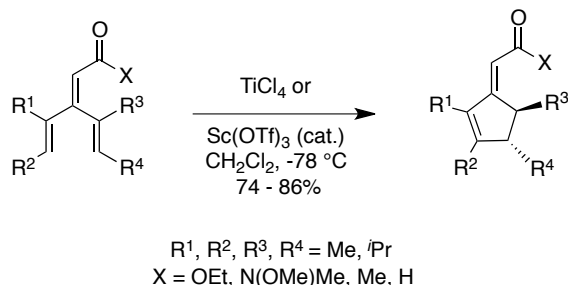


Scheme 1.6 Neutral Pd(0) Catalyzed Cyclization of Diketoester.

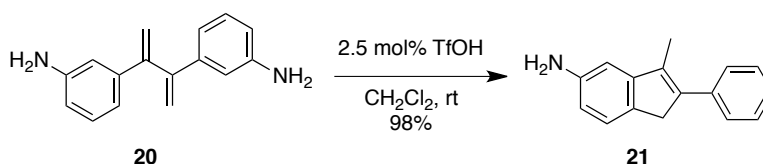
1.1.2. Activation through Cross-conjugated Trienes

A conventional method for substrate activation for the Nazarov cyclization is through metal complexation to a divinyl ketone moiety at the C-3 position. Altering the substitution pattern at the C-3 position raises challenges with regard to initiation of the reaction.⁹ The West group has demonstrated that a cross-conjugated triene can be a substrate for Nazarov cyclization in presence of TiCl_4 or catalytic $\text{Sc}(\text{OTf})_3$ to furnish the cyclized product (Scheme 1.7).¹³ Replacement of the carbonyl moiety with enoate, enamide, enone or enal functionality did not impede the course of cyclization. Notably, only a single diene regioisomer was observed with the endocyclic olefin being *trans* to the carbonyl group. Recently, the Lee group demonstrated that symmetric or unsymmetric diaryl and alkyl aryl-1,3-dienes **20** can participate in Nazarov-type cyclization to furnish substituted

indenes **21** (Scheme 1.8).¹⁴ In the presence of catalytic TfOH, the unsymmetrical dienes underwent cyclization involving the more electron-rich arene.



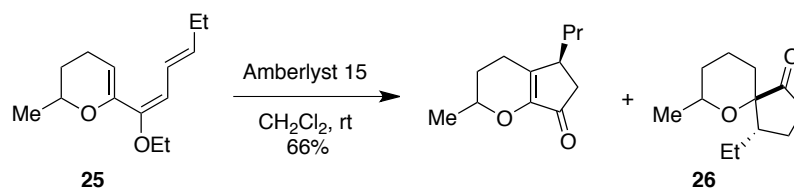
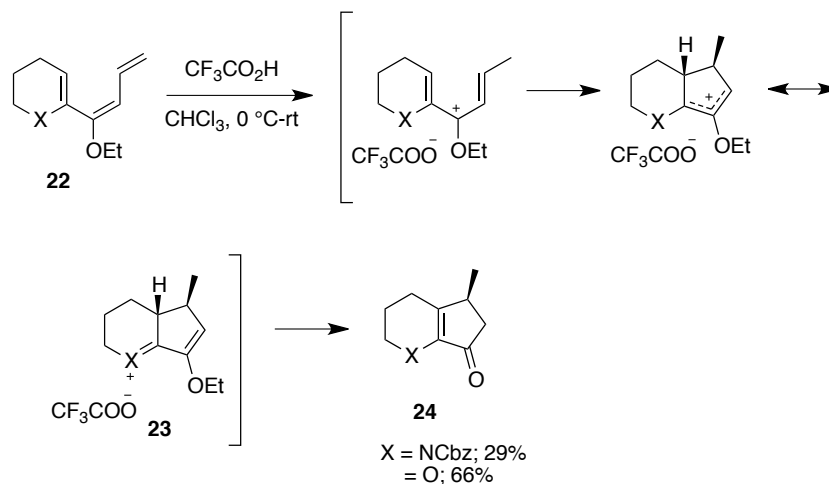
Scheme 1.7 Vinylogous Nazarov Cyclization of Cross-Conjugated Trienes.



Scheme 1.8 Triflic Acid Mediated Cyclization of Cross-Conjugated Triene **20**.

1.1.3. Activation Through Linearly Conjugated Trienes

Proper activation of electron-rich trienes such as **22** derived from the lactam- or lactone-derived vinyl triflates can also trigger a successful Nazarov cyclization, thereby annulating cyclopentenone rings to N- and O-containing heterocycles **24** with high diastereoselectivity and moderate to good yields (Scheme 1.9).¹⁵ The presence of a heteroatom in the ring is crucial for the stabilization of the oxallyl cationic intermediate **23**, which also accounts for the mild activation conditions. A spirocyclic by-product **26** was furnished during the cyclization of the dihydropyran derivative **25** via competing protonation of the dihydropyran olefin.¹⁶

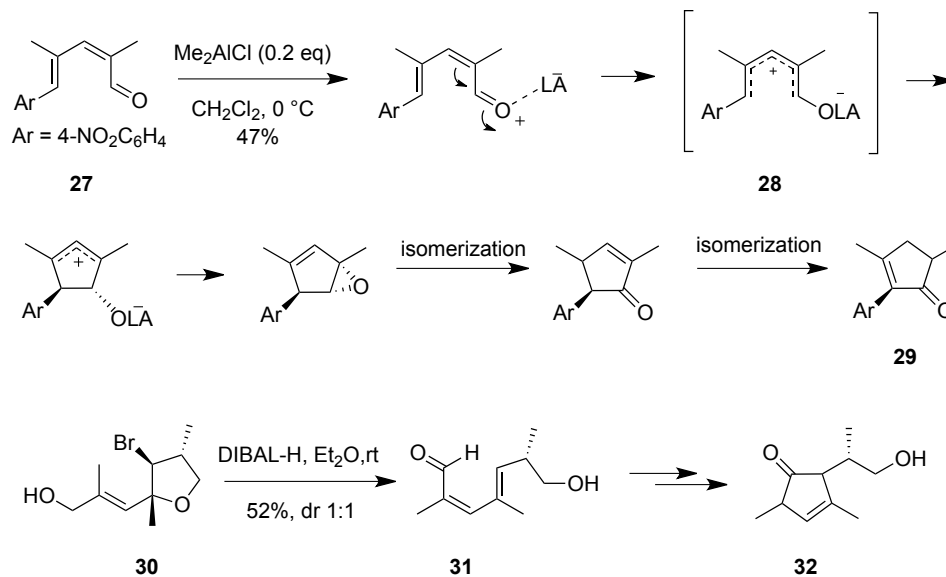


Scheme 1.9 Nazarov Cyclization of Electron-rich Trienes to form Fused Cyclopentenones.

1.1.4. Activation Through Conjugated Dienals

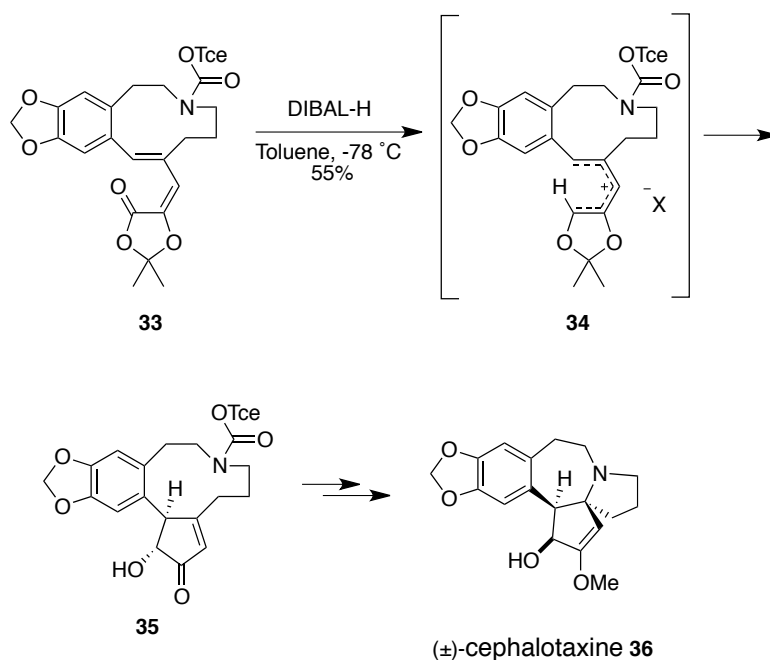
Lewis acid activated electrocyclicization of linearly conjugated dienals or ‘iso-Nazarov’ has also been recently studied. Trauner and coworkers presented the first example of an iso-Nazarov cyclization.¹⁷ They reported the formation of cyclopentenone **29** from pentadienal **27** in presence of Me_2AlCl as Lewis acid (Scheme 1.10). The product **29** is assumed to form through a conrotatory electrocyclicization of an oxy-pentadienyl cation **28**. The resulting cyclopentadienyl cation undergoes further reaction to form a cyclopentadiene epoxide, which finally isomerizes to afford the cyclopentenone **29**. An unusual rearrangement-cyclization cascade of 2-alkenyl-3-bromotetrahydrofuran **30** under DIBAL-H reduction conditions was reported by the Jung group in 2007.¹⁸ The cyclopentenone **32** is presumably formed via the iso-Nazarov cyclization of the

activated form of the dienal **31**. DIBAL-H is most likely to promote the cyclization.



Scheme 1.10 Iso-Nazarov Cyclization of Dienals.

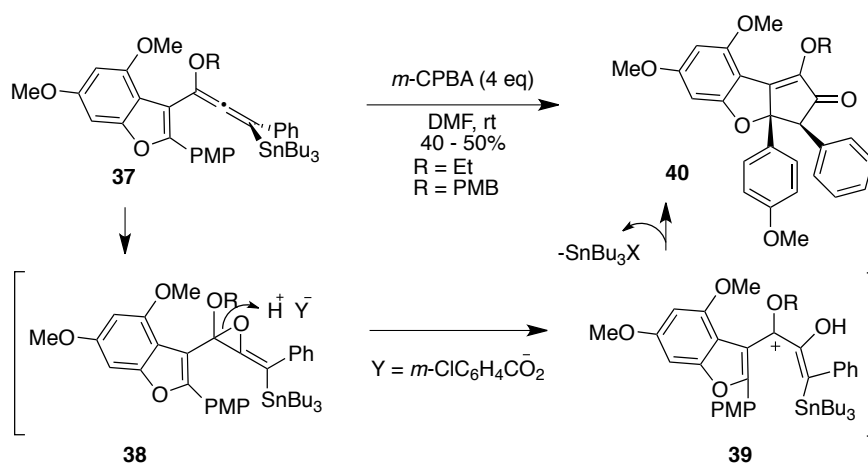
A similar cyclopentannulation protocol (reductive oxy-Nazarov reaction) has been developed by the Li group in conjunction with their studies toward the natural product cephalotaxine **36** (Scheme 1.11).¹⁹ This transformation involved an initial DIBAL-H reduction of vinylalkylidene dioxolanone **33** to form a tethered 1,2-oxidopentadienyl cation **34**, which on subsequent electrocyclic ring closure formed cyclopentenone **35** in a regio- and stereospecific fashion.



Scheme 1.11 Reductive Oxy-Nazarov Cyclization.

1.1.5. Electrophilic Activation of Oxygenated Vinyl Allenes

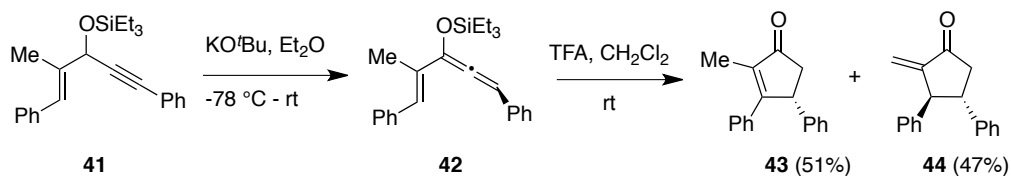
Another alternative route to pentadienyl cation generation involves electrophilic activation of vinyl allenenes. In their recent endeavor to the total synthesis of the natural product rocaglamide, Frontier and co-workers applied this strategy through an oxidative activation.²⁰ Treatment of the alkoxy allene **37** with excess *m*-CPBA gave the cyclized product **40** stereospecifically, but in moderate yield (Scheme 1.12). This domino pathway employed an initial regioselective epoxidation of the alkoxy allene to generate allene oxide **38**. The oxirane ring opening under acidic conditions unveiled the pentadienyl cation **39**, which then underwent conrotatory 4π -electrocyclization to form the fused tricyclic product **40**. This strategy has also been extended to simpler vinyl alkoxyallenes, providing a mild method for the diastereoselective construction of C-4, C-5 disubstituted cyclopentenones.²¹



Scheme 1.12 Oxidative Nazarov Cyclization of Vinyl Allene **37**.

1.1.6. Brønsted Acid Activation of Vinyl Allenes

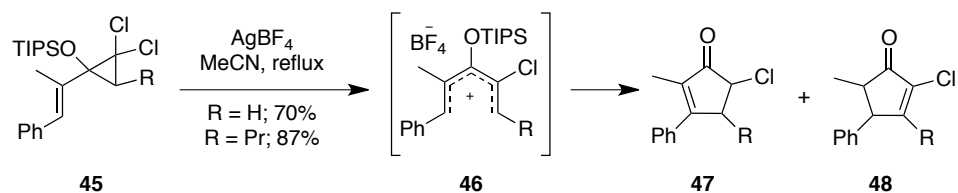
Brønsted acid activation of vinyl allenes provides another way of accessing pentadienyl cations (Scheme 1.13).²² Vinyl siloxyallenes such as **42**, formed *in situ* from enyne **41**, underwent a 4π -electrocyclization upon Brønsted acid (TFA) activation, to form cyclopentenones **43** and **44** in good yields. However, the regiocontrol for the final deprotonation step was poor, resulting in mixtures of cyclopentenones (e.g. **43**) and alkylidene cyclopentenones (e.g. **44**).



Scheme 1.13 Brønsted Acid Mediated Cyclization of Vinyl Allene **41**.

1.1.7. Dihalocyclopropane Nazarov Reaction

Disrotatory electrocyclic ring opening of dihalocyclopropanes under thermal or silver-assisted conditions is well documented. The resulting chloroallyl cations can be subjected to a variety of trapping processes. A dihalocyclopropane, when aptly substituted with an alkene unit, could potentially provide a novel route to a pentadienyl cation. Grant and West have demonstrated that alkenyl and silyloxy substituted cyclopropane **45**, in the presence of Ag(I), opens to pentadienyl cation **46**.²³ Subsequent conrotatory Nazarov cyclization followed by elimination would then provide chlorocyclopentenones **47** or **48** (Scheme 1.14). Complete regioselectivity in the elimination step in favor of more substituted alkene product **47** was observed in substrates lacking alkyl substitution on the cyclopropane.



Scheme 1.14 Silver Assisted Electrocyclization of Vinyl Dihalocyclopropanes.

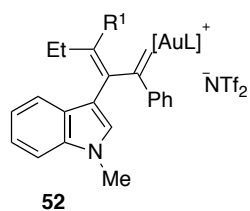
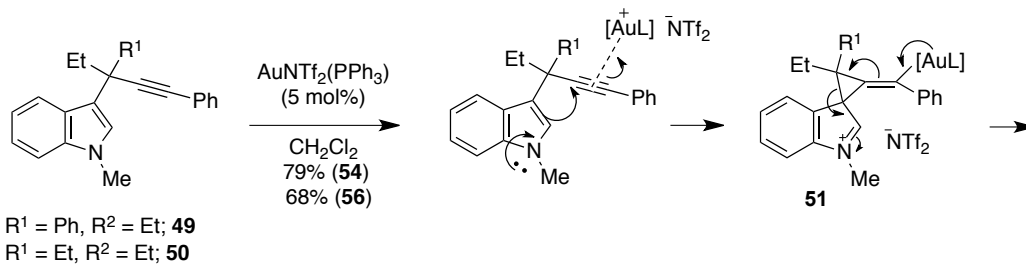
1.2 Generation of Pentadienyl Cation Through Activation of Alkyne

Several different strategies have been developed over the past few years to access species bearing the pentadienylic moiety analogous to the Nazarov intermediate for cyclopentannulation. One of the popular protocols is to activate an alkyne tethered to a distal alkene or aromatic moiety to access divinylmetallocarbene species. The process often involves tandem pathways, thus leading to an increase in molecular complexity in a fast and efficient fashion. Highly functionalized cyclopentane-containing products can be obtained from

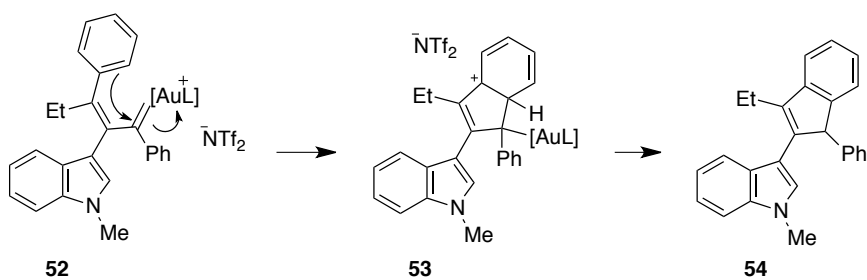
rather simple starting materials in a very step-efficient manner. This aspect is highly significant in terms of their application to natural product synthesis where step-economy is highly desirable.

1.2.1. Nazarov Cyclization via Divinylmetallocarbene Formation Under Gold Catalysis

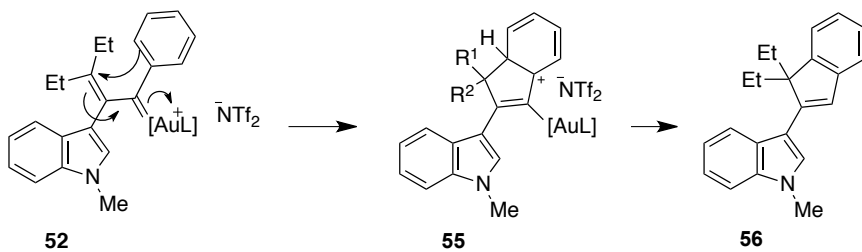
Divinylmetallocarbenes may display pentadienylic character analogous to Lewis or Brønsted acid activated divinyl ketones. A facile way of generating such metallocarbenes is through Au-catalyzed activation of alkynes. Sanz and Rodríguez reported the first gold-catalyzed domino reaction of propargylated indoles triggered by a [1,2]-indolyl migration.²⁴ Interestingly, propargyl indole **49** with an aryl group at the propargyl position gave only **54** as the sole product whereas **56** was formed when **50** was the substrate (Scheme 1.15). Both the fused cyclopentenones **54** and **56** are believed to be formed through a common intermediate **52** after a stepwise [1,2]-indolyl migration.²⁵ Initial coordination of the gold to the alkyne moiety of **49** or **50** would trigger an intramolecular attack of the indole nucleus on the activated alkyne, leading to an alkylidenecyclopropane intermediate **51**. Subsequent rearrangement and [1,2]-indolyl migration through a 4π -electrocyclic ring-opening affords the gold carbenoid **52**. When there is an aryl group at the propargylic position of **52**, a gold-variant of the iso-Nazarov cyclization takes place involving the aryl group leading to intermediate **53**, which then undergoes rearomatization and subsequent protodemetalation to form **54**. On the other hand, when there are two alkyl groups at the propargyl position, the carbenoid intermediate **52** may undergo a gold-variant of the Nazarov cyclization to give **55**. Ultimately a similar rearomatization followed by protodemetalation gives the Nazarov product **56**.



When $\text{R}^1 = \text{Ph}$

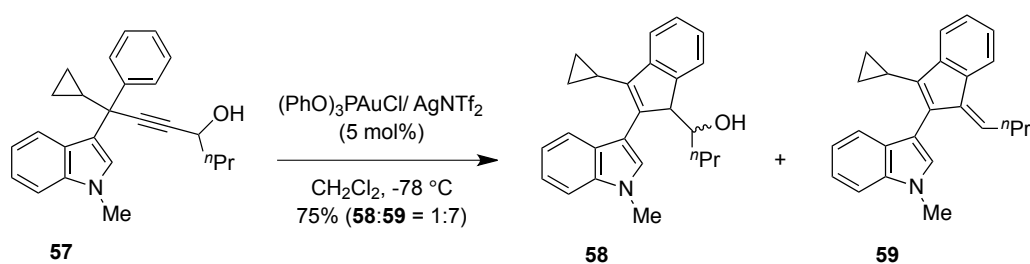


When $\text{R}^1 = \text{Et}$



Scheme 1.15 Au(I) Catalyzed Domino Cyclization of Propargylated Indoles.

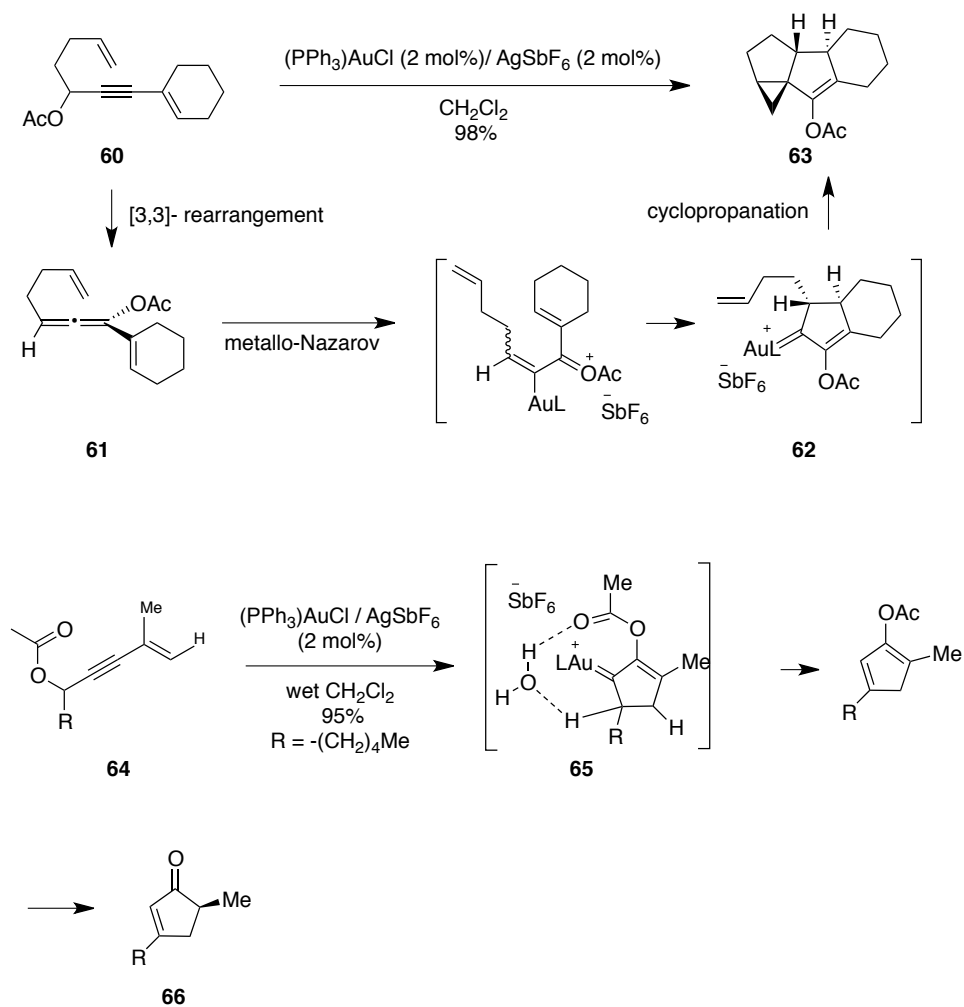
Sanz and coworkers have also reported a tandem Au(I) catalyzed cyclization of 3-propargylindoles **57** possessing a hydroxyl and a *n*-propyl group at the other propargyl position to form 2-indol-3-ylbenzofulvenes **58** and **59** (Scheme 1.16).²⁶ Formation of **58** follows a similar mechanistic route as that shown for the formation of the iso-Nazarov product **54** in Scheme 1.15; however, the methyleneindene derivative **59** is proposed to be formed through an elimination process. The reaction is found to be dependent on the nature of the ligand on the gold complex, the temperature of the reaction and the steric hindrance around the hydroxyl group.



Scheme 1.16 Au(I)-Catalyzed Domino Cyclization to Form 2-indol-3-ylbenzofulvenes.

An interesting gold(I) catalyzed domino cyclization of propargylic acetate **60** has been reported by the Malacria group.²⁷ An initial [3,3]-rearrangement of the propargylic acetate leads to the intermediate **61** which then undergoes a metallo-Nazarov cyclization to generate a cyclopentenylidene gold complex **62** (Scheme 1.17). A subsequent cyclopropanation of **62** involving the tethered alkene provides the tetracyclic product **63** as a single diastereomer in excellent yield. This methodology has been applied to the synthesis of a variety of triquinanes including a short total synthesis of the natural product capnellane.^{26b} A similar domino protocol of [3,3]-rearrangement/Nazarov cyclization and [1,2]-hydride shift of enynyl acetate **64** to cyclopentenone **66** has previously been reported by the Zhang group.²⁸ Best results were obtained when wet

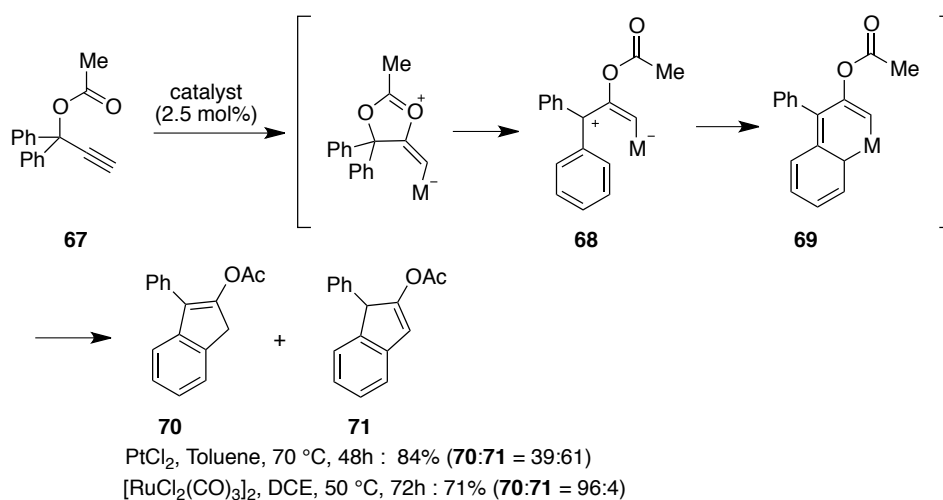
dichloromethane was employed as solvent, prompting the authors to propose a water-assisted proton transfer mechanism involving **65**.^{27b}



Scheme 1.17 Au(I) Catalyzed Domino Cyclization of Enynes involving [3,3]-Rearrangement and Nazarov Cyclization.

1.2.2. Generation of Vinylcarbenoid Species via Other Transition Metal Catalysis

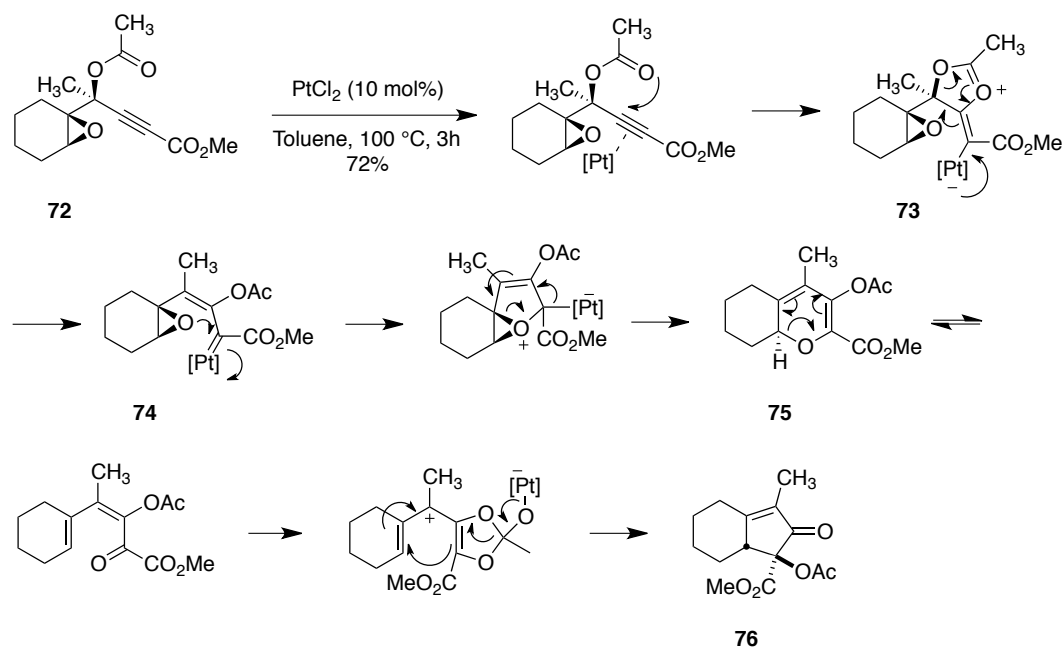
Vinylcarbenoid species can also be generated by other transition metal catalysis. Indenes **70** and **71** have been formed from propargyl ester **67** under platinum or ruthenium catalyzed conditions.²⁹ Metal mediated activation of the alkyne moiety in **67** with a concomitant [1,2]-acetyl shift generated a vinylcarbenoid intermediate **68** (Scheme 1.18). In the presence of a platinum catalyst, a mixture of isomers **70** and **71** were formed, whereas, use of a ruthenium catalyst produced predominantly a single isomer **70**. An alternative mechanism via metallacycle **69** has been proposed for the ruthenium-catalyzed reaction.



Scheme 1.18 Formation of Indenes Under Platinum or Ruthenium Catalysis.

The Sarpong group has reported an efficient one-pot transformation of oxiranyl propargylic esters **72** to 2-cyclopentenones **76** under PtCl₂ catalyzed conditions (Scheme 1.19).³⁰ The reaction is proposed to involve an initial Pt(II) catalyzed 5-*exo-dig* cyclization on the activated alkyne moiety to form the zwitterionic intermediate **73**, which could generate the metalcarbenoid **74**.

Subsequent attack by the epoxide oxygen should finally give rise to the pyran **75** after bond isomerization. An oxa-6 π -electrocyclic opening of the pyran intermediate followed by an iso-Nazarov type cyclization could finally give rise to the observed cyclopentenone **76**.

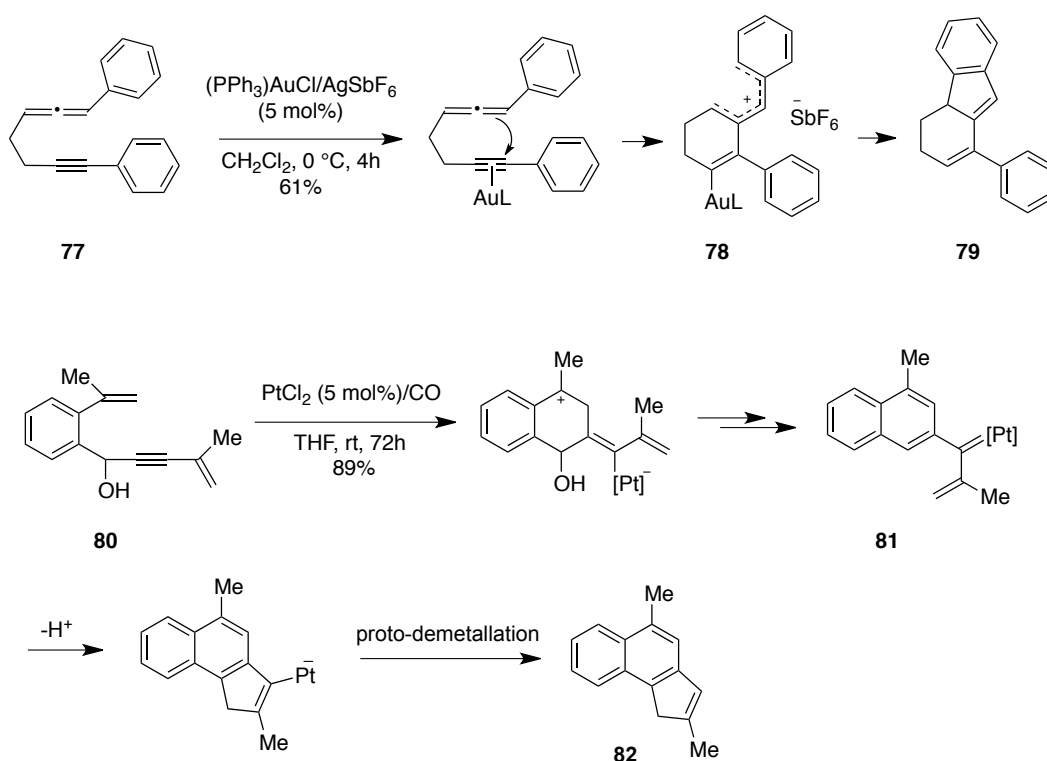


Scheme 1.19 One-Pot Domino Cyclization of Oxiranyl Propargylic Ester **72**.

1.2.3. Activation of Enynes by Transition Metals Toward Nazarov-Type Cyclizations

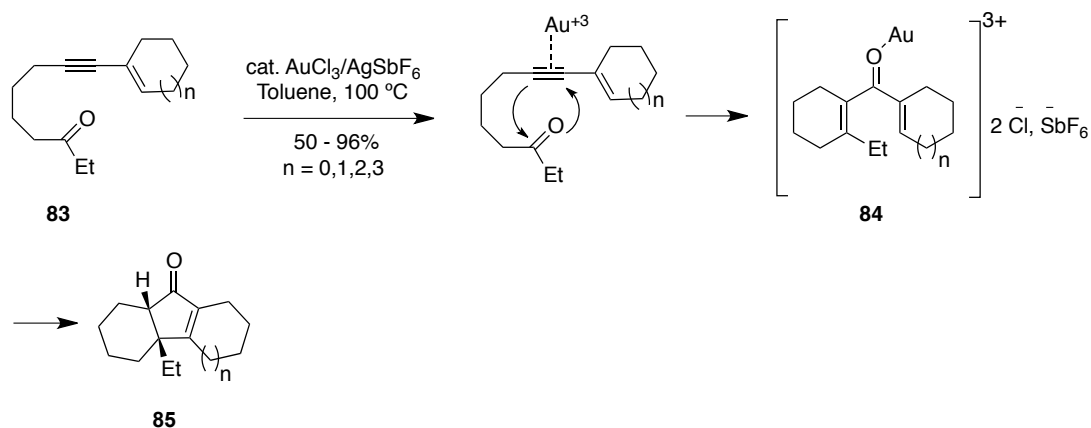
Gold-mediated activation of alkynes can also lead to a Nazarov-type cyclization via a pentadienyl cationic intermediate without involving any formation of a vinylcarbenoid species (Scheme 1.20).³¹ The 1,6-allenynes **77** undergoes a domino 6-*endo-dig* cyclization via Au(I)- π -alkyne intermediate to generate the pentadienyl cationic species **78**. A subsequent Nazarov cyclization of **78** leads to the formation of bicyclo[4.3.0]nonadiene **79**. The PtCl₂/CO catalyst system is found to be efficient in catalyzing 2-alkenyl-(1'-hydroxy-4-en-2-

ynyl)benzenes **80** through a similar cascade transformation to generate cyclopentanaphthalene derivatives **83** in a regioselective manner.³² Metal catalyzed carbophilic activation of the alkyne in **80** triggered a 6-*exo-dig* cyclization, resulting in the formation of the 2-naphthalidene intermediate **81**, thereby setting the stage for the subsequent Nazarov cyclization to afford **82** as the final product.



Scheme 1.20 Metal Catalyzed Domino Cyclizations of Enynes.

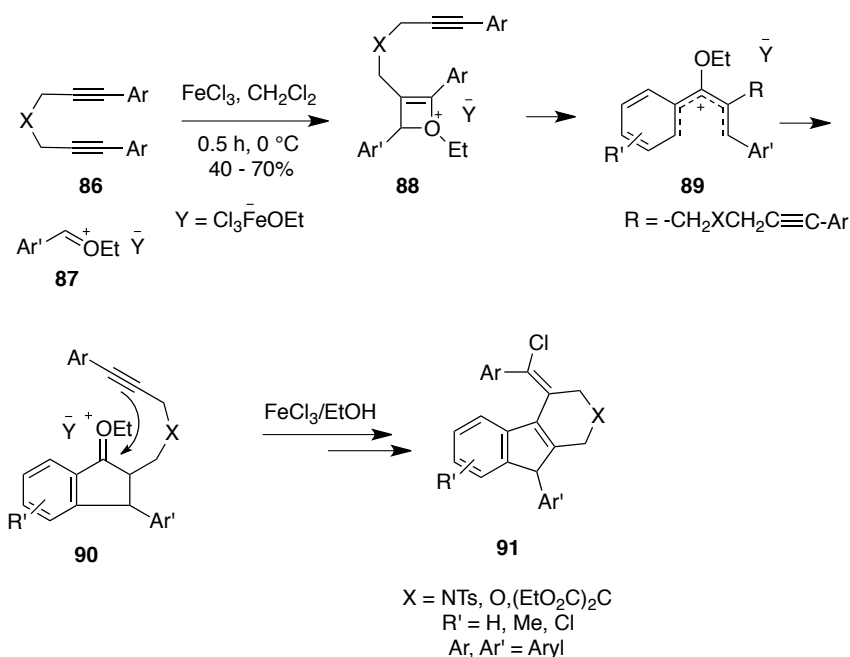
An intramolecular heteroenyne metathesis cyclization of 1,3-enynyl carbonyls **83** in presence of a Au(III) catalyst provides an alternate method of generating the pentadienyl cationic systems such as **84** (Scheme 1.21).³³ In this case, Au (III) performs the dual role of activating both the alkyne and the carbonyl groups. The tricyclic enones **85** are usually formed in excellent yields with good olefin regioselectivity and high diastereoselectivities.



Scheme 1.21 Heteroenyne Metathesis of 1,3-Enynyl Carbonyls **83**.

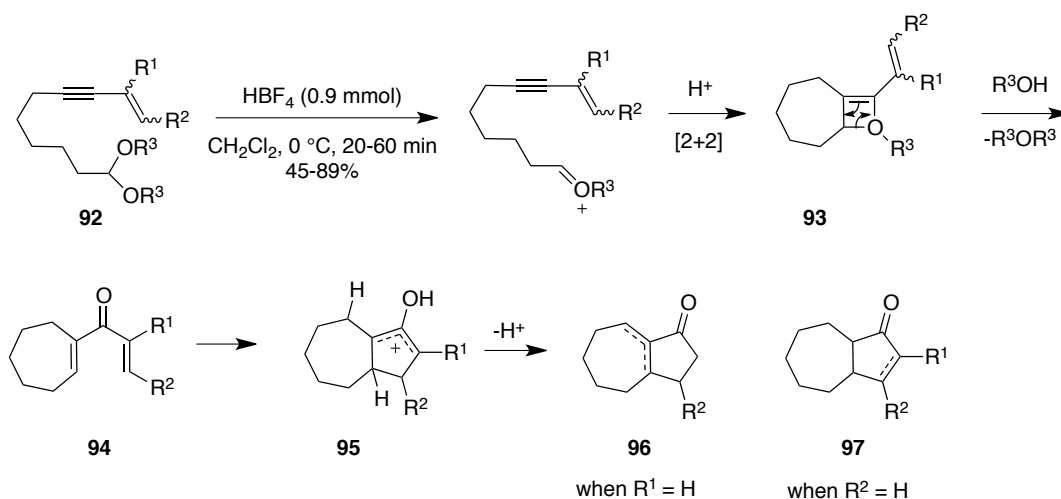
1.2.4. Lewis Acid Mediated Intermolecular Generation of the Pentadienyl Cationic Species

Various different routes of generating the 3-oxygenated pentadienyl cations have been reported in recent years. A tandem cyclization of diyne **86** and oxocarbenium ion **87** in presence of FeCl_3 catalyst has been demonstrated to provide highly functionalized indenenes **91** (Scheme 1.22).³⁴ In this example, diyne **86** undergoes an initial [2+2] cycloaddition with the oxonium ion **87** generated from benzaldehyde acetal by Lewis acid catalysis, to form an oxete intermediate **88**. Electrocyclic ring opening leads to the formation of a pentadienyl cation **89**, thereby setting the protocol for a 4π electrocyclization, to generate another oxocarbenium cation **90**. The tethered alkyne moiety then intercepts the oxocarbenium ion and finally attack by chloride ion provides the indene **91**.



Scheme 1.22 FeCl₃ Catalyzed Cyclization of Diynes **86** in Presence of Aldehyde-Acetal **87**.

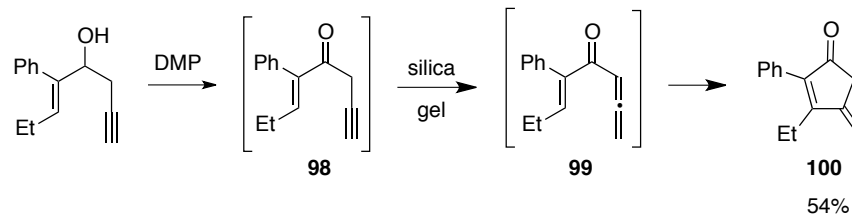
A very similar strategy has been applied by the Saa group in the formation of hydroazulenone skeletons **96** and **97** from enyne acetals **92** (Scheme 1.23).³⁵ Exposure of the enyne acetals to the optimized conditions using HBF₄ as the Brønsted acid catalyst formed the corresponding hydroazulenones in good to excellent yields. The regioselectivity of the product formation was largely dependent on the position of the alkene substituent, R¹ and R², and also on the nature of the tether that controlled the conformation of the oxallyl cationic intermediate. The mechanism is believed to involve an initial Brønsted acid induced oxocarbenium ion formation followed by a [2+2] cycloaddition with the alkyne unit to form the oxete intermediate **93**. Electrocyclic ring opening of the oxete forms the divinyl ketone **94**. Subsequent Nazarov cyclization under Brønsted acid catalyzed conditions forms the oxallyl cationic intermediate **95**. Depending on the presence of a substituent at the α or β position of the alkene, the final elimination step proceeds to form one of the observed bicyclo[5.3.0]decenones **96** or **97**.



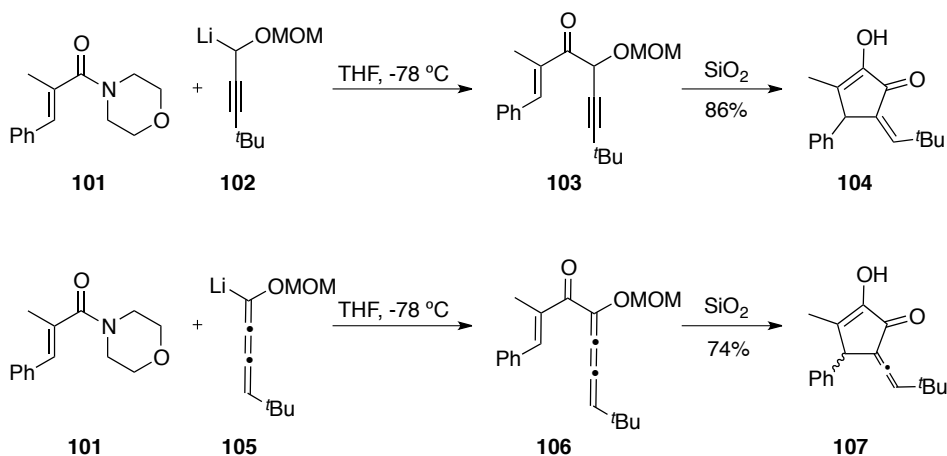
Scheme 1.23 Brønsted Acid Catalyzed Formation of Hydroazulenes **96** or **97**.

1.3 *In situ* Generation of Allenyl Vinyl Ketone

Nazarov cyclization of allenyl vinyl ketone has been an area of active research in the recent past. Hashmi and co-workers first proposed the intermediacy of allenyl vinyl ketones **99** during the cyclization of propargyl vinyl ketones **98** (Scheme 1.24).³⁶ Alkylidene cyclopentenones **99** were formed readily on exposure of propargyl vinyl ketones to silica gel. Later, Tius *et al.* have demonstrated that cyclization of oxyallenones **103**, prepared by the addition of allenyl lithium to enamide **101**, is an efficient method for the preparation of cyclopentenones of type **104** (Scheme 1.25).³⁷ The presence of an electron-releasing group at C-2 position of the ketone seems to enhance the reactivity of the substrates and allows cyclization under extremely mild conditions. They have explored the use of allenyl vinyl ketones extensively in the context of several natural product syntheses.³⁸ Alkoxy cumulenes **106** were also explored for Nazarov cyclization for the first time by Tius and co-workers.³⁹ Treatment of cumulenyl lithium **105** with enamide **101** generates the cumulene intermediate **106**, which undergoes ready cyclization under mild acidic conditions of aqueous workup to provide vinylidenecyclopentenones **107**.

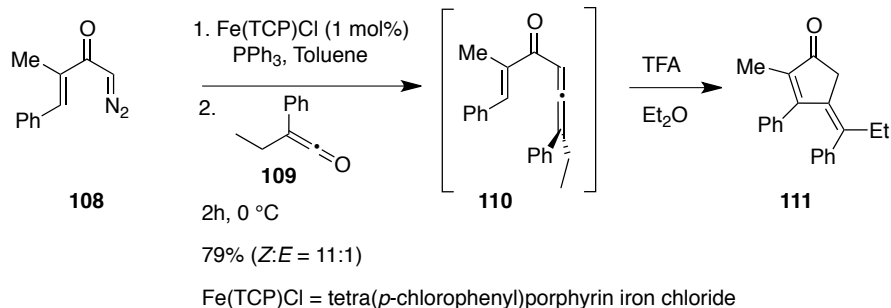


Scheme 1.24 Synthesis and Cyclization of Allenyl Vinyl Ketones.



Scheme 1.25 Nazarov Cyclization of Alkoxy Allenes and Alkoxy Cumulenes.

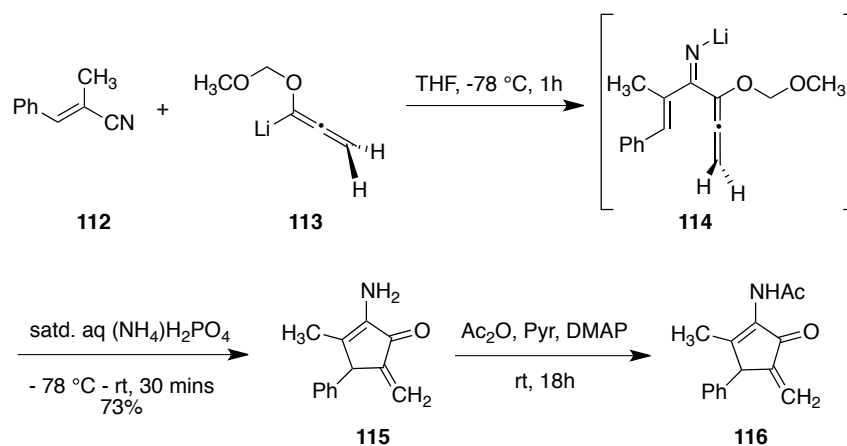
Tang and co-workers developed a method for *in situ* generation of allenyl vinyl ketone **110** and its subsequent Nazarov cyclization (Scheme 1.26).⁴⁰ In this process an unsaturated diazocarbonyl compound **108** undergoes Wittig olefination with ketene **109** to generate the allenyl vinyl ketone intermediate **110**. Subsequent cyclization under acidic conditions gave the cyclopentenone **111**. This is an efficient one-pot strategy to access sensitive allenyl vinyl ketones, which then undergo a facile cyclization to provide cyclopentenone derivatives in high yield and with excellent *Z* stereoselectivity.



Scheme 1.26 Nazarov Cyclization of an *In Situ* Generated Allenyl Vinyl Ketone.

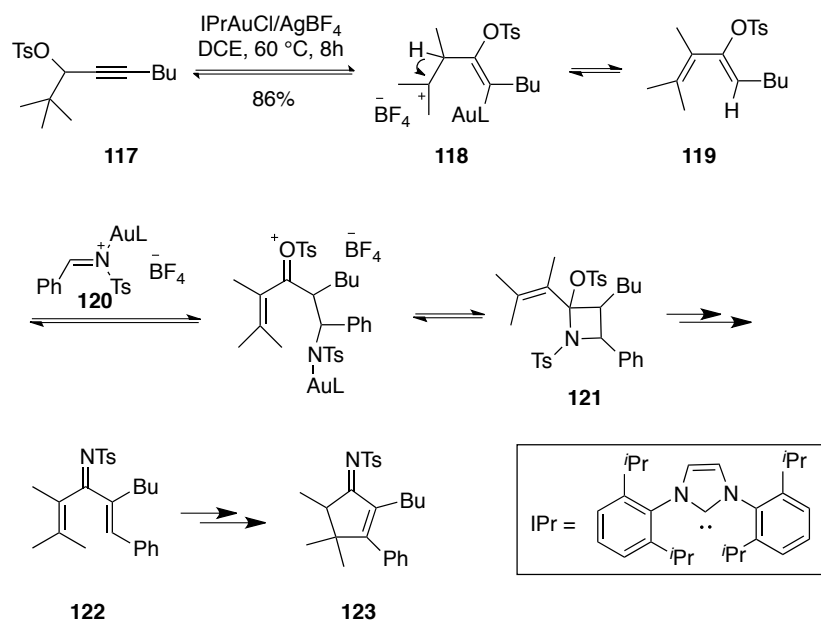
1.4 Imino Nazarov and Aza Nazarov Cyclizations

In 2001 Tius and co-workers first reported the formation of α -aminocyclopentenones **115** in a single operation from α,β -unsaturated nitriles **112** and allenyl nucleophiles **113** via an allenyl vinyl imine intermediate **114** (Scheme 1.27).⁴¹ The cyclopentannulation event was described as an imino Nazarov cyclization. The amines were generally converted to the corresponding acetamides **116** for the ease of handling and storage. Theoretical calculations by the Smith group suggest the unlikelihood of a classical imino Nazarov cyclization due to an unfavorable equilibrium for the cyclization.⁴² However, the formation of the α -aminocyclopentenones **115** is favored by the irreversible loss of the methoxymethyl cation after the cyclization step.



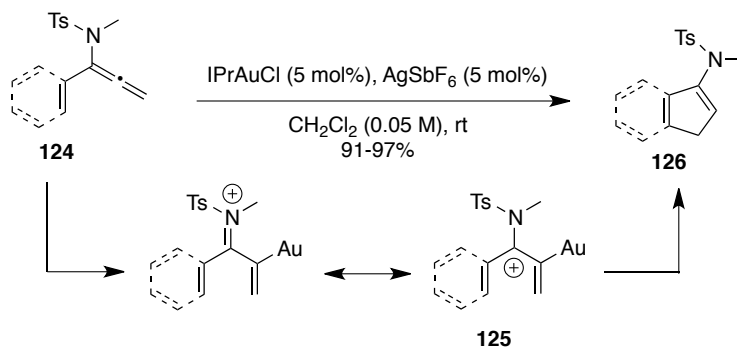
Scheme 1.27 An Imino Nazarov Cyclization to Form α -Aminocyclopentenones **115**.

Cyclopent-2-imines **123** have been reported to be formed through an interesting tandem sequence involving a gold catalyzed activation of propargyl tosylates **117** followed by further reaction with an activated aldimine **120** (Scheme 1.28).⁴³ According to the proposed reaction mechanism, an initial Au(I) activation of the alkyne moiety leads to a [1,2]-tosyl rearrangement inducing an alkyl migration to give **118**. A subsequent elimination provides the diene **119**, which then reacts with the activated aldimine **120** to form a highly strained azetidine intermediate **121**. Finally, a divinyl imine **122** is formed via the electrocyclic ring opening of **121**. In the presence of the gold complex, **122** undergoes a Nazarov-like cyclization to form the cyclopentenyl imine **123**.



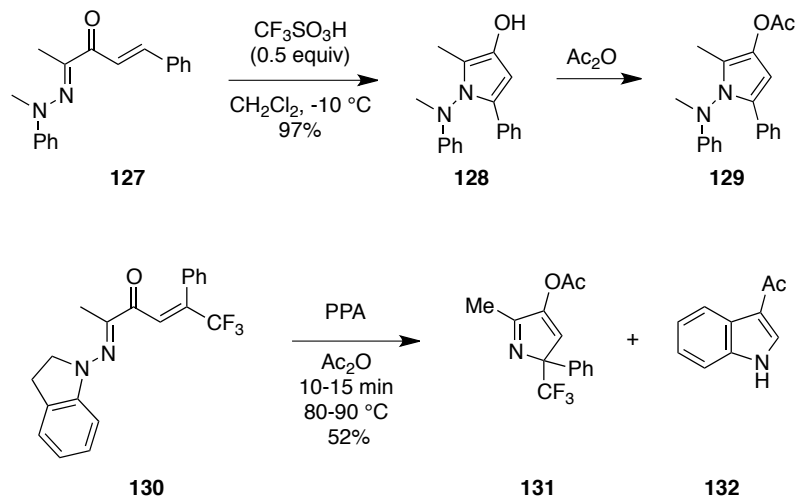
Scheme 1.28 Au(I) Catalyzed Imino Nazarov Cyclization of Propargyl Tosylates.

The Hsung group has demonstrated another very promising example of imino Nazarov cyclization of α -aryl allenamides under Au(I) catalyzed conditions (Scheme 1.29).⁴⁴ Electrocyclization of α -aryl allenamides **124** is assumed to be more favored due to the reduced ability of N-tosyl nitrogen atom to stabilize the pentadienyl cation **125**. The domino cyclization provides an efficient and regioselective protocol in constructing aromatic ring fused cyclopentenamides **126**. The enamide functionality generated through the imino-Nazarov cyclization can be used as an important synthetic handle.



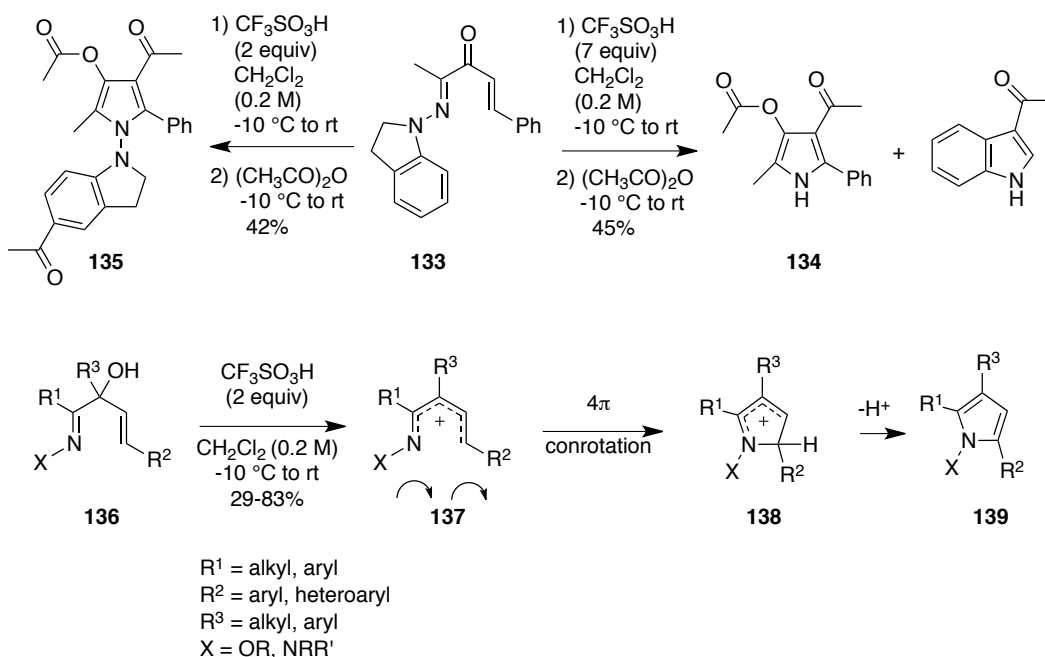
Scheme 1.29 Au(I) Catalyzed Imino Nazarov Cyclization of α -Aryl Allenamides.

Replacement of 1,4-pentadien-3-ones with 1-aza-1,4-pentadien-3-ones can offer an attractive and efficient route to the formation of variably substituted pyrroles through a Nazarov type cyclization. Ciufolini and co-workers first coined the name “aza-Nazarov reaction” during their synthetic endeavor toward camptothecin where a quinoline-containing enone gave an indolizine product in presence of Yb(fod)_3 .⁴⁵ Later, the Würthwein group have shown that hydrazones of the type **127** having nitrogen in the 1-position undergo smooth cyclization to give pyrrole **128** in accordance with their theoretical speculations (Scheme 1.30).⁴⁶ The pyrrole **128** formed through the aza-Nazarov cyclization contains a hydroxyl group at the 3-position which led to the instability of the pyrrole. A quick acetylation to give **129** circumvented this problem. Further studies were carried out with indoline **130** where proton elimination was blocked by double substitution at C-5. In this case, indole **132** was an effective leaving group to produce substituted 1*H*-pyrrole **131**.⁴⁷



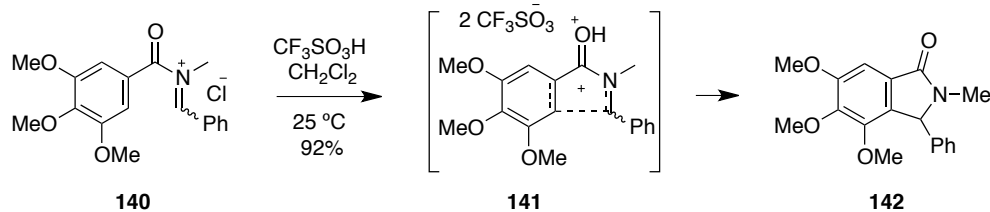
Scheme 1.30 Aza Nazarov Cyclization of Hydrazones to Form Pyrroles.

The same group has also demonstrated the use of excess triflic acid as a “superelectrophile” to form NH-pyrroles **134** through a cascade cyclization of 1-azapenta-1,4-dien-3-one **133** (Scheme 1.31).⁴⁸ Under these conditions **133** undergoes an aza-Nazarov cyclization cascade followed by N-N bond cleavage to give **134** after an acetic anhydride workup. However, use of 2 equivalents of triflic acid only formed the N-indolylpyrrole products **135**. The presence of hydroxyl or acetoxy group at the 3-position of pyrroles can be regarded as a limitation in terms of substitution pattern; additionally a 3-hydroxyl group also renders the pyrrole to be highly unstable. An efficient way to circumvent these limitations was found in the aza-Nazarov cyclization of 1-azapenta-1,4-diene-3-ols **136**.⁴⁹ Treatment of **136** with triflic acid in dilute dichloromethane at -10 °C formed diversely substituted pyrroles **139** in moderate to good yields. The reaction is believed to proceed through the formation of a reactive 1-azapentadienyl cation **137** after protonation of the hydroxyl group of **136** followed by subsequent loss of water. Pyrrole **139** is finally formed by the electrocyclic ring closure of the 1-azapentadienyl cation followed by aromatization of pyrrolium cation **138**.



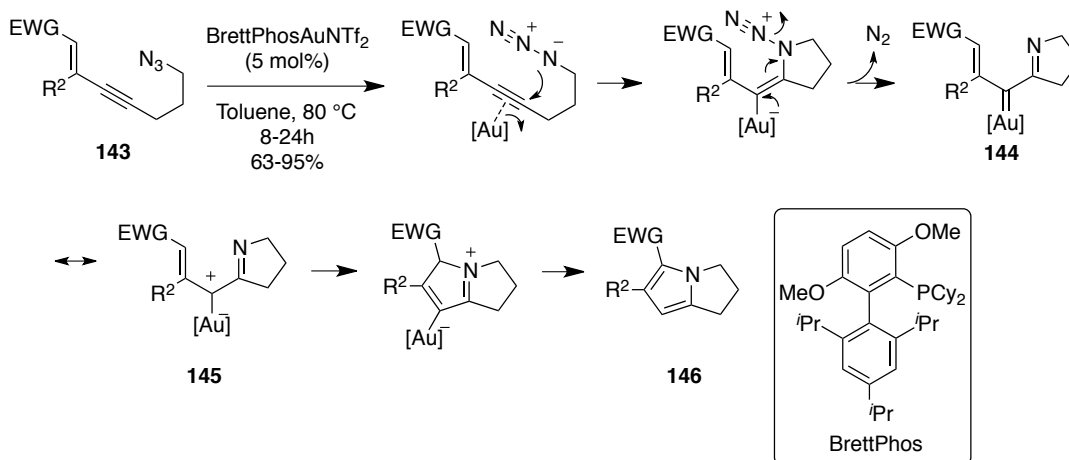
Scheme 1.31 Synthesis of Pyrroles Under Superelectrophilic Conditions via an Aza Nazarov Reaction Cascade.

Klump *et al.* on the other hand reported the aza-Nazarov cyclization of 2-azapentadienone **140** to form a fused bicyclic product **142** (Scheme 1.32).⁵⁰ Theoretical calculations predict that the presence of nitrogen at the 2-position could confer a high activation energy for cyclization, but the cyclization occurred smoothly when N-acyliminium salts **140** were treated with strong acid promoters.^{45a} On the basis of theoretical calculations, Klump and co-workers suggested that the formation of superelectrophilic species such as **141** in the presence of super acid like triflic acid is crucial to the success of these reactions.



Scheme 1.32 Aza Nazarov Cyclization of 2-Azapentadienone **140** under Superelectrophilic Conditions.

2,3-Dihydro-1*H*-pyrrolizines **146** can be formed through a Au(I)-catalyzed domino sequence involving a 4π -electrocyclic ring closure of an 1-azapentadienium species **145** (Scheme 1.33).⁵¹ The reaction entails an initial *5-exo-dig* cyclization of the azido group on to the Au(I)-activated alkyne unit of azidoenynes **143** in a highly regioselective manner to generate α -amino gold carbene **144**. 4π -electrocyclization of its mesomeric form **145** eventually delivers the pyrrole ring of **146**. The presence of an electron-deficient olefin at the distal end of the alkyne moiety minimizes the chance of a competitive *6-endo-dig* cyclization and also provides a setup for the eventual pentannulation following the formation of the gold carbene. The synthetic utility of the protocol has been showcased in a formal synthesis of 7-methoxymitosene, a biologically important compound.

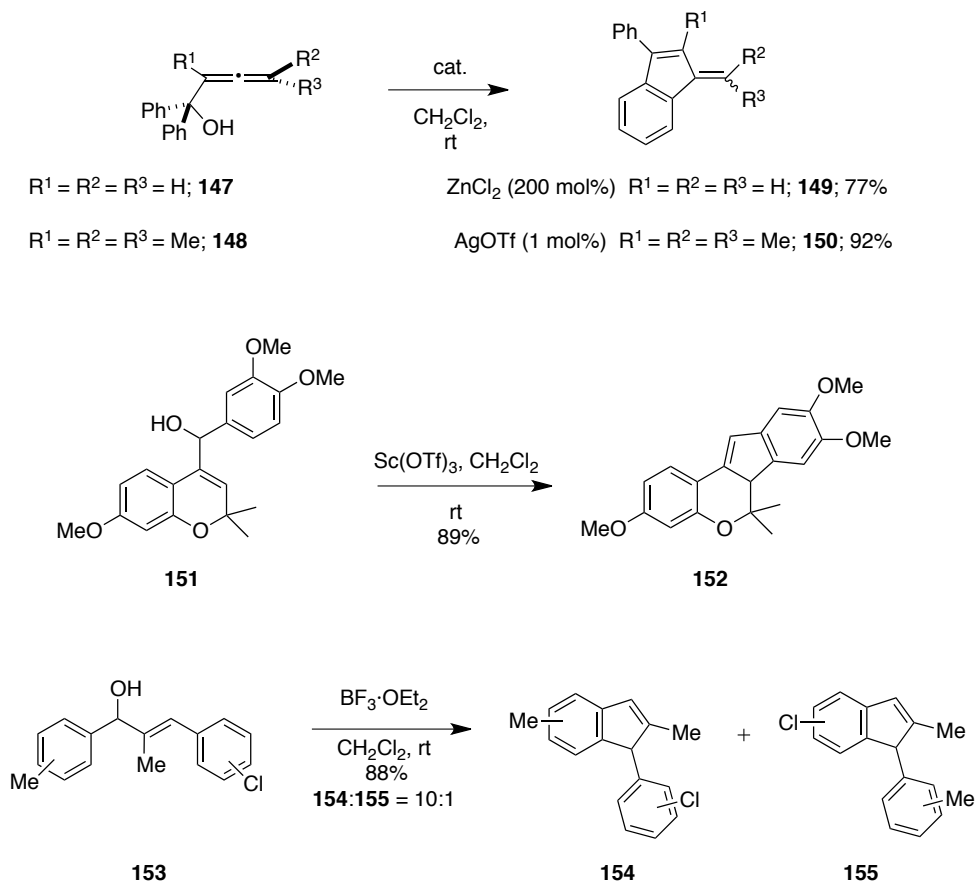


Scheme 1.33 Formation of 2,3-Dihydro-1*H*-Pyrrolizines **146** via Au(I) Catalyzed Tandem Cyclization of Azidoenynes **143**.

1.5 Cyclization of Pentadienyl Carbocation Generated Through Dehydration

Another unconventional route for the generation of pentadienyl carbocation for a 4π -electrocyclization could be achieved via dehydration of a divinyl alcohol. An allenic version of this protocol has been reported by Malacria and Gandon to provide a direct route to benzofulvenes through cyclization of α -hydroxyallenes (Scheme 1.34).⁵² In case of the monosubstituted α -hydroxyallene substrate **147**, ZnCl_2 proved to be a superior catalyst providing benzofulvene **149**, whereas for di- and tetra-substituted allenes such as **148**, AgOTf , TfOH and phosphomolybdic acid (PMA) produced the best yields in the formation of **150**. Interesting polycyclic scaffolds **152** have been synthesized in a similar fashion from diaryl alcohols **151** by the Panda group.⁵³ An electron donating group on the aromatic ring activates the cyclization of the pentadienyl carbocation, whereas lack of substitution leads to a sluggish cyclization and also allylic isomerization of the products. 1,3-diarylallylic alcohols **153** have been shown to provide 1-aryl-1-*H*-indenes **154** and **155** under similar Lewis acidic conditions.⁵⁴ The reaction is proposed to commence through dehydration of the alcohol **153** to form the corresponding 1,3-diarylallylic carbocation. The presence of a substituent at the 2-

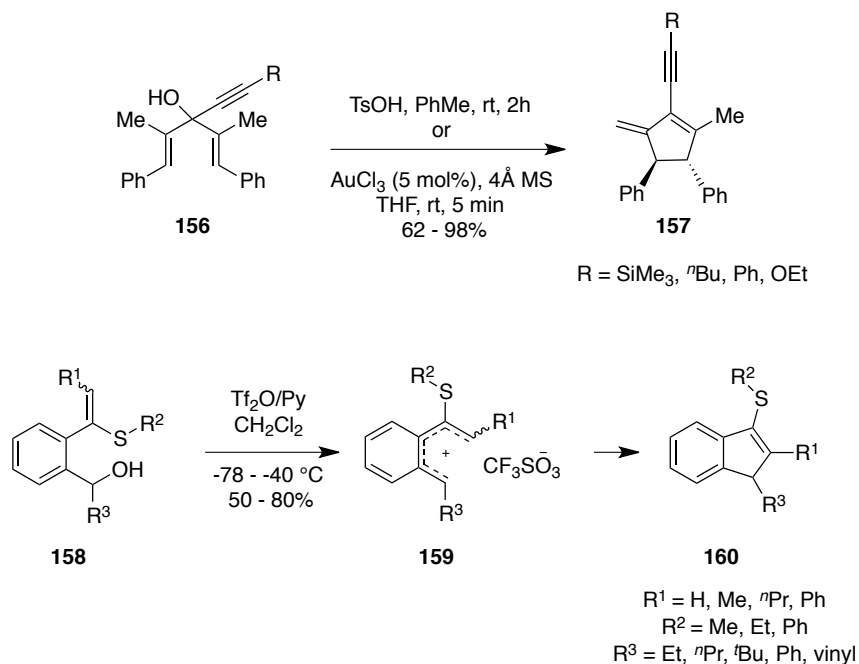
position of the diaryllic alcohols **153** is found to be crucial to attain the reactive U-shaped conformation for the 4π electrocyclicization.



Scheme 1.34 Synthesis of Benzofulvenes via Nazarov Cyclization of Divinyl Alcohol Following a Dehydrative Protocol.

A dehydrative cyclization was also reported by West and co-workers during their studies on the Meyer-Schuster rearrangement of alkynyl carbinols **156** (Scheme 1.35).⁵⁵ Exclusive formation of the cyclized alkyne **157** in good to excellent yields was observed when the reaction was carried out under Au(III) catalyzed conditions in presence of molecular sieves. The stereochemical outcome of this dehydrative cyclization confirmed a Nazarov type conrotatory electrocyclicization. Zhou and co-workers, on the other hand, reported a sulfur-mediated dehydration of [2-(1-thio-vinyl)phenyl]alcohols **158** to generate the

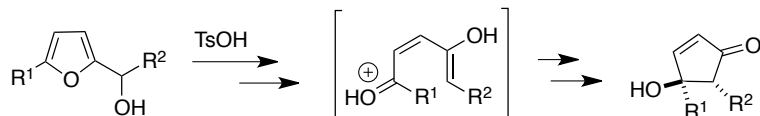
pentadienyl cation **159**, followed by Nazarov-type cyclization to form 3-thio-1*H*-indenes **160**.⁵⁶ The sulfur atom first attacks the triflate protected alcohol in an S_N2 process to afford the sulfonium ion which then releases the pentadienyl carbocation **159**.



Scheme 1.35 Dehydrative Nazarov Cyclization of Divinyl Alcohols.

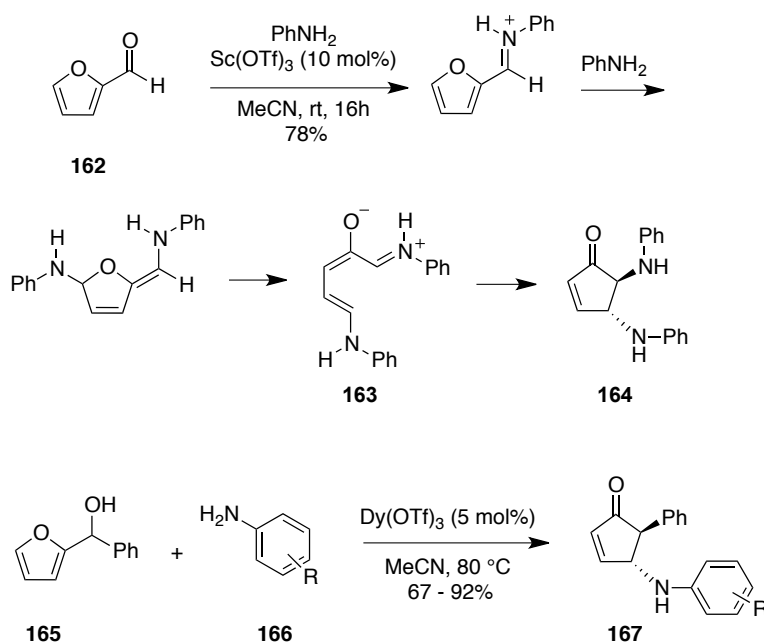
1.6 Piancatelli Reaction

In 1976, Piancatelli and co-workers reported the synthesis of various 4-hydroxycyclopentenones via an acid-catalyzed rearrangement of 2-furylcarbinols (Scheme 1.36).⁵⁷ The overall transformation is believed to proceed through a domino sequence that involves a 4 π electrocyclic ring closure of a pentadienyl cation, closely resembling the Nazarov cyclization. However, the synthetic application of this rearrangement had been largely limited because of the requirement for stoichiometric amounts of acid as activator, dilute reaction conditions and excess water.



Scheme 1.36 The Piancatelli Reaction.

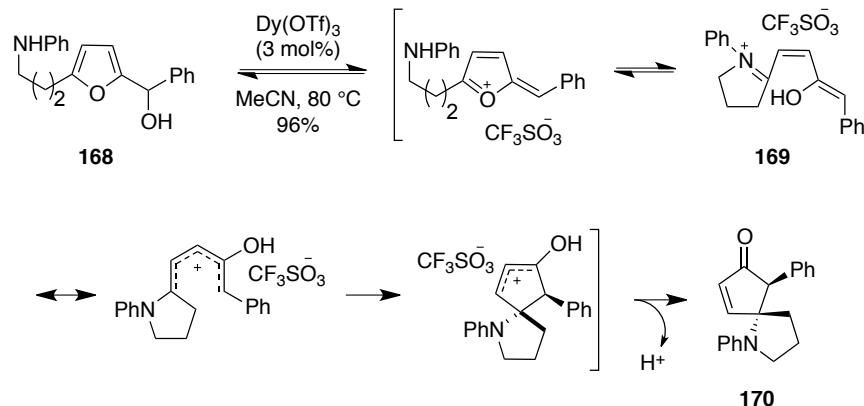
In 2007, the Batey group reported the synthesis of 4,5-diaminocyclopent-2-enones **164** from furan-2-carbaldehyde **162** and aniline in presence of Sc(OTf)₃ as Lewis acid promoter (Scheme 1.37).⁵⁸ Product **164** is formed with exclusive *trans* diastereoselectivity. The overall transformation is proposed to follow a domino pathway involving an initial condensation followed by ring opening to give the pentadienyl imminium ion **163**, which upon electrocyclization afforded **164**, very similar to the Piancatelli reaction. Alaniz and co-workers have developed a mild catalytic aza-Piancatelli protocol for the synthesis of 4-amino-5-alkylcyclopentenones **167** from readily available 2-furylcarbinols **165** and aromatic amines **166**.⁵⁹ Use of 5 mol% of Dy(OTf)₃ was optimal for the conversion with good yields and high *trans* diastereoselectivity. Generally, product isomerization is difficult to control in the Piancatelli rearrangement which could be avoided under the present conditions due to the mild nature of Dy(OTf)₃.



Scheme 1.37 Piancatelli Reactions in Presence of Mild Lewis Acids.

The aza-Piancatelli rearrangement has been applied by the Alaniz group toward the synthesis of azaspirocycles **170** using 2-furylcarbinols **168** with an aminoalkyl side chain.⁶⁰ This is an interesting example of the intramolecular version of the reaction. The Reddy group has recently reported a very similar aza-Piancatelli rearrangement to construct *trans*-4,5-disubstituted cyclopentenones under mild conditions using very low catalyst loading (0.03 mol% PMA).⁶¹ The reaction involves a nucleophilic attack of the tethered amino group on the initially formed oxocarbenium ion, leading to the cyclic imminium ion **169**. Subsequent Nazarov type cyclization affords the azaspirocycle **170** as the final product. The intramolecular aza-Piancatelli rearrangement also proceeds with good *trans* diastereoselectivity, consistent with a 4π electrocyclization. Substrates bearing an electron-donating group adjacent to the alcohol and an electron-withdrawing group on the nucleophilic nitrogen gave the best results in the intramolecular pathway. The intramolecular aza-Piancatelli rearrangement provides an efficient approach to the construction of challenging azaspirocycle motifs **170** by

generating the tertiary stereocenter and the spirocyclic ring system in a single operation.



Scheme 1.38 Intramolecular Aza-Piancatelli Reaction of 2-Furylcarbinols **168**.

1.7 Conclusion

A huge diversity of novel activation strategies has been developed to access cyclopentenone products through Nazarov cyclization. As the pentadienyl cation is generated directly from the starting materials without the involvement of a dienone species the problem of product inhibition can be avoided. Moreover, it offers better opportunity for the development of catalytic asymmetric versions of the reaction, as most of these reactions require very low catalyst loading. Divinylmetallocarbenes are often generated under mild catalytic conditions and through tandem reaction sequences involving tethered olefin or aromatic moieties, thereby increasing molecular complexity in a step and atom economic way.

Bridged bicyclic substrates with an embedded enyne unit as alternate Nazarov precursors may influence the final olefin regioselectivity and the diastereoselectivity of the reaction due to the inherent bonding preferences of these strained systems. In Chapter 2, we addressed this issue in detail. Chapter 4

will discuss the utility of these systems in the progress toward the total synthesis of a taxane natural product, taxinine.

1.8 References

- (1) A portion of this chapter has been submitted for publication: Scadeng, O.; Wu, Y.-K.; Fradette, R. J.; Joy, S.; West, F. G. "The Nazarov Cyclization," In *Comprehensive Organic Synthesis*, 2nd Ed.; Molander, G. A.; Knochel, P. Eds.; Elsevier; Vol. 5, in press.
- (2) Nazarov, I. N.; Zaretskaya, I. I. *Izv. Akad. Nauk SSSR, Ser. Khim.* **1941**, 211.
- (3) (a) Kursanov, D. N.; Parnes, Z. N.; Zaretskaya, I. I.; Nazarov, I. N. *Izv. Akad. Nauk SSSR, Ser. Khim.* **1953**, 114. (b) Nazarov, I. N.; Zaretskaya, I. I.; Parnes, Z. N.; Kursanov, D. N. *Izv. Akad. Nauk SSSR, Ser. Khim.* **1953**, 519. (c) Kursanov, D. N.; Parnes, Z. N.; Zaretskaya, I. I.; Nazarov, I. N. *Izv. Akad. Nauk SSSR, Ser. Khim.* **1954**, 859.
- (4) For recent reviews of Nazarov chemistry: (a) Shimada, N.; Stewart, C.; Tius, M. A. *Tetrahedron* **2011**, *67*, 5851. (b) Vaidya, T.; Eisenberg, R.; Frontier, A. J. *ChemCatChem* **2011**, *3*, 1531. (c) Nakanishi, W.; West, F. G. *Curr. Opin. Drug Discov. Dev.* **2009**, *12*, 732. (d) Pellisier, H. *Tetrahedron* **2005**, *61*, 6479. (e) Frontier, A. J.; Collison, C. *Tetrahedron* **2005**, *61*, 7577. (f) Tius, M. A. *Eur. J. Org. Chem.* **2005**, 2193.
- (5) Nakanishi, W. W., F. G. *Curr. Opin. Drug. Discov.* **2009**, *12*, 732.
- (6) (a) Muxfeldt, H.; Weigele, M.; Rheenen, V. V. *J. Org. Chem.* **1965**, *30*, 3573. (b) Casson, S.; Kocienski, P. *J. Chem. Soc., Perkin Trans. 1* **1994**, 1187. (c) Tius, M. A.; Kwok, C.-K.; Gu, X.-q.; Zhao, C. *Synth. Commun.* **1994**, *24*, 871.
- (7) (a) Bee, C.; Leclerc, E.; Tius, M. A. *Org. Lett.* **2003**, *5*, 4927. (b) Batson W. A.; Sethumadhavan, D.; Tius, M. A. *Org. Lett.* **2005**, *7*, 2771. (c) Uhrich, E. A.; Batson, W. A.; Tius, M. A. *Synthesis* **2006**, 2006, 2139.
- (8) Baldwin, J. E.; *J. Chem. Soc. Chem. Commun.* **1976**, 734.
- (9) Brooks, J. L.; Caruana, P. A.; Frontier, A. J. *J. Am. Chem. Soc.* **2011**, *133*, 12454-12457.
- (10) Brooks, J. L.; Frontier, A. J. *J. Am. Chem. Soc.* **2012**, *134*, 16551.

- (11) Basak, A. K.; Shimada, N.; Bow, W. F.; Vivic, D. A.; Tius, M. A. *J. Am. Chem. Soc.* **2010**, *132*, 8266.
- (12) Shimada, N.; Stewart, C.; Bow, W. F.; Jolit, A.; Wong, K.; Zhou, Z.; Tius, M. A. *Angew. Chem. Int. Ed.* **2012**, *51*, 5727.
- (13) Rieder, C. J.; Winberg, K. J.; West, F. G. *J. Am. Chem. Soc.* **2009**, *131*, 7504.
- (14) Kang, D.; Kim, J.; Oh, S.; Lee, P. H. *Org. Lett.* **2012**, *14*, 5636.
- (15) (a) Prandi, C.; Ferrali, A.; Guarna, A.; Venturello, P.; Occhiato, E. G. *J. Org. Chem.* **2004**, *69*, 7705. (b) Occhiato, E. G.; Prandi, C.; Ferrali, A.; Guarna, A.; Venturello, P. *J. Org. Chem.* **2003**, *68*, 9728.
- (16) Prandi, C.; Deagostino, A.; Venturello, P.; Occhiato, E. G. *Org. Lett.* **2005**, *7*, 4345.
- (17) Miller, A. K.; Banghart, M. R.; Beaudry, C. M.; Suh, J. M.; Trauner, D. *Tetrahedron* **2003**, *59*, 8919.
- (18) Jung, M. E.; Yoo, D. *J. Org. Chem.* **2007**, *72*, 8565.
- (19) Li, W.-D. Z.; Duo, W.-G.; Zhuang, C.-H. *Org. Lett.* **2011**, *13*, 3538.
- (20) Malona, J. A.; Cariou, K.; Spencer, W. T.; Frontier, A. J. *J. Org. Chem.* **2012**, *77*, 1891.
- (21) Spencer, W. T.; Levin, M. D.; Frontier, A. J. *Org. Lett.* **2010**, *13*, 414.
- (22) Wu, Y.-K.; West, F. G. *J. Org. Chem.* **2010**, *75*, 5410.
- (23) (a) Grant, T. N.; West, F. G. *J. Am. Chem. Soc.* **2006**, *128*, 9348. (b) Grant, T. N.; West, F. G. *Org. Lett.* **2007**, *9*, 3789.
- (24) (a) Sanz, R.; Miguel, D.; Rodríguez, F. *Angew. Chem. Int. Ed.* **2008**, *47*, 7354. (b) Álvarez, E.; Miguel, D.; García-García, P.; Fernández-Rodríguez, M. A.; Rodríguez, F.; Sanz, R. *Beilstein J. Org. Chem.* **2011**, *7*, 786.
- (25) Sanz, R.; Miguel, D.; Gohain, M.; García-García, P.; Fernández-Rodríguez, M. A.; González-Pérez, A.; Nieto-Faza, O.; de Lera, Á. R.; Rodríguez, F. *Chem. Eur. J.* **2010**, *16*, 9818.

- (26) Álvarez, E.; Miguel, D.; García-García, P.; Fernández-Rodríguez, M. A.; Rodríguez, F.; Sanz, R. *Synthesis* **2012**, *44*, 1874.
- (27) (a) Lemièrre, G.; Gandon, V.; Cariou, K.; Fukuyama, T.; Dhimane, A.-L.; Fensterbank, L.; Malacria, M. *Org. Lett.* **2007**, *9*, 2207. (b) Lemièrre, G.; Gandon, V.; Cariou, K.; Hours, A.; Fukuyama, T.; Dhimane, A.-L.; Fensterbank, L.; Malacria, M. *J. Am. Chem. Soc.* **2009**, *131*, 2993.
- (28) (a) Zhang, L.; Wang, S. *J. Am. Chem. Soc.* **2006**, *128*, 1442. (b) Shi, F.-Q.; Li, X.; Xia, Y.; Zhang, L.; Yu, Z.-X. *J. Am. Chem. Soc.* **2007**, *129*, 15503.
- (29) Nakanishi, Y.; Miki, K.; Ohe, K. *Tetrahedron* **2007**, *63*, 12138.
- (30) (a) Pujanauski, B. G.; Bhanu Prasad, B. A.; Sarpong, R. *J. Am. Chem. Soc.* **2006**, *128*, 6786. (b) González-Pérez, A. n. B.; Vaz, B. n.; Faza, O. N.; de Lera, Á. R. *J. Org. Chem.* **2012**, *77*, 8733.
- (31) Lin, G.-Y.; Yang, C.-Y.; Liu, R.-S. *J. Org. Chem.* **2007**, *72*, 6753.
- (32) Abu Sohel, S. M.; Lin, S.-H.; Liu, R.-S. *Synlett* **2008**, 745.
- (33) Jin, T.; Yamamoto, Y. *Org. Lett.* **2008**, *10*, 3137.
- (34) Xu, T.; Yang, Q.; Ye, W.; Jiang, Q.; Xu, Z.; Chen, J.; Yu, Z. *Chem. Eur. J.* **2011**, *17*, 10547.
- (35) Escalante, L.; González-Rodríguez, C.; Varela, J. A.; Saá, C. *Angew. Chem. Int. Ed.* **2012**, *51*, 1.
- (36) Stephen, A.; Hashmi, K.; Bats, J. W.; Choi, J.-H.; Schwarz, L. *Tetrahedron Lett.* **1998**, *39*, 7491.
- (37) (a) Forest, J.; Bee, C.; Cordaro, F.; Tius, M. A. *Org. Lett.* **2003**, *5*, 4069. (b) Tius, M. A. *Acc. Chem. Res.* **2003**, *36*, 284.
- (38) (a) Tius, M. A.; Drake, D. J. *Tetrahedron* **1996**, *52*, 14651. (b) Tius, M. A.; Hu, H.; Kawakami, J. K.; Busch-Petersen, J. *J. Org. Chem.* **1998**, *63*, 5971. (c) Tius, M. A.; Busch-Petersen, J.; Yamashita, M. *Tetrahedron Lett.* **1998**, *39*, 4219. (d) Wan, L.; Tius, M. A. *Org. Lett.* **2007**, *9*, 647.
- (39) Leclerc, E.; Tius, M. A. *Org. Lett.* **2003**, *5*, 1171.
- (40) Cao, P.; Sun, X.-L.; Zhu, B.-H.; Shen, Q.; Xie, Z.; Tang, Y. *Org. Lett.* **2009**, *11*, 3048.

- (41) Tius, M. A.; Chu, C. C.; Nieves-Colberg, R. *Tetrahedron Lett.* **2001**, *42*, 2419.
- (42) Smith, D. A.; Ulmer, C. W. *J. Org. Chem.* **1997**, *62*, 5110.
- (43) Suárez-Pantiga, S.; Rubio, E.; Alvarez-Rúa, C.; González, J. M. *Org. Lett.* **2008**, *11*, 13.
- (44) Ma, Z.-X.; He, S.; Song, W.; Hsung, R. P. *Org. Lett.* **2012**, *14*, 5736.
- (45) Ciufolini, M. A.; Roschangar, F. *Tetrahedron* **1997**, *53*, 11049.
- (46) Dieker, J.; Fröhlich, R.; Würthwein, E.-U. *Eur. J. Org. Chem.* **2006**, 5339.
- (47) Ghavtadze, N.; Fröhlich, R.; Würthwein, E.-U. *Eur. J. Org. Chem.* **2008**, 3656.
- (48) Narayan, R.; Daniliuc, C.-G.; Würthwein, E.-U. *Eur. J. Org. Chem.* **2012**, 6021.
- (49) Narayan, R.; Fröhlich, R.; Würthwein, E.-U. *J. Org. Chem.* **2012**, *77*, 1868.
- (50) (a) Klumpp, D. A.; Zhang, Y.; O'Connor, M. J.; Esteves, P. M.; de Almeida, L. S. *Org. Lett.* **2007**, *9*, 3085. (b) Sai, K. K. S.; O'Connor, M. J.; Klumpp, D. A. *Tetrahedron Lett.* **2011**, *52*, 2195.
- (51) Yan, Z.-Y.; Xiao, Y.; Zhang, L. *Angew. Chem. Int. Ed.* **2012**, *51*, 8624.
- (52) Cordier, P.; Aubert, C.; Malacria, M.; Lacôte, E.; Gandon, V. *Angew. Chem. Int. Ed.* **2009**, *48*, 8757.
- (53) Singh, R.; Panda, G. *Org. Biomol. Chem.* **2011**, *9*, 4782.
- (54) Smith, C. D.; Rosocha, G.; Mui, L.; Batey, R. A. *J. Org. Chem.* **2010**, *75*, 4716.
- (55) Rieder, C. J.; Winberg, K. J.; West, F. G. *J. Org. Chem.* **2010**, *76*, 50.
- (56) Zhou, H.; Xie, Y.; Ren, L.; Wang, K. *Adv. Synth. Catal.* **2009**, *351*, 1289.
- (57) Piancatelli, G.; Scettri, A.; Barbadoro, S. *Tetrahedron Lett.* **1976**, *17*, 3555.
- (58) Li, S.-W.; Batey, R. A. *Chem. Commun.* **2007**, 3759.
- (59) Veits, G. K.; Wenz, D. R.; Read de Alaniz, J. *Angew. Chem. Int. Ed.* **2010**, *49*, 9484.

- (60) Palmer, L. I.; Read de Alaniz, J. *Angew. Chem. Int. Ed.* **2011**, *50*, 7167.
- (61) Subba Reddy, B. V.; Narasimhulu, G.; Subba Lakshumma, P.; Vikram Reddy, Y.; Yadav, J. S. *Tetrahedron Lett.* **2012**, *53*, 1776.

Chapter 2

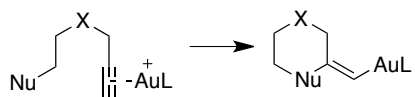
Bridged Bicyclic Enynyl Acetates in a Highly Efficient Domino [3,3]-Propargylic Shift/ Nazarov Cyclization/[1,5]-Hydride Shift Pathway Catalyzed by Au(I)

2.1 Au(I) Mediated Activation of Alkynes

The field of homogeneous catalysis using gold and platinum complexes has experienced an enormous development in the past decade.¹ New synthetic tools have emerged to utilize the distinct reaction profile of these noble metals as highly chemoselective activators of C-C π -bonds.² In particular, their ability to catalyze a variety of cascade reactions, transforming simple starting materials to products with significant complexity has provided chemists with both step and atom economical routes to complex molecules with defined configuration.³

Gold complexes are highly carbophilic Lewis acids, and unlike other transition metal complexes they bind exclusively to sp-hybridization (alkynes) and polarize the substrate toward further nucleophilic addition (Scheme 2.1).^{2a} Both inter and intramolecular nucleophilic additions have been reported.⁴ Nucleophilic attack on such a reactive species leads to the formation of a polarized intermediate that can be termed as a gold “carbenoid.”⁵ However, this may not be the most accurate description of the reactive organo-gold species due

to the vastly different size of the frontier orbitals of gold and carbon, which may preclude any significant back donation from the metal to the ligand.⁶ Thus, it may be more reasonable to depict these intermediates as metal-bound carbocationic species.

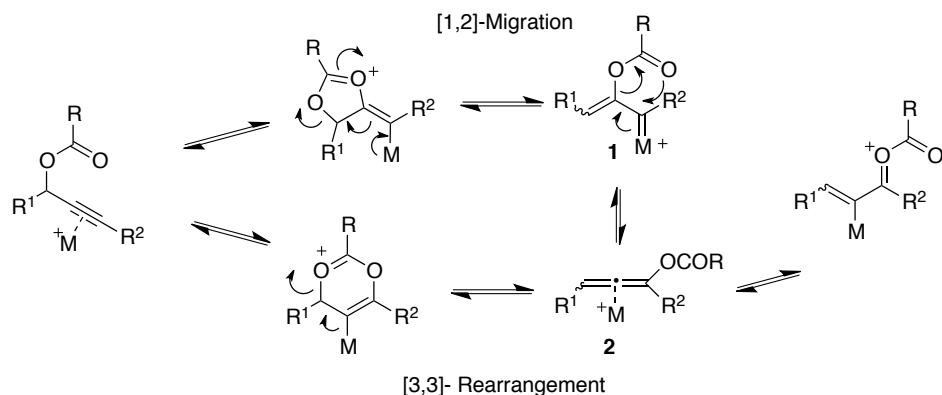


Scheme 2.1 Gold Activation of Alkynes.

2.2 Propargylic Esters in Gold Catalysis

One rapidly expanding area in the field of homogeneous gold catalysis involves the Au(I) catalyzed rearrangement of the propargylic carboxylates.⁷ Upon activation of the alkyne by coordination to the metal, two divergent transformations of the propargylic carboxylates have been proposed, namely [1,2]-acyloxy migration (or [2,3]-rearrangement) and [3,3]-rearrangement (Scheme 2.2).⁸ [1,2]-acyloxy migration involves the formation of an alkenyl gold carbene **1** triggered by a 5-*exo-dig* cyclization of the carbonyl ester on the gold activated alkyne, followed by cleavage of the original C-O bond, completing the transformation. The [3,3]-rearrangement is believed to proceed through an initial 6-*endo-dig* cyclization on the alkyne to form a gold bearing oxocarbenium ion, which can further undergo a ring opening to give a carboxy allene intermediate **2**. The [3,3]-rearrangement is also referred to as the Saucy-Marbet rearrangement, which was first reported in 1967.⁹ These two potentially reversible processes have low activation barriers, and preference for one over the other usually depends on the substitution pattern of the propargyl moiety and the further evolution of the carbenoid intermediate leading to irreversible formation of products.^{7b,10} Calculations by Cavallo and co-workers indicate that a [3,3]-rearrangement can be the net result of two consecutive [1,2]-acyloxy migrations (or [2,3]-

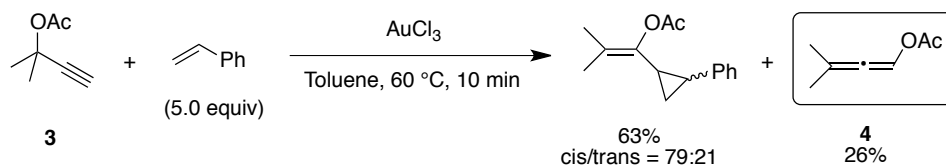
rearrangements); however this pathway has been refuted by the ^{18}O labeling studies by the Toste group.¹¹



Scheme 2.2 Two Possible Pathways of Rearrangements of Propargylic Esters under Gold Activation.

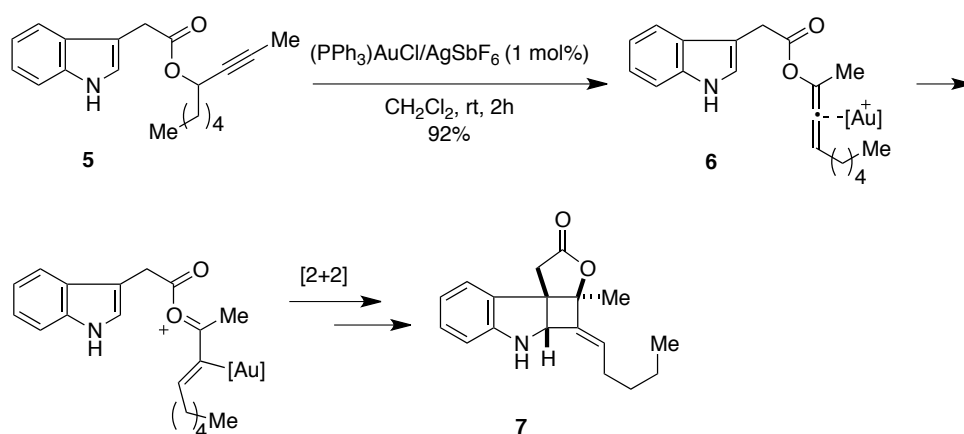
2.2.1. Examples of Gold Catalyzed [3,3]-Rearrangement of Propargylic Esters and Further Evolution of the Vinyl Gold Species

The [3,3]-rearrangement of propargylic esters under gold catalyzed conditions occurs preferably in case of sterically and/or electronically unbiased substrates.¹² An initial example of [3,3]-rearrangement of propargylic acetate **3** was demonstrated in the studies of Ohe and co-workers.¹³ Acetoxyallene **4** was formed as a side product in the AuCl_3 catalyzed reaction of the propargylic acetate (Scheme 2.3).

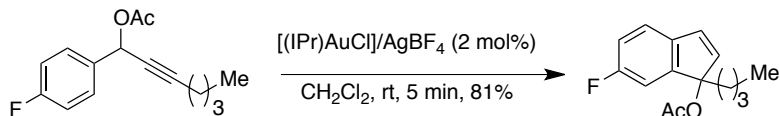


Scheme 2.3 First Report of Acetoxyallene Formation in AuCl_3 Catalyzed Reaction of Propargylic Acetates.

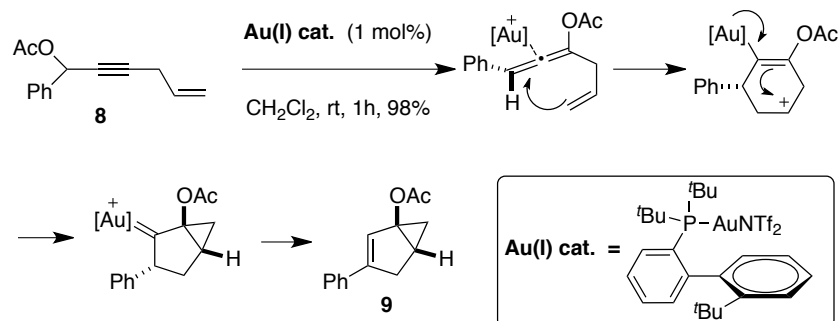
The fact that the gold complex not only activates the alkyne but also the intermediate allene was taken advantage of by the Zhang group in their clever reaction design (Scheme 2.4).¹⁴ Indole-3-acetate **5** was converted to highly functionalized tetracyclic cyclobutane **7** in excellent yield and diastereoselectivity. The reaction is proposed to proceed through an initial [3,3]-rearrangement to form the carboxyallene **6** which on further activation by the same cationic gold(I) species, undergoes a formal [2+2] cycloaddition to give the final product as a tetracyclic cyclobutane **7**. When the R¹ substituent on the propargylic ester is an aryl group, substituted indenenes were reported to be formed in good yields via domino [3,3]-rearrangement and electrophilic aromatic substitution on the oxocarbenium moiety (Scheme 2.5).¹⁵ Substitution at the acetylenic position also seems to be critical to the formation of the final product. When R² is an allyl group as in **8**, bicyclo[3.1.0]hexenes **9** were formed under Au(I) catalyzed conditions (Scheme 2.6).¹⁶ According to the mechanistic rationale, an initial gold(I) activation of the alkyne forms the alkoxy allene through a [3,3]-rearrangement. Further activation of the allene by the same gold(I) catalyst triggers the nucleophilic attack of the pendent alkene leading to a vinyl-gold species. Subsequent cyclopropanation followed by a [1,2]-hydride shift finally produces the product **9**.



Scheme 2.4 Au(I) Catalyzed Formation of Tetracyclic Cyclobutanes.



Scheme 2.5 Formation of Substituted Indenenes via Au(I)-Catalyzed [3,3]-Rearrangement and Electrophilic Aromatic Substitution.



Scheme 2.6 Synthesis of Bicyclo[3.1.0]hexenes from Propargylic Acetates with a Tethered C-C Double Bond.

However, the allenyl acetate formed after [3,3]-rearrangement, in absence of viable nucleophiles, can transform to a vinyl-gold intermediate by the participation of the metal ion. Depending on the molecular architecture, the vinyl-gold intermediate can be intercepted by various reaction pathways including a Nazarov-type cyclization when R² is an alkenyl unit.¹⁷

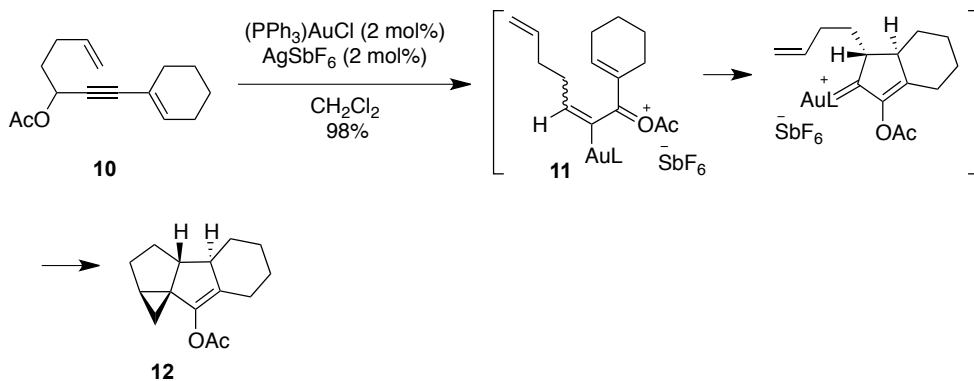
2.3 Gold Catalyzed Domino Reactions of Enynyl Carboxylates Involving Nazarov Cyclization as the Key Step

The Nazarov cyclization involves an electrocyclic ring closure of a pentadienylic carbocation, permitting the stereospecific formation of a carbon-carbon bond preserving orbital symmetry.¹⁸ There has been a renaissance in the study of this versatile transformation due to its utility in the formation of functionalized cyclopentenones. The prevalence of cyclopentane rings in various natural products and bioactive compounds has provided a major impetus in the

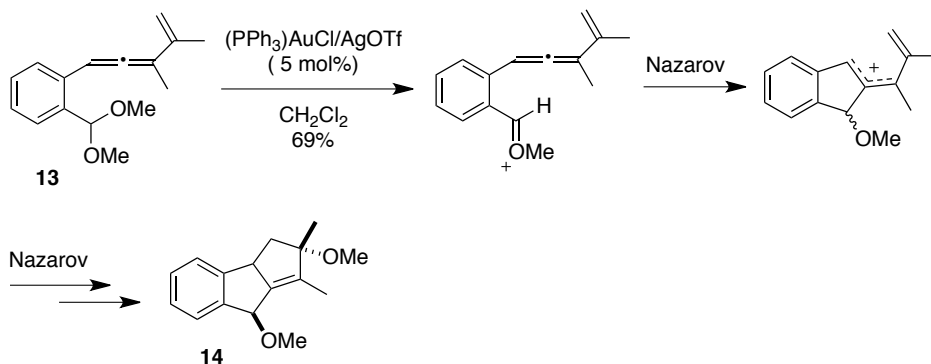
development and refinement of efficient synthetic tools for their construction. In its most traditional format, the Nazarov cyclization involves a strong Lewis or Brønsted acid promoted cyclization of a divinyl ketone, and this can be a limitation for the use of acid-sensitive substrates. Additionally, as both the starting material and the product of the reaction are ketones, a catalyst must bind to the carbonyl of the dienone in preference to that of the cyclopentenone to avoid product inhibition. This is a significant challenge, which often results in the use of high catalyst loading. Quite a bit of recent activity in the area of Nazarov chemistry has focused largely on the development of unconventional precursors to the key pentadienyl carbocation, providing unusual substitution pattern and also allowing milder reaction conditions. Some of the key examples include the use of allenyl vinyl ketones,¹⁹ vinyl cyclopropanes,²⁰ cross-conjugated trienes,²¹ α -diketones,²² and transition-metal mediated *in situ* generation of pentadienyl cation approaches.²³

Propargylic esters are a widely accepted choice in transition metal catalyzed cycloisomerizations due to their ease of preparation allowing for dense functionalization of the core structure. They are also popular due to the plethora of catalytic chemistry involving [2,3]- and [3,3]-rearrangements. Enynyl propargylic esters have recently been reported to participate in domino reaction pathways under Au(I) catalyzed conditions leading to *in situ* generation of a pentadienyl cation-type intermediate.²⁴ Malacria and co-workers have demonstrated a quick formation of cyclopentenone-containing polycyclic structure **12** under Au(I) catalyzed cycloisomerization entailing Nazarov cyclization of the vinyl gold-carbenoid **11** in a domino reaction sequence of the enynyl acetate **10** (Scheme 2.7).²⁵ In this example, a cleverly positioned alkene tether intercepts the gold carbenoid to form the cyclopropane unit in **12**. The yields and diastereoselectivity are excellent in this method. This example elegantly showcases the amount of complexity that can be achieved through the domino reaction pathway of these simple starting materials in a very mild, fast and efficient fashion. This work has also been discussed in detail in Chapter 1

(See page 16). Further, an alkenylallene bearing substrate **13** was shown to undergo a domino iso-Nazarov/Nazarov cyclization when subjected to gold catalyzed conditions to form bicyclo[3.3.0]octene **14** (Scheme 2.8).²⁶



Scheme 2.7 A Tandem Au(I)-Catalyzed Nazarov Cyclization/Cyclopropanation of Gold Carbenoid to Form Polycyclic Products.



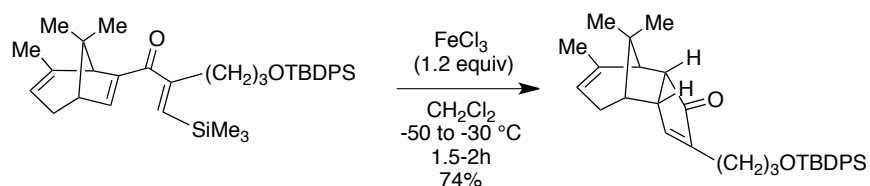
Scheme 2.8 Au(I)-Catalyzed Tandem Iso-Nazarov/Nazarov Cyclization to Form Bicyclo[3.3.0]octene.

2.4 Results and Discussions

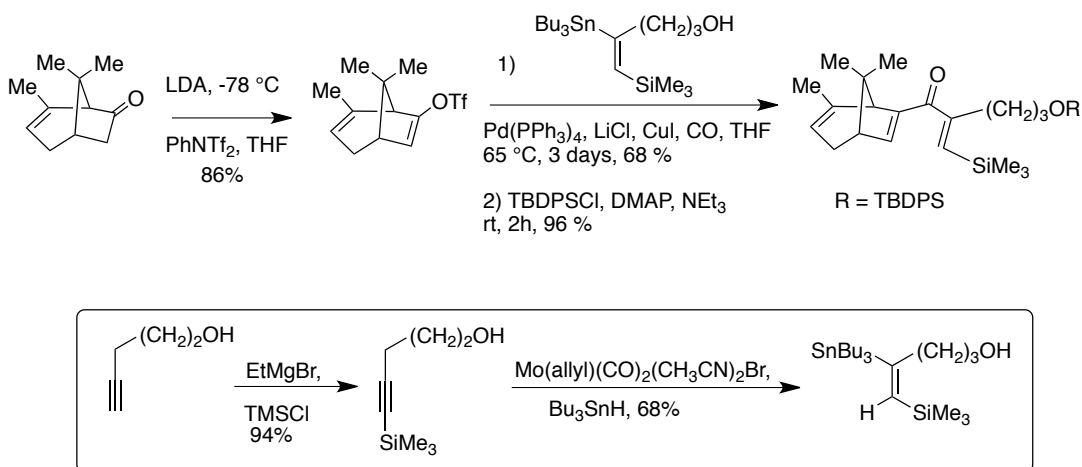
The West group has been engaged in the development of new and unconventional precursors to the Nazarov intermediate. Vinyl

dihalocyclopropanes have been reported to undergo facile electrocyclization after an initial electrocyclic ring opening of the halocyclopropane under Ag(I) assisted conditions.^{20a} A vinyl dihalocyclopropaneamine also has been demonstrated to undergo a similar electrocyclic ring opening to form aminopentadienyl cation followed by subsequent imino-Nazarov cyclization.²⁷ Wu and West have shown that silyl-protected allyl propargyl alcohols can serve as potential Nazarov substrates via sequential base promoted isomerization to siloxy vinyl allenes followed by activation with mild Brønsted acid to give the final cyclopentenone.²⁸

Our interest in bridged bicyclic Nazarov precursors stems from our synthetic endeavor toward a taxane natural product. Our efforts toward the synthesis of a taxane skeleton have been elaborated in detail in Chapter 4. A diastereoselective silicon-directed Nazarov cyclization of a bridged bicyclic dienone forms the key part of the synthetic route (Scheme 2.9).²⁹



Scheme 2.9 Silicon-Directed Nazarov Cyclization of Bridged Bicyclo[3.2.1]octadiene Substrate.



Scheme 2.10 Preparation of the Bicyclo[3.2.1]octene Dienone.

The preparation of the divinyl ketone precursors required for the silicon-directed Nazarov process involves the use of super-stoichiometric quantities of toxic reagents like CO and tributyltin hydride (Scheme 2.10).³⁰ An alternative route to *in situ* generation of the required divinyl ketone was investigated. Moreover, our synthetic approach to a taxane natural product required the migration of the olefin of the silicon-directed Nazarov product to the ring fusion position for the oxidative cleavage to furnish the eight-membered B-ring (Figure 2.1). Standard procedures for installation of the tetrasubstituted olefin often met with difficulties, especially in presence of bulky substituents on the cyclopentenone unit (Scheme 2.11).

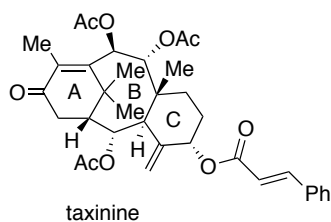
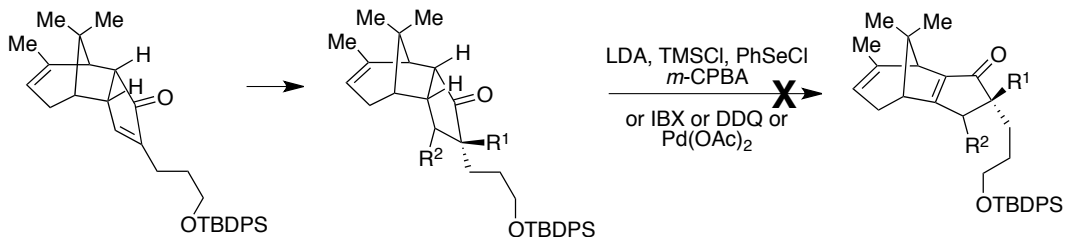
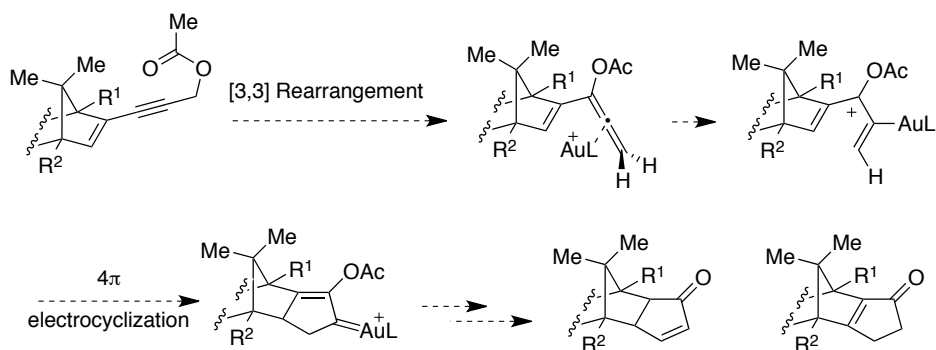


Figure 2.1 The A-B-C Ring System of a Representative Member of the Taxane Family.

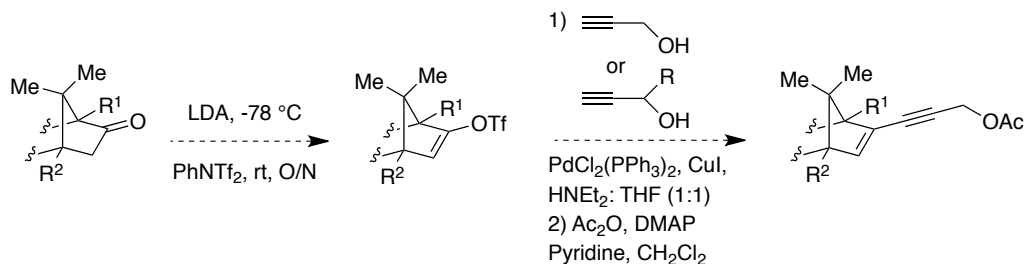


Scheme 2.11 Difficulties in Installation of a Tetra-Substituted Olefin in a Highly Functionalized Cyclopentenone Framework.

Inspired by the pioneering works of Zhang and Malacria on the use of enynyl acetates in their respective Au(I) catalyzed domino [3,3]-rearrangement and Nazarov cyclization, we envisaged that the bridged bicyclic enynyl acetates could potentially provide an alternate route to the cyclopentenones through the formation of divinyl metallocarbenoids (Scheme 2.12). Enynyl acetates were proposed to be accessible easily through a simple procedure involving a palladium(0) mediated Sonogoshira cross-coupling of propargylic alcohols with bridged bicyclic vinyl triflates followed by subsequent acetylation of the alcohol (Scheme 2.13).³¹



Scheme 2.12 Proposed Reaction Pathway for the Conversion of Bridged Bicyclic Enynyl Acetates to Cyclopentenones.

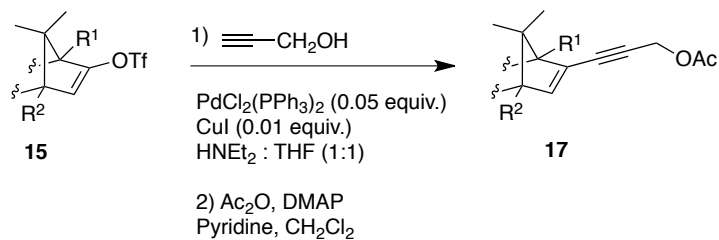


Scheme 2.13 Proposed Pathway for the Preparation of Bridged Bicyclic Enynyl Acetates.

2.4.1. Synthesis of Starting Material

The vinyl triflates **15a-c** were prepared from the corresponding ketones upon treatment with LDA in THF at $-78\text{ }^{\circ}\text{C}$ followed by addition of *N*-phenyl trifluoromethanesulfonimide at the same temperature and then warming to room temperature overnight. The corresponding Sonogoshira coupling of the vinyl triflates **15** with propargyl alcohol in the presence of Pd(II) catalyst under basic conditions provided the enynols **16** cleanly after overnight stirring in good to excellent yields (Table 2.1).³¹ The required enynyl acetates **17a-c** were then formed by acetylation of the enynols.

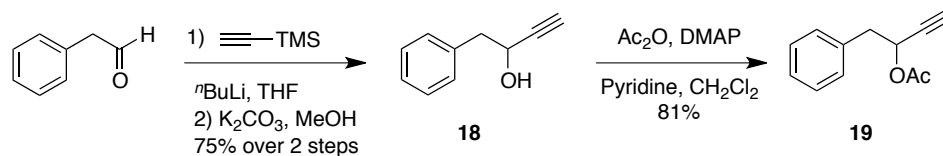
Table 2.1 Sonogoshira Coupling of Bridged Bicyclic Enol Triflates and Propargylic Alcohol.^a



Entry	Enol triflate	Enynyl acetate	Yield (%)
1.	 15a	 17a	83%
2.	 15b	 17b	84%
3.	 15c	 17c	81%

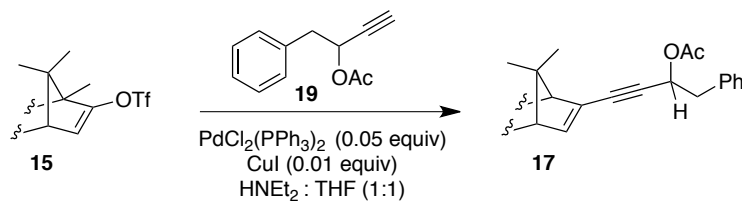
^aStandard Procedure: $\text{Pd}(\text{PPh}_3)_2\text{Cl}_2$ (0.05 equiv) and copper iodide (0.01 equiv) were dissolved in a 1:1 solution of THF:DEA (diethylamine). The solution was degassed with argon for 10 min. The appropriate vinyl triflate **15** (1.0 equiv) was dissolved in THF and the solution was degassed for an additional 10 min before adding to the reaction mixture via a syringe. Propargyl alcohol (1.1 equiv) was added via syringe, and the initial green solution changed from yellow, to orange to red. The THF and DEA were removed under reduced pressure. The residue was purified by silica gel flash chromatography (40% EtOAc in hexanes) to provide the corresponding enynol. To a solution of the enynol (1.0 equiv), pyridine (1.1 equiv), DMAP (5%) in dichloromethane at 0 °C, was slowly added acetic anhydride (2.0 equiv) and the reaction mixture was stirred for 2h at this temperature. The reaction was quenched with aqueous NH_4Cl , followed by extraction, drying (MgSO_4), filtration and concentration under reduced pressure. The residue was purified by silica gel flash chromatography (20% EtOAc in hexanes) to provide the corresponding enynyl acetate **17**. ^bIsolated yields based on vinyl triflates **15**.

Bridged bicyclic enynyl acetates **17d-f** with a benzyl substituent at their C-5 position were synthesized using propargyl acetate **19** as the Sonogoshira coupling partner with the vinyl triflates **15a-c** (Table 2.2). Compound **19** was obtained by acetylation of the propargyl alcohol **18**, which in turn was prepared from phenylacetaldehyde and trimethylsilyl acetylene (Scheme 2.14).



Scheme 2.14 Preparation of the Propargyl Acetate **19**.

Table 2.2 Preparation of C-5 Substituted Bridged Bicyclic Enynyl Acetates via Sonogoshira Coupling.^a

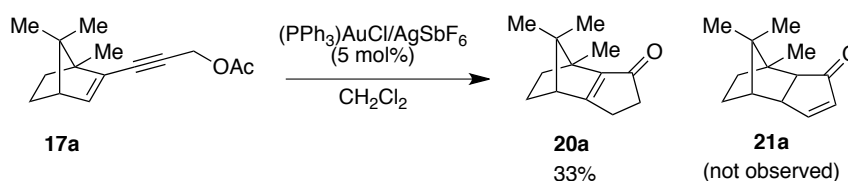


Entry	Enol triflate	Enynyl acetate	Yield (%)
1.	 15a	 17d	87%
2.	 15b	 17e	80%
3.	 15c	 17f	81%

^aStandard Procedure: $\text{Pd}(\text{PPh}_3)_2\text{Cl}_2$ (0.05 equiv) and copper iodide (0.01 equiv) were dissolved in a 1:1 solution of THF:DEA (diethylamine). The solution was degassed with argon for 10 min. The appropriate vinyl triflate **15** (1.0 equiv) was dissolved in THF and the solution was degassed for an additional 10 min before adding to the reaction mixture via a syringe. Propargyl alcohol **19** (1.1 equiv) was added via syringe, and the initial green solution changed from yellow to orange, to red. The THF and DEA were removed under reduced pressure. The residue was purified by silica gel flash chromatography (40% EtOAc in hexanes) to provide the corresponding enynyl acetate **17**. ^bIsolated yields based on vinyl triflates **15**.

2.4.2. Domino [3,3]-Rearrangement/Nazarov Cyclization and [1,5]-Hydride Shift of Enynyl Acetates

The elegant work of the Zhang and Malacria groups suggested to us that the enynyl acetates could potentially undergo cyclization cascade under Au(I) catalysis.^{17,25b} We first sought to explore the reactivity of the enynyl acetate **17a** using 5 mol% of the AuClPPh₃/AgSbF₆ catalyst system. In the event, only partial conversion of the starting material was observed after 12 hours. A catalyst optimization revealed that the starting enynyl acetate underwent complete conversion using 10 mol% of the Au(I) catalyst. To our surprise we found that the cyclization of **17a** produced **20a** as the sole product rather than the expected **21a**¹⁷ through a domino cyclization pathway (Scheme 2.15).

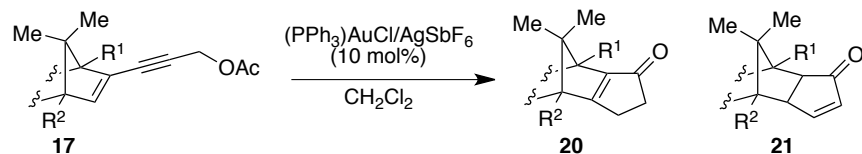


Scheme 2.15 Au(I)-Catalyzed Domino Cyclization of Camphor-Derived Enynyl Acetate.

We set out to examine the scope of this domino transformation and to understand the factors controlling the regioselectivity of the alkene formation. As shown in Table 2.3 (entry 1-3), bicyclic enynyl acetates **17a-c** were found to cyclize to give fused cyclopentenones **20a-c** in moderate to good yields. Unlike the examples of simpler acyclic or cyclic enynyl acetates,¹⁷ cyclization with bridged bicyclic enynyl acetates was found to be a bit sluggish. Attempts to use other gold catalysts such as AuCl₃ proved to be ineffective for the desired transformation. We then set out to examine if substitution of a benzyl group at the propargyl terminus could affect the regiochemical outcome of the cyclopentannulation. Bridged bicyclic enynyl acetates **17d-f** (Table 2.3, entry 4-6)

when subjected to $(\text{PPh}_3)\text{AuCl}/\text{AgSbF}_6$ conditions, showed a complete reversal in regioselectivity during the cycloisomerization cascade forming olefin isomers **21a-c** exclusively in each case. This indicates that the substitution pattern at C-5 of the propargylic terminus plays a crucial role in determining the regiochemistry of olefin formation in the cyclopentenone products. Surprisingly, we found that the diastereoselectivity in the case of the bicyclo[2.2.1]heptenynyl acetate **17d** is favored toward the *endo*-isomer **21d** as confirmed by 2D TROESY correlations (Figure 2.2). This is a highly intriguing result as we have previously reported exclusive *exo*-isomer formation during the Nazarov cyclization of bicyclo[2.2.1]heptene divinyl ketone.^{29a,32}

Table 2.3 (PPh₃)AuCl/AgSbF₆ Catalyzed Formation of Fused Cyclopentenones^a



Entry	Enynyl acetate	Product	Yield (%)
1.	 17a	 20a	77
2.	 17b	 20b	86
3.	 17c	 20c	73
4.	 17d	 21d	78
5.	 17e	 21e	81
6.	 17f	 21f	63

Table 2.3 Continued

^aStandard Procedure: To a solution of bridged bicyclic enynyl acetate **17** (1.31 mmol) in dichloromethane (25.8 mL, 0.05 M) was added AuClPPh₃/AgSbF₆ [pregenerated as 0.01 M solution in dichloromethane by mixing AuCl(PPh₃) (0.13 mmol) with AgSbF₆ (0.13 mmol), 13 mL] at room temperature and the reaction mixture was stirred for 4-5h. Following consumption of **17**, the mixture was treated with one drop of triethylamine and concentrated. The residue was purified by silica gel flash chromatography (20% EtOAc in hexanes) to give the corresponding cyclopentenones **20** or **21**. ^bIsolated yields based on enynyl acetates **17**.

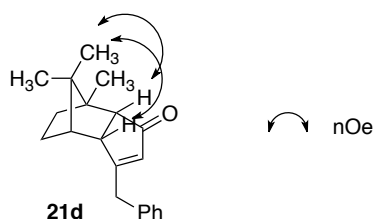
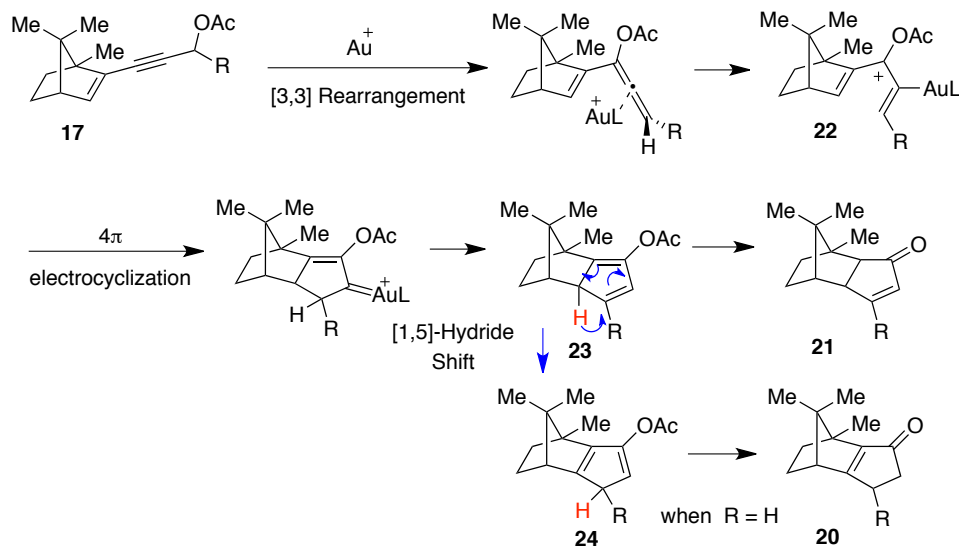


Figure 2.2 Relative Stereochemical Assignment of **21d** Based on 2D TROESY Correlations.

A possible mechanistic rationale to account for the reversal of regioselectivity in the cases of the enynyl acetates **17** as opposed to the observations by Zhang *et al.* is shown in Scheme 2.16.¹⁷ A [3,3]-rearrangement of the enynyl acetate **17** promoted by Au(I) activation of the alkyne leads to an allenyl acetate which on further activation generates the pentadienyl cation **22**. Electrocyclic ring closure of **22** results in the formation of a cyclopentenyl gold-carbenoid. Cyclopentadienyl acetate **23** can be formed through a possible two-step E1-type elimination and proto-deauration mechanism. Finally, isomerization via [1,5]-hydride shift can be proposed to account for the generation of pentadienyl acetate **24**, which hydrolyzes to the corresponding cyclopentenones **20**. Formation of the olefin isomer **21** in the case of bridged bicyclic enynyl acetates with a C-5 substituent can be rationalized by the fact that a [1,2]-hydride shift via a cyclopentadienyl acetate **23** is more favored than a [1,5]-hydride shift due to a lower activation energy barrier for the event. In this case, a [1,5]-hydride shift is a

relatively slower process and requires the presence of a base ($\text{KO}t\text{-Bu}$ in $t\text{-BuOH}$) to promote the isomerization.

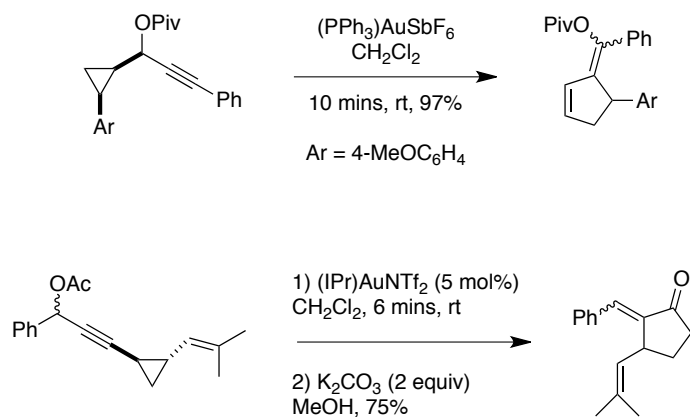


Scheme 2.16 Proposed Mechanistic Pathway for the Formation of Cyclopentenones **20** and **21**.

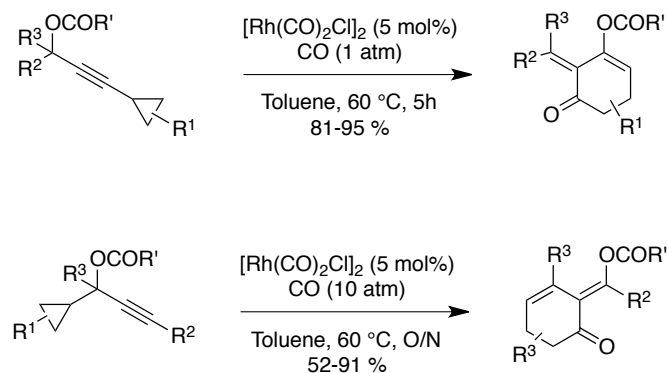
2.4.3. Au(I) Catalyzed Reactions of Cyclopropyl Substituted Enynyl Acetates

The ability of gold(I) species to activate alkynes, alkenes and allenes as strong π -acids is largely attributed to its relativistic effects.³³ However, gold catalysts have also proven to be extremely powerful in triggering ring expansions of strained ring-systems, introducing structural complexity in a very fast and step-economical fashion.³⁴ Works of Toste¹¹ and Nevado³⁵ have demonstrated that cyclopropyl substituted propargylic esters may readily undergo an initial [3,3]-rearrangement of the ester followed by a cyclopropyl ring enlargement to provide substituted cyclopentenones (Scheme 2.17). A key factor influencing the successful evolution of these transformations is the presence of an electron-donating substituent on the cyclopropyl ring being able to stabilize the positive charge developed during the concomitant ring-opening step. On the other hand,

Tang and co-workers have developed a highly efficient Rh(I) catalyzed transformation of cyclopropyl substituted propargylic esters entailing a [3,3]-rearrangement, cyclopropyl ring expansion followed by carbonylation to give substituted cyclohexenones in an atmosphere of CO (Scheme 2.18).³⁶ Both substituted and unsubstituted cyclopropyl moieties underwent facile ring expansions under these conditions.

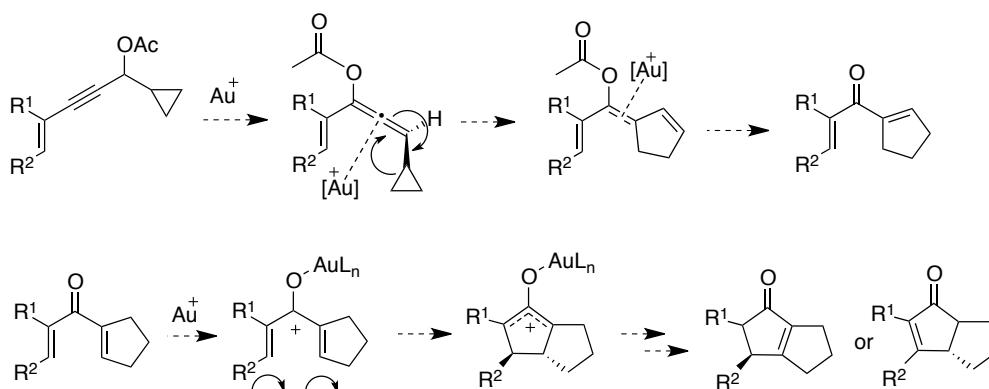


Scheme 2.17 Au(I)-Catalyzed Cyclopropyl Ring Opening to Form Substituted Cyclopentenes.



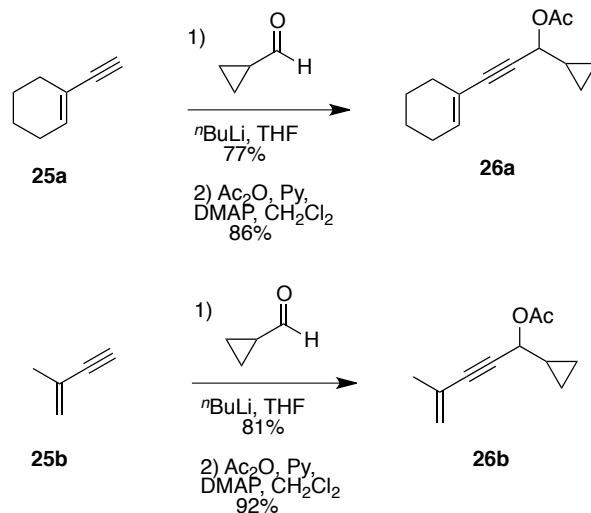
Scheme 2.18 Rh(I)-Catalyzed Domino Cycloisomerization/Carbonylation of Cyclopropyl Propargylic Esters.

We envisioned that placing an alkenyl unit aptly on the other alkynyl terminus of the cyclopropyl substituted propargyl ester could trigger a domino sequence of events as elaborated in Scheme 2.19. We anticipated an usual Saucy-Marbet rearrangement on the Au(I) activated alkyne, followed by cyclopropyl ring expansion to generate a cyclopentenyl acetate species. Bond reorganization may then lead to a pentadienyl cationic intermediate that can potentially undergo a conrotatory 4π -electrocyclic ring closure to form bicyclic products.



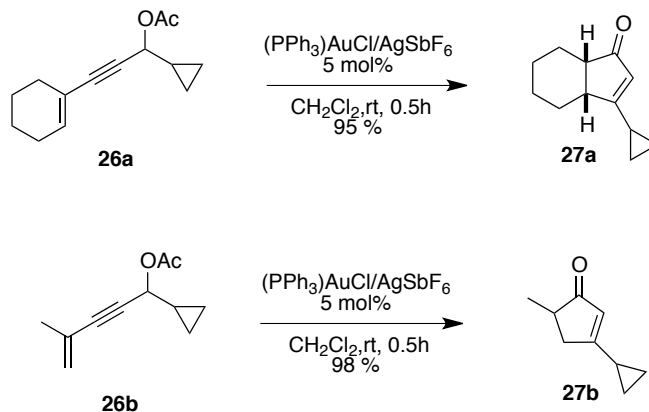
Scheme 2.19 A Proposed Reaction Pathway for Domino Cyclization of Cyclopropyl Enynyl Ester.

The required substrates were synthesized to test our proposed cyclization methodology (Scheme 2.20). *n*-BuLi was added to a solution of the commercially available enyne substrates **25a** and **25b** at -78 °C and stirred at this temperature for 15 min, after which the cyclopropyl carbaldehyde was added neat and the reaction mixture was again stirred for another 15 min. The 2-cyclopropyl substituted enynol was then acetylated under the standard conditions using acetic anhydride as the acetylating agent to obtain the desired 2-cyclopropyl substituted enynyl acetates **26a-b**.



Scheme 2.20 Synthesis of Cyclopropyl Enynyl Acetates.

With cyclopropyl substituted enynyl acetates **26a** and **26b** in hand we sought to explore our cyclization strategy using $(\text{PPh}_3)\text{AuCl}/\text{AgSbF}_6$ as the catalytic system. In the event, we found that only cyclopentenones **27a-b** (Scheme 2.21) were formed with the cyclopropyl moiety being intact. The cyclopropyl substituent behaved as a mere spectator in this cyclization cascade.³⁷ No cyclopropyl ring-opened product was observed and the cyclopentenones were obtained in excellent yields. Lack of an electron-donating group on the cyclopropyl unit could be one reason for its inertness toward ring expansion under the present reaction conditions.



Scheme 2.21 Au(I)-Catalyzed Domino Cyclization of Cyclopropyl Substituted Propargyl Acetates.

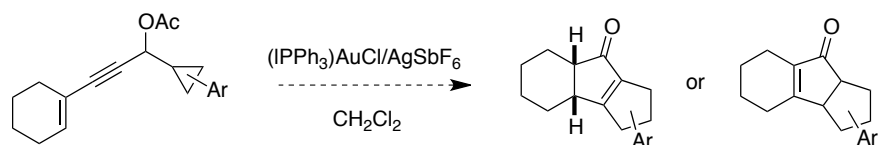
2.5 Conclusion

We have demonstrated a very facile step-economical method of forming highly functionalized fused cyclopentenones in a domino Au(I) catalyzed pathway. The reaction proceeds under mild conditions providing products with good to excellent yields in a very rapid fashion. This methodology provides a shorter route to the bridged bicyclic cyclopentenones, which are important synthetic intermediates. Bridged bicyclic cyclopentenone with the tetra-substituted olefin of type **20c** is a key intermediate to our synthetic route to the taxane skeleton. The present methodology provides an easy direct access to the more substituted bridged bicyclic cyclopentenones with the olefin being installed at the ring fusion carbons. Installation of the tetra-substituted olefin has been proved to be extremely difficult by standard procedures in presence of dense functionality on the cyclopentenone system. In case of camphor-derived cyclopentanones various oxidative reagents like Pd(OAc)₂, IBX, DDQ failed to install the olefin at the ring fusion position. This lack of reactivity is attributed to the high steric congestion at the bottom face (or α -face) of these substrates.

In absence of a substituent at the C-5 position, the thermodynamically favored olefin isomer formation is observed during the cyclization, whereas presence of a substituent altered the result in favor of the other olefin isomer. Finally, introducing a cyclopropyl substituent at one terminus did not influence the course of events.

2.6 Future Plans

Investigation with cyclopropyl substituted enynyl acetates under Au(I) catalyzed conditions only furnished us normal cyclopentenone products. No cyclopropyl ring opened products were obtained. Absence of a suitable substituent on the cyclopropyl ring could be a reason for the lack of reactivity. An electron-donating group on the cyclopropyl unit is known to stabilize the cation once formed after the ring-opening event. Future investigation in this area may focus on the appropriate substitution on the cyclopropyl moiety to trigger the ring expansion in sequence with the [3,3]-rearrangement (Scheme 2.22).



Scheme 2.22 Enynyl Acetates with Substituted Cyclopropyl Unit.

A thorough scan of various Au(I) catalysts and other transition metals may also be exercised. Several new gold catalysts have been developed in the recent past which may be explored to see if the domino cyclization of the bridged bicyclic enynyl acetates can be achieved with an even lower catalyst loading. Scope of the C-5 substituent for the bridged bicyclic enynyl acetates needs to be investigated in further detail to find out if more substituted cyclopentenone regioisomers can be delivered in the presence of a C-5 substituent through a [1,5]-

hydride shift pathway. This might also allow us to delve into the mechanistic course of the reaction in detail and understand the factors affecting the penultimate [1,2] or [1,5]-hydride shifts.

2.7 Experimental

2.7.1. General Information

Reactions were carried out in flame-dried glassware under a positive argon atmosphere unless otherwise stated. Transfer of anhydrous solvents and reagents was accomplished with oven-dried syringes. Solvents were distilled before use: methylene chloride and 1,2-dichloroethane from calcium hydride, tetrahydrofuran from sodium/benzophenone ketyl. All other solvents and commercially available reagents were either purified by standard procedures or used without further purification. Thin layer chromatography was performed on glass plates precoated with 0.25 mm silica gel; the stains for TLC analysis were conducted with 2.5 % *p*-anisaldehyde in AcOH-H₂SO₄-EtOH (1:3:85) and further heating until development of color. Flash chromatography was performed on 230-400 mesh silica gel with the indicated eluents.

Proton nuclear magnetic resonance spectra (¹H NMR) were recorded at 300, 400 MHz or 500 MHz and the chemical shifts are reported on the δ scale (ppm) and the spectra are referenced to residual solvent peaks: CDCl₃ (7.26 ppm, ¹H; 77.06 ppm, ¹³C) as internal standard. Coupling constants (*J*) are reported in Hz. Second order splitting patterns are indicated. Splitting patterns are designated as s, singlet; d, doublet; t, triplet; q, quartet; m, multiplet; br, broad; dd, doublet of doublets, dt, doublet of triplets, etc. Carbon nuclear magnetic resonance spectra (¹³C NMR) were recorded at 100 MHz or 125 MHz and chemical shifts are accurate to one decimal place. Infrared (IR) spectra were measured with a Nicolet Magna 750 FT-IR spectrometer and Nic-Plan FT-IR microscope. Mass spectra

were determined on a Kratos Analytical MS-50 (EI) or Agilent 6220 oaTOF electrospray positive ion mode spectrometer (ESI).

All reagents and catalysts were purchased from Aldrich or Sigma or Strem and were used without further purification unless otherwise stated.

2.7.2. Synthesis and Characterization of Compounds

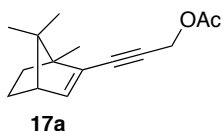
Standard Procedure for the Synthesis of Enynyl Acetates 17(a-c) by Sonogoshira Coupling between Vinyl Triflates 15 and Propargyl alcohol:

Pd(PPh₃)₂Cl₂ (0.11 mmol, 0.05 equiv) and copper iodide (0.22 mmol, 0.1 equiv) were dissolved in a 1:1 solution of THF:DEA (diethylamine) (9.7 mL each) in a flame-dried round bottomed flask. The solution was degassed with argon for 10 min. The appropriate vinyl triflate **15** (2.26 mmol) was dissolved in THF (2 mL) and the solution was degassed for an additional 10 min before it was added to the reaction mixture via a syringe. Propargyl alcohol (2.48 mmol, 1.1 equiv) was added via syringe, and the initial green solution changed from yellow to orange, to red. The THF and DEA were removed under reduced pressure. The residue was purified by silica gel flash chromatography (40% Ethyl Acetate in hexanes) to provide the corresponding enynyl alcohol **16**.

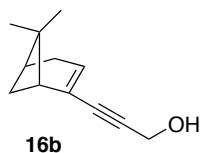
To a solution of the enynol (1.61 mmol), pyridine (8.09 mmol, 1.1 equiv), DMAP (0.08 mmol) in dichloromethane (18 mL) at 0 °C, was slowly added acetic anhydride (3.23 mmol, 2.0 equiv) and the reaction mixture was stirred for 2 h at this temperature. The reaction was first diluted with EtOAc (20 mL). The combined organic solution was then washed with 10% HCl (3 x 20 mL), followed by 1N NaOH (3 x 20 mL) and water (2 x 20 mL). The organic layer was then dried over MgSO₄, filtered and concentrated under reduced pressure. The residue

was purified by silica gel flash chromatography (20% EtOAc in hexanes) to provide the desired enynyl acetate **17**.

Compound **16a** has previously been synthesized and characterized.³¹ Our spectra closely corresponded to the reported data.

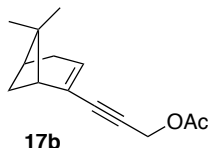


Following the representative procedure, flash chromatography (10% EtOAc in hexanes) gave **17a** as colorless oil, 0.310 g (83% yield): $R_f = 0.82$ (20% EtOAc in hexanes); IR (neat) 3062, 2955, 2871, 2247, 1747, 1366, 1291, 1141 cm^{-1} ; ^1H NMR (500 MHz, CDCl_3) δ 6.27 (d, $J = 3.4$ Hz, 1H), 4.43 (s, 2H), 2.01 (s, 3H), 1.91-1.88 (m, 1H), 1.55 (ddd, $J = 11.9, 9.1, 3.4$ Hz, 1H), 1.07 (m, 2H), 1.05 (s, 3H), 1.00 (ddd, $J = 12.4, 9.1, 3.4$ Hz, 1H), 0.791 (s, 3H), 0.787 (s, 3H); ^{13}C NMR (125 MHz, CDCl_3) δ 171.0, 141.4, 131.7, 91.1, 82.2, 60.6, 56.7, 55.8, 52.3, 31.3, 25.0, 19.8, 19.6, 16.4, 12.0; HRMS (EI, M^+) Calcd for $\text{C}_{15}\text{H}_{20}\text{O}_2$ m/z 232.1463; found m/z 232.1459.

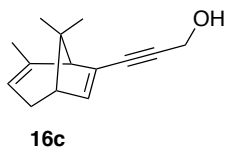


Following the representative procedure, flash chromatography (40% EtOAc in hexanes) gave **16b** as colorless oil, 0.370 g (93% yield): $R_f = 0.52$ (20% EtOAc in hexanes); IR (film) 3329, 2987, 2891, 2245, 1412, 1391, 1298 cm^{-1} ; ^1H NMR (500 MHz, CDCl_3) δ 5.96 (q, $J = 1.9$ Hz, 1H), 4.37 (d, $J = 5.5$ Hz, 2H), 2.40-2.21 (m, 4H), 2.09 (br s, 1H), 1.52-1.48 (m, 1H), 1.26 (s, 3H), 1.21 (d, $J = 9.3$ Hz, 1H), 0.06 (s, 3H); ^{13}C NMR (125 MHz, CDCl_3) δ 130.8, 128.7, 91.0, 86.2, 51.1, 46.8,

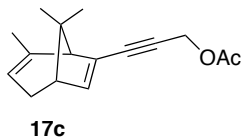
39.9, 31.4, 30.7, 28.4, 25.4, 20.6; HRMS (EI, M⁺) Calcd for C₁₂H₁₆O m/z 176.1201; found m/z 176.1196.



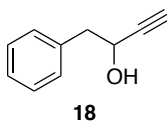
Following the representative procedure, flash chromatography (10% EtOAc in hexanes) gave **17b** as colorless oil, 0.294 g (84% yield): $R_f = 0.83$ (20% EtOAc in hexanes); IR (film) 3009, 2958, 2877, 2245, 1742, 1391, 1298 cm⁻¹; ¹H NMR (500 MHz, CDCl₃) δ 6.07-6.05 (m, 1H), 4.84 (s, 2H), 2.45-2.42 (m, 1H), 2.38-2.35 (m, 1H), 2.31-2.28 (m, 1H), 2.18 (br s, 4H), 1.59 (s, 1H), 1.32 (s, 3H), 1.26 (d, $J = 9.1$ Hz, 1H), 0.91 (s, 3H); ¹³C NMR (125 MHz, CDCl₃) δ 170.4, 132.5, 128.9, 87.2, 82.5, 53.1, 46.8, 40.2, 37.8, 32.1, 31.4, 26.0, 21.0, 20.9; HRMS (EI, M⁺) Calcd for C₁₄H₁₈O₂ m/z 218.1307; found m/z 218.1296.



Following the representative procedure, flash chromatography (40% EtOAc in hexanes) gave **16c** as colorless oil, 0.279 g (86% yield): $R_f = 0.55$ (20% EtOAc in hexanes); IR (film) 3340, 2968, 2934, 2886, 2247, 1384, 1286 cm⁻¹; ¹H NMR (500 MHz, CDCl₃) δ 5.93 (d, $J = 2.9$ Hz, 1H), 5.03-5.02 (m, 1H), 4.46 (d, $J = 5.1$ Hz, 2H), 2.27 (app dpentet, $J = 19.0, 2.5$ Hz, 1H), 2.14-2.12 (m, 2H), 1.81-1.77 (m, 3H), 1.63-1.61 (m, 2H), 1.09 (s, 3H), 1.08 (s, 3H); ¹³C NMR (125 MHz, CDCl₃) δ 140.3, 137.6, 133.5, 116.9, 90.5, 83.4, 59.0, 52.4, 48.0, 44.5, 27.3, 24.4, 20.9, 14.4; HRMS (EI, M⁺) Calcd for C₁₄H₁₈O m/z 202.1358; found m/z 202.1347.

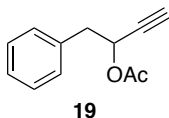


Following the representative procedure, flash chromatography (10% EtOAc in hexanes) gave **17c** as colorless oil, 0.318 g (81% yield): $R_f = 0.76$ (20% EtOAc in hexanes); IR (film) 3105, 2987, 2933, 2816, 2245, 1744, 1286 cm^{-1} ; ^1H NMR (500 MHz, CDCl_3) δ 5.96 (d, $J = 2.9$ Hz, 1H), 5.02-5.00 (m, 1H), 4.86 (s, 2H), 2.24 (app dpentet, $J = 19.0, 2.5$ Hz, 1H), 2.13-2.12 (m, 5H), 1.79-1.76 (m, 4H), 1.58-1.57 (m, 1H), 1.08 (s, 6H); ^{13}C NMR (125 MHz, CDCl_3) δ 170.3, 140.0, 138.1, 132.9, 116.6, 85.8, 83.8, 58.6, 53.0, 47.7, 44.3, 27.0, 26.5, 20.9, 24.0, 20.8; HRMS (EI, M^+) Calcd for $\text{C}_{16}\text{H}_{20}\text{O}_2$ m/z 244.1463; found m/z 244.1447.



In a flame-dried round-bottomed flask trimethylsilyl acetylene (6.0 mmol, 1.5 equiv) was dissolved in THF (8 mL) and stirred at -78 $^\circ\text{C}$ under an inert atmosphere of argon. *n*-BuLi (3.23 mL, 5.3 equiv) was added dropwise to this stirring solution at -78 $^\circ\text{C}$. The reaction mixture was allowed to stir at the same temperature for 15 min. Phenylacetaldehyde (4.0 mmol) was added to the solution and stirred for another 2 h. The reaction mixture was quenched with saturated aqueous solution of NH_4Cl (8 mL) and extracted with Et_2O (2 x 10 mL). The organic layer was collected and the combined organics were washed with brine (2 x 10 mL), dried (MgSO_4) and concentrated under reduced pressure. The crude alcohol (4.0 mmol) was dissolved in MeOH (8 mL) and anhydrous K_2CO_3 (0.80 mmol) was added to the solution at room temperature. The reaction mixture was allowed to stir at room temperature overnight before quenching with saturated aqueous solution of NH_4Cl (8 mL). The solution was extracted with Et_2O (2 x 10 mL) and the organic layer was collected after the separation of two layers. The

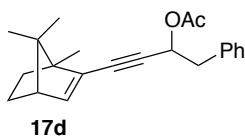
combined organics were washed with H₂O (2 x 10 mL) and brine (2 x 10 mL), dried (MgSO₄) and concentrated under reduced pressure. The crude residue was purified by flash column chromatography (15% EtOAc in hexanes) and gave **18** as a yellow oil, 0.46 g, 75% yield. Compound **18** has been previously characterized and our spectra corresponded closely to the reported data.³⁸



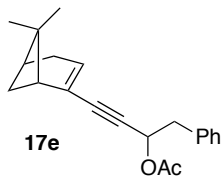
Alcohol **16** (0.402 g, 2.77 mmol) was dissolved in CH₂Cl₂ (20 mL) in a round-bottomed flask. Pyridine (13.9 mmol, 5 equiv), DMAP (0.13 mmol, 0.05 equiv) and Ac₂O (5.54 mmol, 2.0 equiv) were added in a sequence to the solution at room temperature and allowed to stir for 2 h. The reaction mixture was diluted with EtOAc (20 mL) and extracted with 10% HCl (3 x 20 mL) and NaOH (3 x 20 mL). The organic layer was collected and the combined organics were washed with H₂O (2 x 20 mL), dried (MgSO₄) and concentrated under reduced pressure. The crude residue was purified by flash column chromatography (15% EtOAc in hexanes) and gave **19**, 0.419 g (81% yield): R_f = 0.62 (20% EtOAc in hexanes); IR (film) 3287, 2973, 2836, 1740, 1373, 1235 cm⁻¹; ¹H NMR (500 MHz, CDCl₃) δ 7.32-7.27 (m, 5H), 5.53 (dt, *J* = 6.8, 2.2 Hz, 1H), 3.11 (m, 2H), 2.45 (d, *J* = 2.2 Hz, 1H), 2.06 (s, 3H); ¹³C NMR (125 MHz, CDCl₃) δ 170.1, 135.6, 129.4, 128.7, 127.2, 80.7, 74.5, 64.4, 41.3, 21.2. Compound **19** has previously been characterized and our spectra corresponded closely to the literature report.³⁹

Standard Procedure B for the Synthesis of Enynyl Acetates 17(d-f) by Sonogoshira Coupling between Vinyl Triflates 15 and Propargyl Acetate 19:

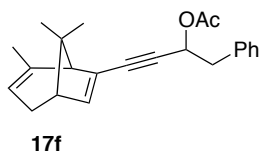
Pd(PPh₃)₂Cl₂ (0.037 mmol, 0.05 equiv) and copper iodide (0.074 mmol, 0.1 equiv) were dissolved in a 1:1 solution of THF:DEA (diethylamine) (4.0 mL each) in a flame-dried round bottomed flask. The solution was degassed with argon for 10 min. The appropriate vinyl triflate **15** (0.740 mmol) was dissolved in THF (0.5 mL) and the solution was degassed for an additional 10 min before adding to the reaction mixture via a syringe. Propargyl acetate **19** (0.814 mmol, 1.1 equiv) was added via syringe, and the initial green solution changed from yellow, to orange to red. The THF and DEA were removed under reduced pressure. The residue was purified by silica gel flash chromatography (20% Ethyl Acetate in hexanes) to provide the corresponding enynyl acetate **17**.



The reaction was carried out at room temperature following the standard procedure B. Flash column chromatography (20% EtOAc in hexanes) gave **17d** as colorless oil, 0.207 g (87% yield): $R_f = 0.72$ (20% EtOAc in hexanes); IR (neat) 2989, 2978, 2937, 2249, 1744, 1634, 1578, 1431, 1389 cm^{-1} ; ¹H NMR (500 MHz, CDCl₃) δ 7.32-7.27 (m, 5H), 6.33 (d, $J = 3.3$ Hz, 1H), 5.80-5.76 (m, 1H), 3.17-3.09 (m, 2H), 2.37 (t, $J = 3.4$ Hz, 1H), 2.08 (s, 3H), 1.93-1.87 (m, 1H), 1.60-1.52 (m, 1H), 1.08-1.01 (m, 1H), 0.99 (s, 3H), 0.93-0.89 (m, 1H), 0.81 (s, 3H), 0.80 (s, 3H); ¹³C NMR (125 MHz, CDCl₃) δ 169.9, 141.1, 136.3, 131.2 (2 x sp²-C), 129.8 (2 x sp²-C), 128.4, 127.0, 89.8, 82.8, 65.6, 56.6, 55.8, 52.2, 41.6, 41.4, 31.1, 24.8, 21.2, 19.7, 11.9; HRMS (EI, M⁺) Calcd for C₂₂H₂₆O₂ m/z 322.1933; found m/z 322.1927.



The reaction was carried out at room temperature following the standard procedure B. Flash column chromatography (20% EtOAc in hexanes) gave **17e** as colorless oil, 0.182 g (80% yield): $R_f = 0.77$ (20% EtOAc in hexanes); IR (film) 3081, 2956, 2933, 2791, 2245, 1745, 1620, 1593, 1487, 1371 cm^{-1} ; ^1H NMR (500 MHz, CDCl_3) δ 7.34-7.27 (m, 5H), 6.01-5.98 (m, 1H), 5.73 (tq, $J = 6.7, 2.4$ Hz, 1H), 3.14-3.06 (m, 2H), 2.44-2.40 (m, 1H), 2.37 (t, $J = 3.1$ Hz, 1H), 2.34 (t, $J = 3.1$ Hz, 1H), 2.25-2.21 (m, 1H), 2.14-2.10 (m, 1H), 2.07 (s, 3H), 1.32 (d, $J = 2.2$ Hz, 3H), 1.24 (dd, $J = 9.0, 1.7$ Hz, 1H), 0.9 (d, $J = 1.8$ Hz, 3H); ^{13}C NMR (125 MHz, CDCl_3) δ 169.2, 135.5, 131.3, 129.2 (2 x $\text{sp}^2\text{-C}$), 128.9, 127.6 (2 x $\text{sp}^2\text{-C}$), 126.6, 86.3, 85.0, 64.7, 46.2, 40.8, 39.6, 37.3, 31.4, 30.7, 25.4, 20.5, 20.4; HRMS (EI, M^+) Calcd for $\text{C}_{21}\text{H}_{24}\text{O}_2$ m/z 308.1776; found m/z 308.1768.

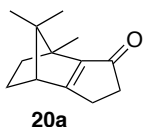


The reaction was carried out at room temperature following the standard procedure B. Flash column chromatography (20% EtOAc in hexanes) gave **17f** as colorless oil, 0.200 g (81% yield): $R_f = 0.79$ (20% EtOAc in hexanes); IR (film) 2962, 2856, 2247, 1746, 1648, 1542, 1498, 1416, 1387 cm^{-1} ; ^1H NMR (500 MHz, CDCl_3) δ 7.34-7.27 (m, 5H), 5.92 (t, $J = 3.3$ Hz, 1H), 5.77 (tq, $J = 6.7, 2.5$ Hz, 1H), 4.99 (br s, 1H), 3.13-3.12 (d, $J = 3.1$ Hz, 2H), 2.29-2.23 (m, 1H), 2.12 (t, $J = 3.1$ Hz, 1H), 2.08 (d, $J = 2.5$ Hz, 3H), 1.80-1.71 (m, 4H), 1.31-1.28 (m, 1H), 1.08 (s, 3H), 1.07 (s, 3H); ^{13}C NMR (125 MHz, CDCl_3) δ 169.7.2, 139.9, 137.6, 135.8, 133.0, 129.7 (2 x $\text{sp}^2\text{-C}$), 128.3 (2 x $\text{sp}^2\text{-C}$), 126.9, 116.5, 88.9, 83.5, 65.2, 58.6,

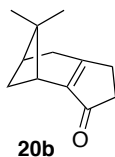
47.7, 44.2, 41.3, 27.0, 26.5, 24.0, 21.0, 20.7; HRMS (EI, M⁺) Calcd for C₂₃H₂₆O₂ m/z 334.1933, found m/z 334.1929.

Standard Procedure for the Synthesis of Cyclopentenones **20a-c** and **21d-f**:

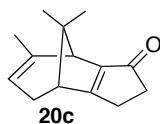
To a solution of the bridged bicyclic enynyl acetate **17** (1.31 mmol) in dichloromethane (25.8 mL, 0.05 M) in a flame-dried round bottomed flask was added AuClPPh₃/AgSbF₆ [pre-generated as 0.01 M solution in dichloromethane by mixing AuCl(PPh₃) (0.13 mmol, 10 mol%) with AgSbF₆ (0.13 mmol, 10 mol%), 13 mL] at room temperature and the reaction mixture was stirred for 2h. The progress of the reaction was monitored through TLC. The mixture was treated with one drop of triethylamine and concentrated under reduced pressure. The residue was purified by silica gel flash chromatography (20% EtOAc in hexanes) to give the corresponding cyclopentenones **20** or **21** as yellow oil.



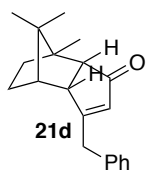
The reaction was carried out at room temperature following the standard procedure. Flash column chromatography (20% EtOAc in hexanes) gave **20a** as yellow oil, 0.191 g (77% yield): R_f = 0.42 (20% EtOAc in hexanes); IR (film) 2956, 2872, 1739, 1701, 1607, 1373 cm⁻¹; ¹H NMR (500 MHz, CDCl₃) δ 2.72-2.66 (m, 1H), 2.63-2.61 (m, 1H), 2.57-2.49 (m, 3H), 2.09-2.04 (m, 1H), 1.78-1.74 (m, 1H), 1.57 (s, 3H), 1.23-1.18 (m, 1H), 1.07-1.00 (m, 1H), 0.88 (s, 3H), 0.83 (s, 3H); ¹³C NMR (125 Hz, CDCl₃) δ 203.5, 189.6, 132.0, 60.4, 53.1, 51.2, 39.3, 32.1, 24.3, 23.9, 19.2, 18.3, 9.9; HRMS (EI, M⁺) Calcd for C₁₃H₁₈O m/z 190.1357; found m/z 190.1357.



The reaction was carried out at room temperature following the standard procedure. Flash column chromatography (20% EtOAc in hexanes) gave **20b** as a yellow oil, 0.199 g (86% yield): $R_f = 0.37$ (20% EtOAc in hexanes); IR (neat) 2973, 2886, 1692, 1632, 1467, 1443, 1389 cm^{-1} ; ^1H NMR (500 MHz, CDCl_3) δ 2.61 (t, $J = 5.6$ Hz, 1H), 2.54-2.44 (m, 7H), 2.18 (sept, $J = 2.9$ Hz, 1H), 1.31 (s, 3H), 1.06 (d, $J = 9.25$ Hz, 1H), 0.67 (s, 3H); ^{13}C NMR (125 Hz, CDCl_3) δ 206.2, 172.8, 149.5, 40.7, 39.8, 37.3, 36.2, 34.0, 32.4, 28.3, 25.8, 21.2; HRMS (APC, $[\text{M}+\text{H}]^+$) Calcd for $\text{C}_{12}\text{H}_{17}\text{O}$ m/z 177.1274; found m/z 177.1273.



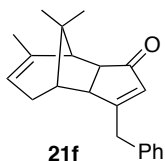
The reaction was carried out at room temperature following the standard procedure. Flash column chromatography (20% EtOAc in hexanes) gave **20c** as a yellow oil, 0.193 g (73% yield): $R_f = 0.24$ (20% EtOAc in hexanes); IR (film) 2989, 2873, 1709, 1645, 1435, 1380 cm^{-1} ; ^1H NMR (500 MHz, CDCl_3) δ 4.99 (m, 1H), 2.75-2.69 (m, 1H), 2.63-2.62 (m, 1H), 2.59-2.55 (m, 2H), 2.35 (m, 2H), 2.33-2.31 (m, 1H), 1.90-1.85 (m, 1H), 1.78-1.77 (m, 3H), 1.16 (s, 3H), 1.07 (s, 3H); ^{13}C NMR (125 MHz, CDCl_3) δ 202.6, 185.5, 156.7, 140.3, 116.5, 49.3, 49.1, 48.4, 39.9, 27.2, 25.3, 23.6, 2.1; HRMS (EI, M^+) Calcd for $\text{C}_{14}\text{H}_{18}\text{O}$ m/z 202.1357; found m/z 202.1357.



The reaction was carried out at room temperature following the standard procedure. Flash column chromatography (20% EtOAc in hexanes) gave **21d** as a yellow oil, 0.286 g (78% yield): $R_f = 0.54$ (20% EtOAc in hexanes); IR (film) 2954, 2885, 1699, 1610, 1453, 1390 cm^{-1} ; ^1H NMR (500 MHz, CDCl_3) δ 7.36-7.22 (m, 5H), 5.72 (dq, $J = 10.2, 1.7$ Hz, 1H), 4.16 (q, $J = 6.5$ Hz, 2H), 2.7 (d, $J = 7.1$ Hz, 1H), 2.54 (dd, $J = 8.5, 2.5$ Hz, 1H), 2.23-2.11 (m, 1H), 2.02-1.96 (m, 1H), 1.71-1.58 (m, 1H), 1.45-1.39 (m, 1H), 1.35-1.27 (m, 1H), 1.16-1.11 (m, 1H), 1.07 (s, 3H), 0.95 (s, 3H), 0.82 (s, 3H); ^{13}C NMR (125 Hz, CDCl_3) δ 182.1, 137.2, 133.3, 132.1, 129.2, 128.9, 127.0, 60.3, 58.2, 54.8, 50.4, 46.8, 39.4, 31.0, 22.8, 20.1, 18.7, 15.5; HRMS (EI, M^+) Calcd for $\text{C}_{20}\text{H}_{24}\text{O}$ m/z 280.1827; found m/z 280.1821.



The reaction was carried out at room temperature following the standard procedure. Flash column chromatography (20% EtOAc in hexanes) gave **21e** as yellow oil, 0.282 g (81% yield): $R_f = 0.55$ (20% EtOAc in hexanes); IR (film) 2993, 2905, 2867, 1703, 1613, 1480, 1437, 1367 cm^{-1} ; ^1H NMR (500 MHz, CDCl_3) δ 7.38-7.22 (m, 5H), 5.92 (s, 1H), 3.17-3.00 (m, 2H), 2.83 (dd, $J = 6.4, 3.0$ Hz, 1H), 2.37 (dd, $J = 9.5, 5.9$ Hz, 1H), 2.21-2.17 (m, 1H), 2.16-2.15 (m, 1H), 2.10-2.08 (m, 2H), 2.02-1.99 (m, 1H), 1.75 (m, 1H), 1.28 (s, 3H), 0.99 (s, 3H); ^{13}C NMR (125 MHz, CDCl_3) δ 212.2, 187.1, 137.6, 132.1, 129.6, 127.7, 51.1, 43.6, 39.2, 38.4, 38.2, 28.6, 27.7, 26.5, 26.2, 21.2; HRMS (EI, M^+) Calcd for $\text{C}_{19}\text{H}_{22}\text{O}$ m/z 266.1670; found m/z 266.1663.

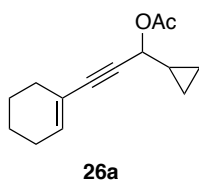


The reaction was carried out at room temperature following the standard procedure. Flash column chromatography (40% EtOAc in hexanes) gave **21f** as yellow oil, 0.241 g (63% yield): $R_f = 0.41$ (20% EtOAc in hexanes); IR (film) 2993, 2897, 2876, 1690, 1613, 1593, 1478, 1431, 1298 cm^{-1} ; ^1H NMR (500 MHz, CDCl_3) δ 7.46–7.27 (m, 5H), 5.72 (app t, $J = 2.0$ Hz, 1H), 5.39 (br s, 1H), 3.13 (dd, $J = 6.9, 3.5$ Hz, 2H), 2.28–2.24 (m, 1H), 2.12–2.11 (m, 1H), 2.08–2.07 (m, 3H), 1.80–1.71 (m, 4H), 1.08–1.07 (m, 6H); ^{13}C NMR (125 Hz, CDCl_3) δ 170.2, 140.4, 138.2, 138.0, 133.4, 130.1, 129.5, 127.3, 117.0, 65.7, 59.0, 48.2, 44.6, 41.8, 27.5, 27.0, 24.4, 21.5, 21.0; HRMS (EI, M^+) Calcd for $\text{C}_{21}\text{H}_{24}\text{O}$ m/z 292.1827; found m/z 292.1823.

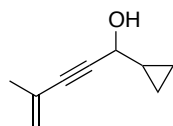
Standard Procedure C for the Synthesis of Enynyl Acetate 26:

To a solution of an enyne **25** (0.24 mL, 2.5 mmol) in THF (5.0 mL) was added *n*-BuLi (1.60 M solution in hexanes, 1.56 mL, 2.5 mmol) at -78 °C and the resulting solution was stirred at the same temperature for 15 min. To this solution was added the cyclopropanaldehyde (0.19 mL, 2.5 mmol) neat via syringe and the reaction was stirred for another 30 min. Aqueous NH_4Cl solution was added to quench the reaction. The resulting mixture was extracted with diethyl ether (3 x 20 mL). The aqueous layer was separated and the combined organic layers were washed with water (2 x 40 mL) and brine (2 x 40 mL) successively, dried over anhydrous MgSO_4 and concentrated under reduced pressure. The residue was then purified through silica gel flash column chromatography (20% EtOAc in hexanes) to yield the corresponding enynyl alcohol.

To a solution of the enynol (1.61 mmol), pyridine (8.09 mmol, 1.1 equiv), DMAP (0.08 mmol) in dichloromethane (18 mL) at 0 °C, was slowly added acetic anhydride (3.23 mmol, 2.0 equiv) and the reaction mixture was stirred for 2h at this temperature. The reaction mixture was first diluted with EtOAc (20 mL). The combined organic solution was then washed with 10% HCl (3 x 20 mL), followed by 1N NaOH (3 x 20 mL) and water (2 x 20 mL). The organic layer was then dried over MgSO₄, filtered and concentrated under reduced pressure. The residue was purified by silica gel flash chromatography (10% EtOAc in hexanes) to provide the desired enynyl acetate **26**.

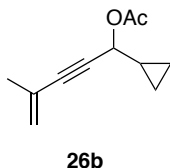


The reaction was carried out at room temperature following the standard procedure C. Flash column chromatography (15% EtOAc in hexanes) gave **26a** as a colorless oil, 0.468 g (86% yield): $R_f = 0.72$ (20% EtOAc in hexanes); IR (film) 3038, 2932, 2874, 2245, 1743, 1416 cm⁻¹; ¹H NMR (500 MHz, CDCl₃) δ 6.09-6.10 (m, 1H), 5.36 (d, $J = 6.7$ Hz, 1H), 2.07-2.01 (m, 7H), 1.63-1.50 (m, 4H), 1.29-1.21 (m, 2H), 0.83-0.89 (m, 1H), 0.41-0.57 (m, 2H); ¹³C NMR (125 Hz, CDCl₃) δ 190.0, 155.9, 139.7, 107.2, 101.5, 87.9, 48.9, 45.5, 42.0, 41.3, 40.9, 34.5, 23.3, 22.0; HRMS (EI, M⁺) Calcd for C₁₄H₁₈O₂ 218.1306; found m/z 218.1300.



Reaction was carried out at room temperature following the standard procedure C. Flash column chromatography (40% EtOAc in hexanes) gave the enynyl alcohol as colorless oil, 0.352 g (81% yield): $R_f = 0.66$ (20% EtOAc in hexanes); IR (film)

3099, 2972, 2872, 2243, 1480, 1370 cm^{-1} ; ^1H NMR (500 MHz, CDCl_3) δ 5.27–5.28 (m, 1H), 5.21 (q, $J = 1.7$ Hz, 1H), 4.31 (t, $J = 5.5$ Hz, 1H), 2.00–2.08 (m, 1H), 1.86 (t, $J = 1.2$ Hz, 3H), 1.21–1.26 (m, 1H), 0.89 (t, $J = 7.2$ Hz, 1H), 0.40–0.56 (m, 3H), ^{13}C NMR (125 Hz, CDCl_3) δ 126.0, 122.2, 86.7, 86.1, 36.8, 27.8, 23.3, 17.1, 3.1, 1.4.

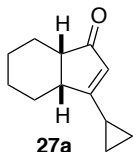


Reaction was carried out at room temperature following the standard procedure C. Flash column chromatography (20% EtOAc in hexanes) gave **26b** as a colorless oil, 0.409 (92% yield): $R_f = 0.62$ (20% EtOAc in hexanes); IR (film) 2986, 2835, 2247, 1748, 1474, 1432 cm^{-1} ; ^1H NMR (500 MHz, CDCl_3) δ 5.34 (d, $J = 6.9$ Hz, 1H), 5.29 (s, 1H), 5.22 (pent, $J = 2.1$ Hz, 1H), 2.07 (s, 3H), 1.84 (t, $J = 1.5$ Hz, 3H), 1.21–1.29 (m, 1H), 0.83–0.87 (m, 1H), 0.41–0.58 (m, 3H); ^{13}C NMR (125 Hz, CDCl_3) δ 170.4, 126.2, 123.1, 86.8, 83.6, 68.1, 23.4, 21.4, 14.7, 3.7, 2.5; HRMS (EI, M^+) Calcd for $\text{C}_{11}\text{H}_{14}\text{O}_2$ 178.0993; found m/z 178.0991.

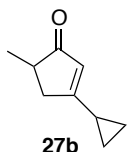
Standard Procedure for the Synthesis of Cyclopentenones **27a** and **27b**:

To a solution of the bridged bicyclic enynyl acetate **26** (1.31 mmol) in dichloromethane (25.8 ml, 0.05 M) in a flame-dried round bottomed flask was added $\text{AuClPPh}_3/\text{AgSbF}_6$ [pre-generated as 0.01 M solution in dichloromethane by mixing $\text{AuCl}(\text{PPh}_3)$ (0.065 mmol, 5 mol%) with AgSbF_6 (0.065 mmol, 5 mol%), 6.5 mL] at room temperature and the reaction mixture was stirred for 0.5 h. The progress of the reaction was monitored through TLC. The mixture was treated with one drop of triethylamine and concentrated under reduced pressure.

The residue was purified by silica gel flash chromatography (20% EtOAc in hexanes) to give the corresponding cyclopentenone **27** as colorless oil.



Reaction was carried out at room temperature following the standard procedure. Flash column chromatography (50% EtOAc in hexanes) gave **27a** as a colorless oil, 0.219 g (95% yield): $R_f = 0.36$ (20% EtOAc in hexanes); IR (film) 2966, 2878, 1617, 1567, 1454, 1377 cm^{-1} ; ^1H NMR (500 MHz, CDCl_3) δ 5.51 (s, 1H), 2.84 (ddd, $J = 9.0, 7.0, 7.0$ Hz, 1H), 2.38 (dd, $J = 6.7, 4.9$ Hz, 1H), 2.05-1.99 (m, 1H), 1.90-1.84 (m, 1H), 1.61-1.45 (m, 4H), 1.31-1.22 (m, 1H), 1.19-0.97 (m, 4H), 0.75-0.65 (m, 2H); ^{13}C NMR (125 Hz, CDCl_3) δ 210.3, 189.4, 121.3, 46.6, 43.7, 28.5, 22.3, 21.6, 21.2, 12.6, 11.7, 10.9; HRMS (EI, M^+) Calcd for $\text{C}_{12}\text{H}_{16}\text{O}$ m/z 176.1201; found m/z 176.1195.



Reaction was carried out at room temperature following the standard procedure. Flash column chromatography (50% EtOAc in hexanes) gave **27b** as a colorless oil, 0.178 g (98% yield): $R_f = 0.22$ (20% EtOAc in hexanes); IR (film) 2978, 2893, 1612, 1477, 1277 cm^{-1} ; ^1H NMR (500 MHz, CDCl_3) δ 5.85 (app t, $J = 1.7$ Hz, 1H), 2.65 (ddd, $J = 18.4, 6.7, 1.6$ Hz, 1H), 2.36 (qd, $J = 7.4, 2.5$ Hz, 1H), 2.0 (app dt, $J = 18.0, 1.9$ Hz, 1H), 1.83-1.78 (m, 1H), 1.13 (d, $J = 7.5$ Hz, 3H), 1.04-1.00 (m, 2H), 0.83-0.81 (m, 2H); ^{13}C NMR (125 Hz, CDCl_3)

δ 211.7, 183.4, 125.8, 40.2, 37.1, 16.5, 14.8, 9.8, 9.7; HRMS (EI, M^+) Calcd for $C_9H_{12}O$ m/z 136.0888; found m/z 136.0879.

2.7 Reference

- (1) (a) Bhunia, S.; Liu, R.-S. *Pure Appl. Chem.* **2012**, *84*, 1749-1757. (b) Fürstner, A.; Davies, P. W. *Angew. Chem. Int. Ed.* **2007**, *46*, 3410-3449.
- (2) (a) Hashmi, A. S. *Angew. Chem.* **2010**, *49*, 5232. (b) Shapiro, N. D.; Toste, F. D. *Synlett* **2010**, 675.
- (3) (a) Fürstner, A. *Chem. Soc. Rev.* **2009**, *38*, 3208. (b) Jiménez-Núñez, E.; Echavarren, A. M. *Chem. Rev.* **2008**, *108*, 3326. (c) Jiménez-Núñez, E.; Echavarren, A. M. *Chem. Commun.* **2007**, 333.
- (4) (a) Li, Z.; Brouwer, C.; He, C. *Chem. Rev.* **2008**, *108*, 3239. (b) Hashmi, A. S. K.; Rudolph, M. *Chem. Soc. Rev.* **2008**, *37*, 1766.
- (5) Salvi, N.; Belpassi, L.; Tarantelli, F. *Chem. Eur. J.* **2010**, *16*, 7231.
- (6) (a) Seidel, G.; Mynott, R.; Fürstner, A. *Angew. Chem. Int. Ed.* **2009**, *48*, 2510. (b) Hashmi, A. S. *Angew. Chem.* **2008**, *47*, 6754.
- (7) (a) Wang, S.; Zhang, G.; Zhang, L. *Synlett* **2010**, 692. (b) Correa, A.; Marion, N.; Fensterbank, L.; Malacria, M.; Nolan, S. P.; Cavallo, L. *Angew. Chem.* **2008**, *47*, 718.
- (8) (a) Marco-Contelles, J.; Soriano, E. *Chem. Eur. J.* **2007**, *13*, 1350. (b) Marion, N.; Nolan, S. P. *Angew. Chem.* **2007**, *46*, 2750.
- (9) (a) Saucy, G.; Marbet, R. *Helv. Chim. Acta* **1967**, *50*, 1158. (b) Saucy, G.; Chopard-Dit-Jean, L. H.; Guex, W.; Ryser, G.; Isler, O. *Helv. Chim. Acta* **1958**, *41*, 160.
- (10) Marion, N.; Lemièrre, G.; Correa, A.; Costabile, C.; Ramón, R. S.; Moreau, X.; de Frémont, P.; Dahmane, R.; Hours, A.; Lesage, D.; Tabet, J.-C.; Goddard, J.-P.; Gandon, V.; Cavallo, L.; Fensterbank, L.; Malacria, M.; Nolan, S. P. *Chem. Eur. J.* **2009**, *15*, 3243.
- (11) Mauleón, P.; Krinsky, J. L.; Toste, F. D. *J. Am. Chem. Soc.* **2009**, *131*, 4513.

- (12) (a) Yu, M.; Zhang, G.; Zhang, L. *Tetrahedron* **2009**, *65*, 1846. (b) Yu, M.; Zhang, G.; Zhang, L. *Org. Lett.* **2007**, *9*, 2147.
- (13) Miki, K.; Ohe, K.; Uemura, S. *J. Org. Chem.* **2003**, *68*, 8505.
- (14) Zhang, L. *J. Am. Chem. Soc.* **2005**, *127*, 16804.
- (15) Marion, N.; Díez-González, S.; de Frémont, P.; Noble, A. R.; Nolan, S. P. *Angew. Chem. Int. Ed.* **2006**, *45*, 3647.
- (16) Buzas, A.; Gagosz, F. *J. Am. Chem. Soc.* **2006**, *128*, 12614.
- (17) Zhang, L.; Wang, S. *J. Am. Chem. Soc.* **2006**, *128*, 1442.
- (18) (a) Woodward, R. B. *Spec. Publ.-Chem. Soc.* **1967**, *21*, 217. (b) Woodward, R. B.; Hoffmann, R. in *The Conservation of Orbital Symmetry*. Verlag Chemie, Weinheim, **1971**, p38-109.
- (19) (a) Stephen, A.; Hashmi, K.; Bats, J. W.; Choi, J.-H.; Schwarz, L. *Tetrahedron Lett.* **1998**, *39*, 7491. (b) Forest, J.; Bee, C.; Cordaro, F.; Tius, M. A. *Org. Lett.* **2003**, *5*, 4069. (c) Tius, M. A. *Acc. Chem. Res.* **2003**, *36*, 284.
- (20) (a) Grant, T. N.; West, F. G. *J. Am. Chem. Soc.* **2006**, *128*, 9348. (b) Grant, T. N.; West, F. G. *Org. Lett.* **2007**, *9*, 3789.
- (21) (a) Rieder, C. J.; Winberg, K. J.; West, F. G. *J. Am. Chem. Soc.* **2009**, *131*, 7504. (b) Kang, D.; Kim, J.; Oh, S.; Lee, P. H. *Org. Lett.* **2012**, *14*, 5636.
- (22) (a) Batson, W. A.; Sethumadhavan, D.; Tius, M. A. *Org. Lett.* **2005**, *7*, 2771. (b) Uhrich, E. A.; Batson, W. A.; Tius, M. A. *Synthesis* **2006**, 2139.
- (23) (a) Lin, G.-Y.; Yang, C.-Y.; Liu, R.-S. *J. Org. Chem.* **2007**, *72*, 6753. (b) Abu Sohel, S. M.; Lin, S.-H.; Liu, R.-S. *Synlett* **2008**, 745.
- (24) Zhang, L.; Wang, S.; Zhang, G. *Synlett* **2010**, 692.
- (25) (a) Lemièrre, G.; Gandon, V.; Cariou, K.; Fukuyama, T.; Dhimane, A.-L.; Fensterbank, L.; Malacria, M. *Org. Lett.* **2007**, *9*, 2207. (b) Lemièrre, G.; Gandon, V.; Cariou, K.; Hours, A.; Fukuyama, T.; Dhimane, A.-L.; Fensterbank, L.; Malacria, M. *J. Am. Chem. Soc.* **2009**, *131*, 2993.
- (26) Bhunia, S.; Liu, R.-S. *J. Am. Chem. Soc.* **2008**, *130*, 16488.
- (27) Bonderoff, S. A. *Unconventional Substrates for the Nazarov and Imino-Nazarov Reactions*, Ph.D. Thesis, University of Alberta, 2012.

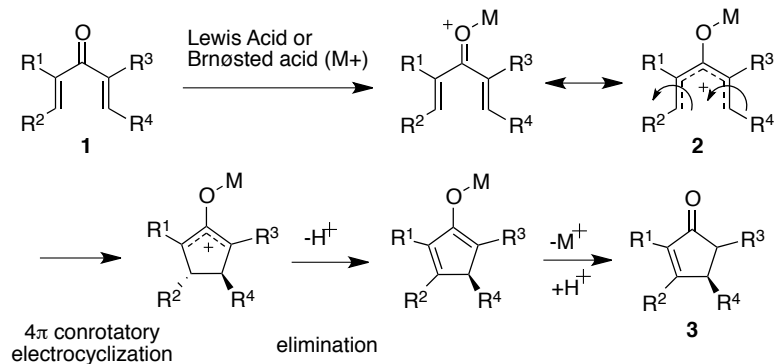
- (28) Wu, Y.-K.; West, F. G. *J. Org. Chem.* **2010**, *75*, 5410.
- (29) (a) Mazzola, R. D.; White, T. D.; Vollmer-Snarr, H. R.; West, F. G. *Org. Lett.* **2005**, *7*, 2799. (b) Giese, S.; Mazzola, R. D.; Amann, C. M.; Arif, A. M.; West, F. G. *Angew. Chem. Int. Ed.* **2005**, *44*, 6546.
- (30) Mazzola, R. D.; Giese, S. Jr.; Benson, C. L.; West, F. G. *J. Org. Chem.* **2003**, *69*, 220.
- (31) Tessier, P. E.; Nguyen, N.; Clay, M. D.; Fallis, A. G. *Org. Lett.* **2005**, *7*, 767.
- (32) (a) Nelson G. Rondan, M. N. P.-R., Pierluigi Caramella, and K. N. Houk *J. Am. Chem. Soc.* **1981**, *103*, 2436. (b) Nelson G. Rondan, M. N. P.-R., Pierluigi Caramella,lb Jiri Mareda, Paul H. Mueller, and K. N. Houk *J. Am. Chem. Soc.* **1982**, *104*, 4974.
- (33) (a) Gorin, D. J.; Toste, F. D. *Nature* **2007**, *446*, 395. (b) Lacour, J.; Linder, D. *Science* **2007**, *317*, 462.
- (34) Lu, B. L.; Dai, L.; Shi, M. *Chem. Soc. Rev.* **2012**, *41*, 3318.
- (35) Garayalde, D.; Gómez-Bengoa, E.; Huang, X.; Goeke, A.; Nevado, C. *J. Am. Chem. Soc.* **2010**, *132*, 4720.
- (36) (a) Shu, D.; Li, X.; Zhang, M.; Robichaux, P. J.; Guzei, I. A.; Tang, W. *J. Org. Chem.* **2012**, *77*, 6463. (b) Li, X.; Zhang, M.; Shu, D.; Robichaux, P. J.; Huang, S.; Tang, W. *Angew. Chem.* **2011**, *50*, 10421.
- (37) Wang, S.; Zhang, L. *J. Am. Chem. Soc.* **2006**, *128*, 8414.
- (38) Burgess, K.; Donk, W. A.; Jarstfer, M. B.; Ohlmeyer, M. J. *J. Am. Chem. Soc.* **1991**, *113*, 6139.
- (39) Detz, R. J.; Abiri, Z.; Griel, R. le; Hiemstra, H.; Maarseveen, J. H. van. *Chem. Eur. J.* **2011**, *17*, 5921.

Chapter 3

Additive Effects in Silicon-Directed Nazarov Cyclization

3.1 Silicon-Directed Nazarov Cyclization

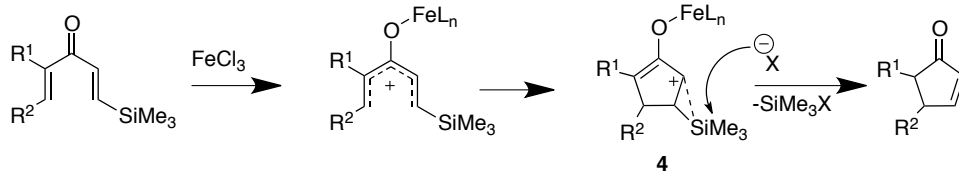
The Nazarov cyclization has emerged as an excellent method for the construction of cyclopentanoid ring systems in natural product synthesis due to the simplicity of the reactants employed and also because of the mildness of the conditions.¹ In its conventional form, the reaction begins with the activation of a cross-conjugated dienone **1** forming a pentadienyl cation **2** (Scheme 3.1).² This cation is a conjugated 4π system capable of undergoing a conrotatory electrocyclic ring closure,³ closing the ring in a stereospecific conrotatory fashion.⁴ This pericyclic process results in a 2-hydroxycyclopentenyl cation, which then undergoes proton elimination and enol tautomerization to form a cyclopentenone **3**.



Scheme 3.1 Nazarov Cyclization of a Divinyl Ketone.

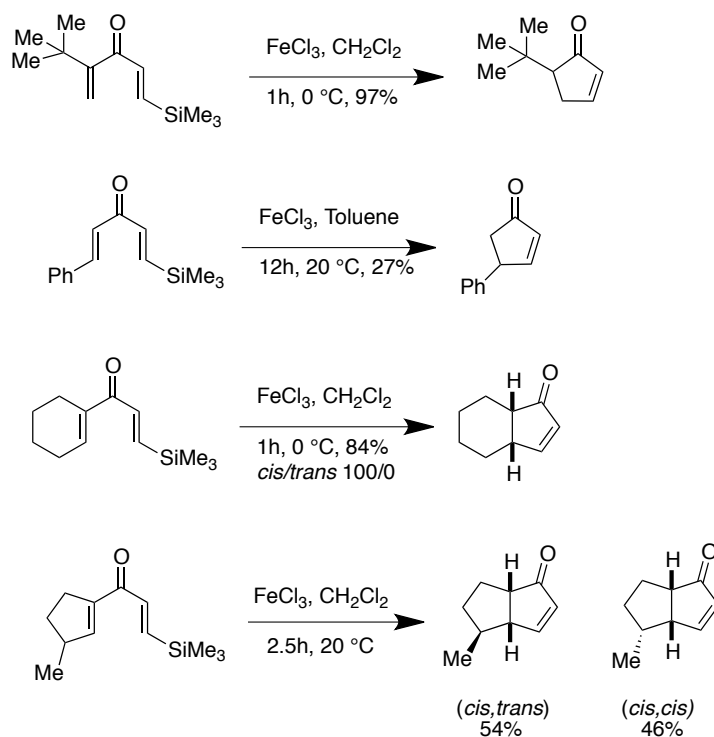
However, the major factor impeding the widespread utilization of the method lies in the penultimate mechanistic step, the elimination, which is often unselective and leads to mixtures of olefin isomers. Denmark and Jones cleverly addressed this problem through the development of the silicon-directed Nazarov cyclization (Scheme 3.2).⁵

Denmark and Jones designed β -silyl substituted divinyl ketones to investigate the ability of silicon to stabilize the oxallyl cationic intermediate **4** formed through electrocyclic cyclization and to control its fate during the elimination step thereafter (Scheme 3.2). The silyl group is expected to localize the cationic charge at the terminus of the allyl cation through a β -cation stabilizing effect and thereby direct a regioselective elimination. At the penultimate step, the silyl group acts as an electrofuge where it leaves intermediate **4** after being captured by a counter-ion of the catalyst or water during the work-up. The C-Si bonding electron pair is then donated to form the olefin of the final cyclopentenone product. The two major benefits of this process are: 1) suppression of undesirable cationic rearrangements, and 2) control of the double bond regiochemistry leading to exclusive formation of one enone isomer, even in cases where this isomer is thermodynamically disfavored.⁶



Scheme 3.2 Silicon-Directed Nazarov Cyclization.

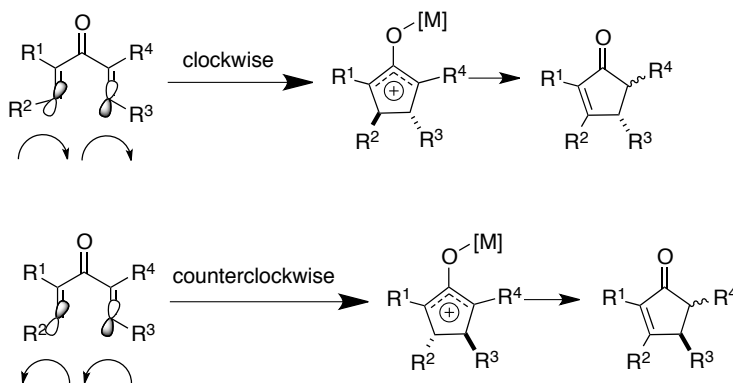
The pioneering work of Denmark and coworkers expanded from the study of silicon-directed Nazarov cyclization of simple acyclic and cyclic dienones to the investigation of the effects of remote stereocenters on the torquoselectivity of the Nazarov cyclization (Scheme 3.3).^{5b,7} Their initial investigation revealed that a cation-stabilizing substituent at the α -position led to rapid cyclization whereas those at the β -position were found to undergo sluggish reaction. In general, the rate of silicon-directed Nazarov cyclization was slower than the undirected one.^{5b}



Scheme 3.3 Effect of Substitution on the Silicon-Directed Nazarov Cyclization.

3.2 Diastereoselective Silicon-Directed Nazarov Cyclizations

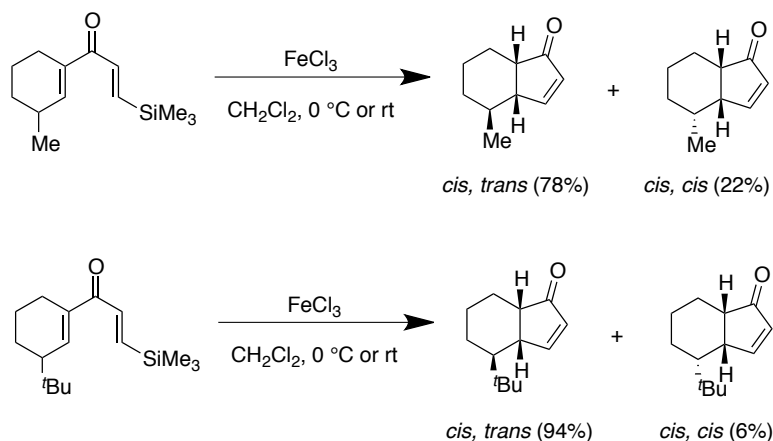
The Nazarov reaction is a pericyclic process involving the concomitant creation of up to two new adjacent stereocenters by a predictable, stereospecific process under the control of orbital symmetry considerations.⁴ However, in the absence of any external or internal stereochemical bias, the electrocyclicization proceeds with equal amounts of clockwise and counterclockwise conrotation, resulting in a racemic mixture (Scheme 3.4). Recently, efforts have been directed at controlling the absolute configuration of the products by imparting a specific direction of conrotation through the introduction of internal or external asymmetric induction (torquoselectivity).⁸ Encasing a portion of the dienone within a ring containing one or more pre-existing stereocenters is one way of controlling the absolute sense of conrotation. In general, the steric bulk exhibited by the substituent(s) on the stereogenic center and its distance from the developing stereogenic centers are the two major factors determining the level of torquoselectivity.⁹



Scheme 3.4 Torquoselectivity in Nazarov Cyclization.

3.2.1. Torquoselectivity Induced through Tetrahedral Chirality

In 1986, the Denmark group first demonstrated the influence of remote stereocenters on the stereochemical outcome of the 4π -electrocyclization process in the context of silicon-directed Nazarov cyclization. The degree of stereocontrol was reported to be modest, with the substituent on the cyclohexane ring *cis* to the ring-fusion protons in the major diastereomer (Scheme 3.5).^{7c} The mechanistic rationale most consistent with the stereochemical outcome of this pericyclic process invokes an early transition state for the cyclization in which the direction of conrotation is controlled by the sterically more favorable approach of the vinyl silane to the less hindered face of the cyclohexenyl unit. The preferred sense of conrotation leads to a better orbital overlap. This was the first report of a diastereoselective Nazarov cyclization.

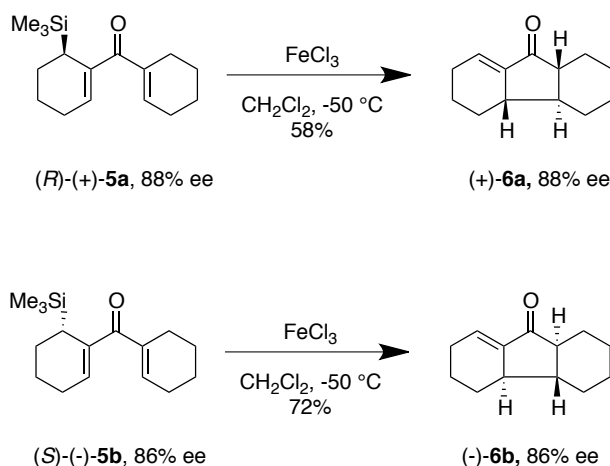


Scheme 3.5 Diastereoselective Nazarov Cyclization: Steric Effect on Torquoselectivity.

3.2.2. Silicon as a Traceless Auxiliary

Work of Denmark and coworkers established that β' -silicon stereocenters can affect the stereochemical outcome of the electrocyclization as traceless chiral

auxiliaries and also lead to a dramatic rate acceleration. Either of the enantiomers of dienone **5** (**a** and **b**) when treated with FeCl_3 , underwent cyclization to form cyclopentenones **6** (**a**, **b**) with retention of enantiomeric purity from the starting dienones (Scheme 3.6).¹⁰ The preferred sense of conrotation in each case was ascribed to the beneficial continuous orbital overlap of the C-Si σ -bond with the developing allyl cation that is permitted through only one direction of conrotation. Again, the double bond regiochemistry was exclusively controlled by the departure of the silyl electrofuge. The original silyl-bearing stereogenic center was lost, but its stereochemical information was transferred to the three newly formed stereocenters.

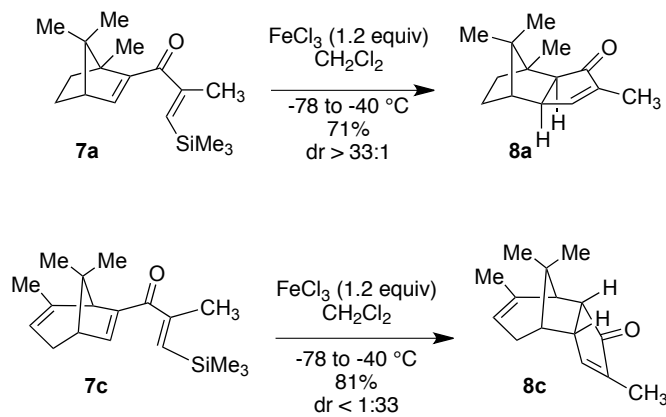


Scheme 3.6 Stereoelectronic Control of Torquoselectivity through an Allylsilane Moiety.

3.2.3. Diastereoselective Nazarov Cyclization of Strained Bridged Bicycles

West and co-workers examined the silicon-directed Nazarov reaction of bridged bicyclic dienones.^{11,12} The observed *exo* selectivity in the formation of cyclopentenone **8a** from the camphor-derived divinyl ketone **7a** is consistent with the known preferences for electrophilic attack of related norbornene-type

derivatives from the *exo* face (Scheme 3.7).¹³ However, an unexpected reversal of torquoselectivity to afford the *endo* product **8c** was observed in the cyclization of the bicyclo[3.2.1]octadienone **7c**. The authors attributed this high diastereofacial selectivity to the stereochemical effect of a remote olefin on the conformational preferences within the six-membered ring of the bicyclic system.¹¹ This was a novel approach to stereocontrol in Nazarov cyclization using the innate facial preferences of strained bridged bicyclic systems.



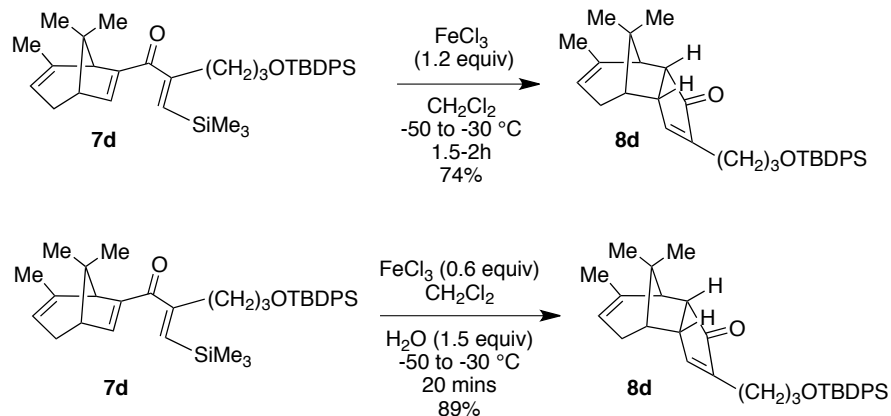
Scheme 3.7 Diastereoselective Nazarov Cyclization of Bridged Bicyclic Dienones.

3.3 Additive Effect in Silicon-Directed Nazarov Cyclization

Our interest in the diastereoselective Nazarov cyclization of bridged bicyclic dienones¹¹ derives from their relevance to an approach to the taxane skeleton.¹⁴ Typically, these cyclizations have employed stoichiometric quantities of Lewis or Brønsted acids and also suffered from reduced yields and undesired product formation when carried out on larger scales. Since its discovery in 1941,^{15,16} the Nazarov cyclization has been keenly investigated and significant advances have been made to expand the scope of this transformation. Although many catalytic conditions have been reported,¹⁷ use of stoichiometric amount of

Lewis or Brønsted acid promoters still remains very common and generally the most effective way to trigger the cyclization.^{1b}

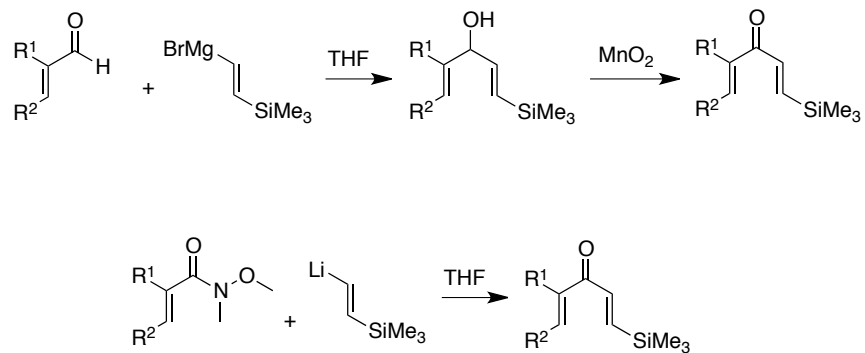
When **7d**, a key intermediate in our approach to a taxane natural product,¹⁸ was subjected to the standard silicon-directed Nazarov conditions, exclusive formation of the *endo* isomer **8d** was observed (Scheme 3.8).¹¹ Unfortunately, low yields accompanied by oligomeric byproduct formation were observed on a larger scale, obviating its application as an early step in the multistep synthesis of a complex natural product. During these early investigations we observed that “aged” FeCl₃ from an old bottle afforded superior yields and a cleaner reaction than a freshly opened, anhydrous reagent. Denmark *et al.* had previously reported that similar reactions failed to work under scrupulously anhydrous conditions with 99.99% FeCl₃ and required addition of water.¹⁰ These observations pointed to the crucial role that moisture might be playing in the success of the cyclization and termination events. This guided us to study the effect of deliberate addition of 1.5 equivalents of water to the solution of bicyclic dienone **7d** prior to the addition of a Lewis acid. As expected, the reaction was found to occur cleanly at a noticeably faster rate providing an even better yield of the desired product **8d** (Scheme 3.8). Only 0.6 equivalents of the Lewis acid (FeCl₃) was enough to promote the cyclization under the present conditions.



Scheme 3.8 Effect of Water as an Additive on the Diastereoselective Nazarov Cyclization of Bicyclo[3.2.1]octadienone.

3.3.1. Synthesis of the Divinyl Ketone Precursors

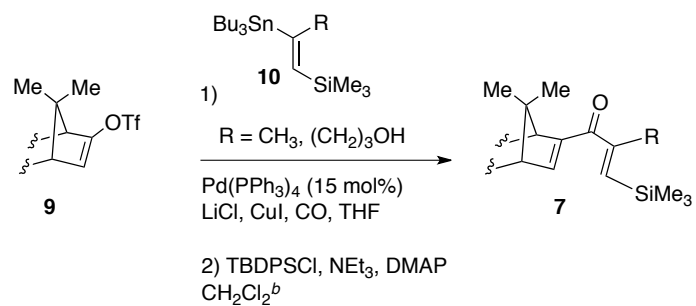
At this point we were interested to investigate the applicability of the present conditions to some of the previously attempted dienone substrates, which have either proved to be completely unreactive or low yielding under classical silicon-directed Nazarov conditions.^{5,19} The simpler divinyl ketones **7e-7l** were mostly synthesized following Denmark's reported procedure, where the vinyl Grignard reagent prepared from the corresponding (2-bromovinyl)trimethylsilane was added to the enal followed by oxidation with MnO_2 (Scheme 3.9).⁵ However, in cases where the appropriate acid chloride or carboxylic acid was commercially available the dienones were prepared through vinyl lithium addition to the corresponding Weinreb amides.²⁰



Scheme 3.9 Preparation of β -Silyl Divinyl Ketones.

The more complex bridged bicyclic dienone precursors **7a-7d** were synthesized by direct Stille cross-coupling approach involving the enol triflates **9a-9b** and alkenyl stannanes **10a-10b** under carbonylative conditions, using CuI as co-catalyst (Table 3.1).²¹

Table 3.1 Preparation of the Bridged Bicyclic Divinyl Ketones.^a



Entry	Enol triflate (9)	Product (7)	Time	Yield (%) ^c
1.			2 days	81% ^a
2.			2.5 days	82% ^{a,b}
3.			3 days	77% ^a
4.			3.5 days	63% ^{a,b}

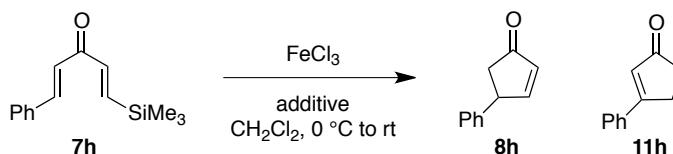
Table 3.1 Continued

^aStandard procedure: A mixture of LiCl (180 mmol) and Pd(PPh₃)₄ (2.1 mmol) in THF (200 mL) was stirred under argon for 15 min. Freshly purified CuI (16 mmol) was added in one solid portion and the dark red solution was saturated with CO (1 atm) for 45 min. A solution of the stannane **10** (54.7 mmol) and enol triflate **9** (45.4 mmol) in THF (100 mL) was added via cannula followed by additional THF (150 mL). The resulting mixture was saturated with CO (1 atm) for an additional 1.5 hours. The reaction mixture was heated to 65 °C and kept under a static pressure of CO until no more enol triflate could be detected by TLC (48 h). The reaction mixture was cooled and the reaction was quenched by the addition of H₂O (200 mL) and diluted with Et₂O (200 mL), followed by extraction, drying (MgSO₄) and concentration under reduced pressure. The residue was purified by silica gel flash chromatography (40% EtOAc in hexanes) to provide the corresponding dienones **7a**, **7c**. ^bTo a solution of the dienones (16.1 mmol) in CH₂Cl₂ (30 mL) was added NEt₃ (22.0 mmol), DMAP (0.92 mmol), and TBDPSCl (19.0 mmol) in this order at room temperature. The resulting mixture was stirred at room temperature before quenching with H₂O (30 mL). The solution was extracted with CH₂Cl₂ (100 mL), dried (MgSO₄) and concentrated under reduced pressure. The crude residue was then purified by flash column chromatography to afford the TBDPS ether protected dienones **7b**, **7d**. ^cIsolated yields based on enol triflates **9**.

3.3.2. Optimization of the Reaction Conditions

Initially, the silicon-directed Nazarov reaction was carried on substrates **7e-7h** (See Table 3.3, page 100) using 1.5 equivalents of water as additive. The reactions proceeded smoothly with the formation of the desired cyclopentenones **8e-8h** in shorter reaction times with better product yields than as reported in the absence of additive. However, the lightly substituted cyclopentenones **8e-8g** suffered from high volatility, which accounted for their relatively low isolated yields. Encouraged by our initial findings, two other hydroxylic additives were examined using the simple β-phenyl substituted dienone substrate **7h**. The choice of the β-phenyl substituted dienone precursor was guided by the low volatility of the corresponding cyclopentenone product, which made product isolation and handling much easier. MeOH was found to be the most promising additive with respect to reaction time and overall yields, affording isomeric cyclopentenones **8h** and **11h** in a combined yield of 79% (Table 3.2, entry 4).

Table 3.2 Effect of Additive and FeCl₃ Stoichiometry.^a



Entry	Additive	FeCl ₃	Time (h)	Yield (%) ^b
1.	-	0.6	18	13% (8h)
2.	H ₂ O	0.6	14.5	67 (1.5:1) ^c
3.	CF ₃ CH ₂ OH	0.6	12-14	62 (1.3:1) ^c
4.	CH ₃ OH	0.6	8	79 (2.0:1) ^c
5.	CH ₃ OH	0.3	17.5	71 (2.5:1) ^c
6.	CH ₃ OH	0.1	84	74 (2.3:1) ^c

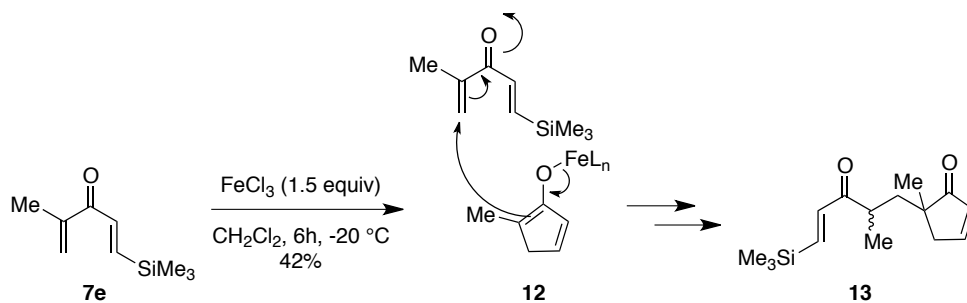
^aStandard Procedure: FeCl₃ was added to a solution of dienone **1e** in CH₂Cl₂ (0.1 M in CH₂Cl₂) at 0 °C. The reaction was stirred at room temperature until completion. After the indicated time, the reaction was quenched with satd. aq. solution of NaHCO₃, followed by extraction, drying (MgSO₄), filtration and chromatographic purification. ^bAll yields given are for isolated product after chromatographic purification. ^cRatios of **8h:11h** were determined after individual product isolation through flash column chromatography.

We also briefly examined Lewis acid stoichiometry under the optimal conditions (Table 3.2, entries 4-6). In the event, 60 mol% catalyst loading was found to be optimal to achieve acceptable yields in reasonable reaction times. The cyclization could be achieved even with 10 mol% catalyst loading; however, the reaction rate was inconveniently slow for use in a multi-step total synthesis.^{5b,7a}

3.3.3. Effect of Additive on the Cyclization of Acyclic Divinyl Ketones

The optimized conditions using 60 mol% of FeCl₃ in the presence of MeOH as additive were applied to test some lightly substituted divinyl ketones **7e-7l**. Dienone **7e**, under classical Nazarov conditions was reported to form **13** as the only observable product (Scheme 3.10).^{5b} This is proposed to be formed by the

Michael addition of the late-stage dienolate intermediate **12** to the unreacted divinyl ketone **7e**. This formation of the Michael adduct could not be prevented even by dilution of the reaction mixture. When the simple α -methyl substituted dienone **7e** was subjected to our modified conditions, it gave the desired 5-methyl-2-cyclopentenone **8e** cleanly (Table 3.3, entry 1). Neither of dimer **13**, nor any other undesired side-product, was isolated. α -Ethyl substituted dienone **7f** (entry 2) also gave the desired 5-ethyl-2-cyclopentenone **8f** without any observable dimer formation. These results may imply that the dienolate formed after Nazarov cyclization is consumed at a faster rate under the present conditions, thereby eliminating the chances of other competitive bimolecular side reactions from occurring.

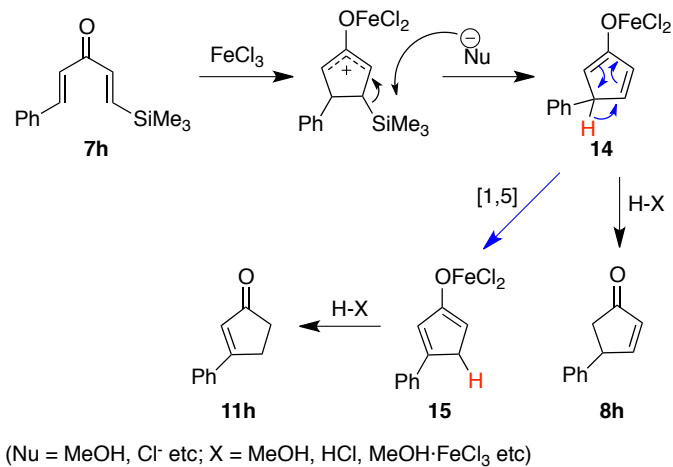


Scheme 3.10 Consumption of the Reactive Dienolate Through Michael Addition Pathway.

There is a general observation that the presence of a β -substituent on the divinyl ketone slows down the cyclization rate. It has been postulated by Denmark in his ingenious study of substituent effects on 4π -electrocyclization that cation-stabilizing β -substituents lower the energy of the pentadienyl cation **2**, leading to a higher activation barrier for the cyclization.^{5b} We examined some of the β -silyl-dienones bearing only a β -substituent on the other olefin (entries 3, 4 and 6). Cyclization of β -methyl substituted dienone **7g** (entry 3) proceeded cleanly to provide the expected product **8g**; however, as noted previously (Table 3.2), β -phenyl substituted dienone **7h** furnished isomeric products **8h** and **11h** under the

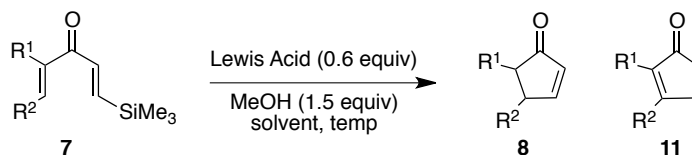
modified conditions (entry 4). The formation of **11h** was quite intriguing since it afforded the olefin at the more substituted position, yet the process accompanied removal of the β -silyl substituent. Competing deprotonation at the benzylic position following electrocyclization, as opposed to desilylation, would provide the observed cyclopentenone regiochemistry, but in that case the product should retain the silyl group. On the other hand, standard desilylation pathway should afford **8h**. A possible explanation for the formation of **11h** is shown below (Scheme 3.11). Assuming preferential removal of the trimethylsilyl electrofuge following the Nazarov cyclization, dienolate **14** should be formed. Protonation of the dienolate would furnish the “normal” desilylative Nazarov product **8h**. However, rearrangement of **14** to the fully conjugated dienolate **15** would provide **11h** upon protonation. This rearrangement could proceed via a [1,5]-hydride shift, as depicted.

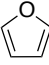
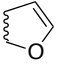
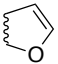

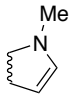
Notably, Nazarov cyclization of **7h** can also be achieved using sub-stoichiometric amounts of $\text{Sc}(\text{OTf})_3$ in the presence of MeOH (entry 5), at higher temperatures (1,2-dichloroethane at reflux). In this case, cyclopentenone **11h** was the sole product, albeit in moderate yield, a result that may be attributed to the preferential consumption of **14** via the [1,5]-hydride shift pathway to give **11h** at the elevated reaction temperature. It should also be noted that when pure **8h** was subjected to the standard reaction conditions for an extended time period, no conversion to the other olefin regioisomer **11h** was observed. This observation rules out the possibility of an isomerization of cyclopentenone **8h** to its more substituted regioisomer **11h** under the reaction conditions. Cyclopentenone **11h** must have formed from the dienone **7h** through a mechanism that does not proceed via **8h**. Dienone **7i** (entry 6) also reacted smoothly under similar conditions to provide **11i** as the only isolable product. Here the “normal” desilylative Nazarov product was not observed at all, which could again be attributed to the more vigorous reaction conditions.



Scheme 3.11 Mechanistic Rationale for the Formation of the Unusual Product **11h**.

Table 3.3 Silicon-Directed Nazarov Cyclization of Simple Acyclic and Cyclic Divinyl Ketones with MeOH as Additive.^a

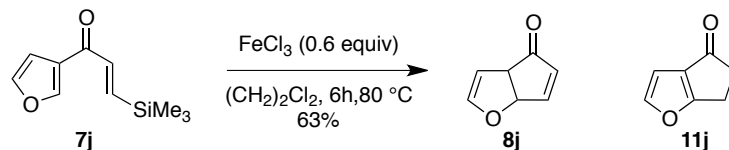


Entry	S.M. (7)	Lewis acid	R ¹	R ²	Solvent	Temp (°C)	Time (h)	Product (8/11)	Yield (%)
1.	7e	FeCl ₃	Me	H	DCM	0	5.5	8e	77 ^b
2.	7f	FeCl ₃	Et	H	DCM	0	6	8f	63 ^b
3.	7g	FeCl ₃	H	Me	DCM	0	16	8g	72 ^b
4.	7h	FeCl ₃	H	Ph	DCM	0	8	8h+11h ^c	79 ^d
5.	7h	Sc(OTf) ₃	H	Ph	DCE	80	12	11h	33 ^{d,e}
6.	7i	FeCl ₃	H		DCE	80	10	11i	60 ^{d,e}
7.	7j	FeCl ₃			DCE	80	10	11j	53 ^{d,e}
8.	7j	Sc(OTf) ₃			DCE	80	16	11j	63 ^{d,e}
9.	7k	FeCl ₃			DCE	80	14	11k	46 ^{d,f}
10.	7l	FeCl ₃		Me	DCE	80	8	11l	63 ^{d,e}

^aStandard Procedure: FeCl₃ or Sc(OTf)₃ (0.6 equiv) was added to a solution of dienone **7** in CH₂Cl₂ (0.1 M in CH₂Cl₂; as in entry 1-4) or (CH₂)₂Cl₂ (0.1 M or 0.05 M; as in entry 5-10) at -30 °C. The reaction was stirred at the indicated temperature until completion. After the indicated time, the reaction was quenched with sat. aq NaHCO₃, followed by extraction, drying (MgSO₄), filtration and chromatographic purification. ^bNMR yields as determined by ¹H NMR spectroscopic analysis of the product relative to an internal standard (PhOCH₃) because of high volatility of the products formed. ^cRatio of **8h:11h** = 2:1. ^dYields are given for isolated products after chromatographic purification. ^eReaction was performed in 0.1 M (CH₂)₂Cl₂ at 80 °C. ^fReaction was performed in 0.05 M (CH₂)₂Cl₂ at 80 °C.

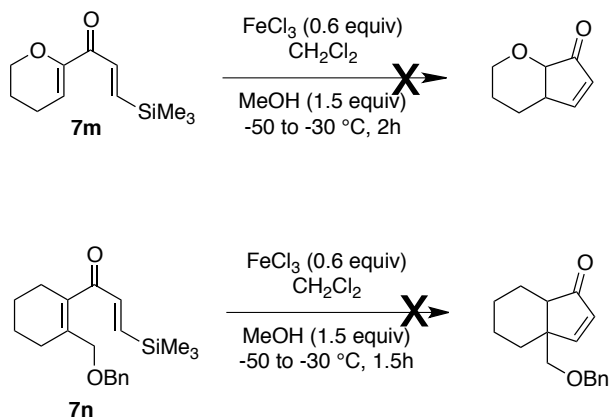
After the initial success with the acyclic divinyl ketones we attempted to apply the same methodology to the more difficult heterocyclic substrates. Enoylfurans (substituted at either the 2- or 3-furyl position) are known to be

typically unreactive under Nazarov cyclization conditions.²² Recently, the Frontier group has demonstrated that 2-substituted furanyl and benzofuranyl enones may cyclize via an alternative Friedel-Crafts alkylation-type pathway instead of the presumed 4π electrocyclization in the presence of Lewis acid.²³ Initially, both the 2- and 3-substituted furans **7j** and **7k** were found to be unreactive when subjected to the optimized conditions using dichloromethane as solvent.¹⁹ The complete lack of consumption of starting material in these cases prompted an examination of reaction at higher temperature in dichloroethane.^{23,24} In DCE at reflux, the starting material **7j** was consumed after overnight stirring, furnishing a single product in 53% yield (entry 7). The ¹H NMR spectrum of the product showed two proton signals whose chemical shifts and coupling constants confirmed the presence of a furan ring, but lacked alkene proton signals corresponding to the cyclopentenone protons as expected from a silyl-directed Nazarov cyclization product **8j** (Scheme 3.12). The structure of the product was then assigned as isomer **11j**. Formation of **11j** can be rationalized by the [1,5]-hydride shift mechanism as has already been postulated for **11h**, and the process is expected to be more facile in this case due to the driving force for rearomatization. Notably, this reaction has also successfully been performed on a 1.68 g (8 mmol) scale, providing the desired cyclopentenone in similar yield with no byproduct formation. When 2-substituted furan **7k** was subjected to similar reaction conditions in dichloroethane at reflux, slow decomposition of the divinyl ketone was observed; however, we were pleased to find that dilution of the reaction mixture to 0.05 M resulted in clean conversion of the 2-furanyl substrate to a single product **11k** *via* Nazarov cyclization (entry 9). This is one of the very few reports of a 2-substituted furan participating in a Nazarov cyclization, most of the past attempts at cationic cyclization of 2-furanyl vinyl ketones have met with little success.^{19, 24, 25} Divinyl ketone **7l** (entry 10) with the N-methyl pyrrole substituent underwent a more facile cyclization under similar conditions to afford **11l** cleanly as the exclusive regioisomer.



Scheme 3.12 Silicon-Directed Nazarov Cyclization of a Furan-Substituted Divinyl Ketone **7j**.

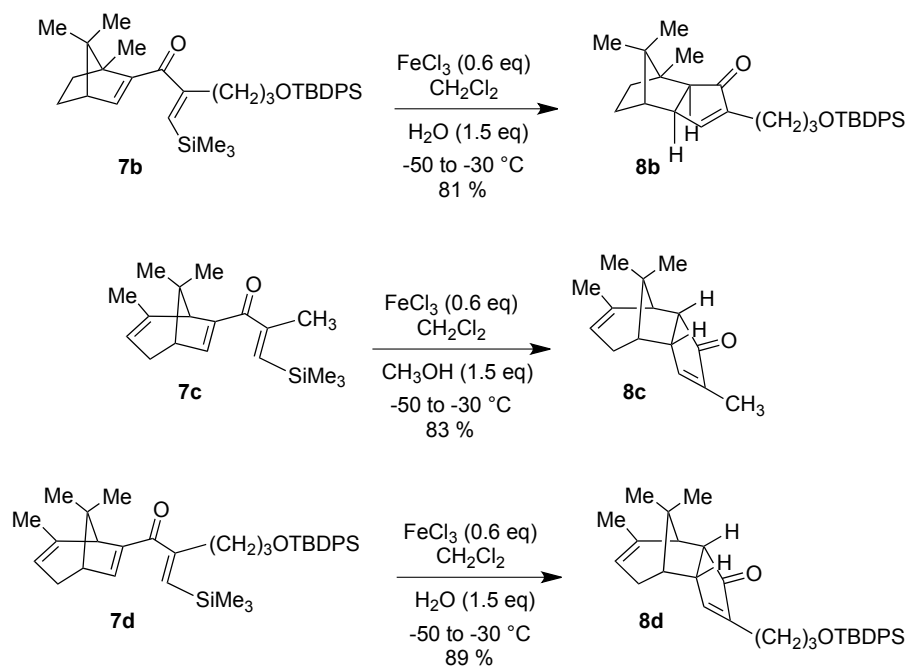
Two other divinyl ketones that were previously found to be unreactive in silyl-directed Nazarov cyclization were also prepared and examined under the new conditions (Scheme 3.13).¹⁹ Cyclic dienones **7m** and **7n** were unreactive at low temperatures in the presence of MeOH as an additive, and underwent slow decomposition at elevated temperatures.



Scheme 3.13 Attempted Silicon-directed Nazarov Cyclization on Cyclic Dienones.

More complex strained bridged bicyclic divinyl ketones were also found to be amenable to these modified reaction conditions (Scheme 3.14). For example, camphor-derived bridged bicyclic dienone **7b** underwent 4π electrocyclization cleanly to furnish the tricyclic cyclopentenone **8b** with complete *exo* selectivity, while bicyclo[3.2.1]octadienones **7c** and **7d** reacted under similar conditions to give the tricyclic enones with complete *endo* selectivity. The probable explanation

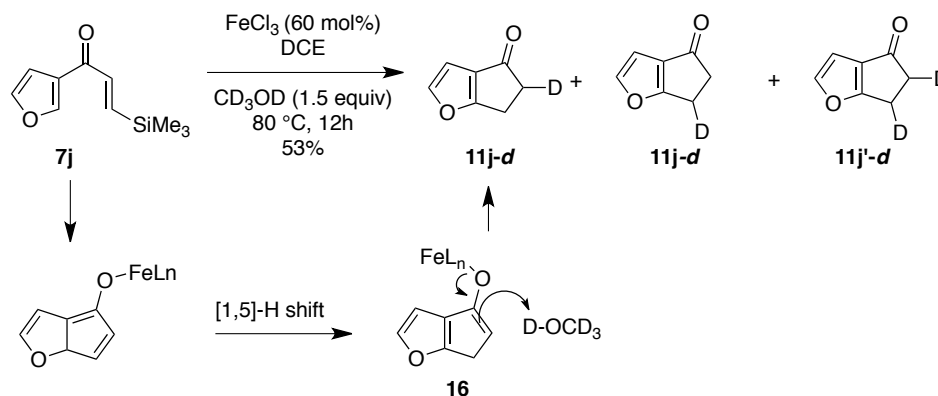
for the stereoselectivity in each case has already been discussed in Section 3.2.3. However, MeOH as an additive led to deprotection of the silyl group on the alcohol tether in case of **7b** and **7d**, prompting us to switch to H₂O as an alternate additive.^{11,26} The product yield for the formation of **7c** is similar to previous observations with BF₃•OEt₂; however, no rearranged product was formed through the participation of the remote tri-substituted olefin in the present investigation.²⁶



Scheme 3.14 Nazarov Cyclization of Strained Bridged Bicyclic Dienones.

The beneficial effect of hydroxylic additives might be ascribed to any of the several possible mechanisms. The explanations include (a) the generation of a Lewis acid-activated Brønsted acid²⁷ from FeCl₃ and MeOH that is a superior catalyst for the initial 4 π -electrocyclization; (b) the presence of a superior silyl scavenger (MeOH or MeOFeX₂); or (c) a more effective proton-transfer agent to quench the dienolate formed after the desilylation step.^{7a} Evidence for the latter

effect was found in a deuterium labeling experiment (Scheme 3.15). When **7j** was subjected to the cyclization conditions using deuterated methanol as the additive, both mono- and di-deuterated products **11j-d** and **11j'-d** were formed and their structures were confirmed through DEPT studies. This study suggests that the additive is aiding in protonation of the unstable dienolate intermediate **16**, which otherwise may decompose by several other pathways, preventing a cleaner reaction. Additionally, we were intrigued about the effect of the additive on the rate of cyclization, since many of the previously unsuccessful substrates were found to cyclize under the present conditions in reasonable time.

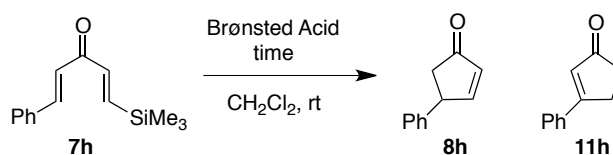


Scheme 3.15 Cyclization in Presence of CD_3OD .

To examine whether the additive was aiding in catalysis through a Brønsted acid via a Lewis acid activation (LBA) mechanism, dienone **7h** was subjected to Brønsted acids of varying strengths (Table 3.4).^{27, 28} Use of 60 mol% TFA failed to promote any cyclization of **7h**; however, when **7h** was subjected to 20 mol% Tf_2NH , approximately 20% conversion to **11h** was observed.²⁸

Cyclopentenone **11h** was formed exclusively in 45% yield with 60 mol% Tf₂NH and in 60% yield when TfOH was employed as the promoter. These results allude to the possible dual role of MeOH in both catalyzing the cyclization step and also in protonation of the reactive dienolate intermediate.²⁹ Finally, compound **7h** was also treated with 1.5 equivalent of dry HCl produced *in situ* by the addition of acetyl chloride to cooled dry methanol, to examine if traces of HCl generated from the Lewis acid promoter FeCl₃ in the solution could be the potential cyclization catalyst. However, no cyclized product was observed under the reaction conditions.

Table 3.4 Cyclization with Brønsted Acid Catalysts.^a



Entry	Brønsted Acid	Amount	Temp (°C)	Time (h)	Yield (%) ^b
1.	TFA	0.6 equiv	rt	48h	-
2.	Tf ₂ NH	0.2 equiv	rt	16h	20% (11h)
3.	Tf ₂ NH	0.6 equiv	rt	12h	45% (11h)
4.	TfOH	0.6 equiv	rt	5h	60% (11h)
5.	HCl	0.6 equiv	rt	8h	-

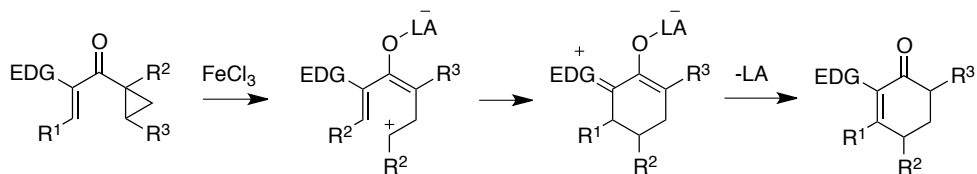
^aStandard Procedure: The chosen Brønsted acid (0.6 equiv) was added to a solution of dienone **7h** in CH₂Cl₂ (0.1 M in CH₂Cl₂) at -30 °C. The reaction was stirred at the indicated temperature until completion. After the indicated time, the reaction was quenched with sat. aq. NaHCO₃, followed by extraction, drying (MgSO₄), filtration and chromatographic purification. ^bYields: Reported for isolated products after chromatographic purification.

3.4 Conclusion

We have demonstrated the beneficial effects of hydroxylic additives such as H₂O or MeOH in silicon-directed Nazarov cyclizations. The additive is believed to both assist in the cyclization by acting as a source of an activated Brønsted acid *in situ* in the presence of FeCl₃ and may also act as a proton source to quench the reactive dienolate in the termination step, which leads to cleaner reactions. The presence of the additive has also successfully eliminated the problem of dimerization observed with some unreactive divinyl ketones. The present reaction conditions offer an efficient method for synthesizing cyclopentenones with high olefin regioselectivity in shorter reaction times and also make it amenable to larger scalability. Even for complex substrates like bridged bicyclic dienones the reaction occurs successfully at large scales within reasonable time. The first successful silicon-directed Nazarov cyclization of 2-substituted furan to cyclopentanone fused furan has also been reported. The newly developed conditions for the silicon-directed Nazarov cyclization are now being applied to our synthetic approach to the taxane skeleton.

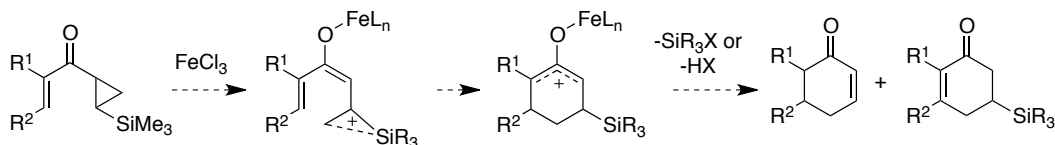
3.5 Future Plans

If one of the double bonds of the divinyl ketone precursor in Nazarov cyclization is replaced with a cyclopropyl group, it opens up the opportunity to create cyclohexanone ring systems, a process termed the homo-Nazarov cyclization (Scheme 3.16).³⁰ The inherent ring strain of cyclopropyl moieties allows their ready participation in various carbon-carbon bond-forming processes. Importantly, in case of the homo-Nazarov cyclization, the reaction does not entail a pericyclic process; rather, cationic opening of the cyclopropyl ketone is followed by cation-olefin cyclization. Proper choice of substituents on the cyclopropyl ring casts a strong effect on its reactivity.^{31,32} Cyclization reactions involving vinyl cyclopropanes are strongly considered to be stepwise in mechanism and can only formally be compared to an electrocyclization process.



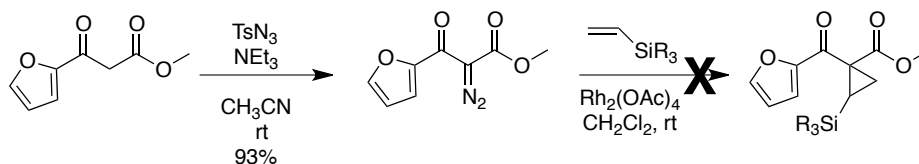
Scheme 3.16 Homo-Nazarov Cyclization.

There have been several recent reports on homo-Nazarov cyclization under mild conditions, which has been achieved by activation of the cyclopropane ring through proper polarization.^{24, 30, 33} We envision that the silicon-directed Nazarov cyclization can be extended to a formal homo-Nazarov cyclization by aptly placing a silyl group directly on the cyclopropyl unit of the precursor. The end product should retain the silyl group that can be used as a synthetic handle for further modifications (Scheme 3.17).



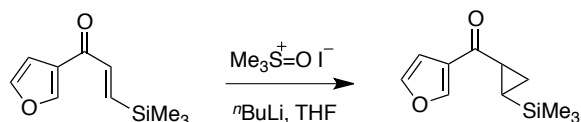
Scheme 3.17 A Possible Silicon-Directed Homo-Nazarov Cyclization.

Attempts at vinyl cyclopropyl ketone synthesis by the addition of a metallocarbene to vinylsilane proved to be unsuccessful (Scheme 3.18).



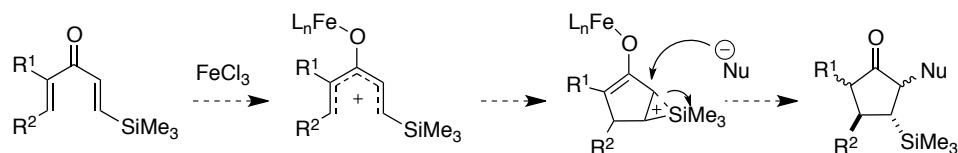
Scheme 3.18 Attempt at the Formation of Substituted Cyclopropane.

An alternative pathway to introduce a cyclopropyl moiety is through a Corey-Chaykovsky cyclopropanation on an α,β -unsaturated ketone.³⁴ The proposed Corey-Chaykovsky cyclopropanation using an *in situ* ylide generation protocol was carried out on furanyl divinyl ketones (Scheme 3.19). The products were formed with moderate yields. Desilylated cyclopropyl vinyl ketone formation was also indicated from the ^1H NMR spectrum. Efforts are to be directed toward optimization of the synthetic procedure for the starting vinyl cyclopropyl ketones. Once the starting materials can be synthesized in reproducible yields, the present additive mediated cyclization conditions can be attempted towards the desired homo-Nazarov cyclization.



Scheme 3.19 Corey-Chaykovsky Cyclopropanation of Furanyl Divinyl Ketone.

Another possible direction is to interrupt the long-lived oxallyl cationic species in the silicon-directed Nazarov cyclization with various different nucleophiles (Scheme 3.20).³⁵ This would lead to the preservation of the two stereogenic centers generated in the conrotatory cyclization. It would be interesting to note if the β -cation stabilizing effect of silicon could direct the regioselectivity of nucleophilic attack on the oxallyl cation. The silyl group on the resulting cyclopentenone can also act as a handle for further synthetic manipulations.



Scheme 3.20 Possible Pathway to an Interrupted Silicon-Directed Nazarov Cyclization.

3.6 Experimental

3.6.1. General Information

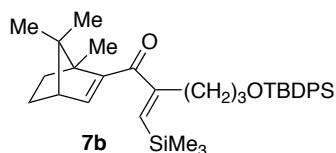
Reactions were carried out in flame-dried glassware under a positive argon atmosphere unless otherwise stated. Transfer of anhydrous solvents and reagents was accomplished with oven-dried syringes. Solvents were distilled before use: methylene chloride and 1,2-dichloroethane from calcium hydride, tetrahydrofuran from sodium/benzophenone ketyl. All other solvents and commercially available reagents were either purified by standard procedures or used without further purification. Thin layer chromatography was performed on glass plates precoated with 0.25 mm silica gel; the stains for TLC analysis were conducted with 2.5 % *p*-anisaldehyde in AcOH-H₂SO₄-EtOH (1:3:85) and further heating until development of color. Flash chromatography was performed on 230-400 mesh silica gel with the indicated eluents.

Proton nuclear magnetic resonance spectra (¹H NMR) were recorded at 300, 400 MHz or 500 MHz and the chemical shifts are reported on the δ scale (ppm) and the spectra are referenced to residual solvent peaks: CDCl₃ (7.26 ppm, ¹H; 77.06 ppm, ¹³C), or CD₃OD (3.31 ppm, ¹H; 49.00 ppm, ¹³C), or (CD₃)₂SO (2.50 ppm, ¹H; 39.52 ppm, ¹³C) as internal standard. Coupling constants (*J*) are reported in Hz. Second order splitting patterns are indicated. Splitting patterns are designated as s, singlet; d, doublet; t, triplet; q, quartet; m, multiplet; br, broad; dd, doublet of doublets, dt, doublet of triplets, etc. Carbon nuclear magnetic

resonance spectra (^{13}C NMR) were recorded at 100 MHz or 125 MHz and chemical shifts are accurate to one decimal place. Infrared (IR) spectra were measured with a Nicolet Magna 750 FT-IR spectrometer and Nic-Plan FT-IR microscope. Mass spectra were determined on a Kratos Analytical MS-50 (EI) or Agilent 6220 oaTOF electrospray positive ion mode spectrometer (ESI).

All reagents and catalysts were purchased from Aldrich or Sigma or Strem and were used without further purification unless otherwise stated.

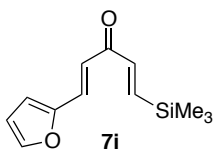
3.6.2. Synthesis and Characterization of Compounds



A mixture of LiCl (0.07g, 1.75 mmol) and Pd(Ph₃)₄ (0.028 g, 0.025 mmol) in THF (5.0 mL) was stirred under argon for 15 min. CuI (0.033 g, 0.175 mmol) was added in one solid portion, and the dark brown mixture was saturated with CO (1 atm) for 20 min. A solution of the stannane (0.29 g, 0.65 mmol) and enol triflate (0.14 g, 0.5 mmol) in THF (10 mL) was added via cannula, and the reaction mixture was saturated with CO (1 atm) for an additional 20 min. The reaction mixture was heated to 65 °C and kept under static pressure until no more enol triflate could be detected by TLC (24-72 h). The reaction mixture was cooled, and the reaction was quenched by the addition of H₂O (20 mL). The layers were separated, and the organic layer was washed with 1N NaOH (2 x 20 mL) and H₂O (20 mL). Drying (MgSO₄), filtered, and concentration under reduced pressure. The crude residue was purified by flash column chromatography (40% EtOAc in hexanes) yielded the alcohol as an orange oil, 0.10 g, 64%. The alcohol (0.11 g, 0.34 mmol) was dissolved in CH₂Cl₂ (2 mL) and stirred in an inert atmosphere of argon. NEt₃ (0.04 g, 0.48 mmol) was added to the solution followed by the

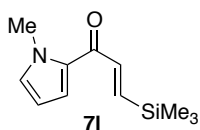
addition of DMAP (0.002 g, 0.017 mmol) and TBDPSCl (0.11 g, 0.41 mmol). The reaction mixture was stirred at the room temperature for 2-4 h before the reaction was quenched by the addition of H₂O (2 mL). The layers were separated and the aqueous layer was extracted with CH₂Cl₂ (6 mL). The combined organics were dried (MgSO₄), filtered and concentrated under reduced pressure. The crude residue was purified by flash column chromatography (10% EtOAc in hexanes) to provide **7b** as a yellow oil, 0.175 g (82% yield): R_f = 0.84 (20% EtOAc in hexanes); IR (thin film) 2962, 2954, 2871, 1633, 1462, 1298 cm⁻¹; ¹H NMR (500 MHz, CDCl₃) δ 7.70–7.62 (m, 4H), 7.39–7.32 (m, 6H), 6.4 (d, *J* = 3.6 Hz, 1H), 6.16 (s, 1H), 3.64–3.59 (m, 2H), 2.64–2.58 (m, 1H), 2.45 (t, *J* = 3.7 Hz, 1H), 2.34–2.40 (m, 1H), 1.91–1.86 (m, 1H), 1.64–1.52 (m, 3H), 1.20 (s, 3H), 1.18–1.13 (m, 1H), 1.05 (s, 9H), 0.98 (ddd, *J* = 12.3, 9.0, 3.8 Hz, 1H), 0.83 (m, 3H), 0.78 (s, 3H), 0.16 (9H); ¹³C NMR (125 MHz, CDCl₃) δ 196.8, 157.0, 149.0, 147.5, 138.0, 135.5, 134.7, 133.8, 129.5, 127.5, 64.0, 55.9, 54.5, 52.6, 32.3, 31.0, 28.6, 26.9, 26.5, 19.5, 19.1, 18.9, 11.3, 0.1; HRMS (EI, M⁺) Calcd for C₃₅H₅₀O₂Si₂ m/z 558.3349; found m/z 558.3341.

Compounds **7a**, **7c** and **7d** have previously been characterized.^{11,12} Our spectra corresponded closely to the published data.



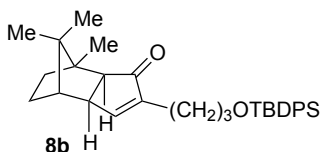
To a solution of (2-bromovinyl)trimethylsilane (0.20 g, 1.03 mmol) in THF (4.6 mL) at -78 °C ^tBuLi (1.75 M, 2.07 mmol, 4.0 equiv) was added dropwise. The reaction mixture was stirred at this temperature for 30 min under an inert atmosphere of argon before transferring slowly to a solution of the known 3-(2-furanyl)-*N*-methoxy-*N*-methyl-(*E*)-2-propenamide³⁶ (0.10 g, 0.51 mmol) in THF (2.3 mL) at -78 °C. The reaction mixture was stirred at this temperature for 30

mins before quenching with saturated aqueous solution of NH_4Cl (10 mL), followed by extraction with HCl (1.0 M, 10 mL) and Et_2O (2 x 10 mL). The organics were collected, dried (MgSO_4) and concentrated under reduced pressure. The crude residue was purified under flash column chromatography (20% EtOAc in hexanes) and afforded dienone **7i**, 0.10 g (91% yield): $R_f = 0.64$ (20% EtOAc in hexanes); IR (thin film) 2962, 2845, 1653, 1596, 1475, 1271 cm^{-1} ; ^1H NMR (500 MHz, CDCl_3) δ 7.48 (d, $J = 1.4$ Hz, 1H), 7.42 (d, $J = 15.3$ Hz, 1H), 7.19 (d, $J = 19.2$ Hz, 1H), 6.98 (d, $J = 15.8$ Hz, 1H), 6.71 (d, $J = 19.0$ Hz, 1H), 6.66 (d, $J = 3.7$ Hz, 1H), 6.47 (dd, $J = 3.4, 1.8$ Hz, 1H), 0.15 (s, 9H); ^{13}C NMR (125 MHz, CDCl_3) δ 208.3, 171.5, 167.2, 164.7, 161.9, 149.6, 140.9, 135.8, 132.5, 18.1; HRMS (EI, M^+) Calcd for $\text{C}_{12}\text{H}_{16}\text{O}_2\text{Si}$ m/z 220.0920; found m/z 220.0917.

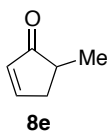


This compound was synthesized in a manner analogous to **7i**. Flash column chromatography (10% EtOAc in hexanes) provided **7l** as a colorless oil, 0.14 g (87% yield): $R_f = 0.72$ (20% EtOAc in hexanes); IR (thin film) 2950, 1665, 1578, 1392, 1237 cm^{-1} ; ^1H NMR (500 MHz, CDCl_3) δ 7.30 (d, $J = 18.7$ Hz, 1H), 7.14 (dd, $J = 4.1, 1.7$ Hz, 1H), 6.94 (dd, $J = 2.2, 2.1$ Hz, 1H), 6.66 (d, $J = 18.9$ Hz, 1H), 6.26 (dd, $J = 4.1, 2.5$ Hz, 1H), 4.07 (s, 3H), 0.26 (s, 9H); ^{13}C NMR (125 MHz, CDCl_3) δ 199.0, 165.0, 158.8, 151.6, 139.5, 128.0, 127.9, 57.6, 18.2; HRMS (EI, M^+) Calcd for $\text{C}_{11}\text{H}_{17}\text{NOSi}$ m/z 207.1079; found m/z 207.1075.

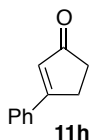
Compounds **7e**, **7f**, **7g**, **7h**, **7j**, **7k**, **7m** and **7n** have previously been characterized.^{5b,7a,19} Our spectra corresponded closely to the published data.



H₂O (17 μ L, 0.94 mmol) was added to a solution of the bridged bicyclic dienone **7b** (0.34 g, 0.62 mmol) in dry dichloromethane (63 mL) and stirred before cooling the solution to -50 °C. FeCl₃ (0.06 mg, 0.40 mmol, 0.6 equiv) was added as one solid portion and the heterogeneous mixture stirred vigorously at -50 °C for 15 min. The reaction mixture was then warmed to -30 °C and continued to stir at this temperature until completion (monitored by TLC). The reaction was then warmed to room temperature before the addition of saturated aqueous solution of NaHCO₃ (44 mL) and the resulting mixture was stirred until two clear phases were observed. The organic phase was separated and the aqueous layer extracted with CH₂Cl₂ (2 \times 92 mL). The combined organic layers were dried (MgSO₄), filtered, and the solvent removed under reduced pressure. The resultant orange oil was purified by flash column chromatography (20% EtOAc in hexanes) to yield the corresponding cyclized product **8b**, 0.25 g (81% yield): *R*_f = 0.76 (20% EtOAc in hexanes); IR (film) 2954, 1697, 1462, 1354, 1231 cm⁻¹; ¹H NMR (500 MHz, CDCl₃) δ 7.70 - 7.68 (m, 4H), 7.46-7.38 (m, 6H), 7.21 (app dt, *J* = 2.9, 1.4 Hz, 1H), 3.68 (t, *J* = 6.5 Hz, 2H), 2.65 (ddq, *J* = 5.2, 2.4, 2.4 Hz, 1H), 2.23 (td, *J* = 5.7, 2.2 Hz, 3H), 1.90 (d, *J* = 4.4 Hz, 1H), 1.86 (dddd, *J* = 12.1, 12.1, 3.9, 3.9 Hz, 1H), 1.75 (q, *J* = 6.9 Hz, 2H), 1.63-1.57 (m, 1H), 1.33-1.28 (m, 1H), 1.23-1.18 (m, 1H), 1.16 (s, 3H), 1.08 (s, 9H), 0.79 (s, 3H), 0.62 (s, 3H); ¹³C NMR (125 MHz, CDCl₃) δ 211.2, 160.1, 147.4, 135.6, 133.9, 129.6, 127.6, 63.4, 59.1, 51.7, 50.5, 47.9, 47.6, 38.0, 29.9, 29.4, 26.9, 23.0, 22.7, 21.3, 19.2, 12.0; HRMS (ESI, [M+Na]⁺) Calcd for C₃₂H₄₂O₂SiNa *m/z* 509.2846; found *m/z* 509.2841.

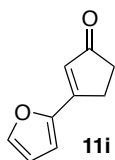


MeOH (0.06 mL, 1.5 mmol) was added to a solution of a dienone **7e** (0.096 g, 1.0 mmol) in dry dichloromethane (10 mL) and stirred before cooling the solution to -30 °C. FeCl₃ (0.09 mg, 0.6 mmol, 0.6 equiv) was added as one solid portion and the heterogeneous mixture was stirred vigorously at -30 °C for 15 min. The reaction mixture was then warmed to 0 °C and stirred at this temperature until completion (monitored by TLC). The reaction was then warmed to room temperature before the addition of saturated NaHCO₃ solution (10 mL) and the resulting mixture was stirred until two clear phases were observed. The organic phase was separated and the aqueous layer extracted with CH₂Cl₂ (2 × 10 mL). The combined organic layers were dried (MgSO₄), filtered, and the solvent removed under reduced pressure. The resultant orange oil was purified by flash column chromatography to yield the corresponding cyclized product **8e** as a yellow oil, 0.058 g (61% yield; 77% by NMR): R_f = 0.35 (20% EtOAc in hexanes); IR (film) 2970, 2942, 2861, 1710, 1445, 1362, 1090 cm⁻¹; ¹H NMR (500 MHz, CDCl₃) δ 7.65 (dt, *J* = 5.5, 2.5 Hz, 1H), 6.16 (dt, *J* = 5.5, 2.0 Hz, 1H), 2.85-2.82 (m, 1H), 2.32 (qd, *J* = 7.5, 2.6 Hz, 1H), 2.27 (m, 1H), 1.18 (d, *J* = 7.5 Hz, 3H); ¹³C NMR (125 MHz, CDCl₃) δ 213.0, 163.0, 133.4, 39.4, 37.8, 15.2; HRMS (EI, M⁺) Calcd for C₆H₈O m/z 96.0575; found m/z 96.0572. This compound has been previously synthesized and characterized.³⁷ Our spectra corresponded closely to the reported data.

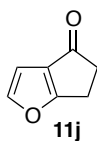


This compound was synthesized in a manner analogous to **8e**. Flash column chromatography (40% EtOAc in hexanes) provided **11h** as a colorless oil, 0.052 g (33% yield): R_f = 0.24 (20% EtOAc in hexanes); IR (thin film) 2923, 1742, 1686, 1603, 1495 cm⁻¹; ¹H NMR (300 MHz, CDCl₃) δ 7.68-7.65 (m, 2H), 7.47-7.20 (m, 3H), 6.58 (t, *J* = 1.8 Hz, 1H), 3.07-3.05 (m, 2H), 2.61-2.58 (m, 2H); ¹³C NMR

(125 MHz, CDCl₃) δ 209.5, 173.9, 134.1, 131.2, 128.9, 127.5, 126.8, 35.3, 28.6; HRMS (EI, M⁺) Calcd for C₁₁H₁₀O m/z 158.0731; found m/z 158.0730. This compound has been previously synthesized and characterized.³⁸ Our spectra corresponded closely to the reported data.

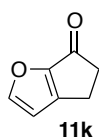


This compound was synthesized in a manner analogous to **8e**. Flash column chromatography (50% EtOAc in hexanes) provided **11i** as a yellow oil, 0.088 g (60% yield): R_f = 0.15 (20% EtOAc in hexanes); IR (film) 2960, 1741, 1587, 1456, 1289 cm⁻¹; ¹H NMR (500 MHz, CDCl₃) δ 7.71–7.70 (m, 1H), 7.51–7.47 (m, 2H), 6.61 (t, *J* = 2Hz, 1H), 3.17–3.08 (m, 2H), 2.64–2.62 (m, 2H); ¹³C NMR (125 MHz, CDCl₃) δ 209.3, 174.0, 134.1, 131.2, 128.9, 127.5, 126.8, 35.3, 28.6; HRMS (EI, M⁺) Calcd for C₉H₈O₂ m/z 148.0730; found m/z 148.0524. This compound has been previously synthesized and characterized.³⁹ Our spectra corresponded closely to the reported data.

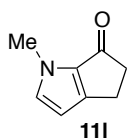


MeOH (0.46 mL, 12 mmol) was added to a stirred solution of the 3-furyl substituted dienone **7j** (0.76 g, 8.0 mmol) in dry dichloroethane (160 mL). FeCl₃ (0.77 mg, 4.8 mmol, 0.6 equiv) was added as one solid portion and the heterogeneous mixture was heated to reflux at 80 °C. The reaction mixture was vigorously stirred at this temperature until completion (monitored by TLC). The reaction was then cooled to room temperature before the addition of saturated

NaHCO₃ solution (160 mL) and the resulting mixture was stirred vigorously until two clear phases were observed. The organic phase was separated and the aqueous layer extracted with CH₂Cl₂ (2 × 200 mL). The combined organic layers were dried (MgSO₄), filtered, and the solvent removed under reduced pressure. The resultant orange oil was purified by flash column chromatography (50% EtOAc in hexanes) to afford **11j** as yellow oil, 0.52 g (53% yield); R_f = 0.28 (20% EtOAc in hexanes); IR (film) 3041, 2954, 1708, 1298 cm⁻¹; ¹H NMR (500 MHz, CDCl₃) δ 7.50 (d, *J* = 2.0 Hz, 1H), 6.52 (d, *J* = 2.0 Hz, 1H), 3.01-2.97 (m, 4H); ¹³C NMR (125 MHz, CDCl₃) δ 195.2, 182.9, 149.5, 128.0, 105.2, 42.1, 22.2; HRMS (EI, M⁺) Calcd for C₇H₆O₂ m/z 122.0367; found m/z 122.0365. This compound has been previously synthesized and characterized.⁴⁰ Our spectra corresponded closely to the reported data.



This compound was synthesized in a manner analogous to **11j**. Flash column chromatography (50% EtOAc in hexanes) provided **11k** as a yellow oil, 0.056 g (46% yield); R_f = 0.22 (20% EtOAc in hexanes); IR (thin film) 3100, 2972, 2933, 2863, 1696, 1367, 1271 cm⁻¹; ¹H NMR (500 MHz, C₆D₆) δ 6.91 (d, *J* = 1.7 Hz, 1H), 5.63 (d, *J* = 1.7 Hz, 1H), 2.27 (t, *J* = 4.5 Hz, 2H), 1.87 (t, *J* = 4.5 Hz, 2H); ¹³C NMR (125 MHz, C₆D₆) δ 186.3, 156.0, 154.9, 152.6, 109.5, 40.6, 18.7 (The ¹H NMR AND ¹³C NMR spectra were taken in C₆D₆ because of the sensitivity of the compound to CDCl₃. HRMS (EI, M⁺) Calcd for C₇H₆O₂ m/z 122.0367; found m/z 122.0368.



This compound was synthesized in a manner analogous to **11j**. Flash column chromatography (50% EtOAc in hexanes) provided **11i** as a yellow oil, 0.085 g (63% yield): $R_f = 0.20$ (20% EtOAc in hexanes); IR (thin film) 3140, 2986, 2843, 1683, 1367 cm^{-1} ; ^1H NMR (500 MHz, CDCl_3) δ 6.92 (d, $J = 1.2$ Hz, 1H), 5.82 (d, $J = 1.2$ Hz, 1H), 3.75 (s, 3H), 2.26 (t, $J = 4.5$ Hz, 2H), 2.67 (t, $J = 4.5$ Hz, 2H); ^{13}C NMR (125 MHz, CDCl_3) δ 187.6, 134.0, 129.9, 127.6, 114.5, 38.6, 32.3, 19.7; HRMS (EI, M^+) Calcd for $\text{C}_8\text{H}_9\text{ON}$ m/z 135.0684; found m/z 135.0675. This compound has been previously synthesized and characterized.⁴¹ Our spectra corresponded closely to the reported data.

Compounds **8a**¹¹, **8c**¹¹, **8d**²⁶, **8f**^{5b}, **8g**^{5b}, **8h**^{5b} have previously been characterized. Our spectra corresponded closely to the published data.

3.7 References

- (1) For reviews see (a) Denmark, S. E. In *Comprehensive Organic Synthesis*; Trost, B.M., Ed.; Pergamon: Oxford, **1991**; Vol. 5, pp 751-784. (b) Habermas, K. L.; Denmark, S. E.; Jones, T. K. *Org. React.* (N.Y.), **1994**; Vol. 45, pp 1-158. (c) Pellissier, H. *Tetrahedron* **2005**, *61*, 6479-6517. (d) Harmata, M. *Chemtracts* **2004**, *17*, 416. (e) Tius, M. A. *Eur. J. Org. Chem.* **2005**, 2193. (f) Frontier, A. J.; Collison, C. *Tetrahedron* **2005**, *61*, 7577. (g) Vaidya, T.; Eisenberg, R.; Frontier, A. J. *ChemCatChem* **2011**, *3*, 1531. (h) N. Shimada, C. Stewart and M. A. Tius, *Tetrahedron* **2011**, *67*, 5851.
- (2) Braude, E. A.; Coles, J.A. *J. Chem. Soc.* **1952**, 1430.
- (3) (a) Kursanov, D. N.; Parnes, Z. N.; Zaretskaya, I. I.; Nazarov, I. N. *Izv. Akad. Nauk SSSR, Ser. Khim.* **1953**, 114. (b) Nazarov, I. N.; Zaretskaya, I. I.; Parnes, Z. N.; Kursanov, D. N. *Izv Akad. Nauk SSSR, Ser. Khim.* **1953**, 519. (c) Kursanov, D. N.; Parnes, Z. N.; Zaretskaya, I. I.; Nazarov, I. N. *Izv. Akad. Nauk SSSR, Ser. Khim.* **1954**, 859.
- (4) (a) Woodward, R. B. *Spec. Publ.-Chem. Soc.* **1967**, *21*, 217. (b) Woodward, R. B.; Hoffmann, R. *Angew. Chem., Int. Ed. Engl.* **1969**, *8*, 781.
- (5) (a) Denmark, S. E.; Jones, T. K. *J. Am. Chem. Soc.* **1982**, *104*, 2642. (b) Jones, T. K.; Denmark, S. E. *Helv. Chim. Acta* **1983**, *66*, 2377.

- (6) Houk, K. N. In *Strain and its Implications in Organic Chemistry*; de Meijere, A., Blechert, S., Eds., Ed.; Kluwer Academic: Dordrecht, **1989**; pp 25-37.
- (7) (a) Jones, T. K.; Denmark, S. E. *Helv. Chim. Acta* **1983**, *66*, 2397. (b) Denmark, S. E.; Klix, R. C. *Tetrahedron* **1988**, *44*, 4043. (c) Denmark, S. E.; Habermas, K. L.; Hite, G. A.; Jones, T. K. *Tetrahedron* **1986**, *42*, 2821. (d) Mehta, G.; Krishnamurthy, N. *J. Chem. Soc., Chem. Commun.* **1986**, 1319.
- (8) Shimada, N.; Stewart, C.; Tius, M. A. *Tetrahedron* **2011**, *67*, 5851.
- (9) Dolbier, W. R.; Koroniak, H.; Houk, K. N.; Sheu, C. *Acc. Chem. Res.* **1996**, *29*, 471.
- (10) (a) Denmark, S. E.; Klix, R. C. *Tetrahedron* **1988**, *44*, 4043. (b) Denmark, S. E.; Wallace, M. A.; Walker, C. B. *J. Org. Chem.* **1990**, *55*, 5543.
- (11) (a) Mazzola, R. D.; White, T. D.; Vollmer-Snarr, H. R.; West, F. G. *Org. Lett.* **2005**, *7*, 2799. (b) White, T. D.; West, F. G. *Tetrahedron Lett.* **2005**, *46*, 5629.
- (12) Benson, C. L.; West, F. G. *Org. Lett.* **2007**, *9*, 2545.
- (13) (a) Rondan, N.G.; Caramella, P.; Houk, K. N. *J. Am. Chem. Soc.* **1981**, *103*, 2436. (b) Rondan, N. G.; Caramella, P.; Ib Jiri Mareda, J.; Mueller, P. H.; Houk, K. N. *J. Am. Chem. Soc.* **1982**, *104*, 4974.
- (14) Nakanishi, W. W., F. G. *Curr. Opin. Drug. Discov.* **2009**, *12*, 732.
- (15) (a) Vorländer, D.; Schroedter, G. *Ber. Dtsch. Chem. Ges.* **1903**, *36*, 1490. (b) Braude, E. A.; Coles, J.A. *J. Chem. Soc.* **1952**, 1430.
- (16) For the first of many communications from Nazarov: Nazarov, I. N.; Zaretskaya, I. I. *Ilz. Akad. Nauk. SSSR. Ser. Khim.* **1941**, 211.
- (17) Vaidya, T.; Eisenberg, R.; Frontier, A. J. *ChemCatChem* **2011**, *3*, 1531.
- (18) Sako, M.; Suzuki, H.; Yamamoto, N.; Hirota, K.; Maki, Y. *J. Chem. Soc., Perkin Trans 1* **1998**, 417.
- (19) Denmark, S. E.; Habermas, K. L.; Hite, G. A. *Helv. Chim. Acta* **1988**, *71*, 168.
- (20) Nahm, S.; Weinreb, S. M. *Tetrahedron Lett.* **1981**, *22*, 3815.

- (21) Mazzola, R. D.; Giese, S.; Benson, C. L.; West, F. G. *J. Org. Chem.* **2003**, *69*, 220.
- (22) (a) Malona, J. A.; Colbourne, J. M.; Frontier, A. J. *Org. Lett.* **2006**, *8*, 5661. (b) He, W.; Huang, J.; Sun, X.; Frontier, A. J. *J. Am. Chem. Soc.* **2007**, *130*, 300. (c) Malona, J. A.; Cariou, K.; Frontier, A. J. *J. Am. Chem. Soc.* **2009**, *131*, 7560. (d) Vaidya, T.; Atesin, A. C.; Herrick, I. R.; Frontier, A. J.; Eisenberg, R. *Angew. Chem. Int. Ed.* **2010**, *49*, 3363.
- (23) Vaidya, T.; Manbeck, G. F.; Chen, S.; Frontier, A. J.; Eisenberg, R. *J. Am. Chem. Soc.* **2011**, *133*, 3300.
- (24) Yadav, V. K.; Kumar, N. V. *Chem. Commun.* **2008**, 3774.
- (25) (a) Kerr, D. J.; Miletic, M.; Chaplin, J. H.; White, J. M.; Flynn, B. L. *Org. Lett.* **2012**, *14*, 1732. (b) Wu, Y.-K.; Niu, T.; West, F. G. *Chem. Commun.* **2012**, *48*, 9186.
- (26) Giese, S.; Mazzola, R. D.; Amann, C. M.; Arif, A. M.; West, F. G. *Angew. Chem. Int. Ed.* **2005**, *44*, 6546.
- (27) Yamamoto, H.; Futatsugi, K. *Angew. Chem. Int. Ed.* **2005**, *44*, 1924.
- (28) Rueping, M.; Koenigs, R. M.; Atodiresei, I. *Chem. Eur. J.* **2010**, *16*, 9350.
- (29) Basak, A. K.; Tius, M. A. *Org. Lett.* **2008**, *10*, 4073.
- (30) De Simone, F.; Saget, T.; Benfatti, F.; Almeida, S.; Waser, J. *Chem. Eur. J.* **2011**, *17*, 14527.
- (31) Piers, E. In *Comprehensive Organic Synthesis*; Trost, B. M., Ed.; Pergamon: New York, **1991**; Vol. 5, pp 971-998.
- (32) For a few selected examples, see: (a) Stork, G.; Marx, M. *J. Am. Chem. Soc.* **1969**, *91*, 2371. (b) Grieco, P. A.; Finkelhor, R. S. *Tetrahedron Lett.* **1974**, *6*, 527. (c) Pohlhaus, P. D.; Sanders, S. D.; Parsons, A. T.; Li, W.; Johnson, J. S. *J. Am. Chem. Soc.* **2008**, *130*, 8642.
- (33) (a) Patil, D. V.; Phun, L. H.; France, S. *Org. Lett.* **2010**, *12*, 5684. (b) Phun, L. H.; Patil, D. V.; Cavitt, M. A.; France, S. *Org. Lett.* **2011**, *13*, 1952.
- (34) Corey, E. J.; Chakovsky, M. *J. Am. Chem. Soc.* **1965**, *87*, 1353.
- (35) Grant, T. N.; Rieder, C. J.; West, F. G. *Chem. Commun.* **2009**, 5676.

- (36) De Simmone, F.; Andres, J.; Torosantucci, R.; Waser, J. *Org. Lett.* **2009**, *11*, 1023.
- (37) Jansen, D. J.; Shenvi, R. A. *J. Am. Chem. Soc.* **2013**, *135*, 1209.
- (38) Nagamine, T.; Kon, Y.; Sato, K. *Chem. Lett.* **2012**, *41*, 744.
- (39) Missiaen, P.; De Clercq, P. J. *Bull. Soc. Chim. Belg.* **1987**, *96*, 105.
- (40) Yamabe, H.; Mizuno, A.; Kusama, H.; Iwasawa, N. *J. Am. Chem. Soc.* **2005**, *127*, 3248.
- (41) Palmer, M. H.; Leitch, D. S.; Greenhalgh, C. W. *Tetrahedron* **1978**, *34*, 1015.

Chapter 4

Some Interesting Novel Reactivities of Advanced Intermediates Towards the Chemical Synthesis of Taxinine

4.1 Biological Significance of Taxinine and its Synthetic Challenges

The taxane diterpenes isolated from yew trees have a common tricyclic core containing a bridgehead olefin (Figure 4.1).¹ Such a unique structural feature accompanied by the presence of a multitude of oxygenated asymmetric centers has made their syntheses extremely challenging.² Furthermore, the remarkable chemotherapeutic potential of the congener Taxol (paclitaxel, Figure 4.1) has accelerated the synthetic efforts towards these targets.³

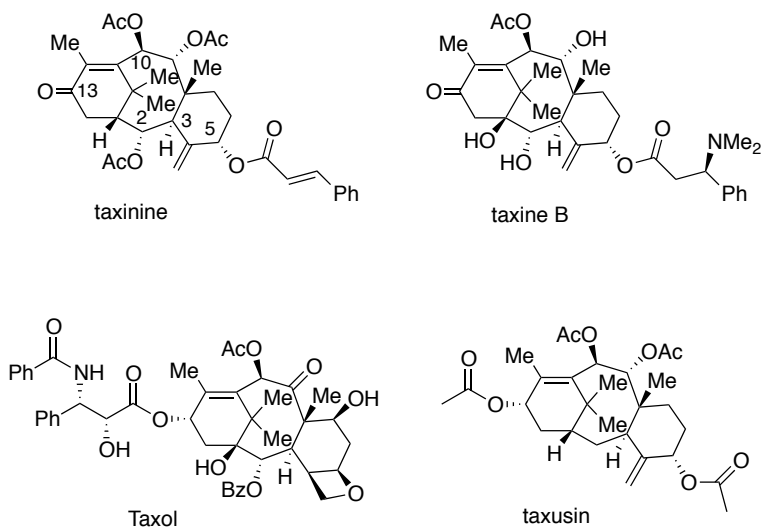


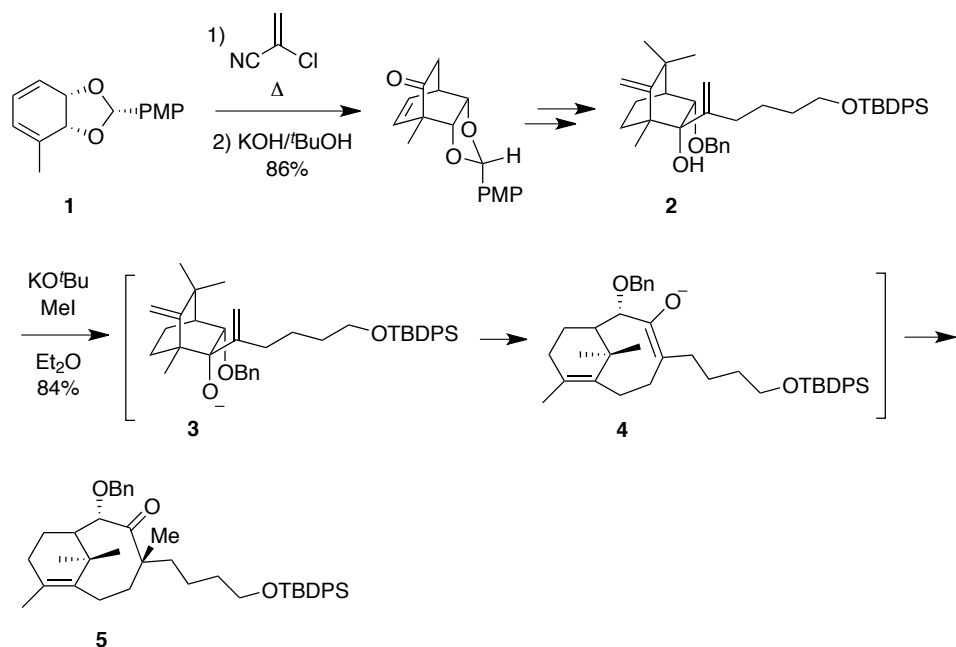
Figure 4.1 Representative Examples of the Members of the Taxane Family.

The crystalline taxane diterpene taxinine (Figure 4.1) was first isolated by ethanol extraction of the needles of the Japanese yew tree in 1925.⁴ This compound has also been identified in the needles, fruits, seeds, twigs, barks of many *Taxus* species. Taxinine was notably the first natural taxoid to be obtained in pure form, as well as the first to be structurally elucidated. Its complex structure was established through a combination of NMR and chemical studies over 30 years ago and subsequently confirmed by X-ray crystallographic methods.⁵ Various studies suggest that, unlike its structural congener paclitaxel, taxinine is a much weaker cytotoxic agent.⁶ However, taxinine has been shown to increase the cellular accumulation of vincristine in multi-drug resistant tumor cells and must, therefore, be regarded as having potential for resensitizing those cells to various anti-cancer agents.⁷ Taxinine has also been identified as an inhibitor of the cell membrane transporter P-glycoprotein, over-expression of which can lead to a rapid efflux of cytotoxic agents from within the cancerous cell.⁸ It is through this process that multi-drug resistance generally develops in a tumor cell. This is a critical problem in cancer chemotherapy, as once initiated, the cancerous cells gain resistance to a wide range of cytotoxic drugs. As a

consequence taxinine has attracted some attention in the scientific community, although no total synthesis has been reported to date.⁹ However, total syntheses of a closely related taxoid, taxusin have been described by several groups.¹⁰ From a synthetic viewpoint, the structural features that make the synthesis of the taxane carbocyclic skeleton difficult are 1) a cyclooctanoid ring structure with a bridgehead olefin 2) stereocontrolled formation of the oxygenated stereocenters at the C9 and C10 positions and 3) the cage-like conformation of the carbocyclic ring system.

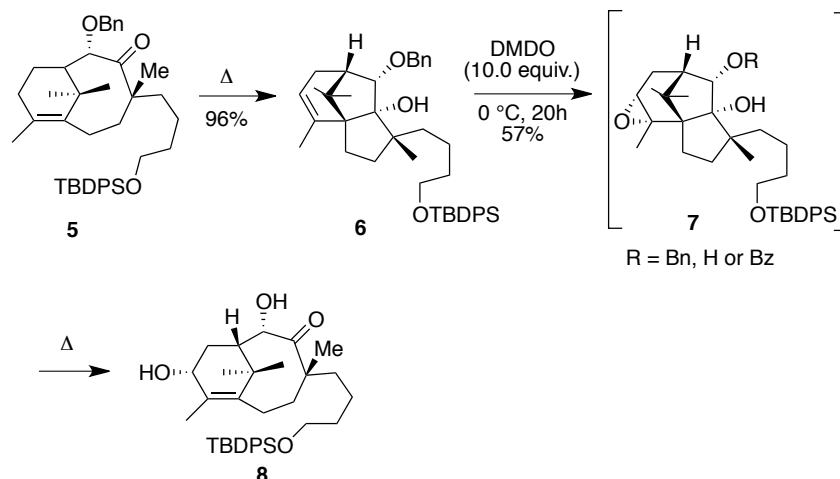
4.2 Enantiospecific Synthesis of the AB-Ring Substructure of Taxinine by the Banwell Group

The Banwell group in 2004 elaborated their approach toward the synthesis of the enantiomer of the natural product taxinine.¹¹ Their work culminated in the stereo-controlled synthesis of the AB-ring substructure incorporating the C8 quaternary carbon stereocenter. The key reaction employed to introduce the cyclooctanoid ring structure was an anionic oxy-Cope rearrangement of the bicyclo[2.2.2]octan-2-one **2** (Scheme 4.1). The bicyclo[2.2.2]octan-2-one **2** in turn, was obtained through a Diels-Alder reaction of the protected cis-1,2-dihydrocatechol **1** with α -chloroacrylonitrile. The homochiral diene **1** is readily available through microbial dihydroxylation of toluene¹² and has already been proved to be a valuable building block for the synthesis of terpenoids.¹³ The anionic oxy-Cope rearrangement was then carried on **2** by treatment with potassium *tert*-butoxide to form the oxyanion **3**, which underwent the desired conversion to form the isomeric enolate **4**. Trapping with methyl iodide gave the desired product **5** in 84% yield.



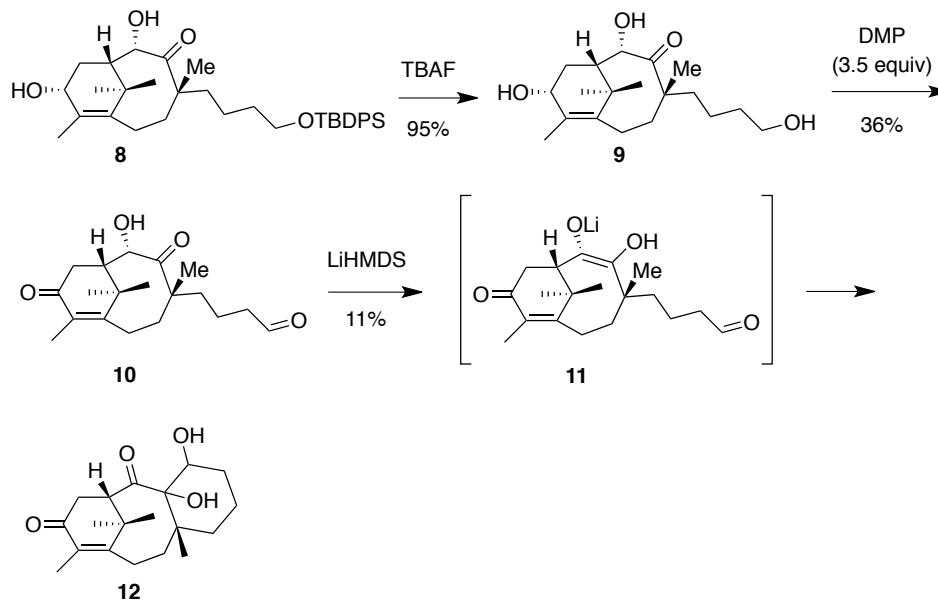
Scheme 4.1 Anionic Oxy-Cope Rearrangement to Construct the AB-Ring System of Taxinine.

A circuitous route was undertaken to introduce the C13 oxygen. The bicyclo[5.3.1]undecanone **5** was subjected to a thermally induced carbonyl-ene reaction affording tricyclic product **6** in 96% yield (Scheme 4.2). Subjection of the latter to epoxidation with 10 equivalents of dimethyl dioxirane (DMDO) afforded an unstable oxirane **7**, which then underwent a thermally promoted facile Grob-type fragmentation to form the target allylic alcohol **8**.¹⁴



Scheme 4.2 Formation of the Allylic Alcohol **8** via Thermal Grob Fragmentation.

Final efforts toward C ring annulation involved an attempt to exploit an aldol-type reaction procedure (Scheme 4.3). To this end, the TBDPS ether in **8** was deprotected under TBAF-mediated conditions to afford the diol **9**, followed by oxidation with DMP to produce the tricarbonyl compound **10**. Treatment of the tricarbonyl compound **10** with LiHMDS did not prove to be very effective, only giving the desired product **12** in small amounts. The reaction is believed to proceed through the formation of an enolate **11** under LiHMDS conditions, followed by aldol reaction with the tethered aldehyde to give the tricyclic product **12**.



Scheme 4.3 Taxinine C-Ring Annulation Attempts Through Aldol Reaction.

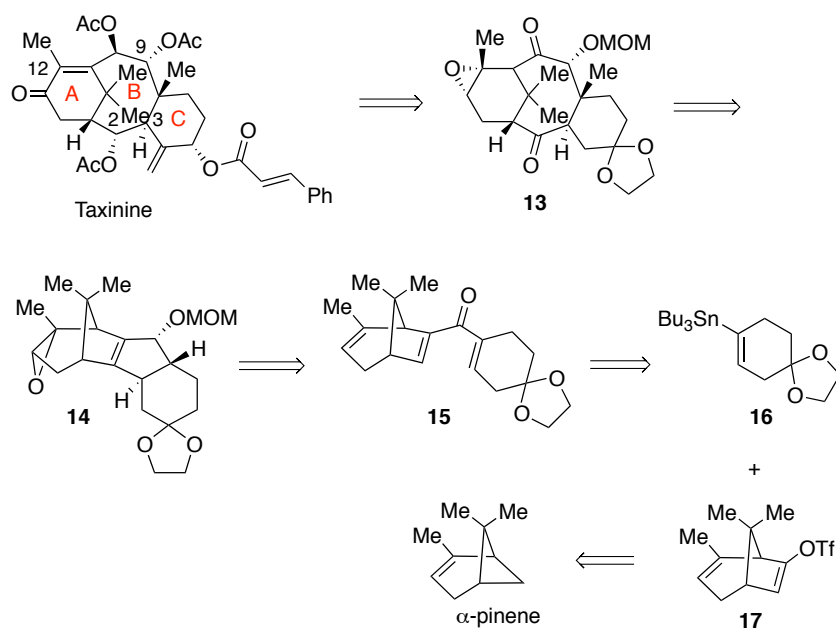
4.3 West Group's Efforts Toward the Total Synthesis of Taxinine

The West group has previously initiated studies into the total synthesis of the natural product taxinine which has culminated in two approaches to a highly advanced intermediate of the natural product through the works of Giese,¹⁵ Mazzola¹⁶ and Benson.¹⁷ Each of their works has highlighted many of the challenging structural aspects associated with this class of compounds. However, each approach had some critical drawbacks that prevented completion of the synthesis.

4.3.1. The First Generation Approach to Taxinine (Giese)

The retrosynthetic route of the first generation approach focused on the synthesis of the diketone **13** as a key intermediate to the natural product taxinine (Scheme 4.4). From this compound, it was envisioned to install the C11-C12

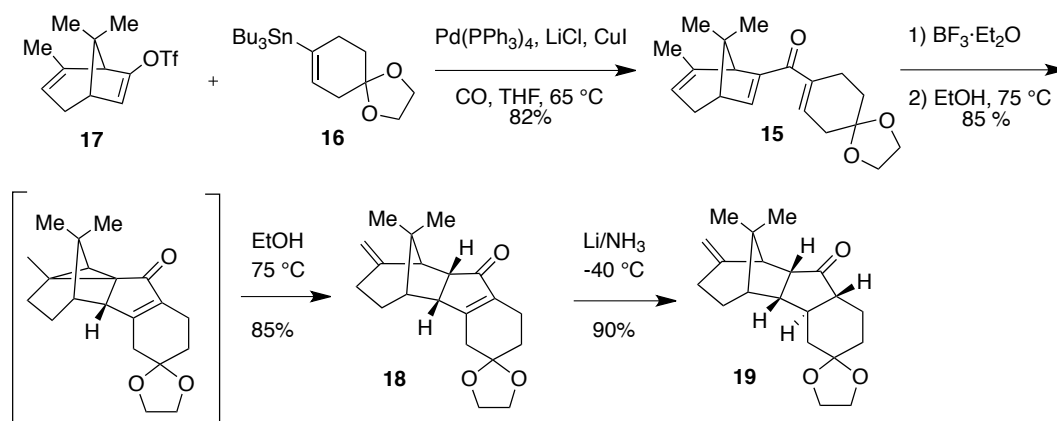
bridgehead olefin through base induced elimination of the epoxide followed by further oxidation state adjustments and protective group manipulations to furnish taxinine. According to the retrosynthetic analysis, the β -epoxy diketone **13** should be obtained through an oxidative cleavage of the C2-C10 olefin in the tricyclic epoxide **14**. The tricyclic epoxide could be accessed through a Nazarov cyclization of the dienone **15**. The divinyl ketone was envisioned to arise from a carbonylative Stille cross coupling of vinyl stannane **16** and enol triflate **17**. The enol triflate could be accessed from α -pinene, an inexpensive chiral, non-racemic starting material.



Scheme 4.4 Retrosynthetic Analysis of Taxinine in the First Generation Approach.

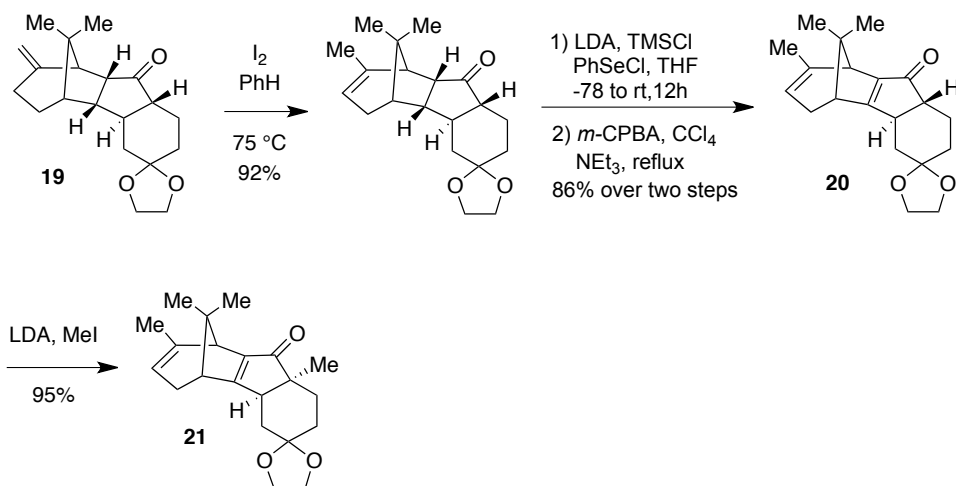
The synthesis began with a crucial carbonylative Stille coupling between a vinyl stannane **16** and enol triflate **17** to access the Nazarov cyclization precursor **15** in good yield (Scheme 4.5).¹⁸ The dienone, upon treatment with $\text{BF}_3 \cdot \text{OEt}_2$ at low temperatures provided a cyclopropyl ketone through the interception of the intermediate allyl cation by the seemingly remote olefin at C12-C13. However,

heating the cyclopropyl ketone in EtOH led to the formation of the rearranged cyclopentenone **18**, which was then carried forward in the synthesis.¹⁹ Finally, dissolving metal conditions successfully gave access to the desired reduced compound **19**, but attempts to methylate at C8 were met with failure. The synthesis was carried forward with the intent to introduce the methyl group at a later stage.



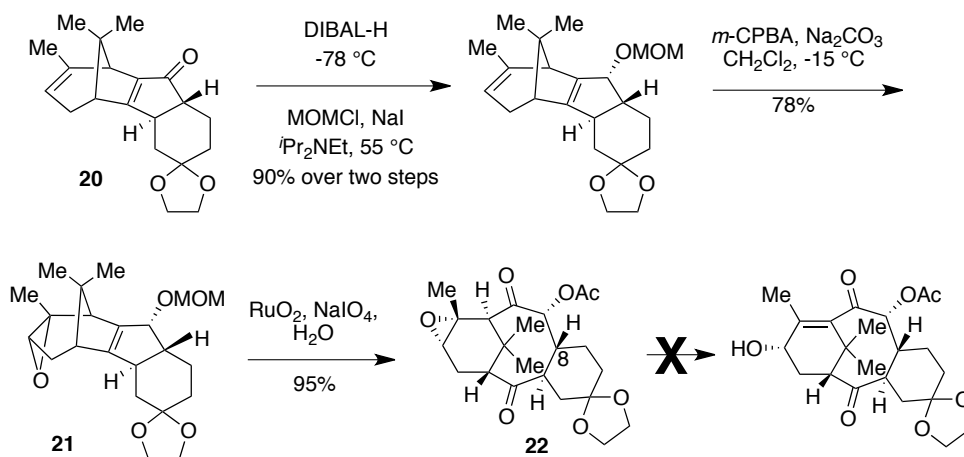
Scheme 4.5 Nazarov Cyclization to Form the Fused Cyclopentenone **19**.

At this point, the exocyclic double bond in **19** was isomerized on treatment with iodine (Scheme 4.6). The C2-C10 olefin was then installed through a highly efficient selenoxide elimination reaction to give **20**. This olefin is crucial for the oxidative cleavage to access the eight-membered B-ring at a later stage. Methylation was attempted at this stage using LDA/MeI conditions and the methyl group was installed successfully with high stereoselectivity to afford enone **21** with excellent yield. However, the methyl group was incorporated with incorrect stereochemistry.



Scheme 4.6 Preparation of the Tetrasubstituted Olefin **21** via Selenoxide Elimination.

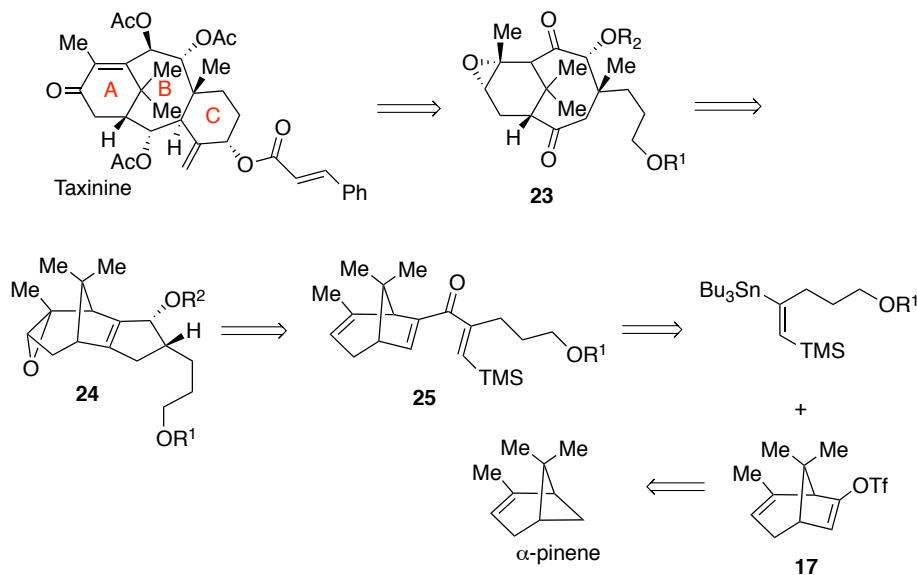
The key oxidative ring opening reaction was attempted on the non-methylated enone **20**. A 1,2-reduction of the enone **20** with DIBAL-H afforded a separable 4:1 α : β mixture of allylic alcohols (Scheme 4.7). The major diastereomer was protected as MOM ether followed by epoxidation of the C12-C13 olefin with *m*-CPBA providing the desired epoxide **21**. The oxidative ring fragmentation was carried out efficiently using RuO_2 in the presence of $NaIO_4$ as the oxidant to furnish the 6-8 bicyclic diketone **22** in excellent yield. Unfortunately, all attempts to open the A-ring epoxide under a range of basic conditions met with failure, producing only complex mixtures. This may be attributed to the conformational preference of the cyclooctanoid ring structure that results in poor alignment of the C11 proton with the adjacent carbonyl, significantly lowering its acidity. This insurmountable roadblock led to the abandonment of this route, and begun efforts in a second generation route to the taxinine skeleton.



Scheme 4.7 Oxidative Cleavage of **21** to Access the Tricyclic Core of the Taxane Skeleton.

4.3.2. The Second Generation Approach to Taxinine (Mazzola)

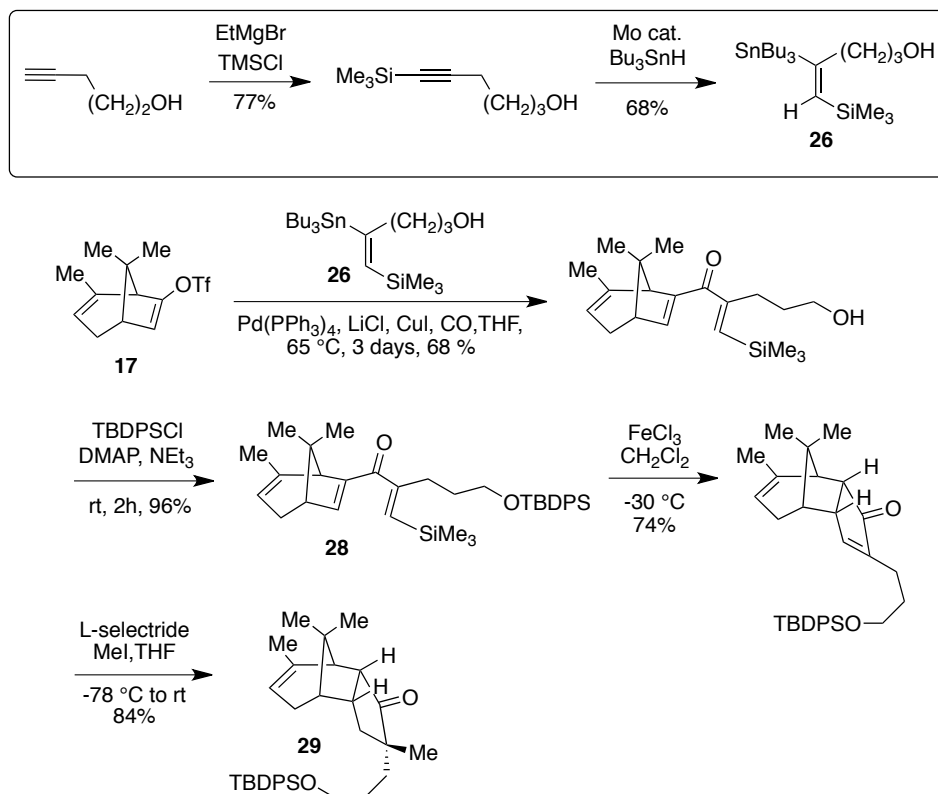
The proposed strategy for the second-generation route to taxinine involved a late stage annulation of the C-ring from an intermediate **23** (Scheme 4.8). This would be revealed by oxidative cleavage of epoxide **24**. Finally, this intermediate would derive, as shown in the first route, from a Nazarov cyclization of dienone **25**, which would in turn be prepared from a carbonylative Stille coupling of enol triflate **17** and a modified vinyl stannane.



Scheme 4.8 Retrosynthetic Scheme for Mazzola's Route.

Stille coupling partner **26** was synthesized via a Mo-catalyzed hydrostannylation reaction of 5-trimethylsilyl-4-pentynol, obtained from 4-pentynol (Scheme 4.9). It was found that the subsequent palladium mediated cross-coupling reaction benefited from the presence of the free alcohol functionality, as its protection resulted in reduction of product yields. Vinyl triflate **17** was then treated with the alcohol **26** in presence of Pd(PPh₃)₄, LiCl and CuI under an atmosphere of CO to afford the corresponding coupling product in 72% yield. However, the subsequent Nazarov cyclization reaction was found to be incompatible with the presence of a free hydroxy group and necessitated the protection of the hydroxy group as the TBDPS ether. The TBDPS-protected dienone **27** was then subjected to the Nazarov cyclization using anhydrous FeCl₃ to afford the desired product **28** in 74% yield with complete *endo* selectivity.²⁰ In this case, no interception of the allylic cation by the remote olefin at C12-C13 was observed. This is attributed to the presence of the trimethylsilyl group, which directs the termination of the cyclization. The crucial step of installing the methyl group to create the C8 quaternary stereocenter was then undertaken. When cyclopentenone **28** was treated with L-Selectride, then methyl iodide, reductive

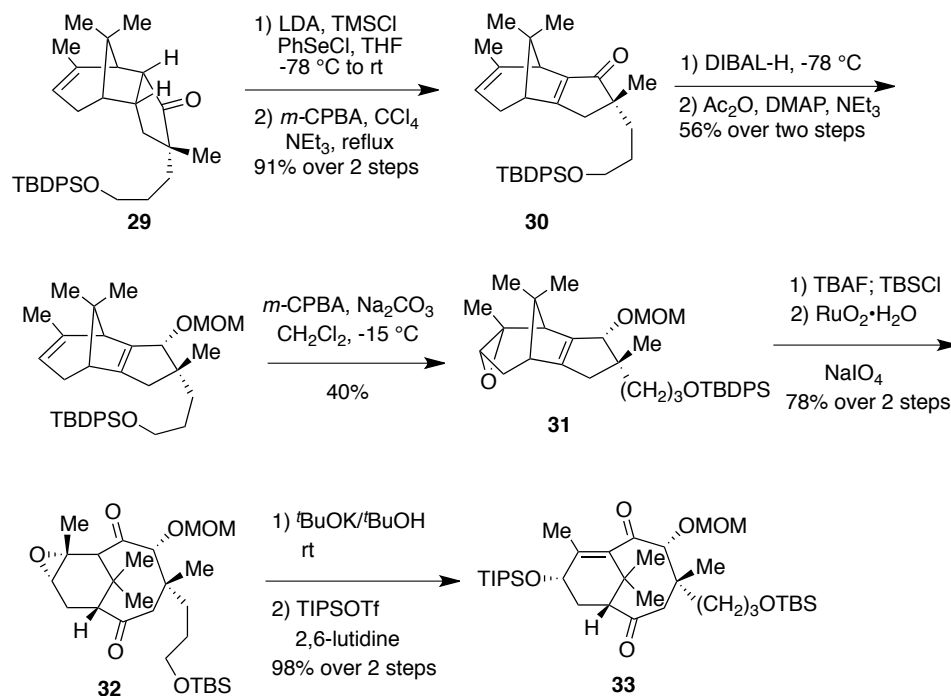
alkylation product **29** was formed without difficulty, unlike the first route where the wrong diastereomer was formed. Methylation is thought to proceed from the β -face of the enolate exclusively to avoid severe steric interactions on the α -face resulting from the cage-like conformation of the tricyclic system.



Scheme 4.9 Silicon-Directed Nazarov Cyclization of a Bridged Bicyclic Dienone **28** and Methylation to Install the Quaternary Stereocenter of **29**.

The tetrasubstituted olefin required for the late stage oxidative cleavage was introduced in the same manner as in the previous route. Ketone **29** was first converted to an α -selenide by treating the TMS enol ether of the ketone with phenylselenenyl chloride. This was followed by oxidation and subsequent *syn*-elimination, furnishing the enone **30** in 91% overall yield (Scheme 4.10). After the efficient installation of the tetrasubstituted olefin, 1,2 reduction of the enone **30** was accomplished by treatment with DIBAL-H, and the resulting crude allylic

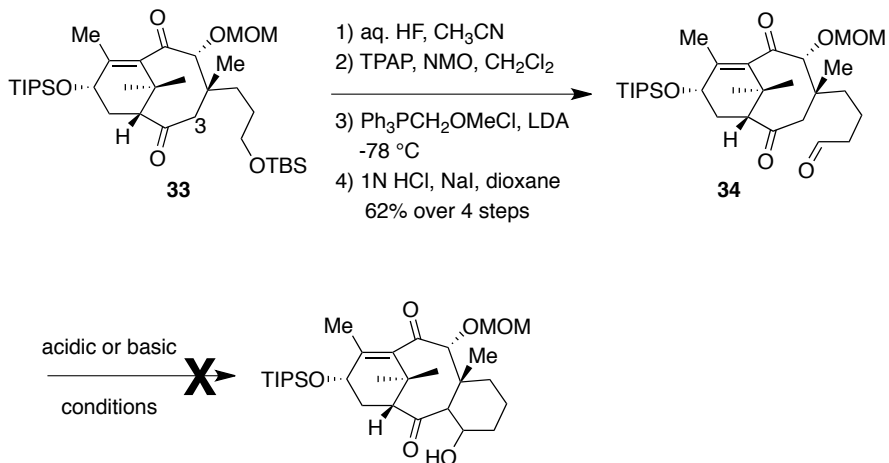
alcohol was directly protected as the MOM ether in 87% yield. The reduction took place exclusively from the more accessible β -face of the molecule setting the C9 oxygenated stereocenter with the correct stereochemistry. The less sterically encumbered A-ring alkene was then epoxidized upon treatment with *m*-CPBA, affording compound **31** in good yield. Prior to the key oxidative fragmentation reaction, exchange of the TBDPS group on the primary alcohol for an alternative siloxy group, which did not contain an aromatic functionality, was found necessary to avoid a low yielding, sluggish reaction in the oxidative cleavage step. To this end, the TBDPS ether was exchanged for TBS ether followed by treatment with $\text{RuO}_2 \cdot 2\text{H}_2\text{O}$ in presence of NaIO_4 as oxidant to furnish the bicyclo[5.3.1]undecane ring system **32** in excellent yield. After successful construction of the eight-membered B-ring, a base induced opening of the epoxide to form the bridgehead olefin was attempted. In the event, treatment with catalytic *t*-BuOK followed by immediate protection of the resulting allylic alcohol with TIPSOTf afforded diketone **33** in excellent yield, in sharp contrast to the earlier study (Scheme 4.7).



Scheme 4.10 Elaboration of Ketone **29** to the AB-Bicyclic Core of Taxinine.

With an efficient route devised for the successful preparation of the AB-bicyclic ring system of taxinine that incorporates the A-ring bridgehead olefin and sets the stereocenters at C8 and C9, a strategy for further elaboration to install the six-membered C-ring was pursued. With an objective to construct the C-ring of taxinine through an aldol type chemistry, compound **33** was converted to aldehyde **34** in 62% yield over a four step sequence (Scheme 4.11). With the aldehyde functionality being installed, an aldol cyclization strategy was investigated for the construction of the six-membered C-ring of the taxane skeleton. Unfortunately, exposure of aldehyde **34** to a range of basic conditions resulted either in decomposition or recovery of starting material. Acidic conditions also resulted in failure. Attempts to access the silyl enol ether via C3 deprotonation also failed. This lack of reactivity was attributed to the particular conformational preferences of the eight-membered ring that rendered deprotonation at C3 center unfavorable due to lack of proper orbital alignment. A

deuterium-labeling experiment also showed deuteration at C1 instead of the desired C3 position. This phenomenon has been observed in other syntheses or approaches to taxane diterpenes as well.²¹



Scheme 4.11 Attempts to Form the Tricyclic Core of the Taxane Skeleton.

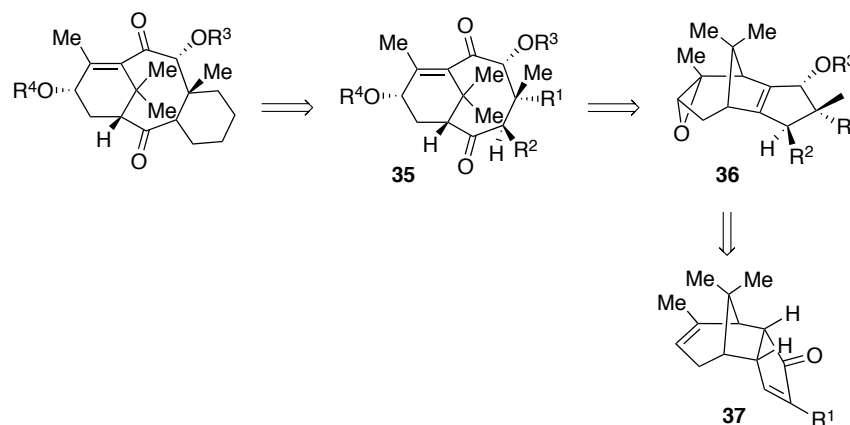
The second-generation approach to the synthesis of taxinine was mostly successful with minor modifications to adjust reactivity. Unfortunately, this linear approach failed to enable the critical C-ring at a late stage of synthesis because of the inability to functionalize the C3 position. The second-generation approach thus required further improvement and led to the development of a third generation route to the natural product.

4.3.3. The Third Generation Approach to Taxinine (Benson)

A third route towards the synthesis of taxinine was conceived with the knowledge from the two routes devised by Giese and Mazzola. In this case, a handle for a later C-ring annulation would be installed at an early stage of the synthesis. It was conceived that the problems associated with the first approach to taxinine could be overcome efficiently because of the additional conformational flexibility that would be granted to the molecule by no longer having the C3

substituent locked into a ring. At a later stage, after revelation of the cyclooctane, this group could facilitate the C-ring construction by two different pathways, dependent on the nature of the substituent. In one, the group might act to further acidify the remaining C3 proton, allowing C-ring closure via an aldol reaction. In the other, the group may serve to migrate the point of ring-closure away from the eight-membered ring, an approach that could then provide a multitude of different ring-closure strategies.

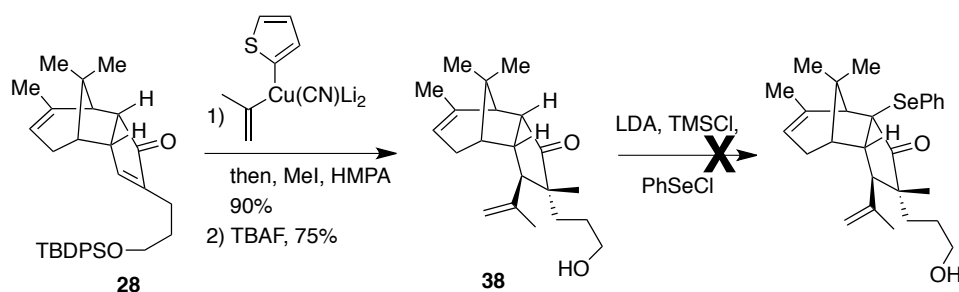
As part of the retrosynthetic analysis, an early functionalization of C3 via conjugate addition to Nazarov product **37** was planned along with the simultaneous methyl trapping of the enolate generated therein (Scheme 4.12). It was hoped that epoxide **36** could be obtained using previously established protocols that on fragmentation would reveal the AB ring system in **35**. In this case, with functionality already in place at C3, facile closure of the C-ring was envisioned using any of several possible bond-constructions.



Scheme 4.12 Retrosynthetic Approach to Taxinine: The Third Generation Approach.

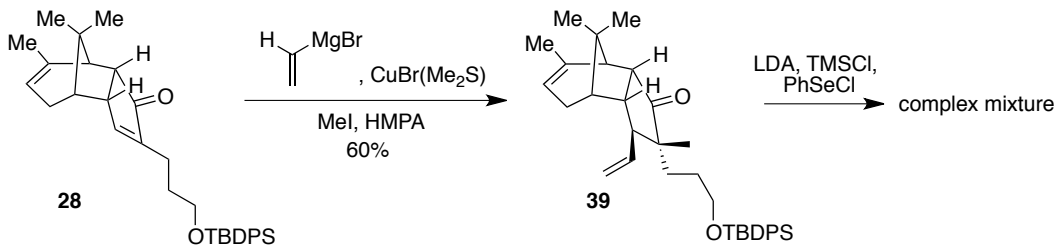
A first attempt at C3 functionalization with an isopropenyl group by conjugate addition to **28** was considered (Scheme 4.13). We believed that this group would provide us with a number of feasible ring closing strategies at the

opportune time. After a few trials, the Lipshutz cuprate, lithium [cyano(1-propen-2-yl)(2-thienyl)cuprate] provided the competent nucleophile for the 1,4-addition.²² Under these conditions the conjugate addition and subsequent methylation followed by deprotection of the TBDPS ether occurred in excellent yield to give C3-substituted ketone **38** as one stereoisomer. Both the nucleophile and the electrophile came from the more accessible β -face of the molecule despite of the steric repulsion that resulted from two groups being *cis* to each other. Unfortunately, attempts to introduce the phenyl selenyl moiety to explore its oxidation to the tetrasubstituted enone met with much resistance.



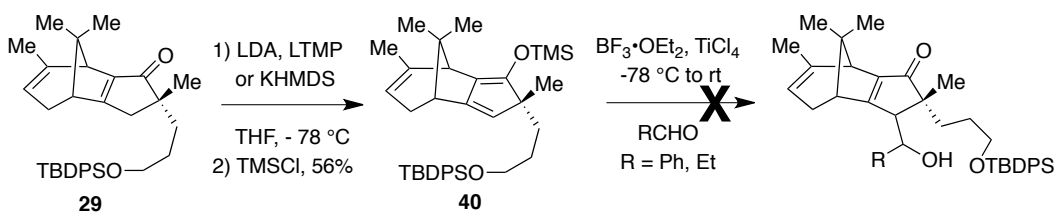
Scheme 4.13 Functionalization of the C3 Position of **28** with Isopropenyl Group.

Another popular dehydrogenation protocol, Saegusa oxidation, employing $\text{Pd}(\text{OAc})_2$ as the oxidant,²³ was attempted, which again met with failure. Steric hindrance of the highly substituted, sterically congested ketone was thought to be responsible for the poor reactivity. Other widely used silyl enol ether oxidation methods employing IBX²⁴ or DDQ²⁵ were not attempted for similar reasons. To modify the reactivity of the sterically congested ketone **28**, the 3-carbon isopropenyl group was replaced with a smaller vinyl group followed by trapping of the intermediate enolate with MeI to form the vinyl-substituted ketone **39** in moderate yield and excellent stereoselectivity (Scheme 4.14). Unfortunately, treatment with PhSeCl only provided a complex mixture. Even a reversal of the sequence of events was attempted but with no favorable result.



Scheme 4.14 Vinylation of the Enone **28** and Attempted α -Selenylation.

In a different approach to C3 functionalization, a vinylogous Mukaiyama aldol reaction employing a siloxy diene and an aldehyde was explored.²⁶ After experimentation with a wide range of bases in presence of TMSCl, it was found that strong bases like LDA, LTMP or KHMDS worked well providing the siloxy diene **40** (Scheme 4.15). Unfortunately, hydrolysis of the siloxy diene **40** to the starting ketone **29** was the only observed outcome under Mukaiyama aldol-type conditions with no indication of incorporating the aldehyde. It seemed that the siloxy diene **40** was too poor a nucleophile to participate in the aldol reaction and this poor nucleophilicity of the dienolate was attributed to steric crowding at both potential reactive sites. The siloxy diene was also extremely sensitive to moisture and readily converted to the ketone **29**.



Scheme 4.15 Generation of the Siloxy Diene **40** from α , β -Unsaturated Ketone **29**.

From the third approach to taxinine, it seemed unlikely that an early incorporation of C3 substituent would help in later C-ring closure through oxidative fragmentation. Steric intolerance of the substituted intermediates

precluded formation of the necessary precursor to oxidative fragmentation. For this reason, a fourth approach to the construction of the taxinine C-ring was considered.

4.3.4. The Fourth Generation Approach to Taxinine (Benson, Nakanishi, Joy)

C-H insertion reactions involving metal-stabilized carbenes, generated via the decomposition of α -diazo ketones or β -keto diazo esters with transition metals have been extensively studied with respect to C-C bond formation.²⁷ Application of a C-H insertion strategy to the synthesis of taxinine seemed a feasible route to the late stage construction of the six-membered C-ring.²⁸ In the target diazo compound **41**, competitive five-membered ring formation was not an option due to the presence of a quaternary center at the γ position (Figure 4.2).

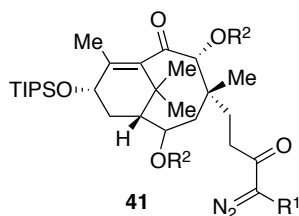
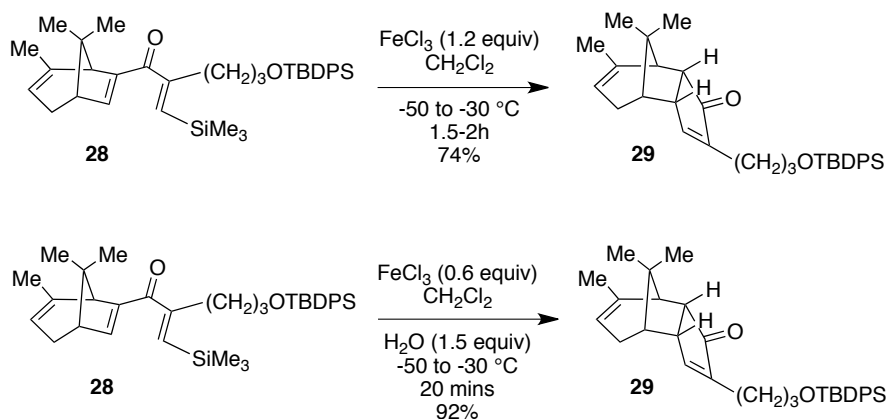


Figure 4.2 Late Stage C-H Insertion Intermediate.

Stork and Nakatani have demonstrated that the presence of an electron-withdrawing group, like a carbonyl, one or two carbons apart may potentially deactivate targeted C-H bonds.²⁹ Thus, the β -position was expected to be inert towards C-H insertion, hindering competitive four-membered ring formation. Moreover, the identity of the protecting group of the C9 hydroxyl required special attention. We decided to protect the hydroxyl group as the electron withdrawing acetate to discourage C-H insertion at the adjacent C9 methine (γ' position).³⁰ It's

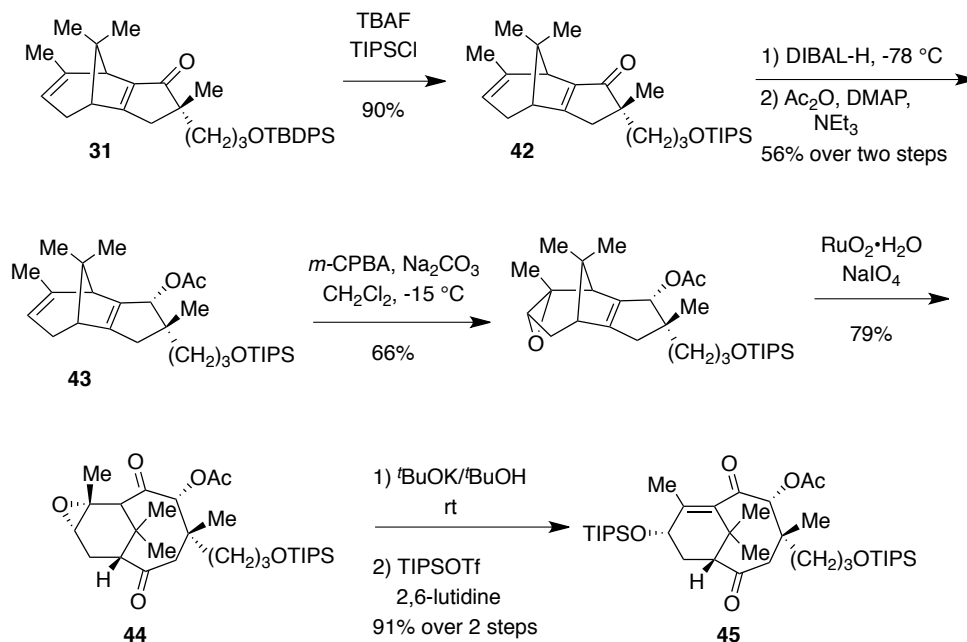
a general observation that the ease of insertion into the targeted C-H bond increases as the reactive carbon becomes more highly substituted ($\text{CH}_3 < \text{CH}_2 < \text{CH}$).³¹ Taking into consideration all of these factors, it was hoped that the desired C-H insertion at C3 should be a feasible approach to furnish the C-ring.

There were certain critical drawbacks of the previous approach that called for attention at this stage before embarking on to the construction of the C-ring. The key Nazarov cyclization step to install the cyclopentenone was often found to be inconsistent when carried out on larger scales. The reaction took a longer time for completion, leading to oligomeric side product formation. We found a way to circumvent this problem by carrying out the cyclization under Lewis acid (FeCl_3) conditions in the presence of hydroxylic additives such as water or methanol. The cyclization of **28** was observed to proceed cleanly, furnishing the desired product **29** in excellent yields even at larger scales (Scheme 4.16). Details of the effect of additives on the silicon-directed Nazarov cyclization have been elaborated in Chapter 3.



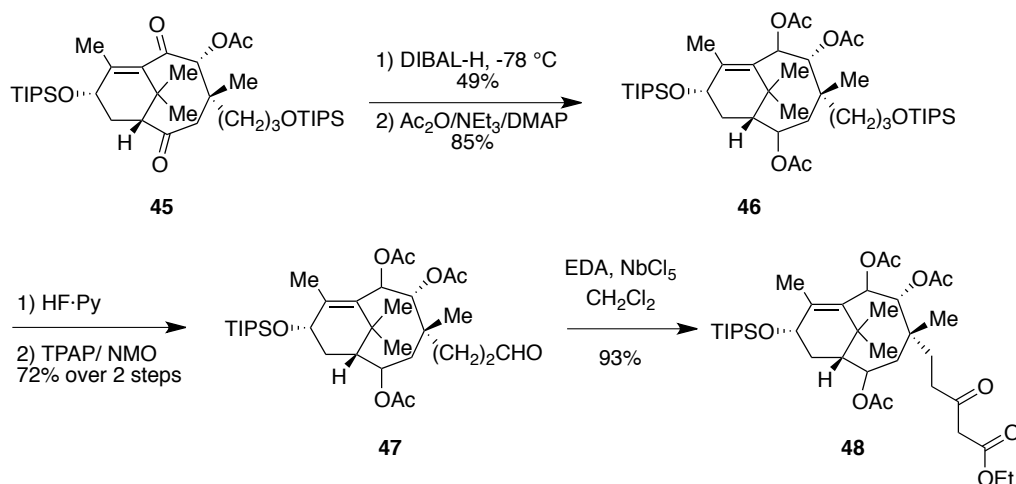
Scheme 4.16 Effect of Additive on the Nazarov Cyclization Step.

Cyclopentenone **29** was then converted to the tetrasubstituted olefin-containing compound **31** over a sequence of four steps. We realized that presence of a labile allylic acetate at C10 could cause a concern for its survival through the subsequent steps required for elaboration to the ring-opened product. In particular, the basic fluoride conditions necessary for deprotection of the TBDPS ether to allow for its exchange to a RuO₄-compatible protective group were worrisome. To avoid this issue, TBDPS exchange was performed prior to reduction and acetylation of **31**. Therefore, **31** was deprotected with TBAF and immediately treated with TIPSCl to furnish enone **42** in 90% yield over two steps (Scheme 4.17). The enone was then subjected to DIBAL-H mediated reduction to give the allylic alcohol, which was subsequently acetylated without intermediate purification to furnish the allylic acetate **43** in 56% yield over two steps. Isolation of **43** required careful chromatographic technique using deactivated silica gel because of unwanted by-product formation under acidic conditions involving the removal of the labile acetate group. Details on the byproduct will be elaborated later in this chapter. The acetate **43** was epoxidized using *m*-CPBA in moderate yield. The epoxide was then treated with RuO₂•2H₂O in the presence of NaIO₄ to cleanly furnish diketone **44** through an oxidative ring cleavage of the tetrasubstituted olefin. On exposure of **44** to catalytic *t*-BuOK, the epoxide was readily opened and the resulting alcohol was protected with TIPSOTf immediately to give **45** in excellent yield.



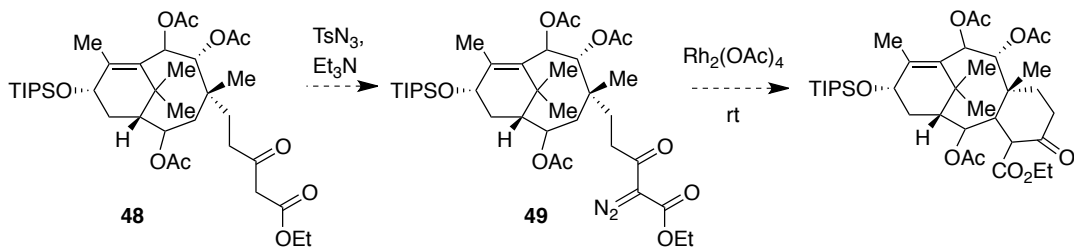
Scheme 4.17 Preparation of the Diketone Intermediate **45**.

DIBAL-H treatment of the diketone **45** produced a triol as the major product due to the simultaneous removal of the acetate protecting group (Scheme 4.18). As had been previously observed in the case of C9-MOM analogs of AB-ring intermediates, the ^1H NMR spectra for the reduced compound also displayed severe peak-broadening of the signals which precluded the option of gaining any information regarding the stereoselectivity of the transformation.³² The triol was thus immediately treated with excess Ac_2O to provide triacetate **46** in good yield. The TIPS protected primary alcohol was then converted to the aldehyde **47** by careful treatment with TBAF, followed by oxidation of the free alcohol to give the aldehyde in 72% yield over two steps. Conversion of **47** to β -keto ester **48** via the Roskamp reaction was found to occur smoothly.³³ The ^1H NMR spectrum indicated the presence of an ethyl ester moiety and HRMS data also confirmed the presence of the desired compound by displaying a molecular ion peak that matched the formula for the proposed structure of **48**.



Scheme 4.18 Conversion of the Diketone **45** to β -Keto ester **48**.

At this point, the β -keto ester **48** was carefully subjected to diazo transfer conditions using TsN₃ and NEt₃ (Scheme 4.19).³⁴ After direct concentration and chromatographic purification using deactivated silica gel, a new compound with lower polarity than the starting material was isolated. A peak in the IR spectrum of the isolated compound at 2133 cm⁻¹ gave evidence for the successful incorporation of the diazo functionality. Unfortunately, when the compound was exposed to Rh₂(OAc)₄, a popular transition metal catalyst for C-H insertion reactions of diazo compounds, no desired product formation was observed. The ¹H NMR spectrum of the crude reaction product closely resembled the starting material **48**. The MS data also provided a molecular ion peak matching the molecular formula of **48**. A possible rationale could be that the desired diazo compound **49** did not form during the diazo transfer reaction and that the peak in the IR spectrum was a result of TsN₃ impurity. Unfortunately, due to the limited availability of material and its potential sensitivity no other spectral data was obtained and the viability of C-H insertion strategy remained unknown at this stage.



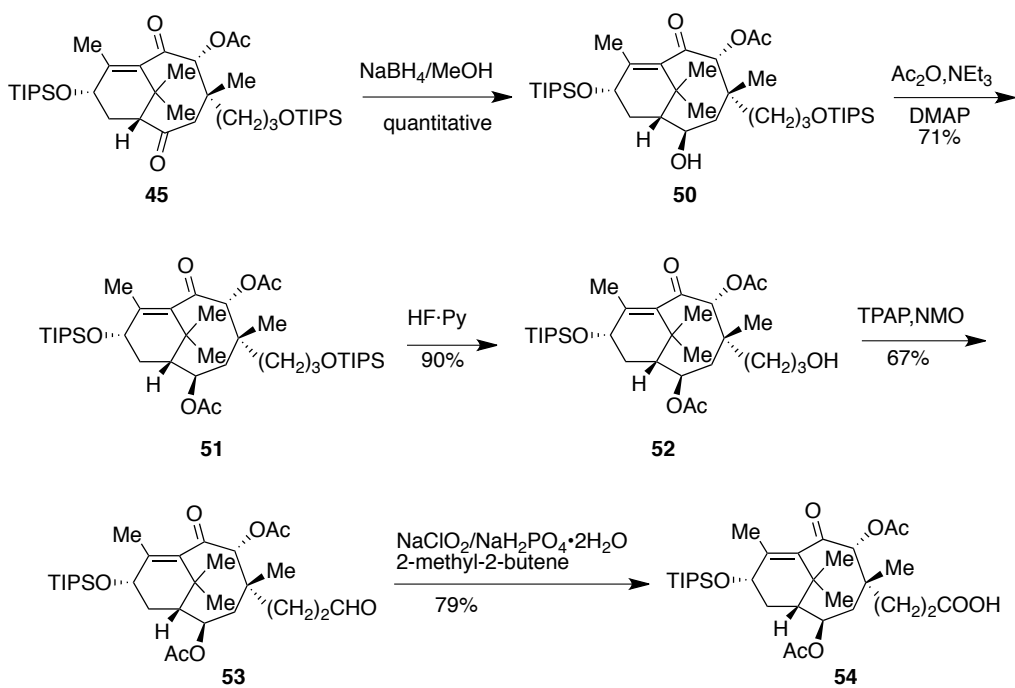
Scheme 4.19 Conversion of **48** to a β -Keto Diazo ester **49** and Attempt at Intramolecular C-H Insertion.

4.4. Results and Discussion

4.4.1. Alternative Attempts at C-Ring Formation (Nakanishi, Joy)

At this point, we decided to take a few steps backward and carry out some key structural modifications that might be helpful for the synthesis of the later intermediates and also for structural elucidation. With this insight, we first investigated the selective reduction of the diketone **45** (Scheme 4.20). Use of a milder reducing agent such as NaBH_4 in methanol instead of DIBAL-H led to a mono-reduction product **50** as a single diastereomer in quantitative yield that was subsequently protected as the acetate **51**. At this stage, the relative stereochemistry of the acetate could be assigned from nOe correlations between the C9 acetate and the bridgehead methyl protons (Figure 4.3). At this point it became clear that **45** underwent selective reduction under NaBH_4 conditions forming the mono-alcohol **50**. The reduction proceeded as expected at the unconjugated carbonyl site C2 leaving the carbonyl moiety at C10 unaffected. The stereoselectivity of the reduction can be attributed to the steric hindrance of the convex face (or β -face) of the molecule due to the presence of the bridging geminal dimethyl groups, which prevents the attack from that face. Comparatively, the concave face (or α -face) is more accessible for a hydride coming in a Bürgi-Dunitz trajectory (Figure 4.3). Removal of the TIPS group under HF/pyridine conditions furnished the corresponding alcohol **52**, which after

oxidation of the primary alcohol provided the aldehyde **53** in 67% yield. At this point we decided to make some structural modifications to the diazo precursor for the planned C-H insertion reaction. Generally, diazo keto-ester is a destabilized diazo compound and is less reactive towards diazo decomposition in the presence of transition metal catalysts. Comparatively, the diazo ketones have been reported to be more reactive toward C-H insertion.³⁵ So it was envisioned that the diazo ketone could be a more effective precursor to the intramolecular C-H insertion reaction. To this end, the aldehyde **53** was oxidized to the carboxylic acid **54** in 79% yield using Pinnick oxidation reaction.³⁶



Scheme 4.20 Elaboration of the Diketone **45** to the Carboxylic Acid **54**.

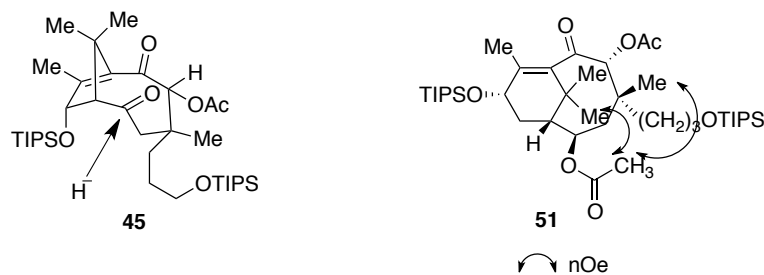
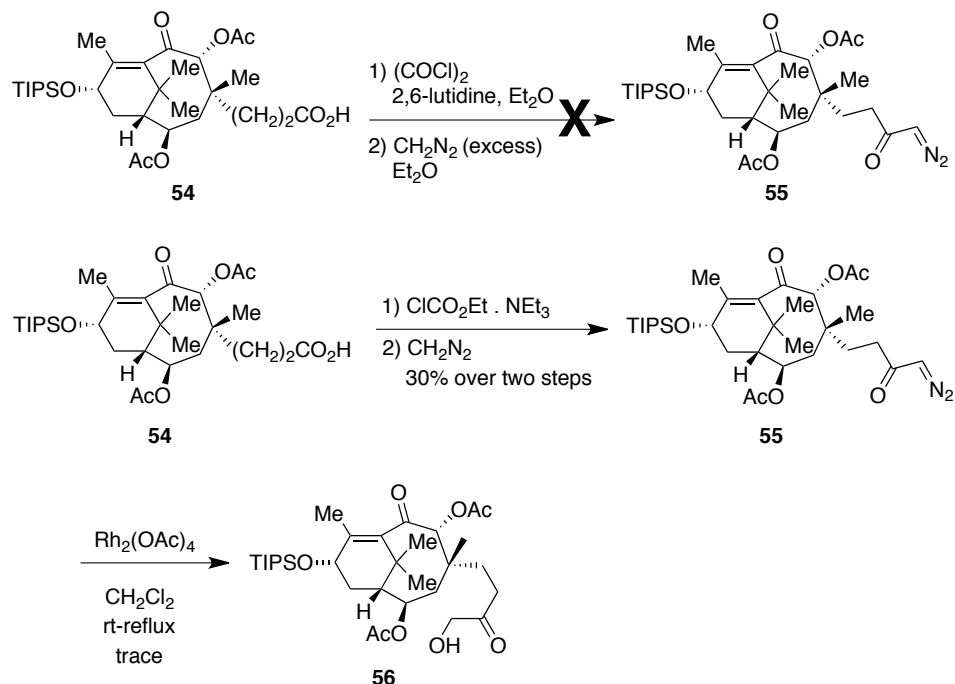


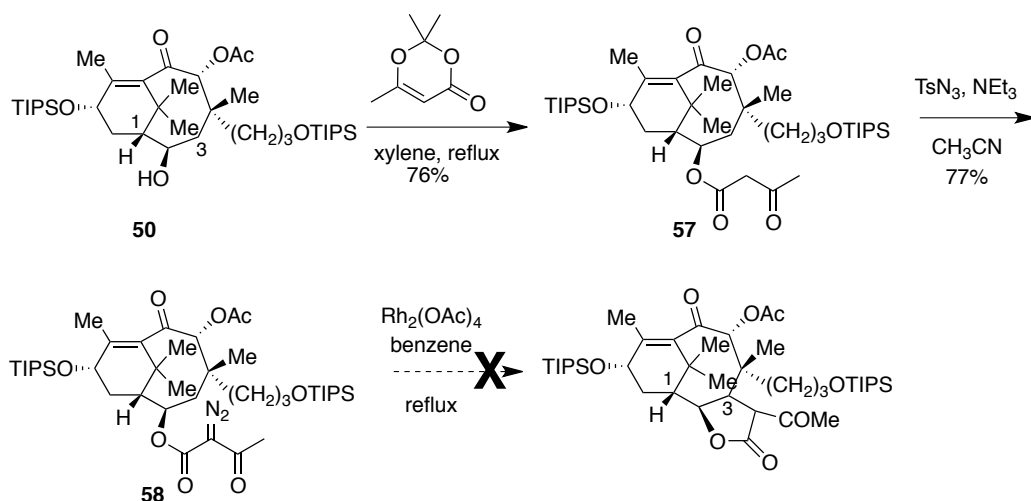
Figure 4.3 Rationale for the Stereoselective Reduction of the Diketone **45** and Relative Stereochemical Assignment of Diacetate **51**.

Treatment of the carboxylic acid with oxalyl chloride in the presence of 2,6-lutidine as base, followed by the addition of excess diazomethane, did not produce the desired diazo compound **55** (Scheme 4.21). The ^1H NMR spectrum of the crude product mixture did not display any useful peaks matching with the proposed compound. In an alternative approach, the carboxylic acid **54** was first converted to the corresponding mixed anhydride on treatment with ethyl chloroformate in the presence of triethylamine, followed by treatment with stoichiometric amount of diazomethane that produced the desired diazo ketone **55** in 63% yield over the two steps. With the key C-H insertion precursor in hand, the transition metal catalyzed cyclization was attempted using dirhodium tetraacetate in dichloromethane. Unfortunately, none of the expected cyclization products were observed. The only compound that was isolated after the reaction displayed a molecular ion peak in HRMS spectrum corresponding to a molecular formula matching with the structure of the alcohol **56**. It seemed that after diazo decomposition the metallocarbene intermediate had been trapped by moisture. However, rigorous removal of moisture did not lead to the desired transformation either.



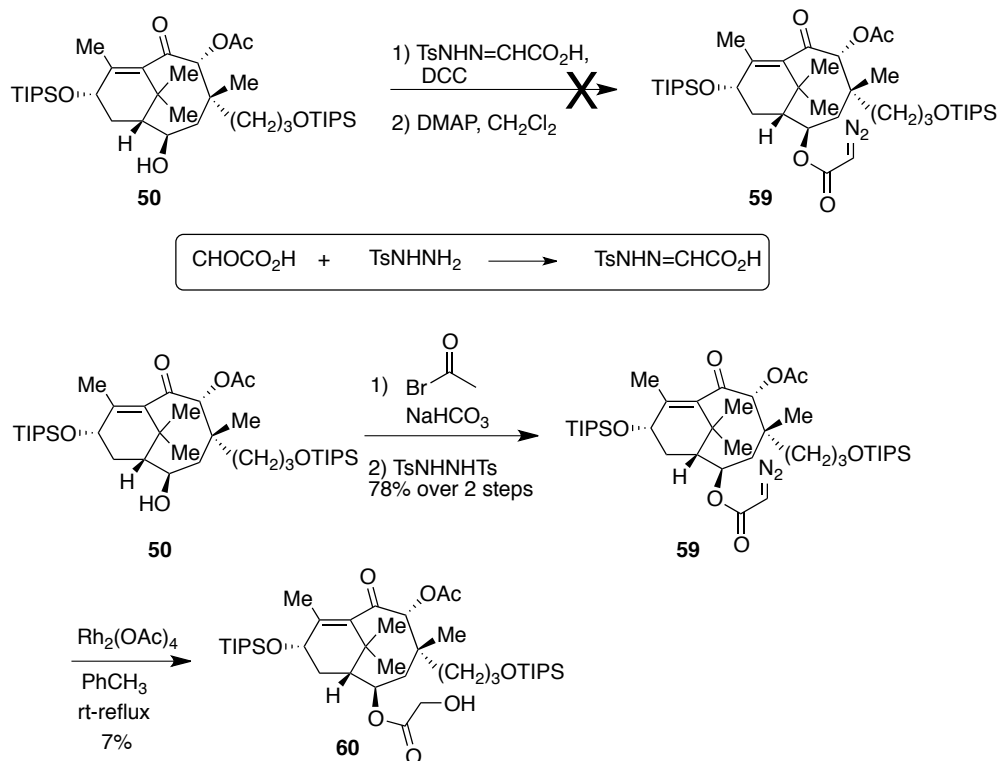
Scheme 4.21 Synthesis of Diazoketone **55** and Attempts at C-Ring Formation.

Failure of the C-ring construction approach under C-H insertion conditions using $\text{Rh}_2(\text{OAc})_4$ can be attributed to the inherent difficulty of the six-membered ring formation under transition metal catalyzed conditions.³⁷ Moreover, the conformation of the eight-membered ring may not allow the metallocarbene to attain the requisite geometry to undergo cyclization.³⁴ We now considered functionalizing the C3 position via intramolecular C-H insertion through an intermediate like **58** (Scheme 4.22). However, the possibly competitive C-1 functionalization could be of major concern in this method. Compound **50** was treated with the diketene acetone adduct (2,2,6-trimethyl-4*H*-1,3-dioxin-4-one) in presence of triethylamine as base to furnish β -ketoester **57** in 76% yield. Under Regitz diazo transfer conditions the diazo ketoester **58** was formed in 30% yield. Unfortunately, treatment of the diazo compound to rhodium catalyst under refluxing benzene conditions did not lead to any desired transformation.



Scheme 4.22 An Alternate Approach to C3 Functionalization.

We then attempted to prepare the diazo ester instead. When compound **50** was treated with (2*E*)-{[(4-methyl phenyl)sulfonyl]hydrazono}ethanoic acid in the presence of DCC followed by further treatment with DMAP, the desired ester was not observed which led us to move to an alternate route (Scheme 4.23). Compound **50** was first converted to an α -bromo acetate, which when treated with *N,N'*-ditosylhydrazine furnished the corresponding diazoacetate **59** successfully in 78% yield over two steps. Treatment of compound **59** with Rh₂(OAc)₄ under a range of conditions provided no fruitful result. Proton signals corresponding to a α -hydroxy ester **60** were only observed in the ¹H NMR spectrum. The HRMS spectrum also provided a molecular ion peak that corresponded to the molecular formula predicted for compound **60**. Unfortunately, due to the small quantity of material available in hand no other conditions could be attempted. At this stage, our investigation with intramolecular C-H insertion mediated C-ring formation remained inconclusive.

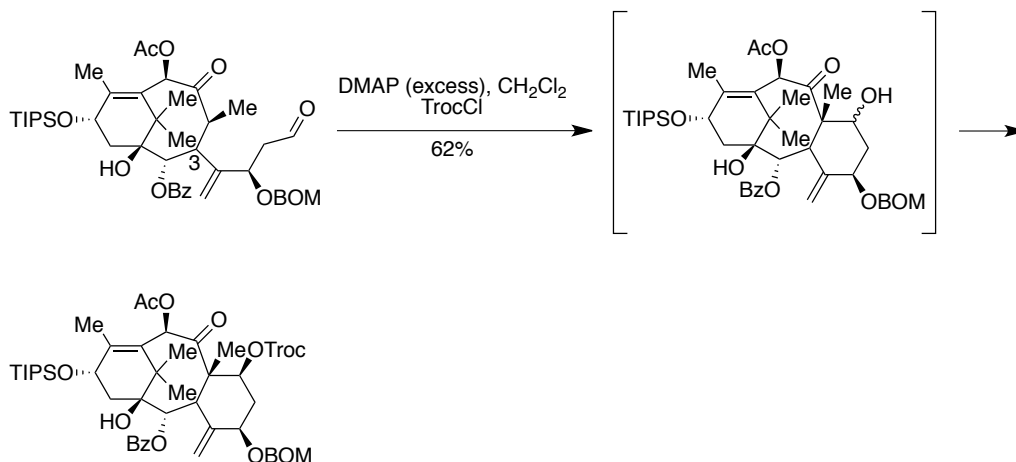


Scheme 4.23 Attempts at the Synthesis of the Diazo Ester **59** and Its Further Elaboration.

4.4.2. Further Attempts at Early Stage C-3 Functionalization of the Taxane Skeleton (Joy)

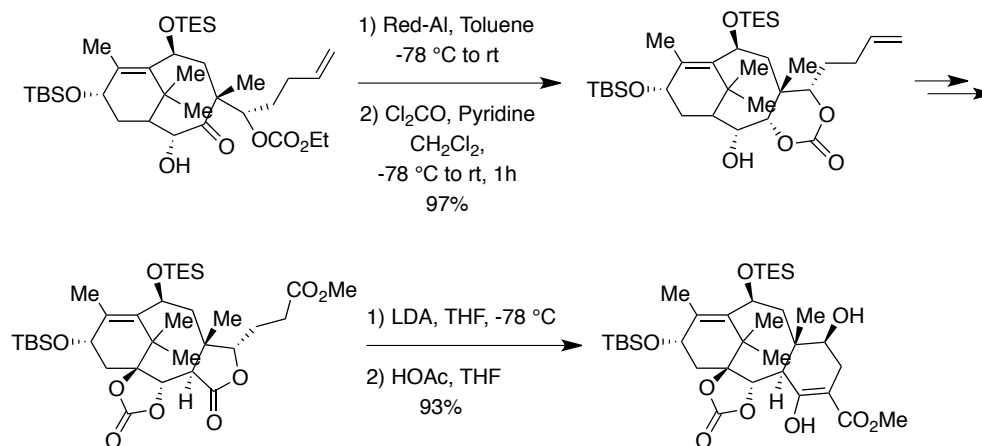
A late stage C-ring formation approach has been a popular strategy in the synthetic studies toward the taxane skeleton of several groups. A key feature to be highlighted here is the fact that most of these routes involved an early functionalization at C3 that was utilized at a later stage for the six-membered ring construction. The strategy used by the Wender group in the elaboration of the AB bicyclic precursor to the ABC tricyclic core was based on a mild aldol cyclization of the AB-bicyclic ketoaldehyde (Scheme 4.24).³⁸ The feasibility of the key aldol cyclization was explored on the AB-bicyclic ketoaldehyde that had a properly functionalized C3 tether. Molecular modeling studies have indicated that the ketoaldehyde possessed the correct B ring conformation placing the C8 hydrogen

in superior alignment with the C9 carbonyl to affect the desired deprotonation.^{38b} In accordance with the theoretical study, exposure of the ketoaldehyde to excess DMAP in dichloromethane provided an epimeric mixture of cyclized alcohols at C7 which, on further treatment with TrocCl, cleanly provided the desired tricyclic product as a single diastereomer.



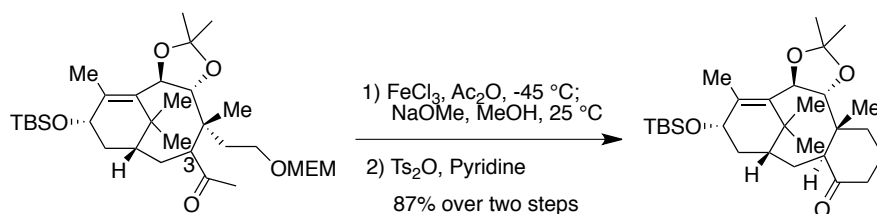
Scheme 4.24 Wender's Route to the Late Stage C-Ring Annulation Using a C3 Tether.

The Holton group had a similar linear strategy during their synthetic endeavor towards paclitaxel (Scheme 4.25).³⁹ According to their synthetic strategy, a late stage intermediate, AB-bicyclic hydroxyl carbonate was subjected to the reducing condition using Red-Al to furnish the triol which, without isolation was converted to the carbonate in excellent yield. The carbonate was then carried through a few steps of functional group modifications to attain the key synthetic intermediate with the correct regio- and stereochemistry of C1, C2, C3, C7, C8, C13 and A-ring olefin. The carbonate was finally subjected to a Dieckmann cyclization protocol using LDA, THF at -78 °C followed by treatment with HOAc in THF to accomplish the cyclization. The enol tautomer of the β -ketoester was formed cleanly with a 93% yield thus establishing the ABC tricyclic core of the natural product paclitaxel.



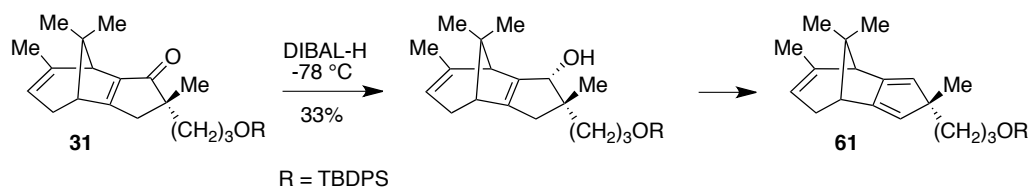
Scheme 4.25 Holton's Strategy for the Construction of the C-Ring.

Taxusin is another tricyclic taxoid natural product whose total synthesis was accomplished by Holton and coworkers in 1988 (Scheme 4.26).⁴⁰ The synthetic route involved a late stage C-ring annulation using appropriately installed C3 and C8 tethers. The bicyclic compound with a keto group at C3 and a two-carbon MEM ether was the chosen cyclization intermediate. Removal of the MEM group provided a mixture of hemiketal and hydroxyketone, which through an unstable tosylate was converted to the tricyclic ketone, thus installing the C-ring of taxusin.



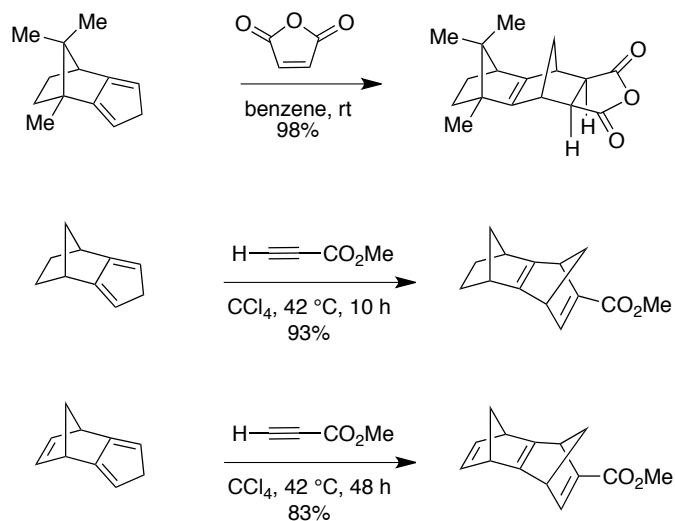
Scheme 4.26 Late Stage C-Ring Annulation Strategy Of the Holton Group Toward the Total Synthesis of Taxusin.

From our synthetic attempts toward the synthesis of the ABC tricyclic core of taxinine we have also learnt that the presence of a bulky C3 functionality might cause serious difficulties during the installation of the tetrasubstituted olefin employing a selenoxide elimination strategy. On the other hand, absence of C3 functionality when the B-ring has already been installed was found to be problematic for C-ring installation through a C-H insertion strategy. This could be attributed to the conformational preference of the eight-membered ring that might not allow the attainment of the seven-membered transition state required for C-H insertion. At this point we thought that the tricyclic diene **61** might be a potential substrate for simultaneous C3 functionalization and tetrasubstituted olefin installation. During the course of our synthesis we observed that the stereoselective enone formation was often complicated by the formation of a much less polar UV-inactive product. This product was identified as the diene compound **61** (Scheme 4.27). It was found that the extent of diene formation was dependent on the acidity of the reaction conditions. The formation of the diene can be attributed to the activation of the alcohol by the residual acidic components derived from DIBAL-H in dichloromethane, leading to elimination. The amount of diene formation was also found to vary with the nature of DIBAL-H solution used: DIBAL-H in dichloromethane afforded the diene as the major product, while DIBAL-H in hexanes provided the allylic alcohol with traces of the diene. The time was also crucial for the reaction. We observed that diene formation increases with time and when the reaction mixture is left for more than 20-25 min there is a rapid conversion of the allylic alcohol to the diene. We envisioned that the diene could be exploited for C3 functionalization. One possible way to utilize the diene to install C3 functionality could be through a hetero-Diels Alder reaction.



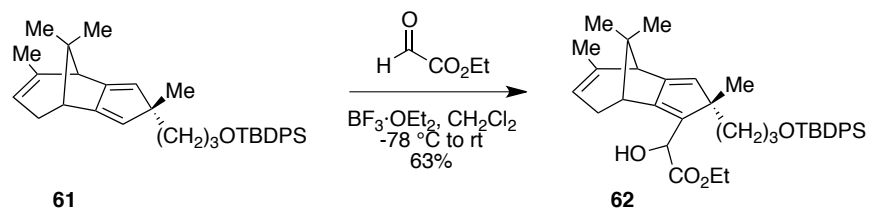
Scheme 4.27 Formation of a Diene Byproduct **61** Under DIBAL-H Reduction of Cyclopentenone **31**.

Paquette and coworkers have performed an extensive study on the stereoselectivity of the Diels-Alder additions to norbornyl and norbornenyl-fused diene systems. The extent and direction of π -facial stereoselectivity as a function of the bicyclic system fused to the diene framework constituted a key part of the study.⁴¹ It has been found that most dienophiles attack the isodicyclopentadienes with predominant *endo* selectivity and similar facial selectivity was also observed for the dihydro derivative (Scheme 4.28).⁴² The stereochemistry of the Diels-Alder addition of a few other isodicyclopentadienes was also explored where they no longer possess the norbornane framework.³⁹ In those examples, Diels-Alder additions occurred through the sterically less encumbered top face in absence of other directive effects.



Scheme 4.28 π -Facial Selectivity in the Diels-Alder Reactions of Isodicyclopentadienes.

The π -facial selectivity of an isodicyclopentadiene of the type **61** that we had in hand was yet to be elucidated. We therefore chose to explore its reactivity with a number of partners. The first dienophile that was chosen for the hetero Diels-Alder reaction was ethyl glyoxalate, a common dienophile for this type of chemistry (Scheme 4.29). When diene **61** was treated with the chosen dienophile under the standard conditions using $\text{BF}_3 \cdot \text{OEt}_2$ in dichloromethane at -78°C followed by warming to room temperature, the starting material was found to be consumed after 30 min and a new spot appeared on the TLC plate. After work-up, isolation and complete spectral analysis the compound was determined to be a formal ene reaction product **62**. ^1H NMR data revealed the disappearance of one of the diene protons around 5.49 ppm. More information on the structure was obtained from two-dimensional NMR study (HMBC), which showed that the proton at 6.10 ppm correlated with the carbon at C11 thereby confirming the structure to be **62** (Figure 4.4).



Scheme 4.29 A Surprising Reactivity of the Isodicyclopentadiene **61** in Presence of Ethyl Glyoxalate as Dienophile.

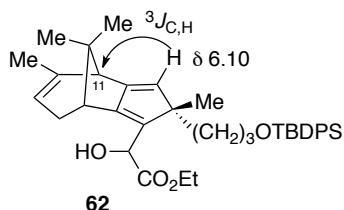
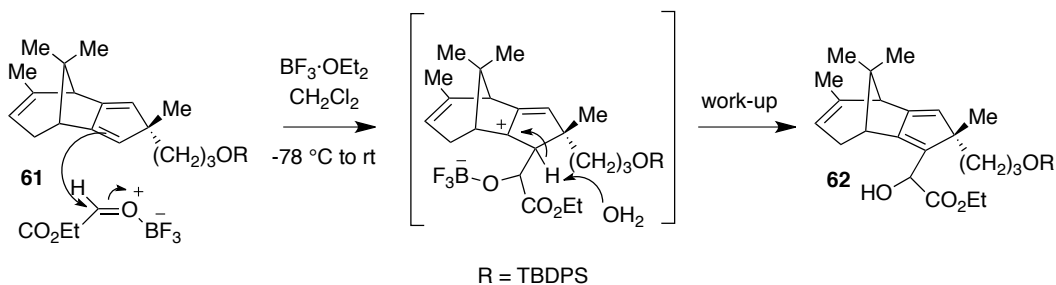


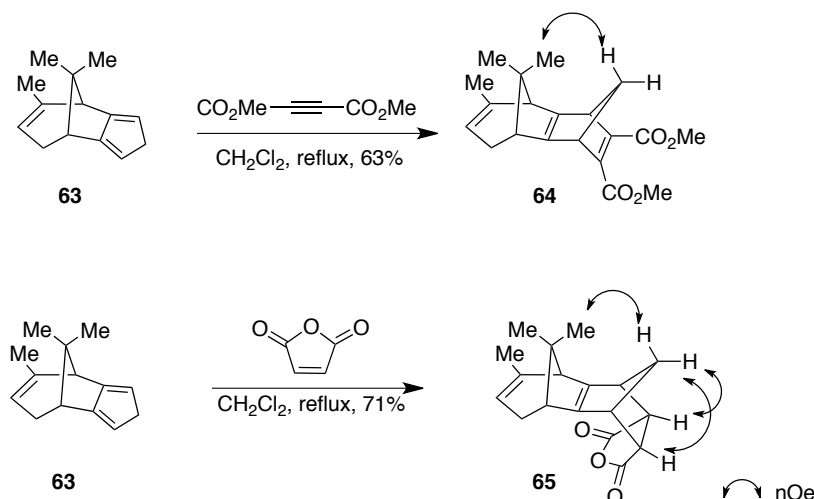
Figure 4.4 Structural Assignment of Compound **62** Based on HMBC Correlations.

The unusual reactivity and regioselectivity of the reaction was highly intriguing. The reaction obviously did not follow the usual course of a hetero Diels-Alder reaction and the diene moiety remained intact at the end of the process. It could possibly follow the course of a regioselective ene-type reaction⁴³ or a Prins-type reaction (Scheme 4.30). The rationale for the observed regioselectivity of this process is however unclear to us.



Scheme 4.30 A Plausible Mechanism for the Formation of the Adduct **62**.

With this interesting result we decided to further explore the reactivity and facial selectivity of this type of isodicyclopentadiene. This is an obvious deviation from our original course of study toward taxinine synthesis; the exploration seemed to be worthwhile nevertheless. To this end, isodicyclopentadiene **63** was treated to a few dienophiles that are frequently used in the study of Diels-Alder reactions (Scheme 4.31). An efficient method of synthesis of the isodicyclopentadiene has been described later in this chapter (See schemes 4.34 and 4.35). At first, the diene **63** was treated with DMAD as the dienophilic source. To a solution of DMAD dissolved in dichloromethane at -30 °C a solution of the diene **63** was added in drop wise fashion. After warming to room temperature, formation of a single product was observed. The adduct **64** was isolated as a single diastereomer. The dienophile as expected underwent reaction from the more accessible bottom face of the diene, avoiding the steric interaction from the bridging methyl groups.⁴⁴ The other dienophile that was tested was maleic anhydride, which when treated with **63** under standard reaction conditions furnished the adduct **65** in 71% yield with similar stereoselectivity. The relative stereochemistry of the two adducts **64** and **65** could be ascertained by detailed analysis of 2D TROESY and ¹³C NMR spectral data (Figure 4.5). Both the dienophiles displayed exclusive below-plane stereoselectivity. The distinctive chemical shifts in the ¹³C NMR spectrum offered further evidence for the *syn*-stereoselectivity of the adduct **64** where the bridgehead methylene carbon resonates at 70.6 ppm which closely resembles the data presented by the Paquette group for their DMAD adducts of several norbornyl-based isodicyclopentadienes.^{42b} Similarly, ¹³C NMR chemical shifts of the methylene bridgehead carbon (50.3 ppm) and the ethanobridge carbons (48.4, 47.8 ppm) of **65** matched closely to the ones observed for the *syn-endo* series of adducts during maleic anhydride addition to various isodicyclopentadienes.^{42b} These data together helped us to confirm the *endo* orientation of the maleic anhydride moiety.



Scheme 4.31 Diels-Alder Reactions of Isodicyclopentadiene **63** with DMAD and Maleic Anhydride as Dienophiles.

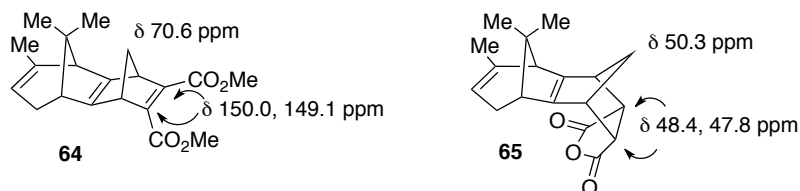
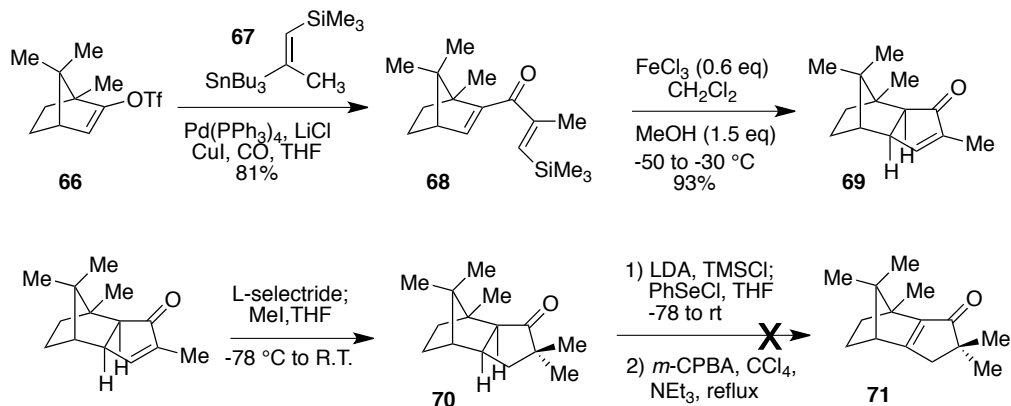


Figure 4.5 Selected ^{13}C NMR Chemical Shift Data of Bridgehead Carbons and Ethano Bridge Carbons of **64** and Ethano Bridge Carbons of **65**.

We decided to prepare camphor-based isodicyclopentadienes to compare the reactivity and stereoselectivity with the isodicyclopentadienes **61** or **63**. We envisioned a similar route for the synthesis of these two involving carbonylative Stille coupling to form the divinyl ketone followed by a Nazarov cyclization to install the five membered ring (Scheme 4.32). The camphor-based dienone **68** was synthesized smoothly from the palladium mediated coupling of the vinyl stannane **67** and camphor enol triflate **66** in 81% yield. Subsequent Nazarov cyclization of the dienone in presence of FeCl_3 as the Lewis acid promoter gave the cyclopentenone **69** in excellent yields with exclusive formation of the *exo* isomer. The tetrasubstituted olefin was required to be installed at this stage.

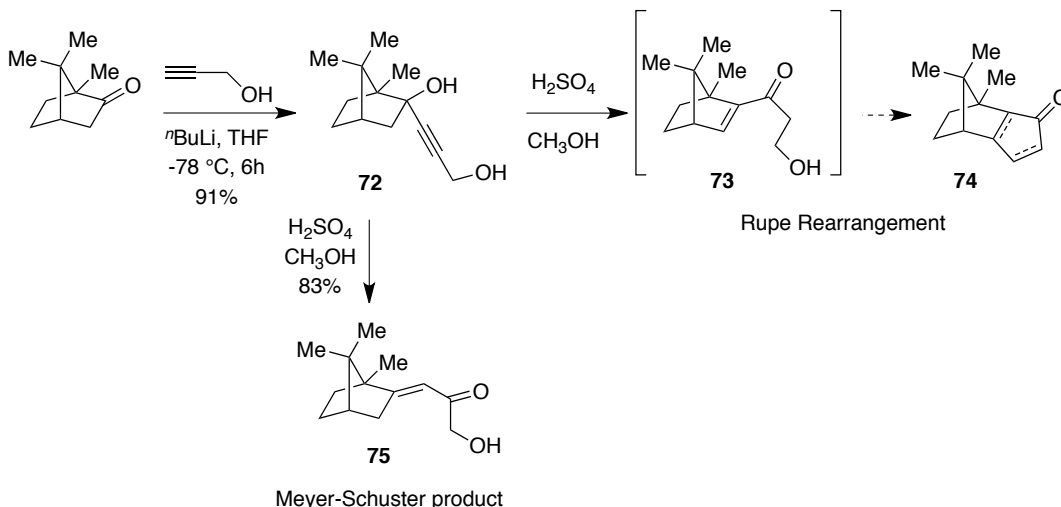
Unfortunately, all attempts at α -selenation failed completely. PhSeCl could not trap the trimethylsilyl enolether of the ketone **70**. The steric demand of the bottom face of the ketone might restrict the approach of a bulky group like phenylselenenyl. Unfortunately, this route had to be dismissed at this stage for the synthesis of camphor-based cyclopentenones **71**.



Scheme 4.32 Attempts at the Synthesis of Cyclopentenone **71**.

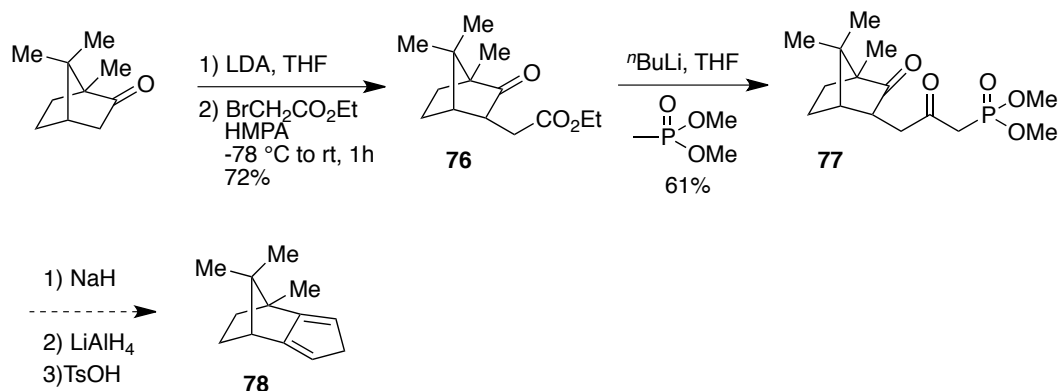
At this point we focused on exploring alternate routes to access the cyclopentenones of type **74**. As a first alternative, Rupe rearrangement of bridged bicyclic propargylic alcohol **72** appeared to be a promising protocol (Scheme 4.33).⁴⁵ Compound **72** was prepared by addition of propargylic alcohol to a solution of the camphor in THF in presence of *n*-BuLi at -78 °C. Propargylic alcohol **72** was then treated with concentrated sulfuric acid in methanol. The reaction went to completion cleanly, leading to a single product. However, spectral data analysis did not indicate the formation of the desired cyclopentenone **74**. The IR spectrum showed the presence of an alcohol group along with a carbonyl moiety. After an initial ^1H NMR spectral analysis we thought that the reaction might have stopped at an intermediate step forming compound **73**. However, detailed spectral analysis confirmed that there was only one CH_2 group present between the carbonyl and the hydroxyl groups. From all these available

data, the structure was revised to be α -hydroxy ketone **75**, a result of Meyer-Schuster rearrangement.⁴⁶



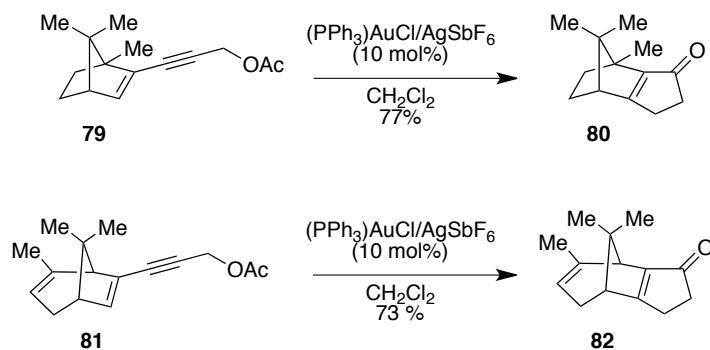
Scheme 4.33 Alternate Attempt at Cyclopentenone **74** Formation.

Volhardt and coworkers, during their study on enantiomerically pure cyclopentadienylmetal complexes, had demonstrated a strategy for the synthesis of similar dienes (Scheme 4.34).⁴⁷ We followed their protocol for the synthesis of isodicyclopentadiene using camphor as the initial model compound. To this end, we carried out an initial alkylation of camphor using ethyl bromoacetate in the presence of HMPA as an additive. Ketoester **76** was formed in 72% yield and was then treated directly with the lithium salt of dimethyl methyl phosphonate that led to the formation of the phosphonate **77**. However, these steps were found to be irreproducible on larger scale, which led us to venture to other possible routes to the desired dienes **78**. NaH mediated cyclization to the cyclopentenone, followed by installation of the olefin under acidic conditions was not explored any further.



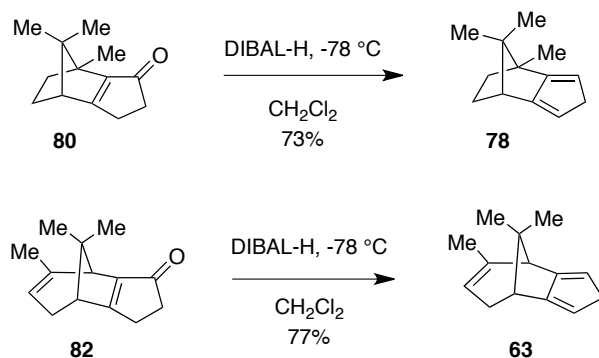
Scheme 4.34 Volhardt's Protocol for the Synthesis of Camphor-Based Diene.

Au(I) catalyzed tandem cyclization reactions of enynylacetates have been demonstrated to be a powerful tool for cyclopentenone synthesis.⁴⁸ We envisioned that in presence of Au(I) catalyst, a camphor-based bridged bicyclic enynyl acetate might also participate in a domino reaction process to give access to fused cyclopentenone with the desired olefin regioisomer in a step-economic fashion. When the enynyl acetate **79** was subjected to (PPh₃)AuCl/AgSbF₆ system the only product that was isolated was the more substituted cyclopentenone isomer **80** as the exclusive regioisomer (Scheme 4.35). This was a highly promising result as the cyclopentenone with a tetrasubstituted olefin is formed directly, which has otherwise been difficult to synthesize under the previous protocol. A similar strategy was also followed for the synthesis of cyclopentenone **82**. As expected, the unsubstituted enynyl acetate **81** reacted cleanly under Au(I) conditions furnishing the more substituted cyclopentenone **82** in good yields. The present domino cyclization strategy also looked promising as an alternate route to the tetrasubstituted olefin containing cyclopentenone intermediate toward taxinine total synthesis. The Au(I) mediated tandem cyclization of bridged bicyclic enynyl acetates has already been discussed in detail in Chapter 2.



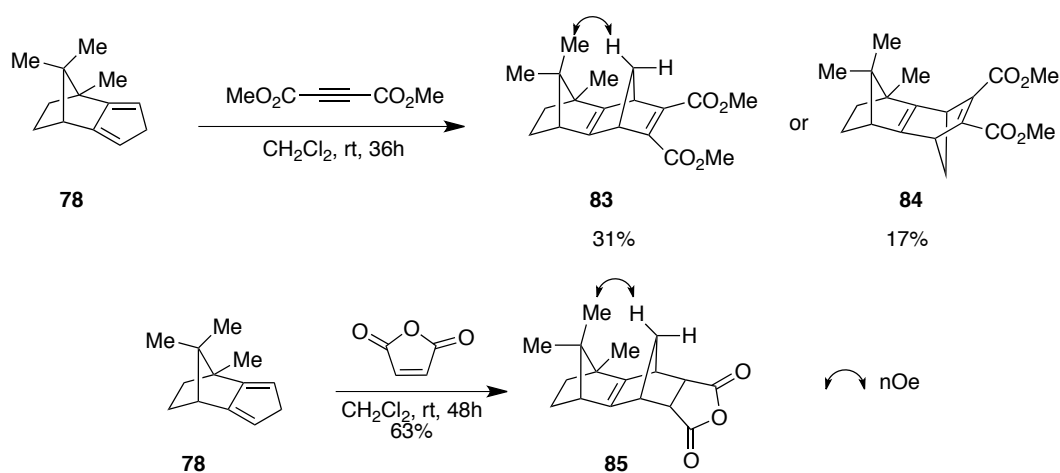
Scheme 4.35 Au(I) mediated Tandem Cyclization for the Synthesis of Cyclopentenones.

The tandem Au(I) catalyzed protocol provided a fast and efficient access to the highly strained bridged bicyclo-fused cyclopentenones. Conversion of the cyclopentenones to the corresponding isodicyclopentadienes required eliminative conditions. As has been observed for compound **31** or **42**, compounds **80** and **82** also furnished the corresponding dienes **78** and **63** under DIBAL-H mediated conditions (Scheme 4.36). Alternatively, a step wise procedure involving NaBH_4 mediated reduction of the ketone followed by elimination in presence of *p*-toluenesulfonic acid also furnished the same products in moderate to good yields.



Scheme 4.36 Conversion of the Cyclopentenones to the Isodicyclopentadienes Under DIBAL-H Mediated Conditions.

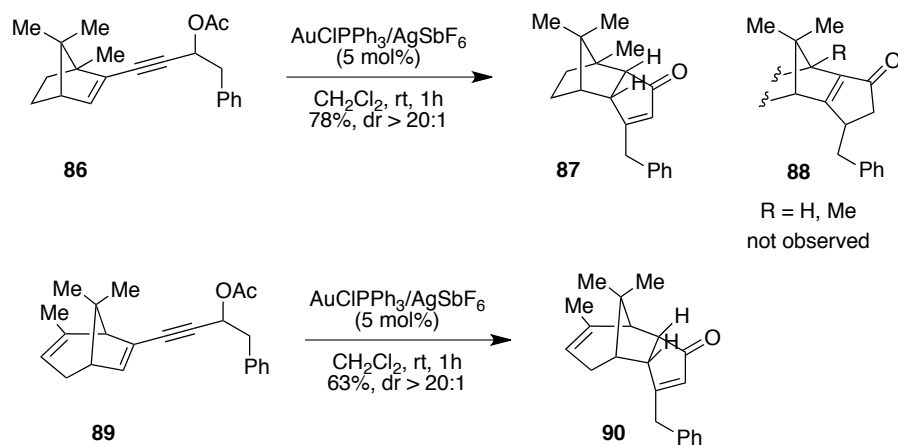
Camphor-based isodicyclopentadienes were then subjected to Diels-Alder reactions in presence of some common dienophiles (Scheme 4.37). Initially camphor-based isodicyclopentadienes were found to undergo rapid polymerization due to the extremely reactive nature of these dienes. These types of dienes have also been demonstrated to undergo facile [1,5]-hydride shifts, which could also be another potential side reaction under these conditions.⁴⁹ We modified the reaction conditions by employing excess of the dienophile. Isodicyclopentadiene **78** reacted with DMAD forming a mixture of *endo* and *exo* isomers (**83** and **84** respectively), *endo* isomer being the predominant product. A similar reactivity profile was observed for the reaction with maleic anhydride furnishing **85** as the only isolable isomer.



Scheme 4.37 Diels-Alder Reactions of Isodicyclopentadiene **78**.

We also attempted to prepare β -substituted cyclopentenones that can subsequently be converted to the corresponding dienes under DIBAL-H conditions. We envisioned that the presence of substituents might restrict [1,5]-hydride shifts in case of isodicyclopentadienes and lead to cleaner adduct formation. Bridged bicyclic enynyl acetates with benzyl substituent at C5 position were prepared (details of the preparation have been provided in Chapter 2). When the enynyl acetate **86** was subjected to the $(\text{PPh}_3)\text{AuCl}/\text{AgSbF}_6$ system

in dichloromethane as solvent, cyclopentenone **87** was formed exclusively through a [1,2]-hydride shift as the penultimate step of the tandem cyclization procedure (Scheme 4.38).⁴⁸ Similarly, cyclopentenone **90** was formed through Au(I) catalyzed tandem cyclization of the C5 substituted enynyl acetates **89** with similar regioselectivity. The scope of the Au(I) catalyzed reaction was found to be limited to the synthesis of cyclopentenones containing the tetrasubstituted olefin when there is no C5 substituent in the starting enynyl acetate. Direct access to cyclopentenones of type **88** failed under the present conditions, which in turn hindered further investigation of the corresponding dienes due to the lack of an efficient synthetic protocol.



Scheme 4.38 Au(I) Catalyzed Cyclization of C5-Substituted Enynyl Acetates

4.5 Conclusion

Our efforts toward the synthesis of taxinine have been unveiled here. Our work began with the goal of introducing functionality at the C3 position of the taxane skeleton to allow C-ring closure. Previous approaches from this group have involved attempts at early incorporation of the six-membered C-ring, and late stage annulation. The first method caused serious challenges in the later intermediates for certain key synthetic manipulations. The AB bicyclic skeleton of

taxane could be accessed easily through the later linear route; however the conformational preference of the eight-membered B-ring did not allow closure of the six-membered C-ring via enolization. The third strategy involved an early C3 functionalization of the taxane core, but further functionalization proved to be difficult due to the steric encumbrance in the resulting intermediates.

With the failure of the above approaches, we decided to investigate a late stage C3 functionalization via intramolecular C-H insertion chemistry. This route seemed to be particularly promising because it does not require any prior activation of the targeted C-H bond. However, proper choice of protecting groups proved to be extremely critical for the preparation of the β -keto ester intermediate. Unfortunately, no cyclization product could be obtained by treating a C8 tethered diazo compound with $\text{Rh}_2(\text{OAc})_4$. Attempts toward C3 functionalization through an alternate C2 tethered diazo compound also met with failure. So far, introduction of a functional group at C3 position has proven to be a difficult task due to the conformational preference of the eight-membered ring that may not allow certain geometry required for the C-H insertion chemistry.

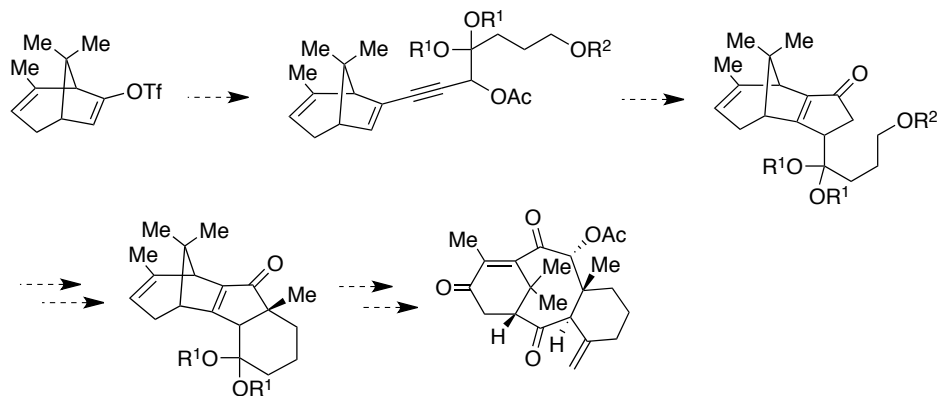
During our synthetic endeavor toward taxinine we became interested in exploring the reactivity of a diene that was formed as a side product in one of the key reactions. We expected to utilize the diene in an attempt to introduce functionality at C3 position after installation of the C2-C10 tetrasubstituted olefin. Some interesting reactivity and π -facial selectivity was observed for the diene during the course of this study. An intriguing ene-type reaction was observed on treatment of the diene with ethyl glyoxalate solution under hetero Diels-Alder type conditions.

We also looked into other possible avenues to the tetrasubstituted olefin containing cyclopentenone intermediate that might later allow an easy access to C3 functionalization and lead to a more concise synthetic route. Au(I) catalyzed

tandem cyclization of the bridged bicyclic enynyl acetate furnished the desired cyclopentenone cleanly. This protocol seemed to be highly promising as it was more step economical, leading to a cyclopentenone with the tetrasubstituted olefin being installed. However, for the purpose of taxinine synthesis we required a proper substituent at the propargylic position, which would later turn into the C3 functionality. Unfortunately, the substituted enynyl acetate led to the other cyclopentenone isomer exclusively.

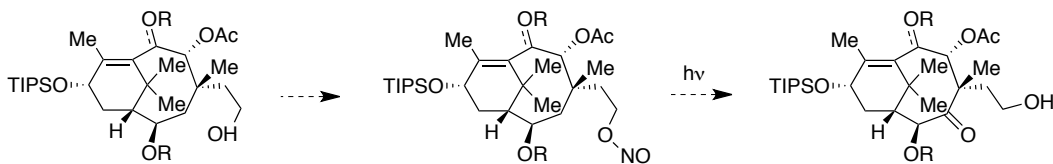
4.6 Future Plans

Au(I) catalyzed tandem protocol involving a Nazarov cyclization is a highly efficient protocol for cyclopentenone synthesis from a relatively simpler starting material. We have already demonstrated in Chapter 2 that bridged bicyclic enynyl acetate can also participate in these reactions to furnish cyclopentenones readily (Scheme 4.39). This protocol may allow C3 functionalization at an early stage. The olefin can also be installed at the C2-C10 positions under base mediated isomerization conditions, which should favor the more thermodynamic product. From here, oxidative cleavage to form the AB bicyclic core of the taxane skeleton, followed by proper manipulation of the C3 tether should provide us avenues to explore the C-ring anulation.



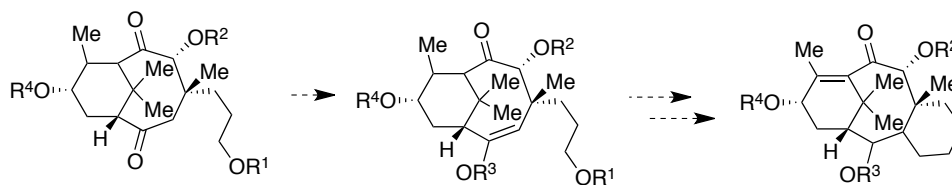
Scheme 4.39 Accessing the Six-Membered C-Ring Via an Early Stage C3 Functionalization.

The absence of C3 functionality has proved to be a major road block in the construction of the six-membered C-ring at the later stage of the synthesis. A carbonyl functionality may be installed through a Barton reaction⁵⁰ on an AB bicyclic intermediate which would then provide us a handle for C-ring annulation (Scheme 4.40).



Scheme 4.40 A Late Stage C3 Functionalization through Barton Reaction.

Alternatively, pyramidalizing the C11-C12 bridgehead olefin via reduction should induce conformational change within the eight-membered ring of the bicyclic intermediate. Annulation of the C-ring through an aldol type protocol could then be attempted (Scheme 4.41). Should positive results be obtained, it may be possible to construct the C-ring prior to the installation of the bridgehead olefin.



Scheme 4.41 Accessing the C3 Enolate via Conformational Change of the Eight-Membered B-ring.

4.7 Experimental

4.7.1. General Information

Reactions were carried out in flame-dried glassware under a positive argon atmosphere unless otherwise stated. Transfer of anhydrous solvents and reagents was accomplished with oven-dried syringes. Solvents were distilled before use: methylene chloride and 1,2-dichloroethane from calcium hydride, tetrahydrofuran from sodium/benzophenone ketyl. All other solvents and commercially available reagents were either purified by standard procedures or used without further purification. Thin layer chromatography was performed on glass plates precoated with 0.25 mm silica gel; the stains for TLC analysis were conducted with 2.5 % *p*-anisaldehyde in AcOH-H₂SO₄-EtOH (1:3:85) and further heating until development of color. Flash chromatography was performed on 230-400 mesh silica gel with the indicated eluents.

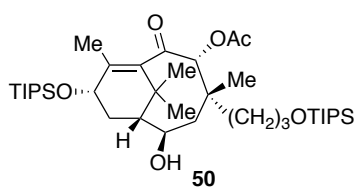
Proton nuclear magnetic resonance spectra (¹H NMR) were recorded at 300, 400 MHz or 500 MHz and the chemical shifts are reported on the δ scale (ppm) and the spectra are referenced to residual solvent peaks: CDCl₃ (7.26 ppm, ¹H; 77.06 ppm, ¹³C), or CD₃OD (3.31 ppm, ¹H; 49.00 ppm, ¹³C) as internal standard. Coupling constants (*J*) are reported in Hz. Second order splitting patterns are indicated. Splitting patterns are designated as s, singlet; d, doublet; t, triplet; q, quartet; m, multiplet; br, broad; dd, doublet of doublets, dt, doublet of

triplets, etc. Carbon nuclear magnetic resonance spectra (^{13}C NMR) were recorded at 100 MHz or 125 MHz and chemical shifts are accurate to one decimal place. Infrared (IR) spectra were measured with a Nicolet Magna 750 FT-IR spectrometer and Nic-Plan FT-IR microscope. Mass spectra were determined on a Kratos Analytical MS-50 (EI) or Agilent 6220 oaTOF electrospray positive ion mode spectrometer (ESI).

All reagents and catalysts were purchased from Aldrich or Sigma or Strem and were used without further purification unless otherwise stated.

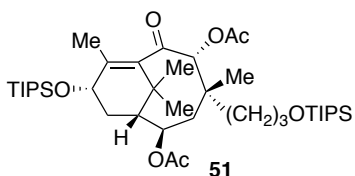
4.7.2. Experimental Procedures and Characterization of Compounds

Compounds **45**,¹⁷ **66**,¹⁸ **68**,¹⁸ **69**,^{19,20} **70**, **72**, **76**,⁴⁷ **77**,⁴⁷ **78**⁴⁷ and **83**,^{42b} **84**,^{42b} **85**^{42b} were synthesized by previously described procedures and our spectra matched closely with the ones reported in the literature. Synthesis and characterization of compounds **79-82** and **86-90** has been described in details in Chapter 2.



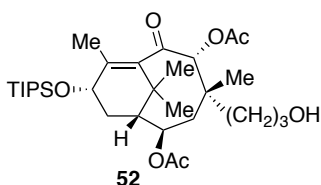
To a solution of diketone **45** (0.042 g, 0.066 mmol) dissolved in MeOH (0.7 mL) and cooled to 0 °C was added NaBH₄ (0.025 g, 0.066 mmol). The mixture was allowed to warm to room temperature and stirred for 2 h. The reaction was quenched by the addition of saturated aqueous Na₂SO₄ and diluted with CH₂Cl₂. The aqueous layer was then extracted with CH₂Cl₂ (3 x 3 mL) and the combined organic extracts were dried over MgSO₄, filtered and concentrated under reduced pressure. The crude residue was purified by column chromatography (30%

EtOAc in hexanes) to give the corresponding alcohol **50** as a white solid, 0.045 g (quantitative yield): $R_f = 0.31$ (20% EtOAc in hexanes); IR (neat) 3484, 2944, 2891, 2866, 1746, 1725, 1692, 1463, 1372, 1243, 1109 cm^{-1} ; ^1H NMR (600 MHz, CDCl_3) δ 5.83 (br s, 1H), 4.64 (br d, $J = 4.3$ Hz, 1H), 4.60 (d, $J = 9.8$ Hz, 1H), 3.75 (br s, 1H), 3.65-3.49 (m, 2H), 2.76-2.71 (m, 1H), 2.20 (s, 3H), 1.88 (br d, $J = 8.5$ Hz, 2H), 1.84 (s, 3H), 1.64-1.45 (m, 9H), 1.12-1.09 (m, 24H), 1.07-1.03 (m, 21H), 0.89 (s, 3H); ^{13}C NMR (125 MHz, CDCl_3 , 15 overlapping sp^3 -Cs corresponding to the TIPS group) δ 198.7, 169.8, 143.1, 141.1, 84.6, 77.8, 67.4, 63.9, 44.4, 40.9, 37.1, 32.4, 29.7, 27.0, 21.5, 20.6, 18.2, 18.1, 18.0, 17.9, 16.7, 12.7, 12.0; HRMS (ESI, $[\text{M}+\text{Na}]^+$) Calcd for $\text{C}_{38}\text{H}_{72}\text{O}_6\text{Si}_2\text{Na}$ m/z 703.4759; found m/z 703.4757.

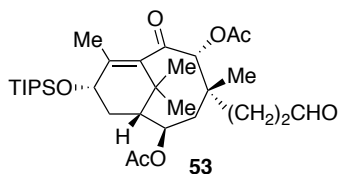


The alcohol **50** (0.038 g, 0.059 mmol) was dissolved in CH_2Cl_2 (0.2 mL). DMAP (0.0004 g, 0.003 mmol) was then added, followed by Ac_2O (75 μL , 0.71 mmol) and NEt_3 (165 μL , 1.18 mmol). The mixture was allowed to stir for 12 h, and then quenched by the addition of 0.3 M HCl (1.0 mL). The aqueous layer was extracted with CH_2Cl_2 (3 x 2 mL). The combined organic fractions were then dried (MgSO_4), filtered and concentrated under reduced pressure. The crude residue was then purified by flash column chromatography (20% EtOAc in hexanes) to give the acetate **51** as a white solid, 0.031 g (71% yield): $R_f = 0.62$ (20% EtOAc in hexanes); IR (neat) 2944, 2891, 2866, 1743, 1700, 1463, 1369, 1236, 1094 cm^{-1} ; ^1H NMR (600 MHz, CDCl_3) δ 6.02 (brs, 1H), 4.64 (s, 1H), 4.60 (d, $J = 9.8$ Hz, 1H), 3.61-3.49 (m, 2H), 2.80-2.72 (m, 1H), 2.17 (s, 3H), 2.04 (s, 3H), 1.85 (s, 3H), 1.68-1.63 (m, 2H), 1.55 (s, 3H), 1.50-1.40 (m, 4H), 1.37-1.34 (m, 1H), 1.23-1.20 (m, 1H), 1.07-1.01 (m, 45H), 0.97 (s, 3H); ^{13}C NMR (125 MHz, CDCl_3 , 16 overlapping sp^3 -Cs

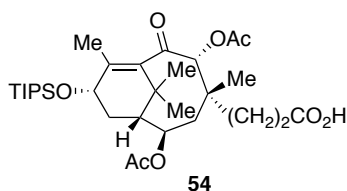
corresponding to the TIPS group) δ 198.7, 170.6, 169.8, 143.6, 141.1, 84.6, 67.8, 65.4, 63.9, 44.4, 40.9, 37.1, 36.6, 32.4, 27.0, 21.5, 24.6, 20.6, 18.2, 18.1, 17.9, 16.7, 15.2, 12.7, 11.9; HRMS (ESI, $[M+Na]^+$) Calcd for $C_{40}H_{74}O_7Si_2Na$ m/z 745.4865; found m/z 745.4860.



The diacetate **51** (0.023 g, 0.041 mmol) was dissolved in CH_3CN (0.5 mL) at room temperature in a polypropylene vial. To this was added 180 μ L of a 1.1 M solution of HF/pyridine (0.16 mmol). The mixture was allowed to stir for 48h and was quenched by the addition of saturated aqueous solution of $NaHCO_3$ (1.0 mL). The aqueous layer was extracted with Et_2O (3 x 5 mL) and the combined organic layers were then dried ($MgSO_4$), filtered and concentrated under reduced pressure. The crude residue was purified by flash column chromatography (40% EtOAc in hexanes) and gave the corresponding primary alcohol **52** as a colorless oil, 0.020 g (90% yield): R_f = 0.64 (20% EtOAc in hexanes); IR (neat) 3469, 2945, 2867, 1741, 1695, 1463, 1371, 1236, 1090 cm^{-1} ; 1H NMR (400 MHz, $CDCl_3$) δ 5.93 (br s, 1H), 5.01 (br s, 1H), 4.63 (d, J = 9.0 Hz, 1H), 3.60-3.52 (m, 2H), 2.81-2.12 (m, 2H), 2.22 (s, 3H), 2.10 (s, 3H), 2.07-1.93 (m, 1H), 1.91 (s, 3H), 1.54 (s, 3H), 1.49-1.44 (m, 3H), 1.22 (br s, 3H), 1.16-1.05 (m, 24H), 0.89 (s, 3H), (OH proton not detected); ^{13}C NMR (125 MHz, $CDCl_3$, 7 overlapping sp^3 -Cs corresponding to the TIPS group) δ 198.7, 170.6, 169.8, 143.5, 141.1, 84.6, 77.8, 67.1, 62.6, 44.4, 40.9, 37.1, 32.4, 29.7, 27.0, 21.5, 20.6, 18.2, 18.1, 18.0, 17.9, 16.7, 12.7, 12.3; HRMS (ESI, $[M+Na]^+$) Calcd for $C_{31}H_{54}O_7SiNa$ m/z 589.3531; found m/z 589.3530.

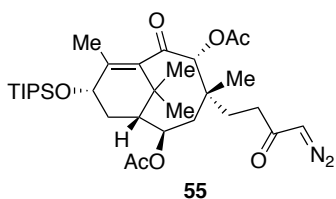


To a solution of the alcohol **52** (0.01 g, 0.015 mmol) in CH_2Cl_2 (0.4 ml) was added 4 Å molecular sieves and NMO (0.12 g, 0.11 mmol), followed by TPAP (0.006 g, 0.001 mmol). The mixture was stirred at room temperature for 15-20 min, and was subsequently filtered through a plug of silica with the aid of 30% EtOAc/hexanes (5 mL). The crude residue was then purified by flash column chromatography (20% EtOAc in hexanes) and gave **53** as colorless oil, 0.006 g (67% yield): $R_f = 0.64$ (20% EtOAc in hexanes); IR (neat) 2944, 2867, 2717, 1741, 1695, 1463, 1371, 1236, 1060 cm^{-1} ; ^1H NMR (400 MHz, CDCl_3) δ 9.71 (s, 1H), 5.97 (br s, 1H), 5.08 (br s, 1H), 4.61 (d, $J = 8.8$ Hz, 1H), 2.82-2.25 (m, 3H), 2.22 (s, 3H), 2.07 (s, 3H), 1.96-1.90 (m, 2H), 1.88 (s, 3H), 1.86-1.80 (m, 2H), 1.52 (s, 3H), 1.30-1.28 (m, 2H), 1.12-1.06 (m, 24H), 1.00 (s, 3H); ^{13}C NMR (125 MHz, CDCl_3 , 7 overlapping sp^3 -Cs corresponding to the TIPS group) δ 200.3, 198.7, 170.6, 169.8, 143.6, 141.1, 84.6, 77.8, 67.4, 44.4, 40.9, 37.1, 32.4, 29.7, 27.0, 21.5, 20.6, 18.2, 18.1, 18.0, 17.9, 16.7, 12.7, 12.3; HRMS (ESI, $[\text{M}+\text{Na}]^+$) Calcd for $\text{C}_{31}\text{H}_{52}\text{O}_7\text{SiNa}$ m/z 587.33749; found m/z 587.33745.



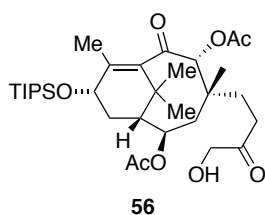
The aldehyde **53** (0.011 g, 0.023 mmol) was dissolved in 2-methyl-2-butene (1.0 mL) and *tert*-BuOH (2.0 mL) and cooled to 0 °C. A solution of NaClO_2 (0.003 g, 0.034 mmol) in aqueous NaH_2PO_4 (1M, 0.03 mL, 0.034 mmol) was then added to the stirred solution of the aldehyde. After 1 h, the reaction was quenched with citric acid (0.5 M, 3.0 mL), extracted with CH_2Cl_2 (3 x 4 mL), dried (MgSO_4) and

concentrated under reduced pressure. The crude residue was purified by flash column chromatography (40% EtOAc in hexanes) and afforded the carboxylic acid **54**, 0.010 g (79% yield): $R_f = 0.43$ (14% EtOAc, 85% hexanes and 1% AcOH); IR (neat) 3349, 2900, 1734, 1643, 1430, 1369, 1060, 1036 cm^{-1} ; ^1H NMR (400 MHz, CDCl_3) δ 5.93 (br s, 1H), 5.28 (br s, 1H), 4.62 (br d, $J = 8.5$ Hz, 1H), 2.85-2.78 (m, 1H), 2.33-2.31 (m, 2H), 2.22 (s, 3H), 2.08 (s, 3H), 1.98-1.89 (m, 1H), 1.87 (s, 3H), 1.84-1.78 (m, 1H), 1.57 (s, 3H), 1.52-1.48 (m, 2H), 1.36-1.26 (m, 2H), 1.15-1.06 (m, 24H), 1.00 (s, 3H), (COOH proton not detected); ^{13}C NMR (125 MHz, CDCl_3 , 7 overlapping sp^3 -Cs corresponding to the TIPS group) δ 198.7, 177.5, 170.6, 169.6, 143.4, 141.1, 84.3, 77.8, 67.4, 44.7, 41.2, 37.1, 32.7, 29.5, 27.3, 21.5, 20.6, 18.3, 18.1, 18.0, 17.9, 16.4, 12.7, 12.3; HRMS (ESI, $[\text{M}+\text{Na}]^+$) Calcd for $\text{C}_{31}\text{H}_{52}\text{O}_8\text{SiNa}$ m/z 603.33244; found m/z 603.33237.

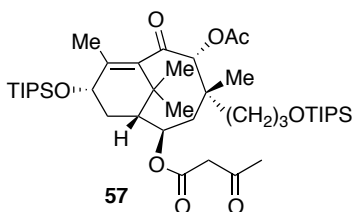


To a stirred solution of carboxylic acid **54** (0.057 g, 0.095 mmol) and triethylamine (1.8 μL , 0.0013 g, 0.013 mmol) in anhydrous diethyl ether (2 mL) was added ethyl chloroformate (1.1 μL , 0.0013 g, 0.012 mmol) dropwise, and the resulting solution was stirred for 2.5 h when a white precipitate formed. The solution of the anhydride was filtered under suction; the residue was washed with diethyl ether and then immediately added to a freshly prepared ethereal solution of diazomethane (~ 1.0 mmol) dropwise.⁵¹ The reaction mixture was stirred overnight and then quenched by addition of glacial acetic acid (5 mL), then poured into a solution of saturated aqueous solution of NaHCO_3 (5 mL) and stirred vigorously for 15 min. The aqueous phase was separated and extracted with ethyl acetate (3 x 5 mL). The combined organic extracts were washed with brine (5 mL), dried (MgSO_4) and concentrated under reduced pressure. The crude

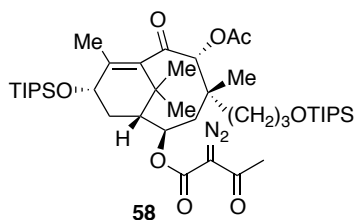
residue was purified by flash column chromatography (30% EtOAc in hexanes) and afforded the diazo ketone **55** as a yellow oil, 0.038 g (67% yield): $R_f = 0.72$ (20% EtOAc in hexanes); IR (neat) 3368, 2945, 2867, 2101, 1742, 1694, 1650, 1462, 1369, 1233 cm^{-1} ; ^1H NMR (500 MHz, CDCl_3) δ 5.97 (br s, 1H), 5.07 (br s, 1H), 4.62 (br d, $J = 10.0$ Hz, 1H), 4.26 (br s, 1H), 2.76-2.64 (m, 1H), 2.22 (s, 3H), 2.18-2.11 (m, 3H), 2.07 (s, 3H), 1.89 (s, 3H), 1.84-1.64 (m, 1H), 1.54 (s, 3H), 1.53-1.1.46 (m, 2H), 1.39-1.22 (m, 2H), 1.10-1.02 (m, 24H), 0.96 (s, 3H); ^{13}C NMR (125 MHz, CDCl_3 , 7 overlapping $\text{sp}^3\text{-Cs}$ corresponding to the TIPS group) δ 198.7, 186.3, 170.6, 169.8, 143.5, 141.1, 84.6, 77.8, 67.4, 46.2, 44.4, 40.9, 37.1, 32.4, 29.7, 27.0, 21.5, 20.6, 18.2, 18.1, 18.0, 17.9, 16.7, 15.2, 12.7, 12.1; HRMS (ESI, $[\text{M}+\text{Na}]^+$) Calcd for $\text{C}_{32}\text{H}_{52}\text{N}_2\text{O}_7\text{SiNa}$ m/z 627.34278; found m/z 627.34267.



To a solution of diazo ketone **55** (0.056 g, 0.076 mmol) in dry benzene (4.0 mL) under argon was added $\text{Rh}_2(\text{OAc})_4$ (0.001 g, 3 mol%) and the resulting mixture was heated to reflux for 3 h. After cooling to room temperature the solvent was removed under reduced pressure and the residue was then purified by flash column chromatography (40% EtOAc in hexanes) to afford **56** as pale yellow oil, in trace amount: $R_f = 0.29$ (20% EtOAc in hexanes); HRMS (ESI, $[\text{M}+\text{Na}]^+$) Calcd for $\text{C}_{32}\text{H}_{54}\text{O}_8\text{SiNa}$ m/z 617.3486; found m/z 617.3484.

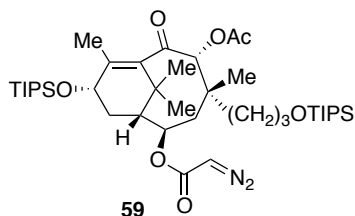


To a stirred solution of alcohol **50** (0.046 g, 0.072 mmol) in xylenes (3.0 mL) under argon, 2,2,6-trimethyl-4H-1,3-dioxin-4-one (34 μ L, 0.033 g, 0.237 mmol) was added. The flask was then fitted with a reflux condenser and placed in an oil bath preheated to 150 $^{\circ}$ C. After 45 min, the mixture was allowed to cool to room temperature and concentrated under reduced pressure. The crude residue was then purified by flash chromatography (35% EtOAc in hexanes) to afford the β -ketoester **57** as a pale yellow oil, 0.041 g (76% yield): $R_f = 0.30$ (20% EtOAc in hexanes); IR (neat) 2944, 2891, 2866, 2136, 1744, 1719, 1697, 1641, 1463, 1371, 1237, 1096 cm^{-1} ; ^1H NMR (500 MHz, CDCl_3) δ 5.89 (br s, 1H), 5.14 (br s, 1H), 4.63 (d, $J = 8.0$ Hz, 1H), 3.62-3.51 (m, 2H), 3.46 (s, 2H), 2.68 (s, 3H), 2.28 (s, 3H), 2.20 (s, 3H), 2.04-1.90 (m, 2H), 1.89 (s, 3H), 1.76-1.42 (m, 4H), 1.56 (s, 3H), 1.18-1.05 (m, 45H), 1.00 (s, 3H); ^{13}C NMR (125 MHz, CDCl_3 , 17 sp^3 -Cs are missing, of which 14 correspond to the TIPS groups) δ 199.2, 198.7, 170.6, 169.8, 143.3, 141.3, 83.6, 77.5, 67.1, 64.3, 44.4, 40.9, 37.1, 32.4, 29.7, 27.0, 21.5, 20.6, 20.3, 18.2, 18.1, 18.0, 17.9, 16.7, 12.7; HRMS (ESI, $[\text{M}+\text{Na}]^+$) Calcd for $\text{C}_{42}\text{H}_{76}\text{O}_8\text{Si}_2\text{Na}$ m/z 787.4974; found m/z 787.4970.



To a stirred solution of acetoacetate **57** (0.04 g, 0.05 mmol) in acetonitrile (3 mL) was added *p*-methylbenzene sulfonyl azide (0.011 g, 0.06 mmol) and the resulting solution was cooled to 0 $^{\circ}$ C. Triethylamine (7 μ L, 0.005 g, 0.05 mmol) was added dropwise, then the mixture was allowed to warm to room temperature and stirred for 14 h. The reaction mixture was then filtered through a pad of silica with the help of CH_2Cl_2 (5 mL). The solution was washed with H_2O (5 mL), dried (MgSO_4) and concentrated under reduced pressure. The crude residue was purified by flash column chromatography (30% EtOAc in hexanes) and afforded

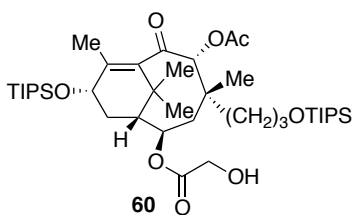
the β -keto diazoester **58** as colorless oil, 0.052 g (77% yield). $R_f = 0.51$ (20% EtOAc in hexanes); IR (neat) 2944, 2892, 2866, 2146, 1735, 1716, 1663, 1463, 1366, 1316, 1237 cm^{-1} ; ^1H NMR (500 MHz, CDCl_3) δ 5.94 (s, 1H), 5.17 (br s, 1H), 4.63 (d, $J = 8.0$ Hz, 1H), 3.63-3.46 (m, 2H), 2.78-2.68 (m, 1H), 2.47 (s, 3H), 2.41-2.22 (m, 1H), 2.20 (s, 3H), 2.04-1.90 (m, 2H), 1.89 (s, 3H), 1.76-1.42 (m, 5H), 1.56 (s, 3H), 1.18-1.05 (m, 45H), 1.00 (s, 3H); ^{13}C NMR (125 MHz, CDCl_3 , 16 sp^3 -Cs are missing of which 14 correspond to the TIPS group) δ 198.9, 189.3, 170.6, 166.7, 143.3, 140.2, 84.7, 77.4, 67.3, 64.5, 58.6, 53.9, 50.2, 46.7, 43.7, 38.5, 35.8, 32.2, 29.7, 28.5, 27.5, 26.9, 23.2, 21.4, 19.3, 12.7; HRMS (ESI, $[\text{M}+\text{Na}]^+$) Calcd for $\text{C}_{42}\text{H}_{74}\text{N}_2\text{O}_8\text{Si}_2\text{Na}$ m/z 813.48778; found m/z 813.48759.



Alcohol **50** (0.054 g, 0.084 mmol) and sodium bicarbonate (0.037 g, 0.44 mmol) were taken in a round-bottomed flask and dissolved in acetonitrile (4.2 mL). The reaction mixture was cooled to 0 °C. Bromoacetyl bromide (0.09 g, 0.44 mmol) was added slowly to this mixture at 0 °C. After stirring at this temperature for 15 min the reaction was quenched with water (5 mL) followed by extraction with CH_2Cl_2 (3 x 5 mL). The organic layer was separated and washed with brine (5 mL), dried (MgSO_4) and concentrated under reduced pressure.

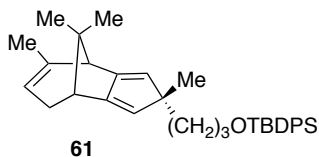
The crude bromoacetate (0.061 g, 0.084 mmol) thus obtained was taken in a flame-dried round-bottomed flask. Bistosylhydrazine (0.11 g, 0.33 mmol) was added to it and the mixture was dissolved in THF (2.0 mL). The reaction mixture was cooled to 0 °C. DBU (0.12 g, 0.84 mmol) was added to the solution at the same temperature and allowed to stir for 20 min. The reaction mixture was quenched by the addition of saturated aqueous solution of NaHCO_3 (2 mL)

followed by extraction with Et₂O (3 x 2 mL). The organic layer was separated and the combined organics were washed with brine (5 mL), dried (MgSO₄) and concentrated under reduced pressure. The crude residue was then purified by flash chromatography (35% EtOAc in hexanes) to afford the diazoester **59** as pale yellow oil, 0.049 g (78% yield): *R_f* = 0.61 (20% EtOAc in hexanes); IR (neat) 2944, 2891, 2866, 2136, 1745, 1698, 1463, 1372, 1237, 1098 cm⁻¹; ¹H NMR (500 MHz, CDCl₃) δ 5.94 (s, 1H), 5.31 (br s, 1H), 4.78 (br s, 1H), 4.66 (d, *J* = 8.5 Hz, 1H), 3.62-3.53 (m, 2H), 2.85-2.78 (m, 1H), 2.20 (s, 3H), 2.14-1.92 (m, 2H), 1.89 (s, 3H), 1.72-1.62 (m, 2H), 1.55 (s, 3H), 1.51-1.29 (m, 2H), 1.26 (s, 3H), 1.24-1.05 (m, 44H), 1.02 (s, 3H); ¹³C NMR (125 MHz, CDCl₃, 15 sp³-Cs are missing of which 14 correspond to the TIPS group) δ 198.7, 171.3, 165.2, 143.5, 140.2, 84.3, 77.6, 67.1, 64.5, 58.6, 53.9, 50.2, 46.2, 43.7, 38.5, 35.8, 32.2, 29.7, 28.5, 27.5, 26.9, 26.6, 25.0, 21.4, 19.3; HRMS (ESI, [M+Na]⁺) Calcd for C₄₀H₇₂N₂O₇Si₂Na m/z 771.4770; found m/z 771.4770.

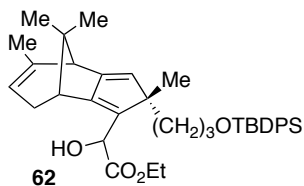


To a solution of diazoester **59** (0.056 g, 0.076 mmol) in dry benzene (4.0 mL) under argon was added Rh₂(OAc)₄ (0.001 g, 3 mol%) and the resulting mixture was heated to reflux for 3 h. After cooling to room temperature the solvent was removed under reduced pressure and the residue was then purified by flash column chromatography (40% EtOAc in hexanes) to afford **60** as yellow oil, 0.004 g (7% yield): *R_f* = 0.29 (20% EtOAc in hexanes); IR (neat) 3477, 2954, 2888, 2863, 1745, 1699, 1464, 1372, 1237, 1098, 1062 cm⁻¹; ¹H NMR (500 MHz, CDCl₃) δ 5.94 (s, 1H), 5.33 (br s, 1H), 4.68-4.61 (m, 1H), 4.16 (d, *J* = 8.5 Hz, 1H), 3.97-3.79 (s, 2H), 3.63-3.51 (m, 2H), 2.83-2.71 (m, 1H), 2.20 (s, 3H), 2.09-1.96 (m, 2H), 1.83 (s, 3H), 1.73-1.62 (m, 2H), 1.57 (s, 3H), 1.54-1.43 (m, 2H),

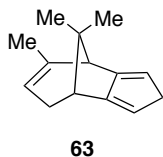
1.26 (s, 3H), 1.24-1.05 (m, 44H), 1.02 (s, 3H); ^{13}C NMR (125 MHz, CDCl_3 , 16 sp^3 -Cs are missing of which 14 correspond to the TIPS group) δ 197.7, 170.6, 166.7, 143.6, 140.7, 84.7, 73.9, 66.6, 65.8, 64.5, 48.0, 42.7, 38.5, 35.8, 32.2, 31.7, 29.7, 28.5, 27.5, 26.9, 19.7, 19.3, 17.7, 12.6; HRMS (ESI, $[\text{M}+\text{Na}]^+$) Calcd for $\text{C}_{40}\text{H}_{74}\text{O}_8\text{Si}_2\text{Na}$ m/z 761.4922; found m/z 771.4922.



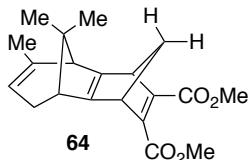
Enone **31** (0.28 g, 0.65 mmol) was dissolved in CH_2Cl_2 (6.5 mL) and cooled to $-78\text{ }^\circ\text{C}$. DIBAL-H (1.0 M solution in CH_2Cl_2 , 670 μL , 0.67 mmol) was added and the mixture was allowed to stir at this temperature for 40 min. The reaction was quenched by the addition of solid $\text{Na}_2\text{SO}_4 \cdot 7\text{H}_2\text{O}$ (0.25 g), and left to stir over 2 h. The mixture was then filtered and concentrated under reduced pressure. The residue was then purified by flash column chromatography (5% EtOAc in hexanes) to give the isodicyclopentadiene **61** a pale yellow oil, 0.245 g (76% yield): $R_f = 0.82$ (20% EtOAc in hexanes); IR (neat) 2945, 2871, 2847, 1567, 1415, 1366, 1291, 1141, 1026, 1005, 825 cm^{-1} ; ^1H NMR (500 MHz, CDCl_3) δ 7.71-7.69 (m, 4H), 7.44-7.37 (m, 6H), 5.57 (d, $J = 1.5$ Hz, 1H), 5.38 (d, $J = 1.5$ Hz, 1H), 5.01 (br s, 1H), 3.48 (t, $J = 6.9$ Hz, 2H), 2.42-2.34 (m, 1H), 2.18 (s, 2H), 1.95-1.88 (m, 1H), 1.65-1.61 (m, 3H), 1.55-1.51 (m, 2H), 1.34-1.26 (m, 2H), 1.15 (m, 4H), 1.09 (s, 2H), 1.04 (s, 3H), 0.01 (s, 9H); ^{13}C NMR (125 MHz, CDCl_3) δ 157.7, 155.1, 144.3, 142.2, 139.7, 134.1, 128.7, 120.2, 117.5, 114.2, 67.7, 61.5, 60.3, 43.1, 37.9, 36.6, 29.8, 26.1, 25.1, 24.1, 21.8, 19.7, 14.8, 0.9; HRMS (EI, M^+) Calcd for $\text{C}_{34}\text{H}_{44}\text{OSi}$ m/z 496.7981; found m/z 496.7981.



In a flame-dried round-bottomed flask isodicyclopentadiene **61** (0.022 g, 0.054 mmol) was taken and dissolved in CH₂Cl₂ (1.5 mL) and allowed to stir under argon. A solution of ethyl glyoxalate (0.025 g, 0.27 mmol) in CH₂Cl₂ (0.5 mL) was added to the solution and the reaction mixture was then cooled to -78 °C. BF₃•OEt₂ (6.7 μL, 0.0076 mmol) was added to the solution dropwise at the same temperature and allowed to stir. The reaction mixture was gradually allowed to warm to room temperature over 1.5 h and then quenched with water (2 mL) and extracted with CH₂Cl₂ (3 x 2 ml). The organic layer was separated and washed with brine (2 mL), dried (MgSO₄) and concentrated under reduced pressure. The crude residue was then purified by flash column chromatography (20% EtOAc in hexanes) and afforded **62** in 63% yield. (*R_f* = 0.66 (20% EtOAc in hexanes); IR (neat) 3451, 3062, 2955, 2871, 1751, 1547, 1416, 1387, 1291, cm⁻¹; ¹H NMR (500 MHz, CDCl₃) δ 7.61-7.60 (m, 4H), 7.37-7.31 (m, 6H), 6.18 (d, *J* = 3.1 Hz, 1H), 5.89 (s, 1H), 4.93 (s, 1H), 3.62-3.59 (m, 2H), 2.54-2.46 (m, 3H), 2.37-2.34 (m, 1H), 2.29-2.24 (m, 1H), 2.21-2.20 (m, 1H), 1.74-1.72 (m, 4H), 1.60-1.55 (m, 2H), 1.03 (s, 4H), 1.01-1.00 (m, 10H), 0.02 (s, 9H); ¹³C NMR (125 MHz, CDCl₃) δ 198.6, 156.5, 153.5, 144.0, 140.8, 135.5, 133.3, 129.6, 128.8, 127.7, 116.2, 63.1, 53.3, 52.3, 48.6, 48.0, 44.3, 32.3, 30.7, 29.7, 29.5, 27.1, 26.9, 26.0, 23.6, 20.6, 19.2, 0.4; HRMS (EI, M⁺) Calcd for C₃₈H₅₀O₄Si m/z 598.3478; found m/z 598.3473.

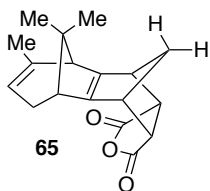


Enone **82** (0.054 g, 0.26 mmol) was dissolved in CH₂Cl₂ (3.5 mL) and cooled to -78 °C. DIBAL-H (1.0 M solution in CH₂Cl₂, 530 μL, 0.53 mmol) was added and the mixture was allowed to stir at this temperature for 40 min. The reaction was quenched by the addition of solid Na₂SO₄•7H₂O (0.15 g), and left to stir over 2 h. The mixture was then filtered and concentrated under reduced pressure. The residue was then purified by flash column chromatography (5% EtOAc in hexanes) to give the isodicyclopentadiene **63** as colorless oil, 0.03 g (77% yield): *R_f* = 0.91 (20% EtOAc in hexanes); IR (neat) 3005, 2978, 2856, 1547, 1444, 1337, 1287, 1171 cm⁻¹; ¹H NMR (500 MHz, CDCl₃) δ 5.87 (br s, 1H), 5.68 (s, 1H), 5.11 (br s, 1H), 2.48-2.42 (m, 1H), 2.37-2.35 (m, 2H), 2.01-1.96 (m, 2H), 1.81 (septet, *J* = 6.8 Hz, 1H), 1.75 (s, 3H), 1.14 (s, 3H), 0.91 (s, 3H); ¹³C NMR (125 MHz, CDCl₃) δ 157.8, 156.5, 138.4, 119.5, 117.4, 113.8, 51.3, 45.7, 42.9, 31.6, 27.6, 26.9, 22.8, 19.9; HRMS (EI, M⁺) Calcd for C₁₄H₁₈ m/z 186.1409; found m/z 186.1403.

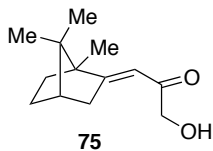


A CH₂Cl₂ solution (10.0 mL) of diene **63** (0.18g, 0.97 mmol) was taken in a flame-dried round-bottomed flask and was stirred at room temperature while a solution of DMAD (0.27 g, 1.95 mmol) in CH₂Cl₂ (1.0 mL) was added to the reaction mixture. The reaction mixture was then stirred at reflux for 3 h under an inert atmosphere of argon before the solvent was removed. The residue was purified through flash chromatography (20% EtOAc in hexanes) to give **64** as yellow oil, 0.200 g (63% yield): *R_f* = 0.69 (20% EtOAc in hexanes); IR (film) 3035, 2978, 2864, 1750, 1727, 1687, 1566, 1463, 1391 cm⁻¹; ¹H NMR (500 MHz, CDCl₃) δ 4.82 (br s, 1H), 3.79 (s, 3H), 3.75 (s, 3H), 2.5 (dt, *J* = 6.9, 1.9 Hz, 1H), 2.34 (d, *J* = 5.3 Hz, 1H), 2.30 (s, 1H), 2.22 (d, *J* = 6.6 Hz, 1H), 2.19 (s, 1H), 1.87 (m, 1H), 1.75 (br s, 1H), 1.61 (s, 3H), 1.49 (m, 1H), 1.20 (s, 3H), 1.03 (s, 3H); ¹³C

NMR (125 MHz, CDCl₃) δ 166.8, 162.2, 152.3, 150.0, 149.1, 148.9, 134.3, 119.0, 70.6, 54.5, 53.6, 52.8, 51.6, 47.6, 47.0, 29.8, 27.6, 23.6, 23.3, 19.8; HRMS (EI, M⁺) Calcd for C₂₀H₂₄O₄ m/z 328.1675; found m/z 328.1669.



A CH₂Cl₂ solution (20.0 mL) of diene **63** (0.32g, 1.72 mmol) was taken in a flame-dried round-bottomed flask and was stirred at room temperature while a solution of maleic anhydride (0.84 g, 8.65 mmol) in CH₂Cl₂ (2.0 mL) was added to the reaction mixture. The reaction mixture was then stirred at reflux for 5 h under an inert atmosphere of argon before the solvent was removed under reduced pressure. The crude residue was purified through flash chromatography (20% EtOAc in hexanes) to give **65** as a yellow oil, 0.347 g (71% yield): R_f = 0.77 (20% EtOAc in hexanes); IR (film) 29961, 2971, 2893, 1748, 1723, 1637, 1563, 1466, 1371 cm⁻¹; ¹H NMR (500 MHz, CDCl₃) δ 4.88 (br s, 1H), 3.40 (br s, 2H), 2.97 (d, J = 8.3 Hz, 1H), 2.78 (d, J = 8.3 Hz, 1H), 2.32 (d, J = 4.9 Hz, 1H), 2.18 (s, 1H), 2.06-2.00 (m, 2H), 1.75-1.72 (m, 1H), 1.70 (s, 3H), 1.46 (dt, J = 10.2, 1.7 Hz, 1H), 1.07 (s, 3H), 1.00 (s, 3H); ¹³C NMR (125 MHz, CDCl₃) δ 172.3, 171.9, 159.3, 146.7, 139.3, 117.4, 53.8, 50.2, 48.4, 47.8, 47.4, 46.7, 45.4, 31.3, 27.4, 24.8, 24.3, 19.7; HRMS (EI, M⁺) Calcd for C₁₈H₂₀O₃ m/z 284.1412; found m/z 284.1407.



A MeOH solution (5.0 mL) of diol **72** (0.25 g, 1.20 mmol) was taken in a flame-dried round-bottomed flask and allowed to stir under argon at 0 °C. Concentrated sulfuric acid (18.0 M, 0.5 mL) was then added to the solution and allowed to stir at the same temperature for 2 h. After completion, the reaction was diluted by addition of ether (5.0 mL). The reaction mixture was then neutralized with sat. NaHCO₃ (5 mL). The aqueous layer was separated and then extracted with ether (2 x 5 mL). The combined organics were dried (MgSO₄) and concentrated under reduced pressure. The crude residue was then purified with flash column chromatography (40% EtOAc in hexanes) to give **75** as a colorless oil, 0.214 g (86% yield): R_f = 0.39 (20% EtOAc in hexanes); IR (neat) 3362, 3071, 2871, 2247, 1687, 1466, 1291 cm⁻¹; ¹H NMR (500 MHz, CDCl₃) δ 5.91 (t, *J* = 2.4 Hz, 1H), 4.25 (d, *J* = 4.3 Hz, 2H), 3.4 (t, *J* = 4.3 Hz, 1H), 2.88 (m, 1H), 2.45 (m, 1H), 1.9 (t, *J* = 4.5 Hz, 1H), 1.82-1.72 (m, 2H), 1.25-1.23 (m, 2H), 0.96 (s, 3H), 0.92 (s, 3H), 0.70 (s, 3H); ¹³C NMR (125 MHz, CDCl₃) δ 198.4, 177.3, 110.9, 68.3, 54.7, 48.4, 44.4, 39.7, 34.0, 27.1, 19.6, 18.8, 12.4; HRMS (EI, M⁺) Calcd for C₁₃H₂₀O₂ m/z 208.1463; found m/z 208.1458.

4.6 References

- (1) (a) Lucas, H. *Arch. Pharm.* **1856**, 85, 145. (b) Kurono, M.; Nakadaira, Y.; Onuma, S.; Sasaki, K.; Nakanishi, K. *Tetrahedron Lett.* **1963**, 4, 2153.
- (2) (a) Swindell, C. S. *Org. Prep. Proced. Znt.* **1991**, 23, 465. (b) Kess, M. H.; Ruel, R.; Miller, W. H.; Kishi, Y. *Tetrahedron Lett.* **1993**, 34, 5999, 6003. (c) Masters, J. J.; Jung, D. K.; Bornmann, W. G.; Danishefsky, S. J. *Tetrahedron Lett.* **1993**, 34, 7253. (d) Swindell, C. S.; Chander, M. C.; Heerding, J. M.; Klimko, P. G.; Rahman, L. T.; Raman, J. V.; Venkataraman, H. *Tetrahedron Lett.* **1993**, 34, 7005.
- (3) (a) Kingston, D. G. I. *Chem. Commun.* **2001**, 867. (b) McGuire, W. P.; Rowinsky, E. K.; Rosenchein, N. B.; Grumbine, F. C.; Ettinger, D. S.; Armstrong, D. K.; Donehower, R. C. *Ann. Intern. Med.* **1989**, 111, 273. (c) Rowinsky, E. K.; Cazenave, L. A.; Donehower, R. C. *J. Natl. Cancer Inst.* **1990**, 82, 1247. (d) Holms, F. A.; Walters, R. S.; Theriault, R. L.; Forman, A. D.; Newton, L. K.; Raber, M. N.; Buzdar, A. U.; Frye, D. K.;

- Hortobagyi, G. N. *J. Natl. Cancer Zmt.* **1991**, 83, 1797. (e) Einzig, A. I.; Hochster, H.; Wiernik, P. H.; Trump, D. L.; Dutcher, J. P.; Garowski, E.; Sasloff, J.; Smith, T. *J. Znuest. New Drugs* **1991**, 9, 59.
- (4) Sako, M.; Suzuki, H.; Yamamoto, N.; Hirota, K.; Maki, Y. *J. Chem. Soc., Perkin Trans 1* **1998**, 417.
- (5) (a) Maki, Y.; Sako, M. *J. Synth. Org. Chem. Jpn* **1993**, 51, 298. (b) Morita, H.; Wei, L.; Gonda, A.; Takeya, K.; Itokawa, H.; Fukaya, H.; Shigemori, H.; Kobayashi, J. *Tetrahedron* **1997**, 53, 4621.
- (6) Kobayashi, J.; Hosoyama, H.; Wang, X.; Shigemori, H.; Koiso, Y.; Iwsaki, S.; Sasaki, T.; Naito, M.; Tsuruo, T. *Bioorg. Med. Chem. Lett.* **1997**, 7, 393.
- (7) Hosoyama, H.; Shigemori, H.; Tomida, A.; Tsuruo, T.; Kobayashi, J. *Bioorg. Med. Chem. Lett.* **1999**, 9, 389.
- (8) Gottesman, M. M.; Fojo, T.; Bates, S. E. *Nat. Rev. Cancer* **2002**, 2, 48.
- (9) Winkler, J. D.; Bhattacharya, S. K.; Batey, R. A. *Tetrahedron Lett.* **1996**, 37, 8069.
- (10) Kuwajima, I.; Kusama, H. *Synlett.* **2000**, 1385.
- (11) (a) Banwell, M. G.; Darnos, P.; Hockless, D. C. R. *Aust. J. Chem.* 2004, 57, 41-52. (b) Banwell, M. G.; McLeod, M. D.; Riches, A. G. *Aust. J. Chem.* 2004, 57, 53-66.
- (12) Hudlicky, T.; Gonzalez, D.; Gibson, D. T. *Aldrichchimica Acta* **1999**, 32, 35.
- (13) Banwell, M. G.; Edwards, A. J.; Harfoot, G. J.; Jolliffe, K. A.; McLeod, M. D.; McRae, K. J.; Stewart, S. G.; Vögtle, M. *Pure Appl. Chem.* **2003**, 75, 223.
- (14) Wender, P. A.; Badham, N. F.; Conway, S. P.; Floreancig, P. E.; Glass, T. E.; Gräncher, C.; Houze, J. B.; Jänichen, J.; Lee, D.; Marquess, D. G.; McGrane, P. L.; Meng, W.; Mucciario, T. P.; Muhlebach, M.; Mnatchus, M. G.; Paulsen, H.; Rawlins, D. B.; Satkofsky, J.; Shuker, A. J.; Sutton, J. C.; Taylor, R. E.; Tomoka, K. *J. Am. Chem. Soc.* **1997**, 119, 2755.
- (15) Giese, S. *Intermolecular Nucleophilic Trapping of Nazarov-Derived Oxyallyl Intermediates and Their Application Toward Total Synthesis of Taxinine*, Ph.D. Thesis, University of Utah, 2000.

- (16) Mazzola, R. D., Jr. *Torquoselectivity in the Nazarov Cyclization of Facially Biased Dienones and their Application Toward Total Synthesis of Taxinine*, Ph.D. Thesis, University of Utah, 2000.
- (17) Benson, C. L. *Electrocyclization Reactions: Studies on Torquoselectivity and Application Toward the Total Synthesis of Taxinine*, Ph.D. Thesis, University of Alberta, 2007.
- (18) Mazzola, R. D., Jr.; Giese, S.; Benson, C. L.; West, F. G. *J. Org. Chem.* **2004**, *69*, 220.
- (19) Giese, S.; Mazzola, R. D., Jr.; Amann, C. M.; Arif, A. M.; West, F. G. *Angew. Chem. Int. Ed. Engl.* **2005**, *44*, 6546.
- (20) Mazzola, R. D., Jr.; White, T. D.; Vollmer-Snarr, H. R.; West, F. G. *Org. Lett.* **2005**, *7*, 2799.
- (21) (a) Mukaiyama, T.; Shiina, I.; Iwadare, H.; Saitoh, M.; Nishimura, T.; Ohkawa, N.; Sakoh, H.; Nishimura, K.; Tani, Y.; Hasegawa, M.; Yamada, K.; Saitoh, K. *Chem. Eur. J.* **1999**, *5*, 121. (b) Stork, G.; Manabe, K.; Liu, L.; *J. Am. Chem. Soc.* **1998**, *120*, 1337.
- (22) Lipshutz, B. H.; Koerner, M.; Parker, D. A. *Tetrahedron Lett.* **1987**, *28*, 945.
- (23) Ito, Y.; Saegusa, T. *J. Org. Chem.* **1978**, *43*, 1011.
- (24) Nicolaou, K. C.; Zhong, Y. L.; Baran, P. S. *J. Am. Chem. Soc.* **2000**, *122*, 7596.
- (25) Walker, D.; Hiebert, J. D. *Chem. Rev.* **1967**, *67*, 153.
- (26) For a review of the vinylogous Mukaiyama aldol reaction see: Casiraghi, G.; Zanardi, F.; Appendino, G.; Rassa, G. *Chem. Rev.* **2000**, *100*, 1929.
- (27) (a) Das Sarma, K.; Zhang, J.; Curran, T. T. *J. Org. Chem.* **2007**, *72*, 3311. (b) Saito, S.; Nagahara, T.; Shiozawa, M.; Nakadai, M.; Yamamoto, H. *J. Am. Chem. Soc.* **2003**, *125*, 6200. (c) Bella, M.; Piancatelli, G.; Squarcia, A.; Trolli, C. *Tetrahedron Lett.* **2000**, *41*, 3699.
- (28) (a) Adams, J.; Poupart, M. -A.; Grenier, L.; Schaller, C.; Ouimet, N.; Frenette, R. *Tetrahedron Lett.* **1989**, *30*, 1749. (b) Ballabio, M.; Malatesta, V.; Ruggieri, D.; Temperilli, A. *Gazz. Chim. Ital.* **1988**, *118*, 375.
- (29) Stork, G.; Nakatani, K. *Tetrahedron Lett.* **1988**, *29*, 2283.

- (30) (a) Adams, J.; Poupart, M.-A.; Grenier, L.; Schaller, C.; Ouimet, N.; Frenette, R. *Tetrahedron Lett.* **1989**, *30*, 1749. (b) Wang, P.; Adams, J. *J. Am. Chem. Soc.* **1994**, *116*, 3296.
- (31) Taber, D. F.; Ruckle, R. E. *J. Am. Chem. Soc.* **1986**, *108*, 7686.
- (32) Nyangulu, J. M.; Nelson, K. M.; Rose, P. A.; Gai, Y.; Loewen, M.; Lougheed, B.; Quail, J.W.; Cutler, A. J.; Abrams, S. R. *Org. Biomol. Chem.* **2006**, *4*, 1400.
- (33) Holmquist, C. R.; Roskamp, E. J. *J. Org. Chem.* **1989**, *54*, 3258. (b) Yadav, J. S.; Subba-Reddy, B. V.; Eeshwaraiyah, B.; Reddy, P. N. *Tetrahedron.* **2005**, *61*, 875.
- (34) Regitz, M. *Angew. Chem. Int. Ed. Engl.* **1967**, *6*, 733.
- (35) Doyle, M. P. *Chem. Rev.* **1986**, *86*, 919.
- (36) Bal, B. S.; Childers, W. E., Jr.; Pinnick, H. W. *Tetrahedron*, **1981**, *37*, 2091.
- (37) Nakamura, E.; Yoshikai, N.; Yamanaka, M. *J. Am. Chem. Soc.* **2002**, *124*, 7181.
- (38) (a) Wender, P. A.; Badham, N. F.; Conway, S. P.; Floreancig, P. E.; Glass, T. E.; Granicher, C.; Houze, J. B.; Janichen, J.; Lee, D.; Marquess, D. G.; McGrane, P. L.; Meng, W.; Mucciario, T. P.; Muhlebach, M.; Natchus, M. G.; Paulsen, H.; Rawlins, D. B.; Satkofsky, J.; Shuker, A. J.; Sutton, J. C.; Taylor, R. E.; Tomooka, K. *J. Am. Chem. Soc.* **1997**, *119*, 2755. (b) Wender, P. A.; Badham, N. F.; Conway, S. P.; Floreancig, P. E.; Glass, T. E.; Houze, J. B.; Krauss, N. E.; Lee, D.; Marquess, D. G.; McGrane, P. L.; Meng, W.; Natchus, M. G.; Shuker, A. J.; Sutton, J. C.; Taylor, R. E. *J. Am. Chem. Soc.* **1997**, *119*, 2757.
- (39) (a) Holton, R. A.; Somoza, C.; Kim, H. B.; Liang, F.; Biediger, R. J.; Boatman, D.; Shindo, M.; Smith, C. C.; Kim, S.; Nadizadeh, H.; Suzuki, Y.; Tao, C.; Vu, P.; Tang, S.; Zhang, P.; Murthi, K. K.; Gentile, L. S.; Liu, J. H. *J. Am. Chem. Soc.* **1994**, *116*, 1597. (b) Holton, R. A.; Kim, H. B.; Somoza, C.; Liang, F.; Biediger, R. J.; Boatman, D.; Shindo, M.; Smith, C. C.; Kim, S.; Nadizadeh, H.; Suzuki, Y.; Tao, C.; Vu, P.; Tang, S.; Zhang, P.; Murthi, K. K.; Gentile, L. S.; Liu, J. H. *J. Am. Chem. Soc.* **1994**, *116*, 1599.
- (40) Holton, R. A.; Juo, R. R.; Kim, H. B.; Williams, A. D.; Harusawa, S.; Lowenthal, R. E.; Yogai, S. *J. Am. Chem. Soc.* **1988**, *110*, 6558.

- (41) Hickey, E. R.; Paquette, L. A. *J. Am. Chem. Soc.* **1995**, *117*, 163.
- (42) (a) Brown, F. K.; Houk, K. N. *J. Am. Chem. Soc.* **1985**, *107*, 1971. (b) Paquette, L. A.; Hayes, P. C.; Charumilind, P.; Böhm, M. C.; Gleiter, R.; Blount, J. F. *J. Am. Chem. Soc.* **1983**, *105*, 3148.
- (43) Gotoh, H.; Masui, R.; Ogino, H.; Shoji, M.; Hayashi, Y. *Angew. Chem. Int. Ed. Engl.* **2006**, *45*, 6853.
- (44) Paquette, L. A.; Hayes, P. C.; Charumilind, P.; Bohm, M. C.; Gleiter, R.; Blount, J. F. *J. Am. Chem. Soc.* **1983**, *105*, 3148.
- (45) Hennion, G. F.; Davis, R. B.; Maloney, D. E. *J. Am. Chem. Soc.* **1949**, *71*, 2813.
- (46) Meyer, K. H.; Schuster, K. *Ber.* **1922**, *55*, 819.
- (47) Halterman, R. L.; Volhardt, P. C. *Organometallics* **1988**, *7*, 883.
- (48) Zhang, L.; Wang, S. *J. Am. Chem. Soc.* **2006**, *128*, 1442.
- (49) Subramanyam, R.; Bartlett, P. D.; Iglesias, G. Y. M. Watson, W. H.; Galloy, J. *J. Org. Chem.* **1982**, *47*, 4491.
- (50) Barton, D. H. R.; Beaton, J. M.; Geller, L. E.; Pechet, M. M. *J. Am. Chem. Soc.* **1961**, *83*, 4076.
- (51) Hopps, H. B. *Aldrichimica Acta*, **1970**, *3*, 9.

Chapter 5

Prion Inhibition with Multivalent PrP^{Sc} Binding Compounds¹

5.1 Prions and Transmissible Spongiform Encephalopathies

Prions are defined as proteinaceous infectious particles that are responsible for various transmissible spongiform encephalopathies (TSEs).² The name was first coined by Dr. Stanley B. Prusiner in 1982, and is derived from the words ‘protein’ and ‘infection.’³ Prion is the disease-causing form of the naturally occurring protein called cellular prion protein (PrP^C). PrP^C is located primarily on the surface of central nervous system cells, but can also be found in other tissues of mammalian body.⁴ Molecular modeling studies predicted that PrP^C is a four-helix bundle protein containing four regions of secondary structure.⁵ Fourier transform infrared (FTIR) and circular dichroism (CD) later showed that PrP^C consists of about 40% α -helix, with minimal β -sheet, consistent with the structural predictions.⁶

Prions are unique pathogens, having no nucleic acid in contrast to viruses, bacteria, fungi and other pathogens. Lacking nucleic acid, prions cannot reproduce in the usual way. Instead they replicate by stimulating normal cellular protein to fold into its isoform called PrP^{Sc}, prion protein scrapie, the first TSE discovered. PrP^{Sc} formation is considered to be a post-translational process

involving only a conformational change in PrP^c.⁷ Models of PrP^{Sc} suggest that formation of the disease causing isoform involves refolding to generate motifs containing substantial amounts of β -sheet secondary structure. The mechanism through which the normal prion protein (PrP^c) is recruited to refold into its pathogenic isoform (PrP^{Sc}) is not clearly understood, and is the subject of extensive research.⁷ The normal prion protein is broken down by protease enzymes but the abnormal form is resistant to these enzymes and hence they accumulate in brain tissue through replication forming aggregates with characteristics often similar to amyloid fibrils.⁸ After PrP^c adopts the structure of PrP^{Sc}, it starts accumulating in the cell's lysosomes. As it accumulates, the lysosomes swell and eventually burst, releasing the proteolytic enzymes and PrP^{Sc} into the cell. As this process occurs simultaneously in different neural cells, the entire brain tissue is slowly riddled with dead neural cells, leading to a spongiform appearance that characterizes the prion diseases.⁹

5.1.1. Prion Replication Models

The central molecular event in the replication of mammalian prions, in context of the protein-only model, is the self-propagating conversion of PrP^c to the misfolded PrP^{Sc}.¹⁰ Two different mechanisms have been proposed for this protein-based replication process. One hypothesis is based on the heterodimer refolding model (also known as the template assistance model), according to which PrP^{Sc} exists as a thermodynamically more stable monomer than PrP^c.⁵ But this thermodynamically favored conformer is kinetically inaccessible. Under these circumstances, the conversion involves heterodimer formation between PrP^{Sc} and PrP^c, with PrP^{Sc} acting as a monomeric template that catalyzes the refolding of PrP^c to a thermodynamically more stable conformation of PrP^{Sc}. While this mechanism is fairly plausible, there is a serious lack of experimental evidence for the existence of a stable PrP^{Sc} monomer. By contrast, there is data indicating that an aggregation process is intimately involved with the conversion of PrP^c, and the infectious agent is oligomeric in nature.¹¹

The hypothesis consistent with the oligomeric nature of PrP^{Sc} is the nucleated polymerization model proposed by Lansbury.¹² According to this mechanism, conversion between PrP^C and PrP^{Sc} is reversible, but the PrP^{Sc} monomer is less stable than PrP^C. Stabilization of PrP^{Sc} monomers occurs upon intermolecular (allosteric) interaction with other PrP^{Sc} molecules. However, once the nucleus has formed, monomeric PrP^C can add to it, thereby adopting the conformation of PrP^{Sc}. According to this hypothesis, the rate-limiting step is the nucleation and not the conformational conversion.

5.1.2. Transmissible Spongiform Encephalopathies (TSEs)

Prion diseases, also known as transmissible spongiform encephalopathies (TSEs) are a group of infectious neurodegenerative diseases affecting many mammals, including humans.¹³ These diseases are characterized by neuronal accumulation of abnormal protein deposits, often composed of amyloid-like fibrils. Brain vacuolation (i.e. formation of vacuoles in the brain), astrogliosis that involves an abnormal increase in the number of astrocytes due to the destruction of nearby neurons, neuronal apoptosis causing death of neuronal cells are the other common features. The best known form of the disease in humans is the Creutzfeldt-Jakob disease (CJD);¹⁴ other examples include a new variant Creutzfeldt-Jakob disease (nvCJD),¹⁵ Gerstmann-Straussler-Scheincker syndrome (GSS), fatal familial insomnia,¹⁶ kuru,¹⁶ scrapie in sheep and goat,¹⁷ bovine spongiform encephalopathy in cattle (commonly known as mad cow disease)¹⁷ and chronic wasting disease in deer and elk.

The transmissibility of TSEs was first demonstrated accidentally in 1937, when a population of Scottish sheep were inoculated against louping-ill virus (i.e. a virus causing louping-ill disease also known as ovine encephalomyelitis in sheep) in sheep with a formalin extract of brain tissue, that was subsequently found to be contaminated with the scrapie agent.^{1,18} Stunningly, after two years 10% of the sheep developed scrapie. Scrapie was subsequently transmitted

experimentally to sheep and mice.¹⁹ In 1959, Hadlow suggested that kuru, a CNS degenerative disease found among the cannibalistic tribe of New Guinea, might be similar to scrapie as the pathologies of these diseases share many features,²⁰ and this was demonstrated in 1966 by transmission of kuru to chimpanzees in the seminal work of Gajdusek.²¹ Due to the unusually long incubation period between exposure to the pathogen and the onset of symptoms scientists had initially predicted it to be a “slow virus”.²² However, in 1967 Alper and co-workers demonstrated that the scrapie agent was extremely resistant to treatments that normally destroy nucleic acids, like UV and other ionizing radiations.²³ These results ruled out the possibility of viruses or other known pathogens to be the infectious agent, and led to alternate hypotheses.²⁴ In 1967, Griffith first introduced the ‘protein-only hypothesis’ for the propagation of TSEs,²⁵ which was later investigated by the Prusiner group.²⁶

The etiology of TSEs may be sporadic, genetic or through transmission via ingestion of infected foods or via blood transfusion.²⁷ Sporadic TSEs are most common in animals where normal prion protein may spontaneously change into the infectious form. Inherited cases arise from a change or mutation of the normal protein to the abnormal form. TSEs cannot be transmitted through the air or through touching or most other forms of casual contact. However, they may be transmitted through contact with infected tissue, bodily fluids, or contaminated medical instruments. Normal sterilization procedures such as boiling or irradiation do not prevent transmission of TSEs. In 1986 in England, bovine spongiform encephalopathy (BSE) spread in cattle in an epidemic fashion. This happened because the healthy cattle were fed with processed remains of infected animals.

Symptoms of TSEs in human primarily include personality changes. Anxiety and depression are fairly common features. Patients may show serious cognitive deficits with time. Disturbance in balance and gait are also seen. Affected individuals may also experience attacks of seizures at later stages of the disease.

TSEs became a major concern and received significant attention after 1994, when the new variant of CJD (nvCJD) was first reported in young adults and teenagers in Britain.²⁸ This new form of prion disease, nvCJD occurs from exposure to beef products that are contaminated with bovine spongiform encephalopathy (BSE). CJD generally affects men and women of ages between 50 and 75 years whereas the variant form affects mostly young adults and the duration of the disease is longer. The initial symptoms are mostly psychiatric in origin, making correct diagnosis even more difficult.

5.2 Challenges and Recent Progress in Prion Research

All prion diseases are invariably fatal due to the lack of a successful treatment or cure. Current development of therapeutics for prion diseases relies heavily on the observation that prion pathogenesis coincides with the cellular prion protein (PrP^C) undergoing a conformational change into a β -sheet-rich isoform PrP^{Sc}. Presently, one of the most promising therapeutic approaches for prion diseases relies on interference with PrP^{Sc} amplification and accumulation. Evidence from cell culture and *in vivo* studies also suggest that once formation of PrP^{Sc} is inhibited, clearance of PrP^{Sc} can occur. However, the lack of mechanistic details for the protein conversion process, combined with the inability to obtain a detailed three-dimensional structure for PrP^{Sc} has greatly hindered progress in this area. Despite of identification of a number of compounds being capable of inhibiting PrP^{Sc} accumulation and also cleaning PrP^{Sc} from infected cell lines, little therapeutic efficacy *in vivo* has been achieved, and no viable treatments of these fatal neurodegenerative disorders are currently available. In order to understand the mechanism of human prion disease, develop rational therapeutics, improve decontamination protocols and diagnostic tools, effective and appropriate experimental models are essential. However, very few experimental approaches are available for studying the disease since incubation time, neuropathology, immune responses and behaviour can only be studied in an animal model.

Recent development in prion research mainly focuses in four main areas; genetic techniques, immunomodulation, immunotherapeutics and discovery of anti-prion compounds.²⁹

One effective approach in the field of transgenic modeling was developed by the Collinge group to inhibit further development of prion diseases in the infected mice by knocking out neuronal PrP^C through transgenic techniques at the early or mid stage of incubation period.³⁰ The result of these studies also validates the hypothesis that the presence of PrP^C is critical for the propagation and development of the prion diseases. However, this research is still at the experimental level and is not directly applicable to humans. Other transgenic experiments have also been reported.³¹

Immunomodulation of the prion disease is another area of active research.^{29,32,33,34} Methods of immunomodulation that are found to prolong incubation time slightly or modestly include: (a) active immunization with prion peptide prior to infection,³⁵ (b) passive immunization;³⁶ (c) immunostimulations;³⁷ and (d) a combination of immunosuppression and anti-inflammatory agent treatment.^{38,39}

Historically, vaccination has been used as a means for protecting both humans and animals from infectious pathogens. Similar approaches are being developed for prion diseases such as CJD and the new variant form (nvCJD). The impetus for this initially came from *in vitro* studies demonstrating a reduction in prion infectivity after incubation of inoculum with anti-PrP antibodies by Gabizon *et al.* in 1988⁴⁰ and later the *in vitro* inhibition of PrP^C conversion to PrP^{Sc} by antibodies (Horiuchi and Caughey in 1999).⁴¹ Subsequently, Enari *et al.* in 2001 successfully inhibited *in vitro* PrP^{Sc} replication in scrapie-infected N2a neuroblastoma cells by treating the cultures with the anti-PrP antibody.⁴² Intriguingly, not only did they succeed in preventing infection of cells by pre-treating with antibody, but also were able to clear scrapie (as represented by PrP^{Sc}

formation) from chronically infected cells using the same approach. This provided a very important insight into how anti-PrP antibodies may be used to abrogate prion replication. Other anti-prion antibodies with specificity and high affinity have been discovered through *in vitro* screening and animal model testing, which are able to reduce infectivity and inhibit PrP^{Sc} accumulation.²⁹

There has been an ongoing effort to develop new small molecules that stabilize the native protein PrP^C and make the conformational change to PrP^{Sc} an energetically less favourable process, thereby blocking the formation of PrP^{Sc}.⁴³ This effort could also improve our knowledge about the mechanism of formation and clearance of PrP^{Sc}. Alternatively, there is also a search for molecules that effectively destabilize PrP^{Sc} either by rendering it protease sensitive and enhancing its chance of clearance, or by binding to PrP^{Sc} and preventing it from serving as a template for replication. The later possibility has been suggested as the mechanism of action of Congo red.⁴⁴

Another strategy could involve preventing formation of molecular complexes by interfering with the interaction between PrP^C and PrP^{Sc}. Several small molecules have been reported to bind to PrP^C and stabilize it against its conformational change to PrP^{Sc}, with the aim of identifying and developing novel prion disease therapeutics. Prusiner and co-workers conducted a computational search on the Available Chemical Directory for molecules that could mimic the dominant negative inhibition of prion replication by polymorphic variants of PrP.⁴⁵ Pyridine dicarbonitriles **1-4** (Figure 5.1) inhibited PrP^{Sc} formation in a dose dependent manner, albeit at high concentrations (IC₅₀ range from 18 to 60 μM).⁴⁶ Additional optimization around this scaffold led to the identification of further compounds **5-7**⁴⁷ (Figure 5.2) with enhanced potency compared to compound **3**, and were found to reduce PrP^{Sc} accumulation to below 30% relative to an untreated control at 50 nM. On the other hand, novel bifunctional diketopiperazine derivatives **8** and **9** (Figure 5.3) were reported by Bolognesi *et al.* with an EC₅₀ of 4 and 15 μM respectively, against prion replication in ScGT1

cells while showing low cytotoxicity.⁴⁸ The planar conformation of this scaffold is proposed to be the major determinant for activity in these classes of compounds. Studies on the mode-of-action demonstrated that **8** might interact directly with the recombinant prion protein to prevent its conversion to the misfolded isoform. Several other classes of chemical compounds have been shown to possess anti-prion activities and the list includes acridines (e.g. quinacrine and other related tricyclic scaffolds),⁴⁹ dimeric and chimeric analogues of statins,⁵⁰ 2,4-Diphenylthiazole and 2,4-Diphenyloxazole amide,⁵¹ and pyrazolones.⁵² However, it seems highly unlikely that these small molecules could be therapeutically useful as most were originally designed to target other diseases (like malaria) and have not been optimized for anti-prion effects in humans or for crossing the blood-brain barrier.⁵³

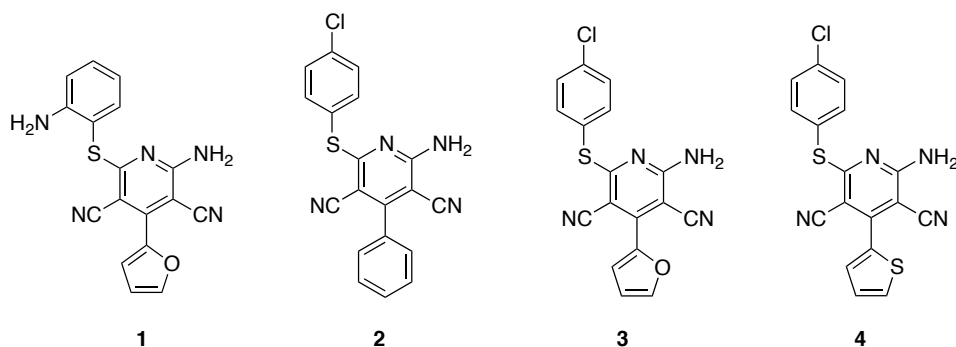


Figure 5.1 Pyridine Dicarbonitrile Scaffold for Dose Dependent Prion Inhibition.

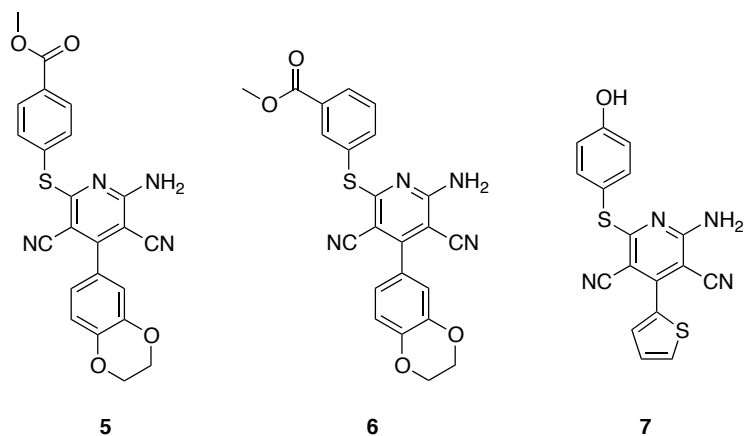


Figure 5.2 Pyridine Dicarbonitrile Scaffolds with Enhanced Potency.

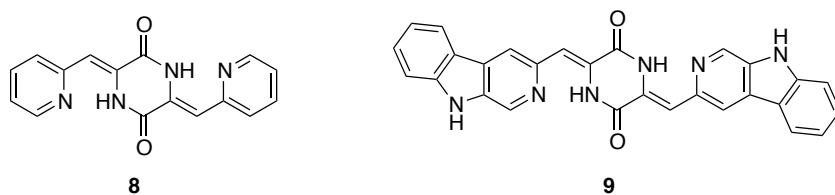


Figure 5.3 Diketopiperazines as Prion Replication Inhibitors.

5.3 Results and Discussions

Many small molecules have been identified to have promising anti-prion effects, and they are effective in some cases in either prolonging incubation time or reducing severity of prion diseases in animal models; however, it still remains unknown whether they will also be effective in humans. Quinacrine (Figure 5.4) is among the most potent compounds, and several groups have reported an IC_{50} ranging from ~ 0.25 to $0.5 \mu\text{M}$ in neuroblastoma cells.⁵⁴ This activity may be partially attributed to an affinity for a PrP carboxy-terminal binding site comprised of Tyr225, Tyr226, and Gln227 (with a K_D ranging from 1 to $5 \mu\text{M}$).⁵⁵

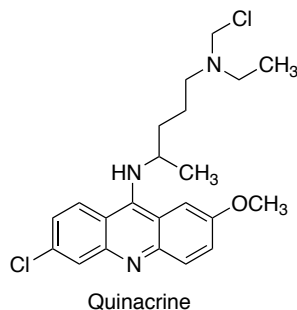


Figure 5.4 Quinacrine: A Potent Anti-Prion Compound.

As synthetic organic chemists, our strategy was to take advantage of the existing small molecules, which are known to have promising anti-prion features, and to make multivalent molecules containing multiple binding units with a goal of attaining improved binding affinity towards PrP^{Sc}. Specifically, the main objective of this project was to synthesize a library of multimeric (dimeric, trimeric or tetrameric) compounds with two, three or four effective binding units. Based on the oligomeric nature of PrP^{Sc},^{56,57} we planned to explore multivalent molecules with a view of increasing potency without altering the effects upon cell viability.

Besides their anticipated higher binding affinity and anti-prion effects, the multivalent molecules might also offer two additional benefits, including determination of the 3D structure of PrP^{Sc} and early detection and location of prion *in vivo*. The 3D structure of PrP^{Sc} is still unclear, and because PrP^{Sc} tends to aggregate to form insoluble plaques, the crystal structure has been difficult to obtain. With the help of multivalent compounds that have high affinity towards PrP^{Sc}, it is possible that one particular soluble PrP^{Sc} oligomer may be selectively stabilized through interaction with a multivalent binder and induced to crystallize. Although relatively unlikely, the potential importance of such a result makes it well worth the effort. If a crystal can indeed be obtained, the 3D structure of PrP^{Sc} may be revealed by X-ray crystallography. Elucidation of the 3D structure of

PrP^{Sc} is highly significant in terms of greater understanding of the binding affinity and hence in drug development.

The second potential benefit of our proposed strategy is that the availability of multivalent fluorescent compounds may facilitate early detection and location of prion *in vivo*. Although some anti-prion compounds such as acridine are fluorescent and can be activated to give off fluorescent signals *in vivo* by binding to prion, their relatively weak signals hinder practical applications. Multivalent fluorescent compounds, on the other hand, may provide much stronger signals due to their higher binding affinity towards PrP^{Sc}. Our plan was to synthesize and find new multivalent fluorescent compounds with high affinity towards PrP^{Sc} by utilizing these monomeric fluorescent compounds as binding sites. If these compounds can concentrate in the area where there is a high concentration of PrP^{Sc}, they will help early detection of prion infection *in vivo* or contamination of surgical instruments or animal processing facilities. Early diagnosis of prion diseases is particularly crucial for effective treatment because the incubation time in prion diseases is usually very long, increasing the chances of extensive damage to the central nervous system by the time symptoms present.

5.3.1. Planning and Synthesis of Multivalent PrP^{Sc} Binding Molecules

In our study, we had envisioned using linear and cyclic linkers to attach multiple chloroquinoline or acridine rings to di-, tri- or tetra-valent scaffolds composed of Congo red dye, trimesic acid, or tetraphenylporphyrin tetracarboxylic acid, respectively. These molecules were to be applied to cells chronically infected with mouse-adapted prions, as described herein.

Disubstituted Congo red, trisubstituted benzene rings and tetrasubstituted porphyrins were selected as scaffolds for the library synthesis of three categories of multivalent compounds for mainly two reasons (Figure 5.5); firstly, these

molecules should be able to provide a rigid and flat platform so that the binding units can be extended to different directions. Secondly, the multivalency of the core scaffolds should allow them to link to several monomeric binding units, which are anticipated to generate structures with enhanced PrP^{Sc} binding affinity. Congo Red and porphyrins are already known to have some binding affinity that could act in synergy with the effects of chloroquinoline or acridine units. Moreover, in the case of porphyrins, the fluorescent nature of these molecules can be utilized in synthesizing multivalent binding molecules with fluorescent activity using porphyrin as the core.^{58,59}

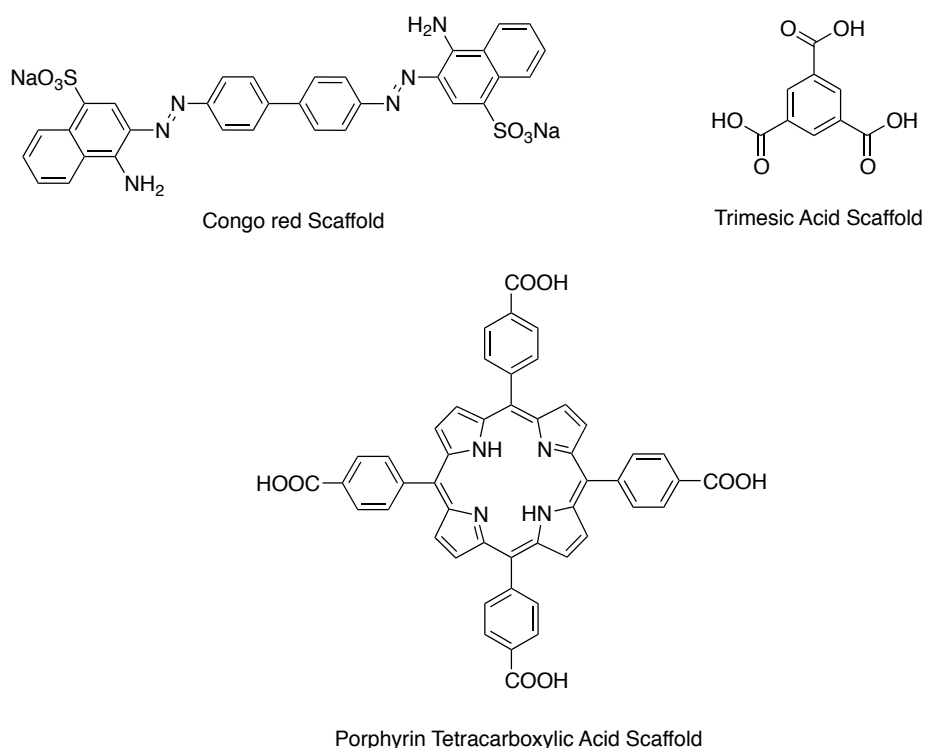


Figure 5.5 Structures of the Selected Multivalent Scaffolds.

Diamines were chosen as linkers to connect the monomeric binding units to the scaffold, either through amide bond formation or palladium catalyzed coupling reactions (Figure 5.6). These diamines were chosen as linkers because of their varying lengths and rigidity. By building target molecules that have linkers

with different lengths, it was hoped that an optimum linker length could be found to fit in the spaces of the aggregates of PrP^{Sc}, and thus optimize binding efficacy.

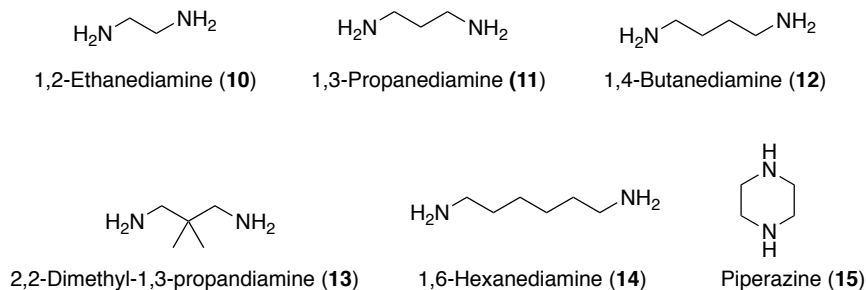


Figure 5.6 Structures of the Chosen Diamine Linkers.

The 4,7-dichloro-quinoline and 6,9-dichloro-2-methoxy acridine were chosen as the monomeric binding units, because they have already been demonstrated to have high binding affinity towards PrP^{Sc} and anti-prion activity (Figure 5.7). It was anticipated that the binding affinity of the multivalent target molecules would be significantly enhanced through multivalent interaction between these known anti-prion binding units and the aggregates of PrP^{Sc} fibrils. In addition, acridines are fluorescent compounds, and the target molecules may be fluorescent if acridines are used as the binding units.

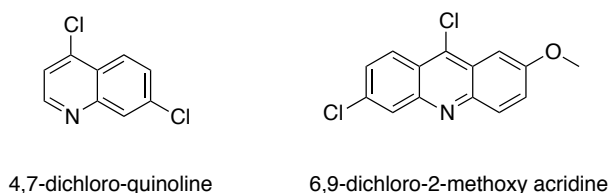


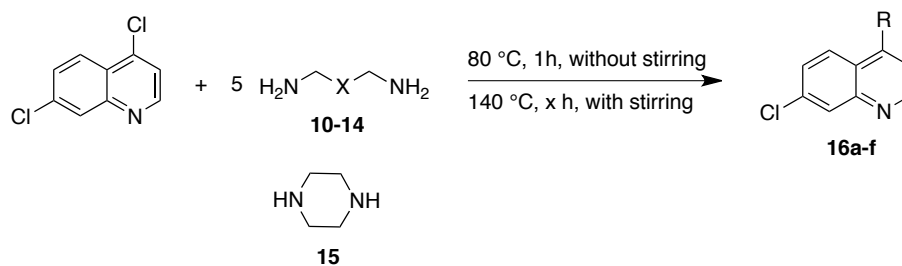
Figure 5.7 The Chosen Monomeric Binding Units.

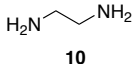
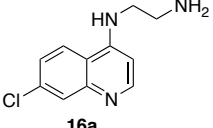
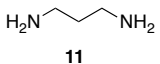
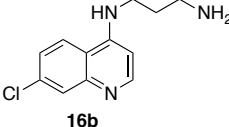
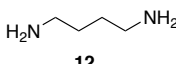
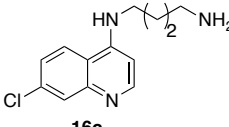
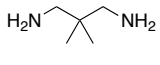
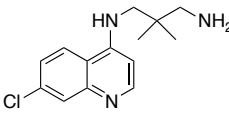
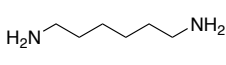
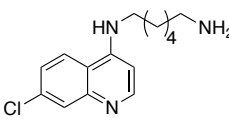
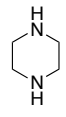
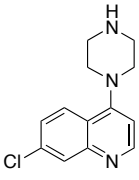
5.3.2. Synthesis of Anti-Prion Compounds: Attachment of Chloroquinoline and Acridine Linkers to the Scaffolding Units

Synthetic preparation of the *N*-(7-chloroquinolin-4-yl)-alkyl-diamine adducts and the trimesic acid-based scaffolding compounds were carried out by me. The preparation of the porphyrin-based compounds and the 3,3'-dicarboxy derivative of Congo red were accomplished by two other coworkers, Mr. Linghui Yu and Dr. Lei Li, respectively.

Chloroquinoline-diamine adducts **16** were readily prepared from the corresponding diamines **10-15** and 4,7-dichloroquinoline (Table 5.1). Preparation of *N*-(7-chloroquinolin-4-yl)-alkyl-diamine adducts **16a-f** was accomplished by heating a neat mixture of diamine **10-15** and 4,7-dichloroquinoline in a 5:1 ratio, over a few hours.⁶⁰ The diamine linkers were obtained in moderate to good yields after chromatographic purification. Three other diamine linkers based on the 6,9-dichloro-2-methoxy acridine monomeric binding unit were also prepared following a similar protocol (Figure 5.8).

Table 5.1 Synthesis of *N*-(7-chloroquinolin-4-yl)-alkyl-diamine adducts **16a-f**.^a



Entry	Diamine	Time (h)	Products (16)	Yield ^b (%)
1.	 10	14h	 16a	73%
2.	 11	12h	 16b	77%
3.	 12	24h	 16c	65%
4.	 13	10h	 16d	79%
5.	 14	14h	 16e	55%
6.	 15	8h	 16f	57%

^aStandard Procedure: A mixture of 4,7-dichloroquinoline (1.5 mmol) and required diamines (7.5 mmol) was heated at 80 °C for one hour without any stirring and then warmed up to 140 °C for the required time as indicated. Once the starting material was consumed (based on TLC), the reaction was quenched with 5 ml concentrated NaOH, followed by extraction with CH₂Cl₂ and brine, drying (MgSO₄), filtration and concentration in vacuo to give the required *N*-(7-chloroquinolin-4-yl)-alkyl-diamine adducts. ^bIsolated yields after chromatographic purification.

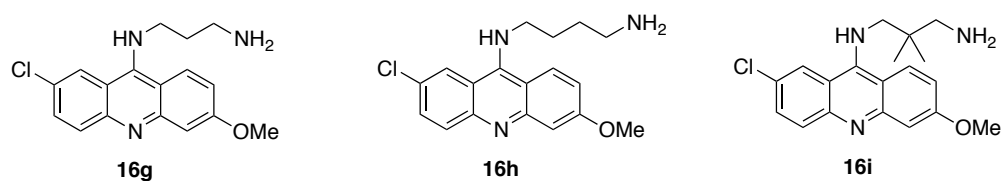
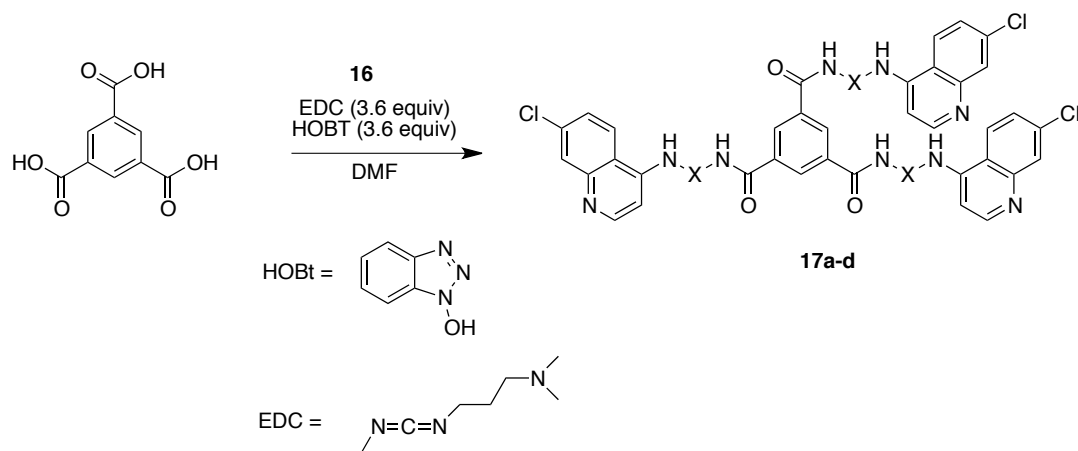


Figure 5.8 Acridine Based Diamine Linkers.

In order to synthesize trivalent PrP^{Sc} binding molecules, trimesic acid was chosen as the scaffold because the composition of its aromatic ring structure provides a convenient and symmetric scaffold upon which three moieties can be mounted at positions 1, 3, and 5. The molecule is commercially available and, to the best of our knowledge, has never been explored in the context of prion biology. The monomeric units **16a-f** were coupled to trimesic acid under standard amide bond forming conditions to afford the trivalent products **17a-d** (Table 5.2).⁶¹ In general, these molecules display poor solubility in water and most of the standard organic solvents, which makes purification a formidable task. Most of these compounds were purified either by repeated precipitation or column chromatography using 5% NEt₃ and 60% EtOAc in Hexanes.

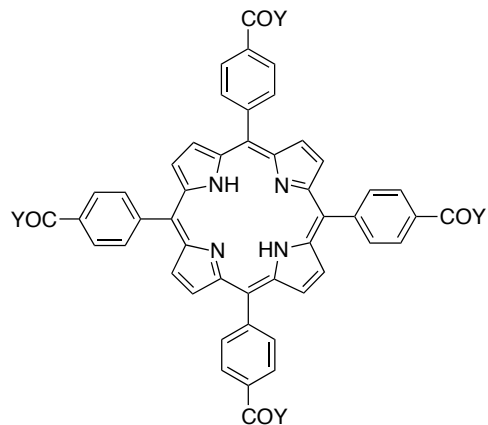
Table 5.2 Preparation of Trivalent Anti-Prion Compounds **17a-d** using Trimesic Acid as the Scaffold.^a



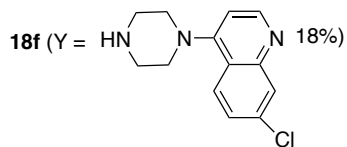
Entry	Binders (16)	Time (h)	Product (17)	Yield ^b (%)
1.		24h	17a	79%
2.		24h	17b	73%
3.		72h	17c	33%
4.		15h	17d	67%

^aStandard Procedure: A mixture of *N'*-(7-chloro-quinolin-4-yl)-ethane-1,2-diamine **16** (1.8 mmol), trimesic acid (0.5 mmol), 1-Hydroxybenzotriazole (HOBT) (1.8 mmol) and 1-Ethyl-3-(3-dimethylaminopropyl)carbodiimide hydrochloride (EDC) (1.8 mmol) in DMF (33 ml) was stirred at RT for 24 h. The reaction mixture was cooled and the solid was filtered. The solid product was washed with methanol and then water to remove any excess amine residue. The solid obtained after filtration was dried under reduced pressure to afford the desired compound **17**. ^bIsolated yields after chromatographic purification.

Mr. Linghui Yu had prepared the corresponding porphyrin-based tetrameric compounds **18a-i** (Figure 5.9) following a similar amide bond formation protocol. We also sought to modify the known anti-prion compound Congo red through tethering quinolone moieties to the amino acid groups on the naphthalene rings. Suitable conditions for this derivatization eluded us. As an alternative, Dr Lei Li prepared the 3,3'-dicarboxy analogue **19** (Figure 5.10) of Congo red. The known 3,3'-benzenedicarboxylic acid was subjected to diazotization followed by treatment with 4-amino-1-naphthalenesulfonic acid to afford **19** as a reddish brown solid. Once again, derivatization with quinoline-containing linkers proved to be unfruitful, and we did not pursue multivalent compound synthesis based upon Congo red-derived cores any further. Again, most of these compounds were highly polar and standard laboratory purification methods failed in isolating these compounds. However, repeated extractions and selective precipitations could afford the compounds as solids.



- 18a** (Y = NH[CH₂]₂NH-7-Cl-4-quinoliny) 82%
18b (Y = NH[CH₂]₃NH-7-Cl-4-quinoliny) 70%
18c (Y = NH[CH₂]₄NH-7-Cl-4-quinoliny) 70%
18d (Y = NH[CH₂]₆NH-7-Cl-4-quinoliny) 61%
18e (Y = NHCH₂CMe₂CH₂NH-7-Cl-4-quinoliny) 5%



- 18g** (Y = NH[CH₂]₃NH-Acr) 75%
18h (Y = NH[CH₂]₄NH-7-Acr) 57%
18i (Y = NHCH₂CMe₂CH₂NH-Acr) 54%

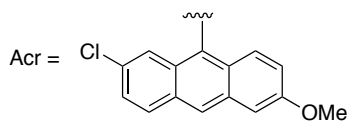


Figure 5.9 Tetravalent Anti-Prion Compounds **18a-i** Using Tetraphenylporphyrin Tetracarboxylic Acid as the Scaffold.

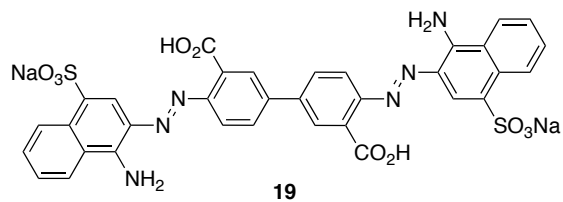


Figure 5.10 The 3,3' Dicarboxy Analogue of Congo Red as an Anti-Prion Compound.

5.4 Biological Studies on the Anti-Prion Compounds

The biological studies described in this section have been carried out by our collaborators in the Westaway Lab from the Centre for Prions and Protein Folding Diseases, University Of Alberta. The study includes cytotoxicity tests for the linkers **16a-i** as well as for the newly synthesized binding compounds **17a-d**, **18a-i** and **19** followed by *in vitro* cell studies using treated-SMB and ScN2A cells for detection of anti-prion activity.

5.4.1. Cytotoxicity of Monomeric Units and their Respective Scaffolding Compounds

As a preamble to considering disease related effects, toxicity studies were performed to identify compounds with deleterious side effects that would limit *in vivo* utility. Neuroblastoma N2a cells have been reported to tolerate quinacrine at concentrations up to 2.5 μM ,^{54a,d,e} while neither chloroquine (Figure 5.11) nor various acridines were previously found to hinder cell viability at concentrations < 4 μM .^{54a,62} We synthesized 4,7-dichloroquinoline and 6,9-dichloro-2-methoxyacridine-based compounds **16a-f** and **16g-i** that contain variable linkers within the side chain at position four of the nitrogen-containing ring. To determine whether the addition of the linker fragment to chloroquinoline, acridine or attachment to the scaffolding molecules enhanced the cytotoxicity of these molecules in comparison to quinacrine, we evaluated mitochondrial activity of SMB cells using a treatment period of 48 hours, a regimen validated by treatment with DMSO. The repertoire of scaffolds, chloroquinoline moieties, and synthetic molecules containing chloroquinoline were all found to be less toxic than quinacrine. In a prior analysis by Cope *et al.*,⁶³ compounds were considered to be cytotoxic if the mitochondrial activity of the cells fell below 70% of the untreated control. Following this criterion, only **17b** and **18f** were found to be slightly cytotoxic at a concentration of 2.5 μM . In contrast, all independent acridine moieties were more toxic than quinacrine.

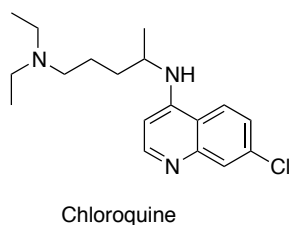


Figure 5.11 Chloroquine as an Anti-Prion Compound.

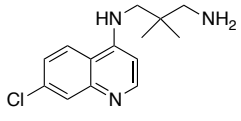
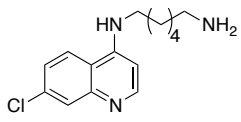
5.4.2. Ability of Chloroquinoline and Acridine Fragments to Clear PrP^{Sc} *In Vitro*

Since our primary goal was to synthesize compounds with greater anti-prion efficacy than quinacrine, the previous treatment protocol was altered to make it more stringent by starting with a higher cell confluence, thus increasing the initial PrP^{Sc} titer.^{54c} This scheme was evaluated by treating SMB and ScN2a cells that persistently propagate PrP^{Sc} with two well-studied anti-prion agents of particular interest in this study, quinacrine and Congo red. Both compounds reduced PrP^{Sc} by $\geq 70\%$, but neither completely cleared the misfolded protein as observed with the previous method and hence called for a lower PrP^{Sc} titer.

Before considering the effectiveness of scaffolded conjugates, SMB cells were subjected to the 7-chloroquinoline and acridine moieties in their monomeric form. Despite having similar bicyclic backbones, the 7-chloroquinoline moieties had contrasting effects on PrP^{Sc} accumulation in the cells. Compound **16d**, possessing the most effective anti-prion activity, consisted of a five carbon branched linker that reduced PrP^{Sc} levels in a dose-dependent manner. Compounds consisting of linear carbon chain linkers of various lengths (**16a**, **16b**, **16c** and **16e**) displayed an intriguing enhancement in the amount of PrP^{Sc} accumulated when treated at low concentrations and with reduction only apparent at higher concentrations. The compound **16e** having the longest linear carbon chain linker, displayed this characteristic to the greatest extent, with an almost

two-fold enhancement maintained between 0.3 to 2.5 μM , while PrP^{Sc} levels are reduced in the presence of 5 μM **16e** (Table 5.3). **16f** was the only compound possessing a rigid cyclic linker and was found to have no notable effects upon PrP^{Sc} levels at concentrations \leq 2.5 μM . On the contrary, independent acridine moieties only possessed PrP^{Sc} inhibiting activity. However, anti-prion activity of the acridine moieties is correlated with their cytotoxicity, thus limiting their ability for completely ridding the cells of PrP^{Sc}. This finding led us to focus on scaffolds bearing the 7-chloroquinoline moieties.

Table 5.3 Anti-Prion Activity of Independent Chloroquinoline Moieties.

Entry	Binders (16)	SMB Cell Concentration (μM)	PrP ^{Sc} Inhibition (%)
1.	 <p>16d</p>	0.6 μM	40 \pm 19%
2.	 <p>16e</p>	0.6 μM	2.07 \pm 0.32% ^b

^aSummarized results of Western Blot Analysis carried out to determine the efficiency of PrP^{Sc} clearance from SMB cells treated for 6 days with 7-chloroquinoline binding compounds. ^bReported for PrP^{Sc} enhancement detected after 6 days treatment of SMB cells with **16e** at 0.6 μM concentration.

5.4.3. Effect of Novel Congo Red Derivative on PrP^{Sc} Propagation in Cultured Cells

Despite our inability to link the quinoline or acridine units to the Congo red core, the modified Congo red core was nonetheless examined for antiprion activity. As previously reported for Congo red itself,⁶⁴ elevated PrP^{Sc} levels were generated in SMB cells treated with the derivative of Congo red **19**, and unlike the unmodified structure of Congo red that cleared > 90% PrP^{Sc} in SMB cells at a

concentration of 2.5 μM , an inhibitory effect was never reached for the present case.

5.4.4. Tetraphenylporphyrin Tetracarboxylic Acid Scaffolding Compounds as Anti-Prion Agents

Porphyrins and other tetrapyrrole compounds are anti-prion molecules that contain a large aromatic ring system known to bind PrP^{Sc} with a potency that is influenced by metal ions (i.e. Fe^{3+} , Mn^{3+} , Co^{3+} , Cu^{2+} , and Ni^{2+}).^{65,66,67,68} The anti-prion activity of tetraphenyl porphyrin molecules in which the 7-chloroquinoline moieties containing various diamine linkers were attached at four *meso* positions of tetraphenylporphyrin tetracarboxylic acid, were tested. Surprisingly, only a single chloroquinoline scaffolding compound **18a** containing the smallest linear carbon chain linker, $-(\text{CH}_2)_2-$, reduced PrP^{Sc} in a dose-dependent manner. Moreover, attachment of acridine moieties at homologous sites on the tetraphenylporphyrin tetracarboxylic acid scaffold, generated compounds **18g-i** that negated the anti-prion activity observed in their monomeric form while simultaneously decreasing their cytotoxicity.

5.4.5. Enhanced Anti-Prion Activity of Trimesic Acid-Based Chloroquinoline Scaffolds.

Trimesic acid is a commercially available compound that had never been tested earlier in the context of prion treatment. The presence of carboxylic acid group at 1, 3 and 5 positions provides us with three handles for elaboration. We envisioned that connecting three binding units such as 7-chloroquinoline or acridine moieties may lead to enhanced binding ability and hence higher anti-prion activity. However, first, the empty trimesic acid scaffold was applied to SMB cells and at concentrations $\leq 2.5 \mu\text{M}$ lacked anti-prion activity, while at 5 μM depleted PrP^{Sc} by nearly 40%. Once 7-chloroquinoline moieties were attached

to the trimesic acid scaffold, all were found capable of efficiently decreasing PrP^{Sc} levels at a minimum concentration of 1.25 μ M. Moreover, attachment of chloroquinoline moieties with linear (**17a** and **17b**) or branched (**17c**) carbon chain linkers generated compounds with the highest anti-prion activity, as demonstrated by their ability to rid > 95% PrP^{Sc} at high concentrations (Table 5.4). However the compound linked by a piperazine ring **17d** was found to be less effective. In fact, 5 μ M of either **17b** or **17c** appeared to “cure” SMB cells of PrP^{Sc} ($0.04 \pm 0.04\%$ for both), which are figures superior to the treatment with quinacrine or Congo red with regard to IC₅₀. By switching to the alternative regimen as described by others,^{54c} an even lower concentration of **17b** and **17c** was required to eradicate PrP^{Sc} from the SMB cells.

Table 5.4 Efficient Clearance of PrP^{Sc} with Trimesic Acid Scaffolds for Treated-SMB Cells.^a

Entry	Anti-Prion Compounds	SMB Cell Concentration (μ M)	PrP ^{Sc} inhibition (%)
1.	Congo Red	5.0 μ M	> 90%
2.	Quinocrine	5.0 μ M	> 70%
3.	Trimesic Acid	5.0 μ M	> 40%
4.	17a	5.0 μ M	> 95%
5.	17b	5.0 μ M	~ 100%
6.	17c	5.0 μ M	> 70%
7.	17d	5.0 μ M	~ 100%

^aSummarized results of Western Blot Analysis carried out to determine the efficiency of PrP^{Sc} clearance from SMB cells treated for 6 days with various anti-prion compounds.

5.4.6. Ability of 17b and 17c to Eradicate PrP^{Sc} of a Different Prion Strain

To evaluate the spectrum of anti-prion activity for **17b** and **17c**, ScN2a cells, which consist of a different cell type and prion strain than SMB cells were also treated. ScN2a cells are a neuroblastoma-derived population of neuronal

subtypes chronically infected with RML prions,⁶³ while SMB cells have been described as mesodermal cells that persistently support the replication of 139A prions.⁶⁹ Although compound potency was restricted in comparison to treatment of SMB cells, **17b** still had the capacity to decrease PrP^{Sc} in a dose-dependent manner. However, anti-prion activity of **17c** was significantly reduced in ScN2a cells with PrP^{Sc} being maintained at concentrations ranging from 0.3 to 2.5 μ M and slightly reduced at 5 μ M.

5.5 Rationale for the Anti-Prion Activity of Various Scaffolded Compounds

Quinacrine, an anti-prion compound, is a tricyclic acridine containing a quinoline ring with an aliphatic side chain. Previous studies have demonstrated that the anti-prion potency of quinacrine is shared with its derivatives including chloroquine and various acridines, in some cases without severely affecting PrP binding.^{54a,54c,55a,70,71,72} Here, we postulated that the number of quinoline or acridine moieties attached to a scaffold would have an additive effect on the binding affinity. This in turn is expected to affect the anti-prion activity exhibited by the moiety in its monomeric form along with any intrinsic activity possessed by the scaffold itself. Support for this concept comes from the enhanced anti-prion effect of quinacrine and its derivatives by synthesizing multiple cyclic structures such as biquinine, biquinidine, biquinoline,⁷⁰ bis-acridine,⁷³ and hybrid heterocyclic compounds.^{54b,74}

5.5.1. Anti-Prion Activity of Compounds

We synthesized six chloroquinoline and four acridine moieties containing a linear, branched, or cyclic linker within the side chain at position four of the nitrogen-containing ring. In the SMB model system, the expected additive anti-prion effect was best observed after linking three homologous chloroquinoline moieties of **16a**, **16b** or **16d** to the trimesic acid scaffold in the synthesis of **17a**,

17b and **17c** respectively. Therefore, 2-carbon, 3-carbon linkers $(\text{CH}_2)_2$, $(\text{CH}_2)_3$ and the branched chain linkers $(\text{CH}_2\text{CMe}_2\text{CH}_2)$ were superior to the 4-carbon and 6-carbon $(\text{CH}_2)_4$, $(\text{CH}_2)_6$ and cyclic linkers. However, once four **16a**, **16b** or **16d** units were linked to the tetraphenylporphyrin tetracarboxylic acid scaffold, none shared the ability to reduce PrP^{Sc} *in vitro*. This finding was unexpected because Caughey and co-workers had demonstrated that a variety of similar tetrapyrroles clear PrP^{Sc} efficiently from cultured cells.⁷⁵ In contrast to the tetrapyrroles with the highest anti-prion activity, tetraphenylporphyrin tetracarboxylic acid, as used here, was neither sulfonated nor synthesized with a metal atom bound to the central core of the porphyrin ring system.⁷³ The lack of anti-prion activity may also be attributed to the larger size of the tetrahydroporphyrin tetracarboxylic acid core structure, which may prevent the chloroquinoline moiety linked to it from reaching the endolysosomes, which some studies have indicated to be the primary site of inhibition by quinacrine.^{55c} These features may be exploited in the future to improve the anti-prion activity of the scaffold part of the molecule. In comparison to the monomeric and tertaphenylporphyrin tetracarboxylic acid structures, an advantageous feature of the trimesic acid scaffold may be the triangular positioning of the chloroquinoline moieties at the 1, 3 and 5-positions of the trimesic acid core. This structural feature could potentially maximize interaction with PrP^{Sc} assemblies if the trimeric structure predicted by computational modeling based on negative stain electron microscopy of 2-D crystals and X-ray fiber diffraction holds true.^{76,77,78}

5.5.2. Role of Cell Type and Prion Strain in Anti-Prion Activity

Two of the most effective compounds for reducing PrP^{Sc} , **17b** and **17c**, were applied to ScN2a cells to better understand the scope of their anti-prion spectrum. Interestingly, **17b** maintained activity in ScN2a cells, whereas **17c** became largely inactive. Chronically-infected ScN2a cells differ from SMB cells in two respects: they are neuroblastoma cells infected with RML prions, while SMB cells are mesodermal fibroblasts supporting 139A prions.^{63,68} Although both

139A and RML prion strains originated from the mouse-adapted “Chandler” scrapie isolate,^{79,80} it is possible that continuous replication of the prion strains in these contrasting cell lines has allowed the prion agent to diverge and adapt to their respective cell types, a difference previously observed when infecting another cell culture model with these two prion strains.⁸¹ In parallel to our findings for **17b** and **17c**, the efficiency with which quinacrine clears PrP^{Sc} from cultured cells appears to be influenced by cell type, as well as the infecting prion strain.^{54d, 55d}

5.5.3. PrP^{Sc} Enhancing Compounds

Several compounds were unexpectedly found to elevate the level of PrP^{Sc}. This finding was unusual in the fact that only a short list of molecules possess this characteristic including plasminogen,⁸² bacterial GroEL,⁸³ yeast heat shock protein 104,⁸⁴ sulfated glycans⁸⁵ and certain polyanionic macromolecules such as RNA.⁸⁶ In our study, compounds most efficacious for enhancing the PrP^{Sc} accumulation were free chloroquinoline subunits containing lengthy linear carbon chains (**16c** and **16e**) and a tetraphenylporphyrin tetracarboxylic acid scaffolding compound linked to chloroquinoline by a three carbon linear chain (**18b**). These compounds were found to maintain their stimulatory effect at concentrations ranging from 0.3 μ M through 2.5 μ M, but at higher dosages returned PrP^{Sc} to basal levels or depressed them. None of the trimeric acid scaffolding compounds possessed this property, with the exception of 0.3 μ M **17d**, which contains a cyclic piperazine linker. Since chloroquinoline is known to bind PrP,^{55a-c, 77} we speculate that the ability to enhance PrP^{Sc} may stem from stabilization of PrP^{Sc} oligomeric assemblies. The dicarboxylated Congo red derivative **19** was also found to stimulate the PrP^{Sc} formation at most concentrations. This exemplifies the fact that dicarboxylation may be unique in disrupting the planarity and or torsional mobility of the phenyl rings essential for PrP^{Sc} binding.

5.6 Conclusion

We were able to target PrP^{Sc} propagation most efficiently by synthesizing scaffolding compounds in which chloroquinoline subunits, rather than acridine moieties, were attached to bind PrP^{Sc}. Since quinacrine lacks the ability to chemically degrade PrP^{Sc} *in vitro*, direct interaction potentially allows quinacrine and its derivatives to block prion propagation by preferential binding of PrP^{Sc} over PrP^C.^{55b} Despite having fewer attachment sites for chloroquinoline, the trimesic acid was discovered to serve as a better scaffolding compound than tetraphenylporphyrin tetracarboxylic acid. Furthermore, we found that 3,3'-carboxylation of Congo red rendered the compound unsuitable for clearing PrP^{Sc}. More importantly, PrP^{Sc} levels were increased by 3,3'-carboxylated Congo red as well as several chloroquinoline-based molecules.

5.7 Future Plans

The work described in this chapter has been published as a part of a full paper and the project is more or less complete. However, there is still scope of improvements in the development of new molecules with better efficacy in prion inhibition. A particularly interesting extension of the present work could be the synthesis of multivalent fluorescent compounds. A possible route to achieve this, is to replace one of the binding units with a fluorophore. One example of the fluorophore is the cyanine dye Cy5 (Figure 5.11), which can avoid quenching by azo dye, porphyrins or the acridine binder, because it emits at longer wavelength.⁸⁷ Two other potential ways of preparation may include simple installation of fluorescent binding units or usage of fluorescent scaffolds. Successful synthesis of these molecules with high affinity toward PrP^{Sc} will help early detection of prion infection *in vivo* and contamination of surgical instruments or animal processing facilities.

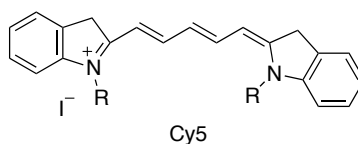


Figure 5.12 Cyanine dye Cy5 as a Fluorophore.

The multivalent anti-prion compounds synthesized in the present study are mostly of high molecular weight and are insoluble in water, which might limit their application as drug molecules. We need to modify these compounds to make them more “drug-like.” This might be done by controlling the length of the linker or the structure of the scaffold. Molecules based on trimesic acid scaffold have the lowest molecular weights and according to our present results they are the best candidates if they can be modified to make them more water soluble. Another crucial requirement for a central nervous system (CNS) drug is to cross the blood brain barrier (BBB). One possible way to test this for the present molecules would require *in vitro* assessment of brain penetration using primary bovine and human brain endothelial cells.

5.8 Experimental

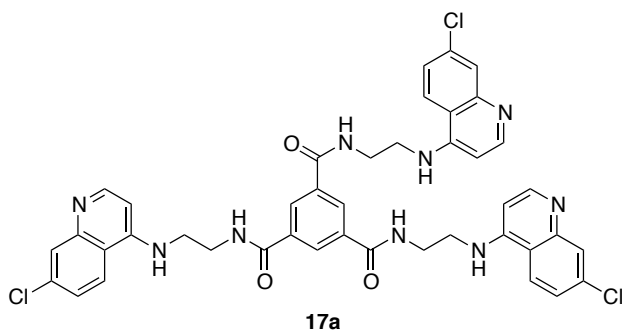
5.8.1. General Information

Reactions were conducted in oven-dried (110 °C) glassware under a positive argon atmosphere unless otherwise noted. Transfer of anhydrous solvents, reagents or mixtures was accomplished with oven-dried syringes or via cannulae. Solvents were distilled before use: dichloromethane over calcium hydride; tetrahydrofuran and diethyl ether over sodium benzophenone ketyl; toluene over sodium metal. Thin layer chromatography (TLC) was performed on 0.25 mm thick *precoated* silica gel plates (*Merck Fertigplatten Kieselgel 60F254*). Flash chromatography columns were packed with 230-240 mesh silica gel.

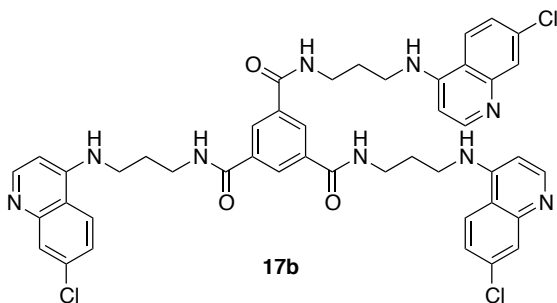
Proton nuclear magnetic resonance spectra (^1H NMR) were recorded at 300, 400 MHz or 500 MHz and the chemical shifts are reported on the δ scale (ppm) and the spectra are referenced to residual solvent peaks: CDCl_3 (7.26 ppm, ^1H ; 77.06 ppm, ^{13}C), or CD_3OD (3.31 ppm, ^1H ; 49.00 ppm, ^{13}C), or $(\text{CD}_3)_2\text{SO}$ (2.50 ppm, ^1H ; 39.52 ppm, ^{13}C) as internal standard. Coupling constants (J) are reported in Hz. Second order splitting patterns are indicated. Splitting patterns are designated as s, singlet; d, doublet; t, triplet; q, quartet; m, multiplet; br, broad; dd, doublet of doublets, dt, doublet of triplets, etc. Carbon nuclear magnetic resonance spectra (^{13}C NMR) were recorded at 100 MHz or 125 MHz and chemical shifts are accurate to one decimal place. Infrared (IR) spectra were measured with a Nicolet Magna 750 FT-IR spectrometer and Nic-Plan FT-IR microscope. Mass spectra were determined on a Agilent 6220 oaTOF electrospray positive ion mode spectrometer (ESI) or a Bruker Daltonics Apex-Qe FTICR MS high resolution MALDI spectrometer.

All reagents and catalysts were purchased from Aldrich or Sigma or Strem and were used without further purification unless otherwise stated. The preparation of N-(7-chloroquinolin-4-yl)-alkyl diamine compounds **16a-f** and N-(6-Chloro-2-methoxy acridin-9-yl)-alkyl diamine compounds **16g-i** were carried out by using literature procedures.^{88,89,90}

5.8.2. Synthesis and Characterization of Compounds

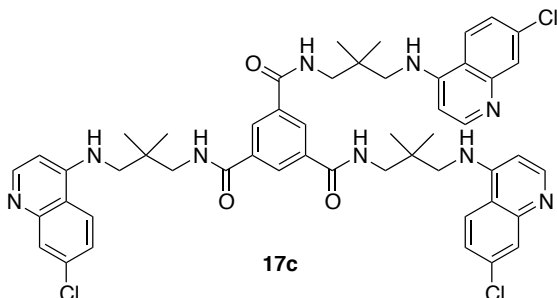


17a: A mixture of N'-(7-chloro-quinolin-4-yl)-ethane-1,2-diamine **16a** (1.8 mmol), trimesic acid (0.5 mmol), 1-Hydroxybenzotriazole (HOBt) (1.8 mmol) and 1-Ethyl-3-(3-dimethylaminopropyl)carbodiimide hydrochloride (EDAC) (1.8 mmol) in DMF (33 mL) was stirred at RT for 24 h. The reaction mixture was cooled and the solid was filtered. The solid product was washed with methanol and then water to remove any excess amine residue. The solid obtained after filtration was dried under high vacuum to afford the desired compound **17a** as a white solid, 0.32 g (79 % yield): IR (neat) 3496, 3339, 3068, 2898, 1644, 1613, 1582, 1536 cm^{-1} . ^1H NMR (400 MHz, *d*-DMSO) δ 8.96 (t, $J = 0.8$ Hz, 3H), 8.48 (s, 3H), 8.41 (d, $J = 5.6$ Hz, 3H), 8.19 (d, $J = 8.8$ Hz, 3H), 7.78 (d, $J = 2.4$ Hz, 3H), 7.48 (t, $J = 0.8$ Hz, 3H), 7.44 (dd, $J = 9.2, 2.4$ Hz, 3H), 6.65 (d, $J = 5.6$ Hz, 3H), 3.52-3.50 (m, $J = 27$ Hz, 12H); ^{13}C NMR (125 MHz, *d*-DMSO) δ 165.5, 154.1, 144.9, 140.9, 136.6, 134.3, 128.6, 126.0, 125.2, 120.9, 115.9, 98.5, 42.1, 37.7; HRMS (ESI, $([\text{M}+\text{H}]^+)$) Calcd for $\text{C}_{42}\text{H}_{37}\text{Cl}_3\text{N}_9\text{O}_3$ m/z 820.2079; found m/z 820.2073.

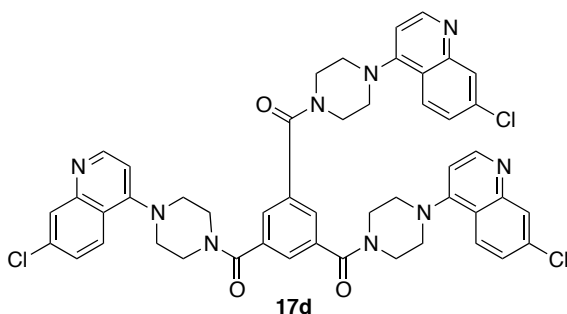


17b: General procedure A was used in the preparation and purification of **17b** as a white solid, 0.31 g (73% yield): IR (neat) 3318, 3074, 2947, 2906, 1673, 1656, 1643, 1592, 1547 cm^{-1} ; ^1H NMR (400 MHz, *d*-DMSO) δ 8.61 (s, 3H), 8.42 (d, $J = 6.0$ Hz, 3H), 8.38 (d, $J = 9.1$ Hz, 3H), 8.28 (br s, 3H), 7.82-7.79 (m, 3H), 7.80 (d, $J = 2.2$ Hz, 3H), 7.41 (dd, $J = 9.1, 2.2$ Hz, 3H), 6.57 (d, $J = 6.0$ Hz, 3H), 3.62-3.59 (m, 12H), 1.98-1.90 (m, 6H); ^{13}C NMR (100 MHz, *d*-DMSO) δ 164.9, 152.6, 146.1, 140.2, 135.6, 134.3, 128.2, 125.1, 124.6, 122.0, 115.8, 98.2, 40.1, 36.6,

27.0; HRMS (ESI, $[M+H]^+$) Calcd for $C_{45}H_{43}Cl_3N_9O_3$ m/z 862.2549; found m/z 862.2541.



17c: General procedure A was used in the preparation and purification of **17c** yellow solid, 0.15 g (33% yield): IR (neat) 3310, 3033, 2995, 2543, 1649, 1596, 1529, 1496, 1449 cm^{-1} ; 1H NMR (400 MHz, CD_3OD) δ 8.85 (d, $J = 0.9$ Hz, 3H), 8.61 (d, $J = 8.9$ Hz, 3H), 8.47 (s, 3H), 8.34 (d, $J = 2.1$ Hz, 3H), 7.84 (s, 3H), 7.80 (d, $J = 2.2$ Hz, 3H), 7.69 (dd, $J = 9.1, 2.1$ Hz, 3H), 6.65 (d, $J = 5.6$ Hz, 3H), 3.42-3.41 (m, 6H), 3.06-3.05 (m, 6H), 1.11-1.09 (m, 18H); ^{13}C NMR (125 MHz, CD_3OD) δ 167.1, 153.3, 147.3, 141.0, 135.8, 133.3, 128.6, 125.5, 124.8, 122.3, 116.4, 98.7, 61.1, 54.2, 32.4, 21.6; HRMS (ESI, $[M+H]^+$) Calcd for $C_{51}H_{55}Cl_3N_9O_3$ m/z 946.3493; found m/z 946.3489.



17d: General procedure A was used in the preparation and purification of **17d** as a yellow solid, 0.30 g (67% yield): IR (neat) 3479, 3212, 3042, 2865, 2653, 1636, 1604, 1585, 1539, 1506, 1429 cm^{-1} ; 1H NMR (400 MHz, CD_3OD) δ 8.55 (d, $J =$

6.9 Hz, 3H), 8.28 (d, $J = 8.9$ Hz, 3H), 7.96 (d, $J = 2.1$ Hz, 3H), 7.83 (s, 3H), 7.69 (dd, $J = 9.1, 2.1$ Hz, 3H), 7.23 (d, $J = 6.9$ Hz, 3H), 4.07-4.05 (m, 24 H); ^{13}C NMR (125 MHz, CD_3OD) δ 166.1, 151.7, 148.3, 146.1, 135.6, 134.4, 128.2, 125.3, 124.6, 122.3, 114.9, 98.4, 57.3, 49.3; HRMS (ESI, $([\text{M}+\text{H}]^+)$) Calcd for $\text{C}_{48}\text{H}_{43}\text{Cl}_3\text{N}_9\text{O}_3$ m/z 898.2549; found m/z 898.2544.

5.9 References

- (1) A version of this chapter has previously been published: Mays, C. E.; Joy, S.; Li, L.; Yu, L.; Genovesi, S.; West, F. G.; Westaway, D. *Biomaterials* **2012**, *33*, 6808.
- (2) Gambetti, P.; Peterson, R. B.; Parchi, P.; Chen, S. G.; Capellari, S.; Goldfarb, L.; Gabizon, R.; Montagna, P.; Lugaresi, E.; Piccardo, P.; Ghetti, B. In *Prion Biology and Diseases*, ed. Prusiner, S. B. (Cold Spring Harbor Lab. Press, Plainview, NY), **1999**, pp 509-583.
- (3) Prusiner, S. B. *Science* **1982**, *216*, 136.
- (4) Shyng, S. L.; Heuser, J. E.; Harris, D. A. *J. Cell Biol.* **1994**, *125*, 1239.
- (5) (a) Pan, K.-M.; Baldwin, M.; Nguyen, J.; Gasset, M.; Serban, A.; Groth, D.; Mehlhorn, I.; Huang, Z.; Fletterick, R. J.; Cohen, F. E.; Prusiner, S. B. *Proc. Natl. Acad. Sci. USA* **1993**, *90*, 10962. (b) Prusiner, S. B. *Proc. Natl. Acad. Sci. USA* **1998**, *95*, 13363.
- (6) Prusiner, S. B. *Science* **1991**, *252*, 1515.
- (7) (a) Brazier, M. W.; Wall, V. A.; Brazier, B. W.; Masters, C. L.; Collins, S. J. *Exp. Rev. Anti. Infect. Ther.* **2009**, *7*, 83. (b) Riesner, D. *Br. Med. Bull.* **2003**, *66*, 21.
- (8) (a) Prusiner, S. B. *Science* **1982**, *216*, 136. (b) Bellinger-Kawahara, C.; Diener, T. O.; McKinley, M. P.; Groth, D. F.; Smith, D. R.; Prusiner, S. B. *Virology* **1987**, *160*, 271.
- (9) Claudio, S.; Joaquin, C. *Nat. Med.* **2004**, S63.
- (10) (a) Cohen, F. E.; Pan, K. M.; Huang, Z.; Baldwin, M.; Fletterick, R. J.; Prusiner, S. B.; *Science* **1994**, *265*, 530. (b) Eigen, M. *Biophysical Chemistry* **1996**, *63*, A1.

- (11) (a) Swietnicki, W.; Morillas, M.; Chen, S. G.; Gambetti, P.; Surewicz, W. K. *Biochemistry* **1999**, *39*, 424. (b) Morillas, M.; Vanik, D. L.; Surewicz, W. K. *Biochemistry* **2001**, *40*, 6982. (c) Kocisko, D. A.; Come, J. H.; Priola, S. A.; Suzette, A.; Chesebro, B.; Raymond, G. J.; Lansbury, P.T.; Caughey, B. *Nature* **1994**, *370*, 471. (d) Maiti, N. R.; Surewicz, W. K. *J. Biol. Chem.* **2001**, *276*, 2427. (e) Caughey, B.; Lansbury Jr, P. T. *Annu. Rev. Neurosci.* **2003**, *26*, 267.
- (12) Jarrett, J. T.; Lansbury Jr, P. T. *Cell* **1993**, *73*, 1055.
- (13) Belay, E. D. *Annu. Rev. Microbiol.* **1999**, *53*, 283.
- (14) Richardson, E. P.; Masters, C. L. *Brain Pathol.* **1995**, *5*, 33.
- (15) Schonberger, L. B. *Infect. Disease Clinics of North Am.* 1998, *12*, 111.
- (16) Reder, A. T.; Mednick, A. S.; Brown, P.; Spire, J. P.; Van Cauter, E.; Wollmann, R. L.; Cervenàková, L.; Goldfarb, L. G.; Garay, A.; Ovsiew, F.; Gajdusek, D. C.; Roos, R. P. *Neurology* **1995**, *45*, 1068.
- (17) Prusiner, S. B.; Scott, M.; Foster, D.; Pan, K.-M.; Groth, D.; Mirenda, C.; Torchia, M.; Yang, S.-L.; Serban, D.; Carlson, G. A.; Hoppe, P. C.; Westaway, D.; DeArmond, S. J. *Cell* **1990**, *63*, 673.
- (18) Gordon, W.S. *Vet. Rec.* **1946**, *58*, 516.
- (19) Sigurdsson, B. *Br. Vet. J.* **1954**, *110*, 341.
- (20) Hadlow, W. J. *Lancet* 1959, *2*, 289.
- (21) Gajdusek, D. C.; Gibbs, C. J.; Alpers, M. *Nature* **1966**, *209*, 794.
- (22) Cho, H. J. *Nature* **1976**, *262*, 411.
- (23) Alper, T.; Cramp, W.A.; Haig, D.A.; Clarke, M.C. *Nature* **1967**, *214*, 764.
- (24) Kimberlin, R.H. *Nature* **1982**, *297*, 107.
- (25) Griffith, J.S. *Nature* **1967**, *215*, 1043.
- (26) Prusiner, S.B. *Science* **1982**, *216*, 136.
- (27) Prusiner, S. B. *Annu. Rev. Microbiol.* **1989**, *43*, 345.
- (28) Will, R. G.; Ironside, J. W.; Zeidler, M.; Cousens, S. N.; Estibeiro, K.;

- Alperovitch, A.; Poser, S.; Pocchiari, M.; Hofman, A.; Smith, P. G. *Lancet* **1996**, *347*, 921.
- (29) (a) Trevitt, C. R. *Brain* **2006**, *129*, 2241. (b) He, J.; Zhang, Y.; Hong, T., *Sci. China Life Sci.* **2010**, *53*, 959.
- (30) (a) Mallucci, G.; Dickinson, A.; Linehan, J.; Klöhn, P.-C.; Brandner, S.; Collinge, J. *Science* **2003**, *302*, 871. (b) Wadsworth, J.D.F.; Asante, E.A.; Collinge, J. *Neuropath. Appl. Neuro.* **2010**, *36*, 576.
- (31) Meier, P.; Genoud, N.; Prinz, M.; Maissen, M.; Ilicke, T. R.; Zurbriggen, A.; Raeber, A. J.; Aguzzi, A. *Cell* **2003**, *113*, 49.
- (32) He, J.; Zhang, Y.; Hong, T. *Sci. China Life Sci.* **2010**, *53*, 959.
- (33) Sakaguchi, S.; Ishibashi, D.; Matsuda, H. *Expert Opin. Ther. Pat.* **2009**, *19*, 907.
- (34) Aguzzi, A.; Heppner, F. L.; Heikenwalder, M.; Prinz, M.; Mertz, K.; Seeger, H.; Glatzel, M. *Br. Med. Bull.* **2003**, *66*, 141.
- (35) Sigurdsson, E.; Brown, D.; Daniels, M.; Kascsak, R.; Kascsak, R.; Carp, R. *Am. J. Pathol.* **2002**, *161*, 7.
- (36) Wisniewski, T.; Goni, F. *Exp. Rev. Vacc.* **2010**, *9*, 1441.
- (37) Sethi, S.; Lipford, G.; Wagner, H.; Kretzschmar, H., *Lancet* **2002**, *360*, 229.
- (38) Outram, G.; Dickinson, A.; Fraser, H. *Nature* **1974**, *249*, 855.
- (39) Outram, G.; Dickinson, A.; Fraser, H. *Lancet* **1975**, *1*, 198.
- (40) Gabizon, R.; McKinley, M. P.; Groth, D.; Prusiner, S. B. *Proc. Natl. Acad. Sci. USA* **1988**, *85*, 6617.
- (41) Horiuchi, M.; Caughey, B. *EMBO J.* **1999**, *18*, 3193.
- (42) Enari, M.; Flechsig, E.; Weissmann, C. *Proc. Natl. Acad. Sci. USA* **2001**, *98*, 9295.
- (43) Tatzelt, J.; Prusiner, S. B.; Welch, W. J. *EMBO J.* **1996**, *15*, 6363.
- (44) Caspi, S.; Halimi, M.; Yanai, A.; Sasson, S. B.; Taraboulos, A.; Gabizon, R. *J. Biol. Chem.* **1998**, *273*, 3484.

- (45) Perrier, V.; Wallace, A. C.; Kaneko, K.; Safar, J.; Prusiner, S. B.; Cohen, F. E. *Proc. Natl. Acad. Sci. U.S.A.* **2000**, *97*, 6073.
- (46) Kaneko, K.; Zulianello, L.; Scott, M.; Cooper, C. M.; Wallace, A. C.; James, T. L.; Cohen, F. E.; Prusiner, S. B. *Proc. Natl. Acad. Sci. U.S.A.* **1997**, *94*, 10069.
- (47) (a) Reddy, T. R.; Mutter, R.; Heal, W.; Guo, K.; Gillet, V. J.; Pratt, S.; Chen, B. *J. Med. Chem.* **2006**, *49*, 607. (b) Guo, K.; Mutter, R.; Heal, W.; Reddy, T. R.; Cope, H.; Pratt, S.; Thompson, M. J.; Chen, B. *Eur. J. Med. Chem.* **2008**, *43*, 93.
- (48) Bolognesi, M. L.; Ai Tran, H. N.; Staderini, M.; Monaco, A.; López-Cobeñas, A.; Bongarzone, S.; Biarnés, X.; López-Alvarado, P.; Cabezas, N.; Caramelli, M.; Carloni, P.; Menéndez, J. C.; Legname, G. *ChemMedChem* **2010**, *5*, 1324.
- (49) (a) Korth, C.; May, B. C.; Cohen, F. E.; Prusiner, S. B. *Proc. Natl. Acad. Sci. U.S.A.* **2001**, *98*, 9836-9841. (b) May, B. C.; Witkop, J.; Sherrill, J.; Anderson, M. O.; Madrid, P. B.; Zorn, J. A.; Prusiner, S. B.; Cohen, F. E.; Guy, R. K. *Bioorg. Med. Chem. Lett.* **2006**, *16*, 4913.
- (50) a) May, B. C.; Fafarman, A. T.; Hong, S. B.; Rogers, M.; Deady, L. W.; Prusiner, S. B.; Cohen, F. E. *Proc. Natl. Acad. Sci. U.S.A.* **2003**, *100*, 3416. b) Dollinger, S.; Lober, S.; Klingenstein, R.; Korth, C.; Gmeiner, P. A. *J. Med. Chem.* **2006**, *49*, 6591. c) Kempster, S.; Bate, C.; Williams, A. *NeuroReport* **2007**, *18*, 479.
- (51) Heal, W.; Thompson, M. J.; Mutter, R.; Cope, H.; Louth, J. C.; Chen, B. *J. Med. Chem.* **2007**, *50*, 1347-1353.
- (52) Kimata, A.; Nakagawa, H.; Ohyama, R.; Fukuuchi, T.; Ohta, S.; Suzuki, T.; Miyata, N. *J. Med. Chem.* **2007**, *50*, 5053.
- (53) Gallardo-Godoy, A.; Gevertz, J.; Fife, K. L.; Silber, B. M.; Prusiner, S. B.; Renslo, A.R. *J. Med. Chem.* **2011**, *54*, 1010.
- (54) (a) Doh-ura, K.; Iwaki, T.; Caughey, B. *J. Virol.* **2000**, *74*, 4894-4897. (b) Dollinger S, Löber, S.; Klingenstein, R.; Korth, C.; Gmeiner, P. *J. Med. Chem.* **2006**, *49*, 6591. (c) Korth, C.; May, B.; Cohen, F.; Prusiner S. B. *Proc. Natl. Acad. Sci. U.S.A.* **2001**, *14*, 9836. (d) Nguyen, T.; Sakasegawa, Y.; Doh-ura, K.; Go, M.-L. *Eur. J. Med. Chem.* **2011**, *46*, 2917. (e) Ryou, C.; Legname, G.; Peretz, D.; Craig, J.C.; Baldwin, M.A.; Prusiner, S.B. *Lab Invest.* **2003**, *83*, 837.

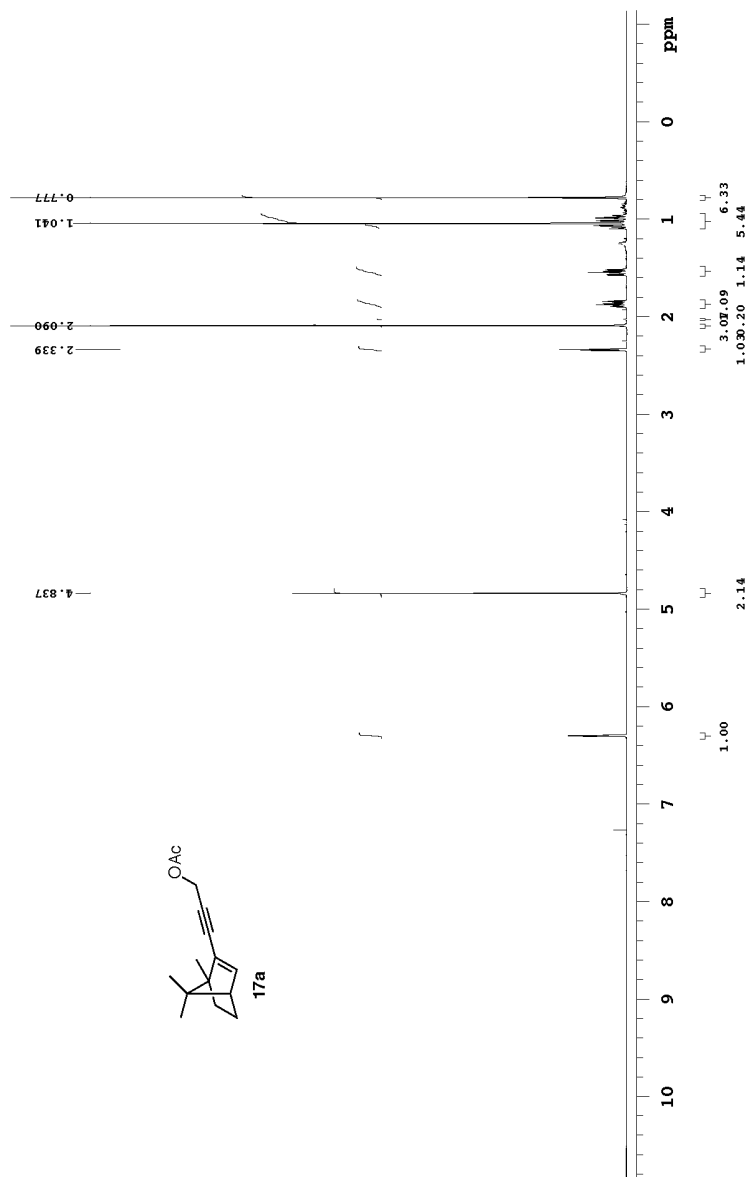
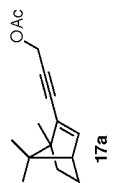
- (55) (a) Kawatake, S.; Nishimura, Y.; Sakaguchi, S.; Iwaki, T.; Doh-ura, K. *Biol. Pharm. Bull.* **2006**, *29*, 927. (b) Phuan, P.-W.; Zorn, J.A.; Safar, J.; Giles, K.; Prusiner, S.B.; Cohen, F. E et al. *J. Gen. Virol.* **2007**, *88*, 1392. (c) Touil, F.; Pratt S, Mutter R, Chen B. *J. Pharm. Biomed. Anal.* **2006**, *40*, 822. (d) Vogtherr, M.; Grimme, S.; Elshorst, B.; Jacobs, D. M.; Fiebig, K.; Griesinger, C. et al. *J. Med. Chem.* **2003**, *46*, 3563. (e) Barret, A.; Tagliavini, F.; Forloni, G.; Bate, C.; Salmona, M.; Colombo, L. et al. *J Virol.* **2003**, *77*, 8462.
- (56) Prusiner, S. B.; McKinley, M. P.; Bowman, K. A.; Bolton, D. C.; Bendheim, P. E.; Groth, D. F. et al. *Cell.* **1983**, *35*, 349.
- (57) Merz, P. A.; Somerville, R. A.; Wisniewski, H. M.; Iqbal, K. *Acta Neuropathol. (Berl)*. **1981**, *54*, 63.
- (58) Milgrom, L. R. *The Colours of Life: An Introduction to the Chemistry of Porphyrins and Related Compounds*. Oxford, 1997, Vol. 225, pp 547-593.
- (59) Yasuhiro, I.; Yuko, N.; Masahiko, I.; Masaharu, N.; Shigenobu, F. *Inorg. Chem.* **2000**, *39*, 4793.
- (60) Musonda, C. C.; Little, S.; Yardly, V.; Chibale, K. *Bioorg. Med. Chem. Lett.* **2007**, *17*, 4733-4736.
- (61) Wolfgang, K.; Geiger, R. *Chem. Ber.* **2006**, *103*, 788.
- (62) Bongarzone, S.; Tran, H. N. A.; Cavalli, A.; Roberti, M.; Carloni, P.; Legname, G. et al. *J. Med Chem.* **2010**, *53*, 8197.
- (63) Cope, H.; Mutter, R.; Heal, W.; Pascoe, C.; Brown, P.; Pratt, S. Chen, B. *Eur. J. Med. Chem.* **2006**, *41*, 1124.
- (64) Demaimay, R.; Harper, J.; Gordon, H.; Weaver, D.; Chesebro, B.; Caughey, B. *J. Neurochem.* **1998**, *71*, 2534.
- (65) Butler, D. A.; Scott, M. R. D.; Bockman, J. M.; Borchelt, D. R.; Taraboulos, A.; Hsiao, K. K. et al. *J Virol.* **1988**, *62*, 1558.
- (66) Lim, Y.-B.; Mays, C. E.; Kim, Y.; Titlow, W. B.; Ryou, C. *Biomaterials.* **2010**, *31*, 2025.
- (67) Nguyen Thi, H. T.; Lee, C.-Y.; Teruya, K.; Ong, W. -Y.; Doh-ura, K.; Go, M.-L. *Bioorg. Med. Chem.* **2008**, *16*, 6737.
- (68) Cope, H.; Mutter, R.; Heal, W.; Pascoe, C.; Brown, P.; Pratt, S. et al. *Eur. J. Med. Chem.* **2006**, *41*, 1124.

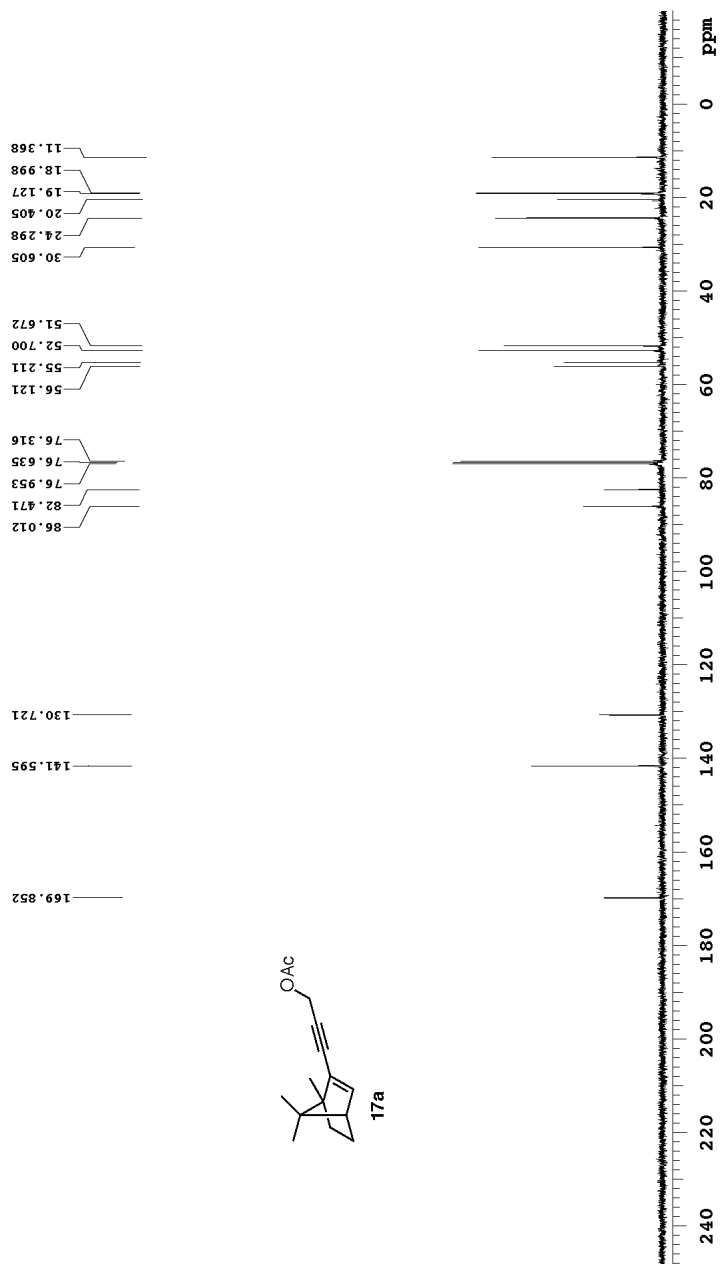
- (69) Caughey, W. S.; Raymond, L.D.; Horiuchi, M.; Caughey, B. *Proc. Natl. Acad. Sci. U. S. A.* **1998**, *95*, 12117.
- (70) Rudyk, H.; Knaggs, M.H.; Vasiljevic, S.; Hope, J.; Birkett, C.; Gilbert, I. H. *Eur. J. Med. Chem.* **2003**, *38*, 567-579.
- (71) Maxson, L.; Wong, C.; Herrmann, L. M.; Caughey, B.; Baron, G. S. *Anal. Biochem.* **2003**, *323*, 54.
- (72) Priola, S. A.; Raines, A.; Caughey, W. *J. Infect. Dis.* **2003**, *188*, 699.
- (73) Priola, S. A.; Raines, A.; Caughey, W. S. *Science.* **2000**, *287*, 1503.
- (74) Butler, D.A.; Scott, M.R.D.; Bockman, J. M.; Borchelt, D. R.; Taraboulos, A.; Hsiao, K.K. et al. *J. Virol.* **1988**, *62*, 1558-1564.
- (75) Caughey, W. S.; Priola, S. A.; Kocisko, D. A.; Raymond, L. D.; Ward, A.; Caughey, B. *Antimicrob. Agents Chemother.* **2007**, *51*, 3887.
- (76) Bosque, P. J.; Prusiner, S. B. *J. Virol.* **2000**, *74*, 4377.
- (77) Birkett, C. R.; Hennion, R. M.; Bembridge, D. A.; Clarke, M.C.; Chree, A.; Bruce, M. E.; Bostock, C. J. *EMBO J.* **2001**, *20*, 3351.
- (78) Murakami-Kubo, I.; Doh-Ura, K.; Ishikawa, K.; Kawatake, S.; Sasaki, K.; Kira, J.; Ohta, S.; Iwaki, T. *J. Virol.* **2004**, *78*, 1281.
- (79) May, B. C. H.; Fafarman, A. T.; Hong, S. B.; Rogers, M.; Deady, L.W.; Prusiner, S. B.; Cohen, F. E. *Proc. Natl. Acad. Sci. U S A.* **2003**, *100*, 3416.
- (80) Klingenstein, R.; Löber, S.; Kujala, P.; Godsave, S.; Leliveld, S. R.; Gmeiner, P.; Peters, P. J.; Korth, C. *J. Neurochem.* **2006**, *98*, 748.
- (81) Caughey, B.; Caughey, W. S.; Kocisko, D. A.; Lee, K. S.; Silveira, J. R.; Morrey, J. D. *Acc. Chem. Res.* **2006**, *39*, 646.
- (82) Govaerts, C.; Wille, H.; Prusiner, S. B.; Cohen, F. E. *Proc. Natl. Acad. Sci. U. S. A.* **2004**, *101*, 8342.
- (83) DebBurman, S.K.; Raymond, G. J.; Caughey, B.; Lindquist, S. *Proc. Natl. Acad. Sci. U. S. A.* **1997**, *94*, 13938.
- (84) Wong, C.; Xiong, L.-W.; Horiuchi, M.; Raymond, L.; Wehrly, K.; Chesebro, B. *EMBO J.* **2001**, *20*, 377.

- (85) (a) Deleault, N.R.; Lucassen, R. W.; Supattapone, S. *Nature*. **2003**, *425*, 717. (b) Wang, F.; Wang, X.; Yuan, C.G.; Ma, J. *Science*. **2010**, *327*, 1132. (c) Deleault, N. R.; Geoghegan, J. C.; Nishina, K.; Kascsak, R.; Williamson, R.A.; Supattapone, S. *J. Biol. Chem.* **2005**, *280*, 26873.
- (86) Iwaniuk, D. P.; Whetmore, E. D.; Rosa, N.; Ekoue-Kovi, K.; Alumasa, J.; de Dios, A. C. et al. *Bioorg. Med. Chem.* **2009**, *17*, 6560.
- (87) Rojas Ruiz, F. A.; García-Sánchez, R. N.; Estupiñan, S.V.; Gómez-Barrio, A.; Torres, A. D. F.; Pérez-Solórzano, B. M.; Nogal-Ruiz, J. J.; Martínez-Fernández, A. R.; Kouznetsov, V. V. *Bioorg. Med. Chem.* **2011**, *19*, 4562.
- (88) Biot, C.; Daher, W.; Ndiaye, C. M.; Melnyk, P.; Pradines, B.; Chavain, N.; Pellet, A.; Fraisse, L.; Pelinski, L.; Jarry, C.; Khalife, J.; Forbar-Bares, I.; Dives, D. *J. Med. Chem.* **2006**, *49*, 4707.
- (89) Clarke, M. C.; Haig, D. A. *Nature*. **1970**, *225*, 100.
- (90) Southwick, P. L.; Ernst, L. A.; Tauriello, E. W.; Parker, S. R.; Mujumdar, R. B.; Mujumdar, S. R.; Clever, H. A.; Waggoner, A. S., *Cytometry* **1990**, *11*, 418.

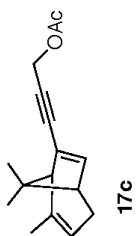
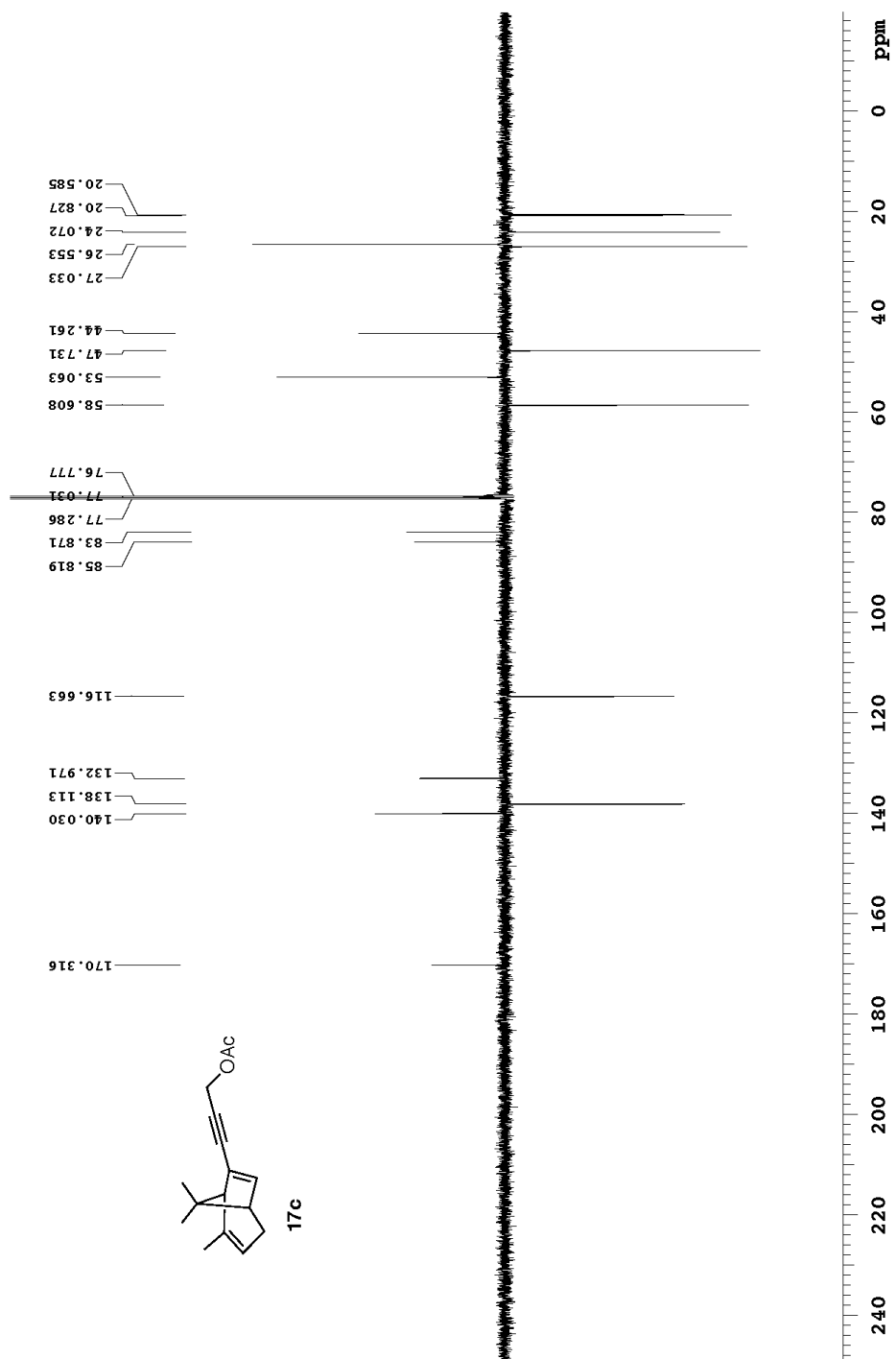
Appendix I (Selected NMR Spectra)

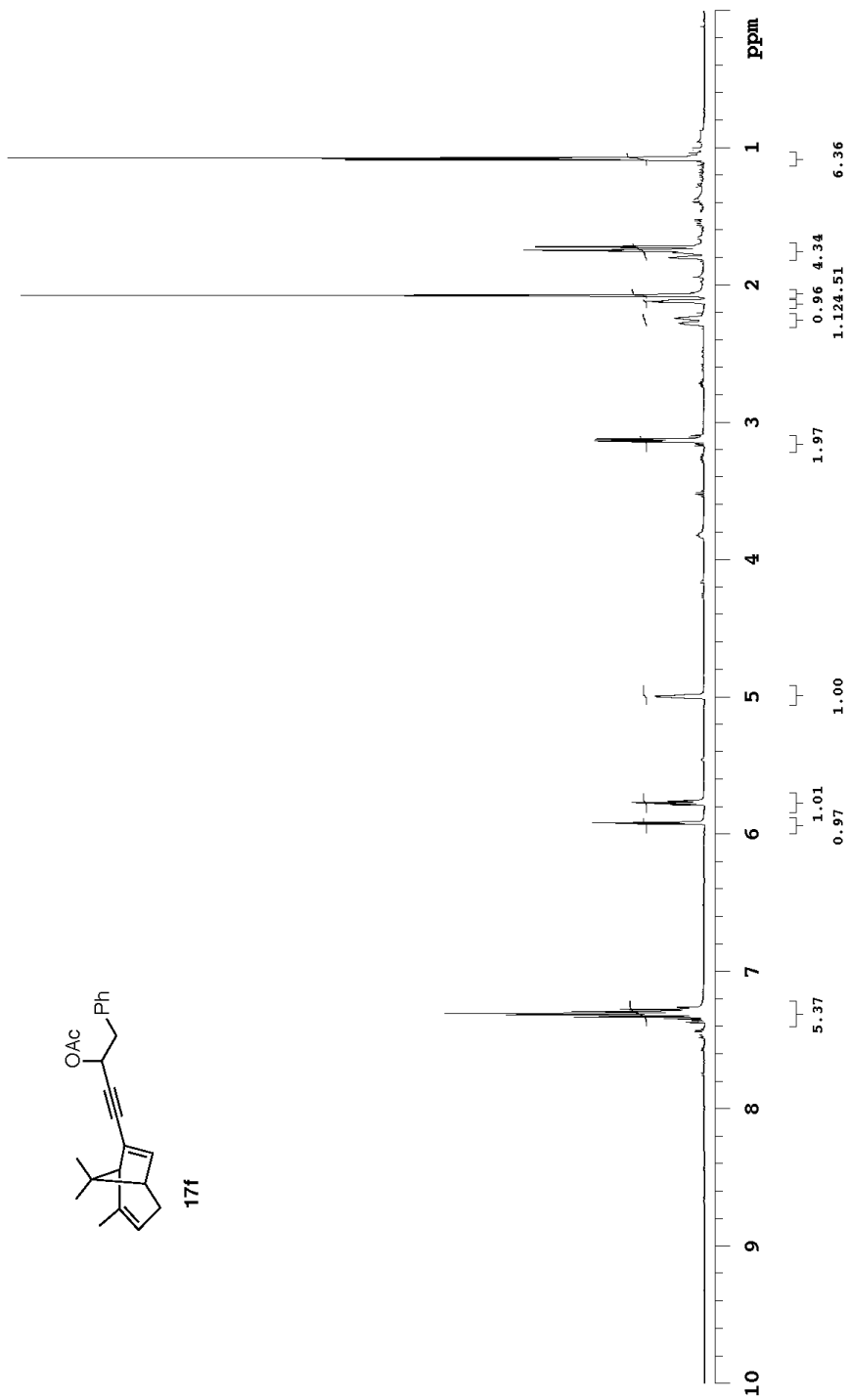
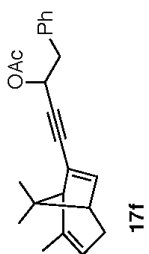
Chapter 2

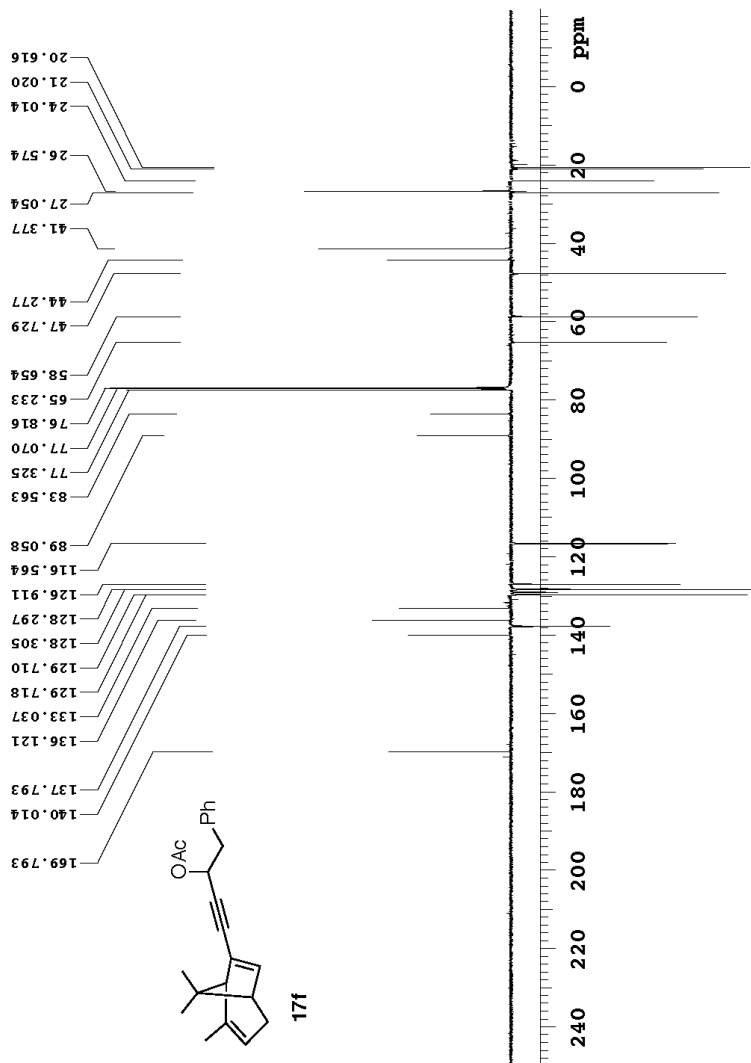


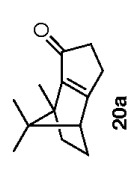
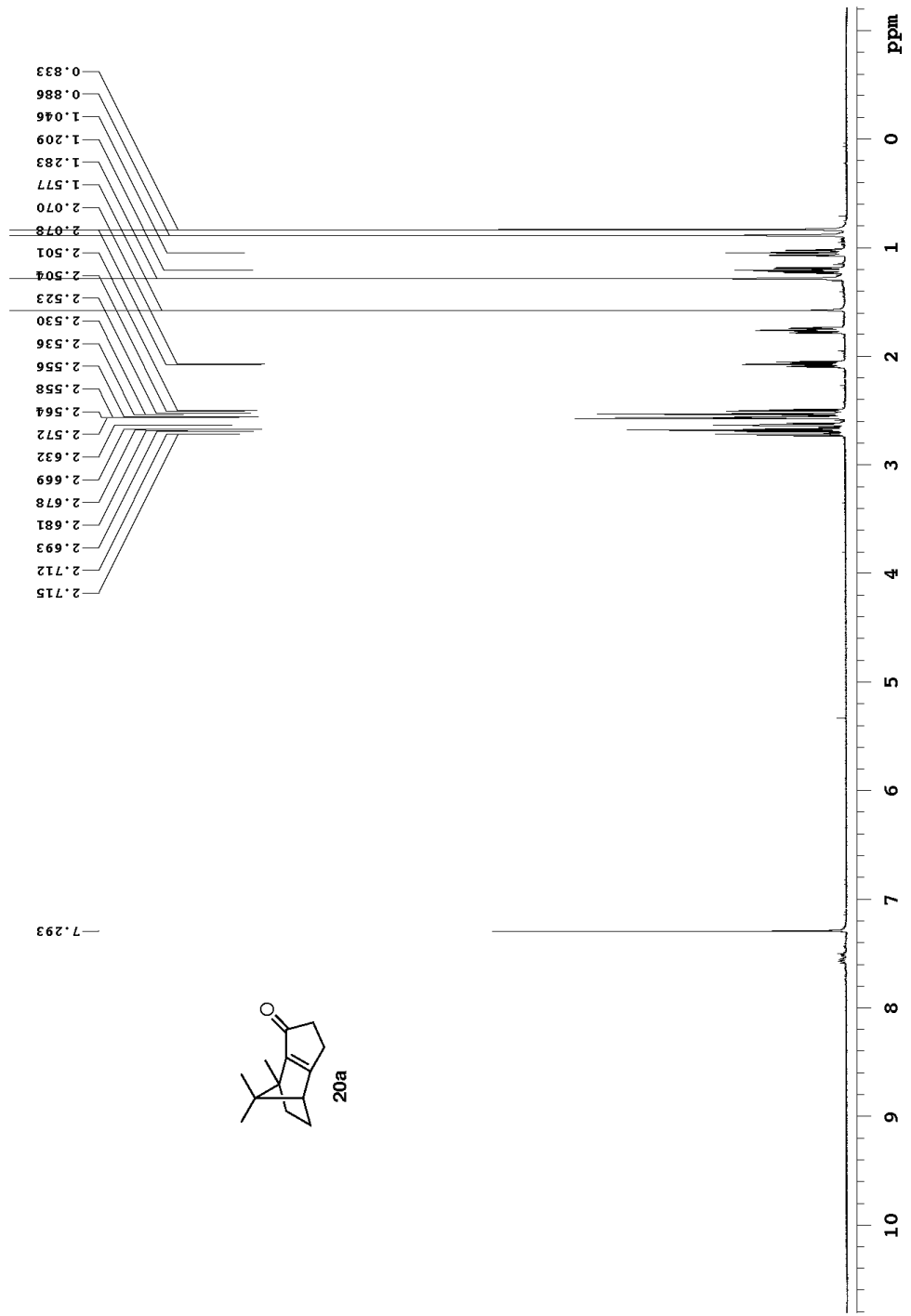


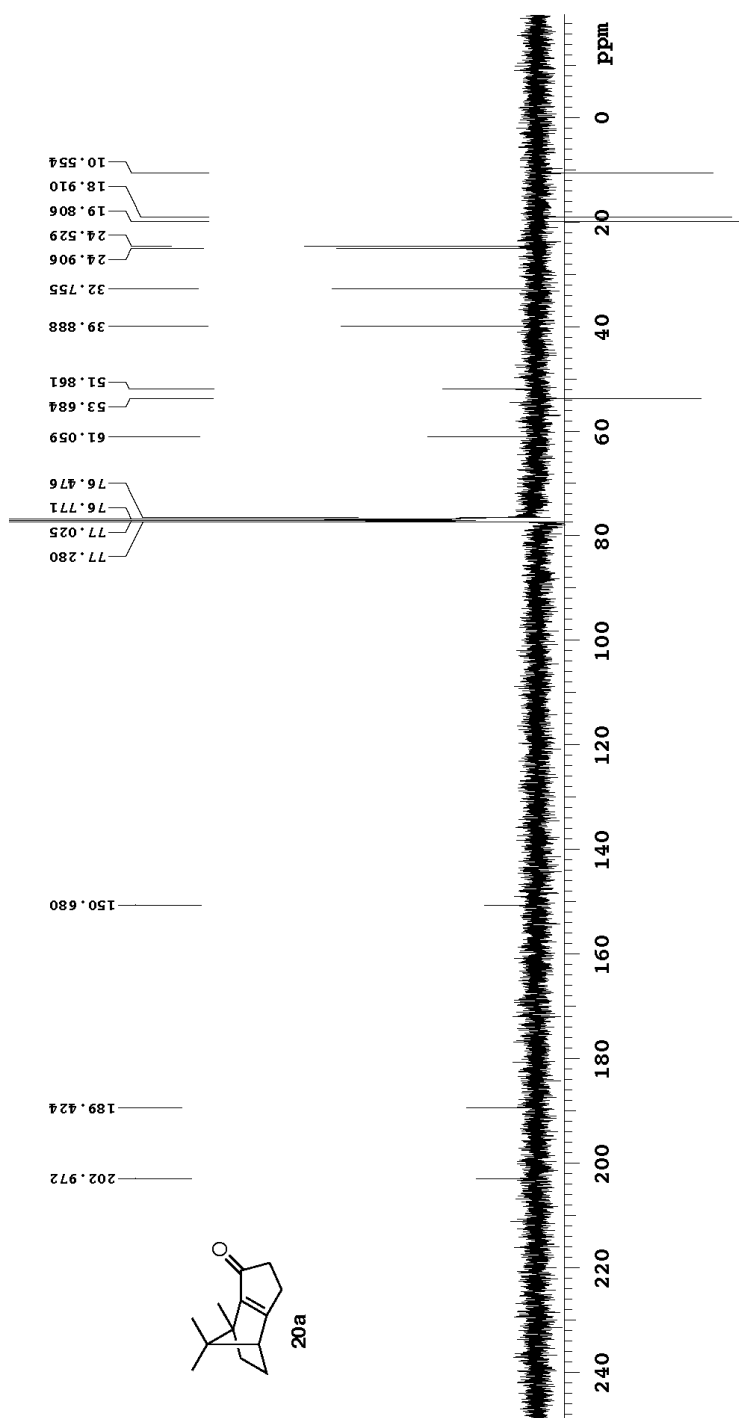


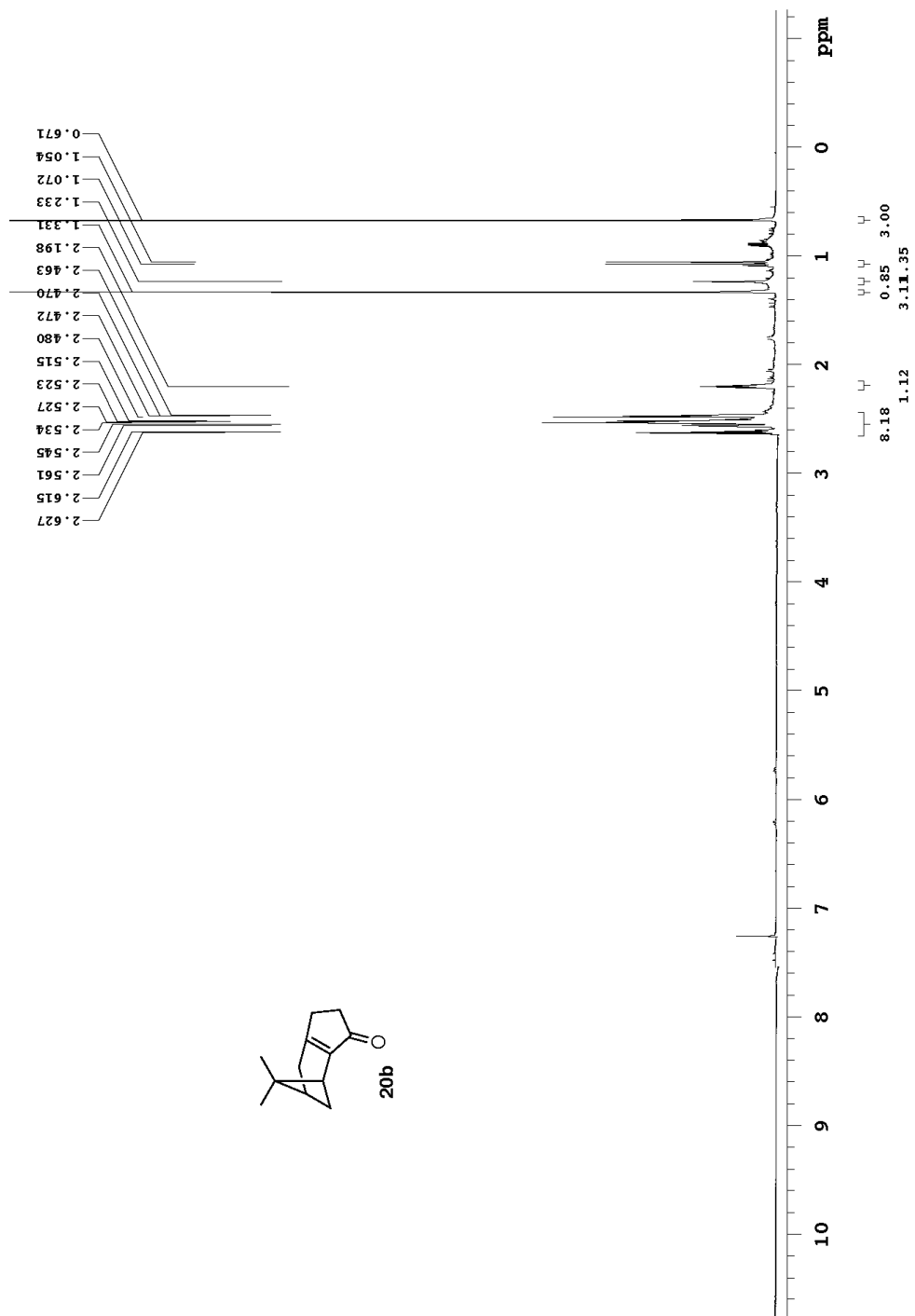
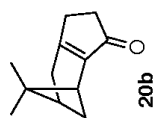


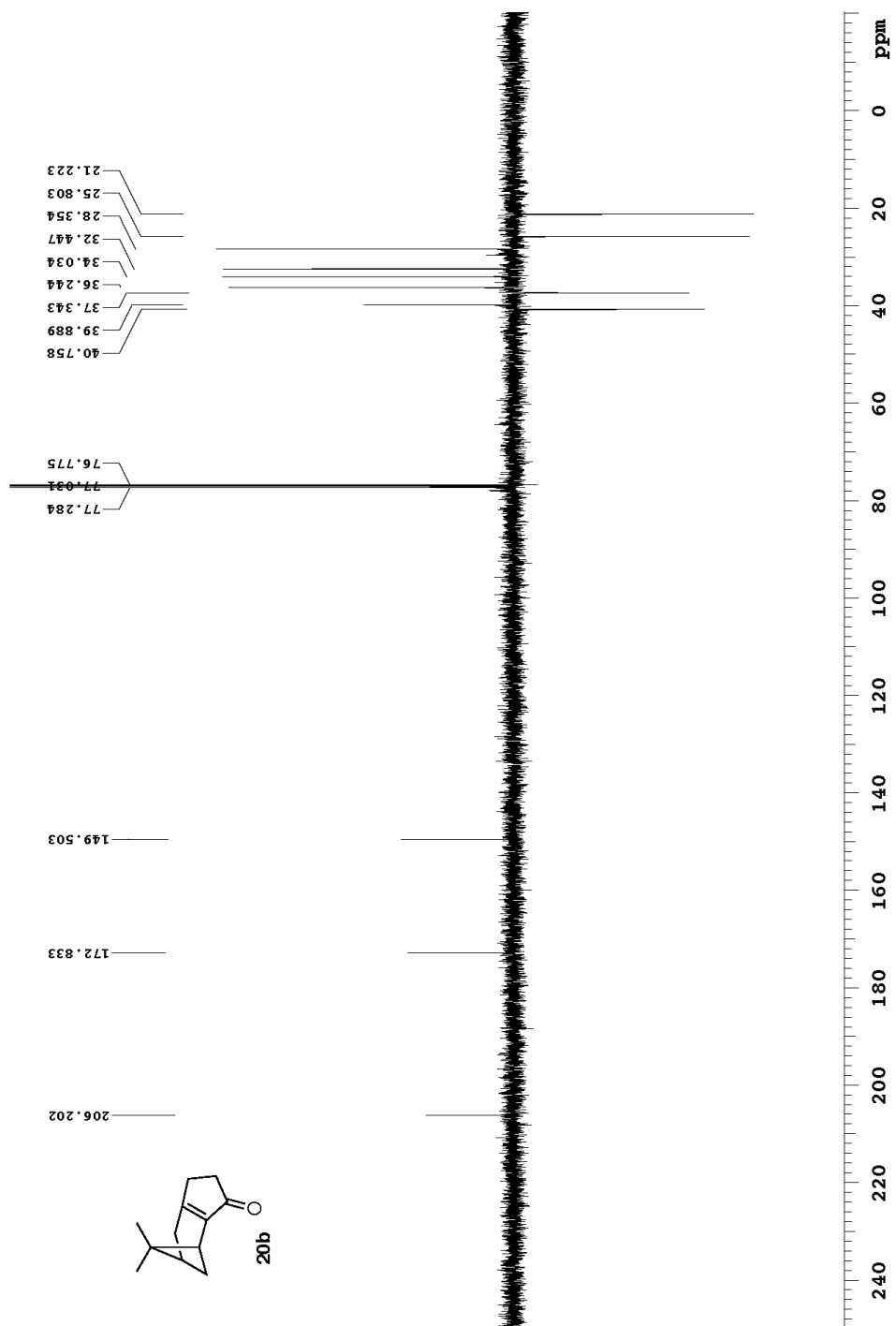


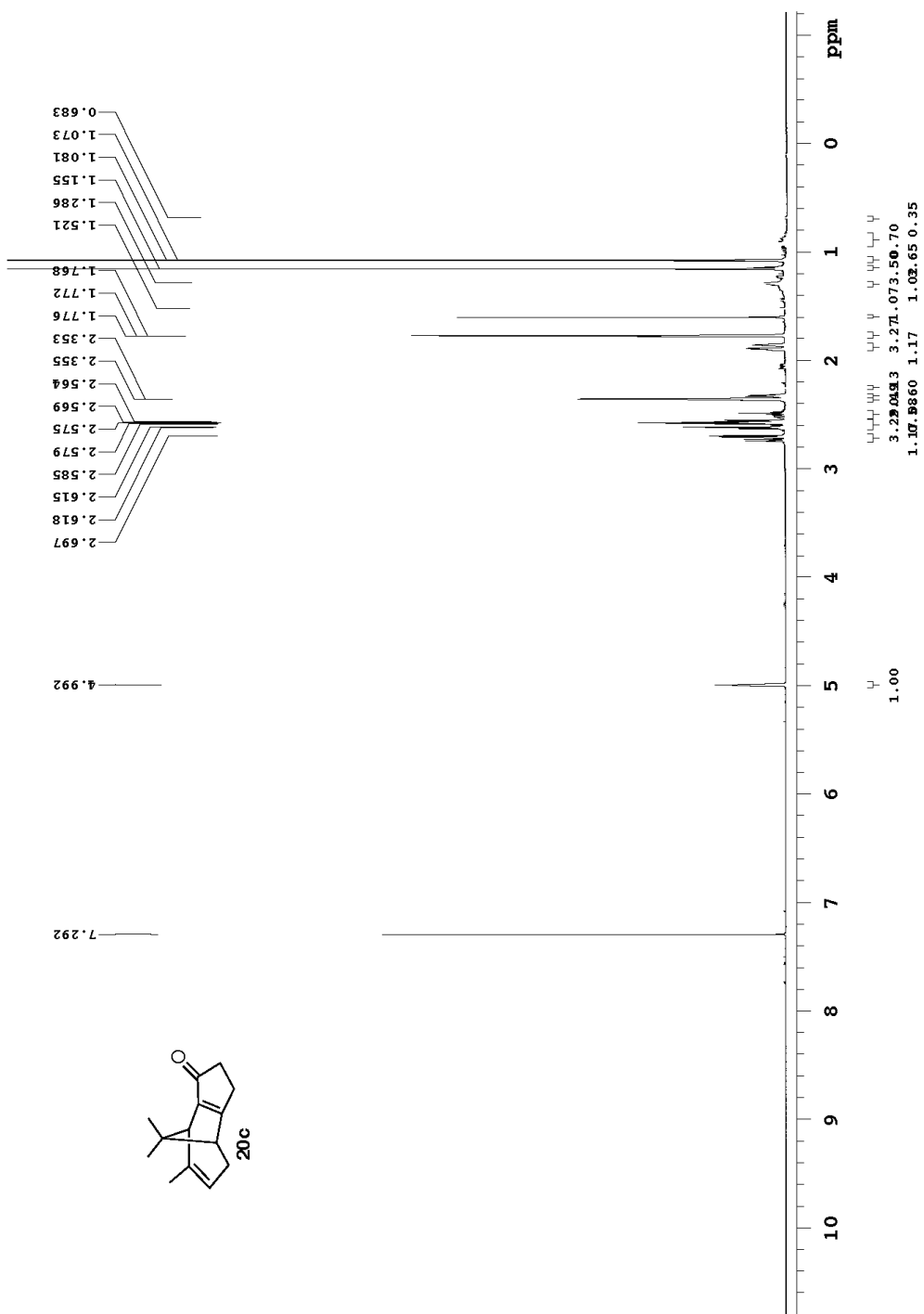


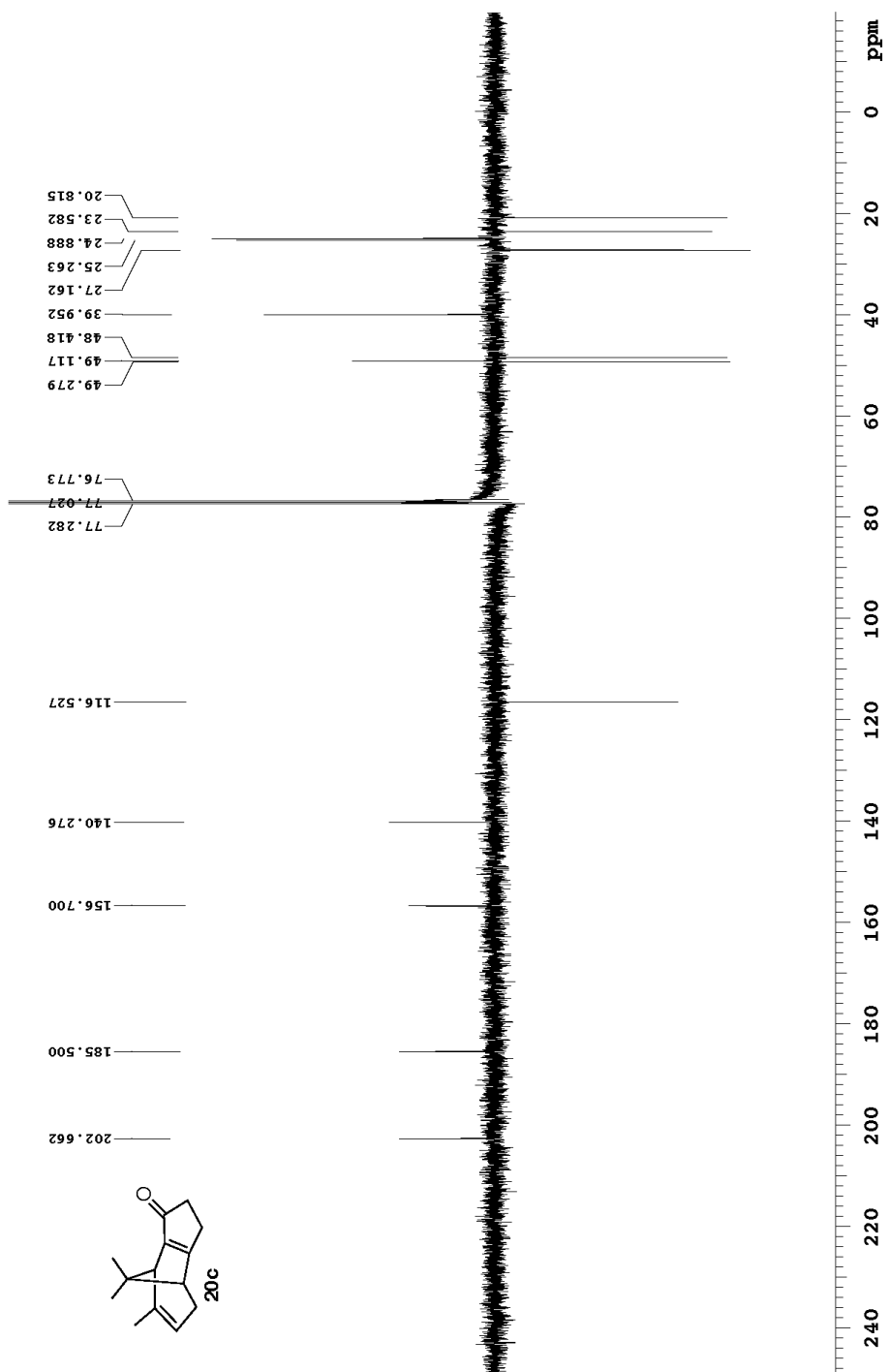


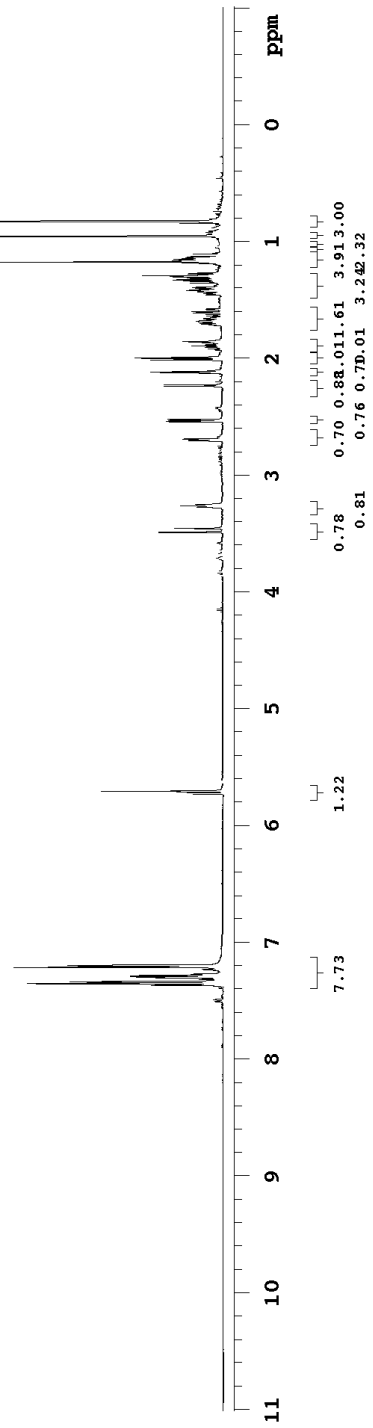
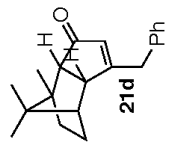


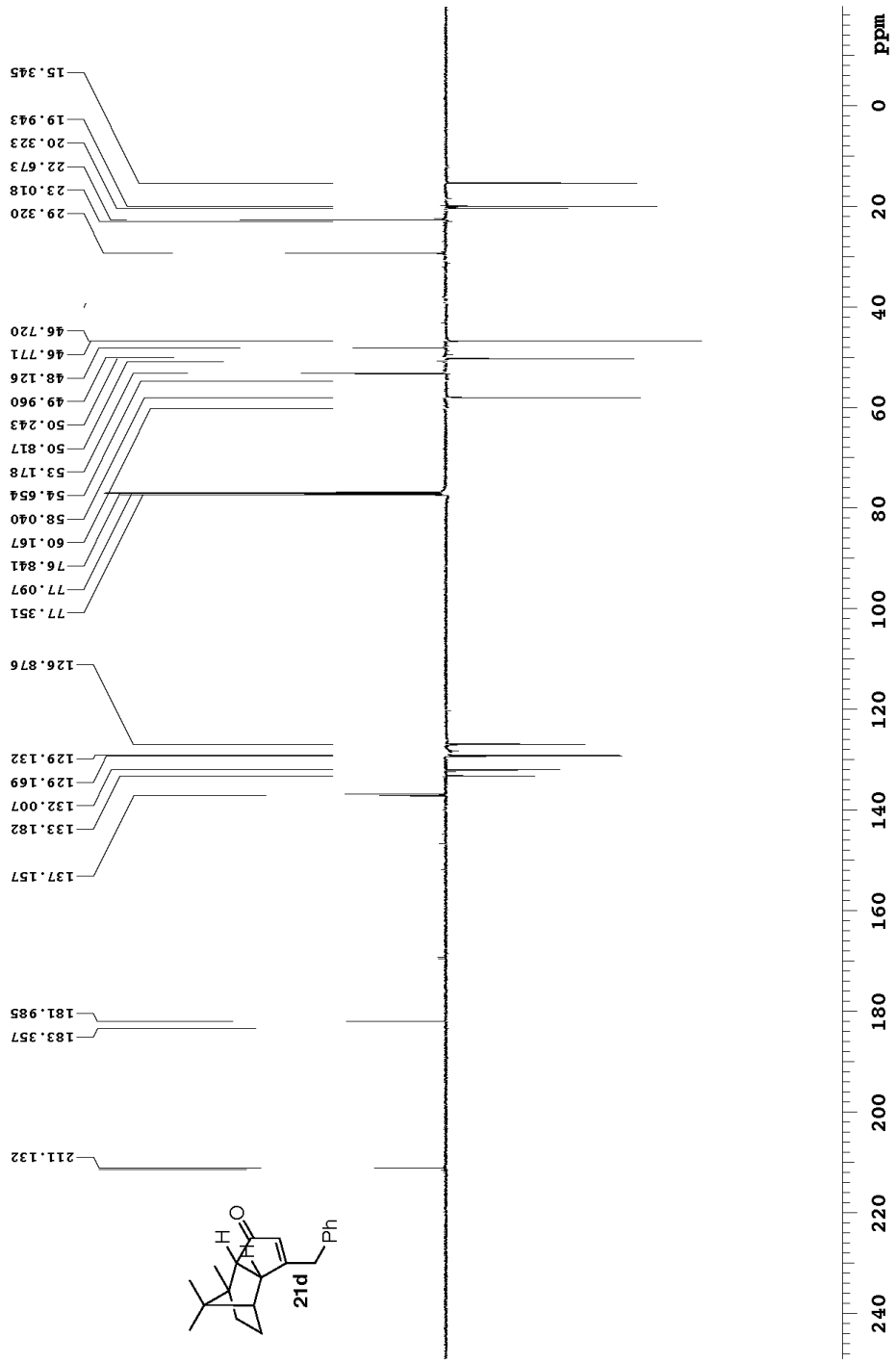


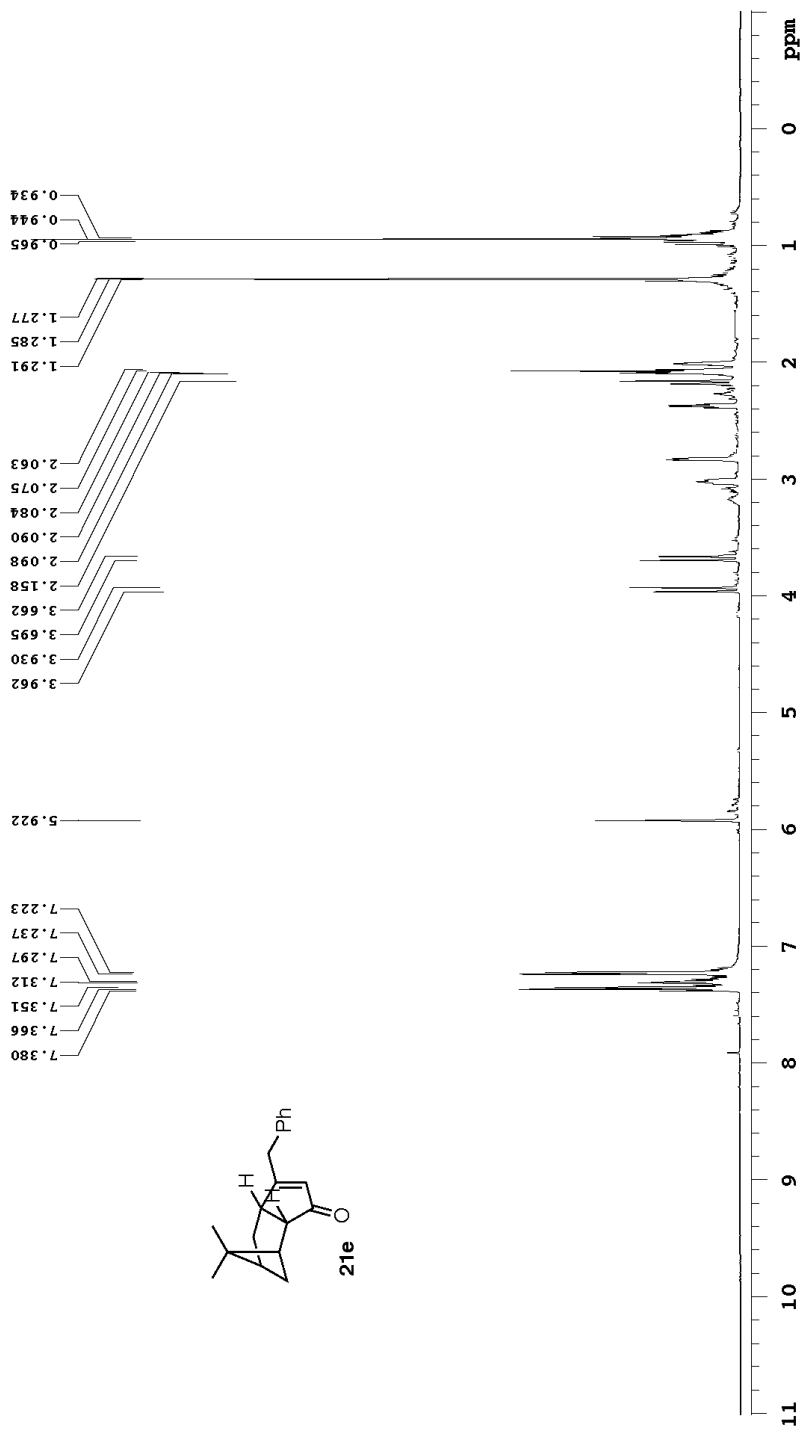


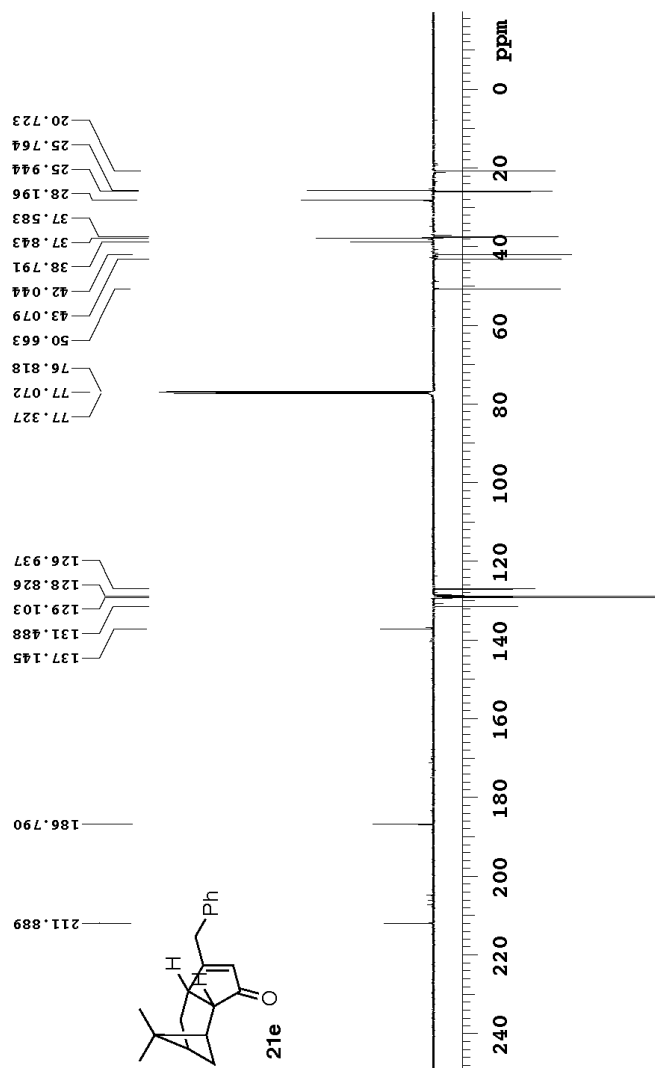


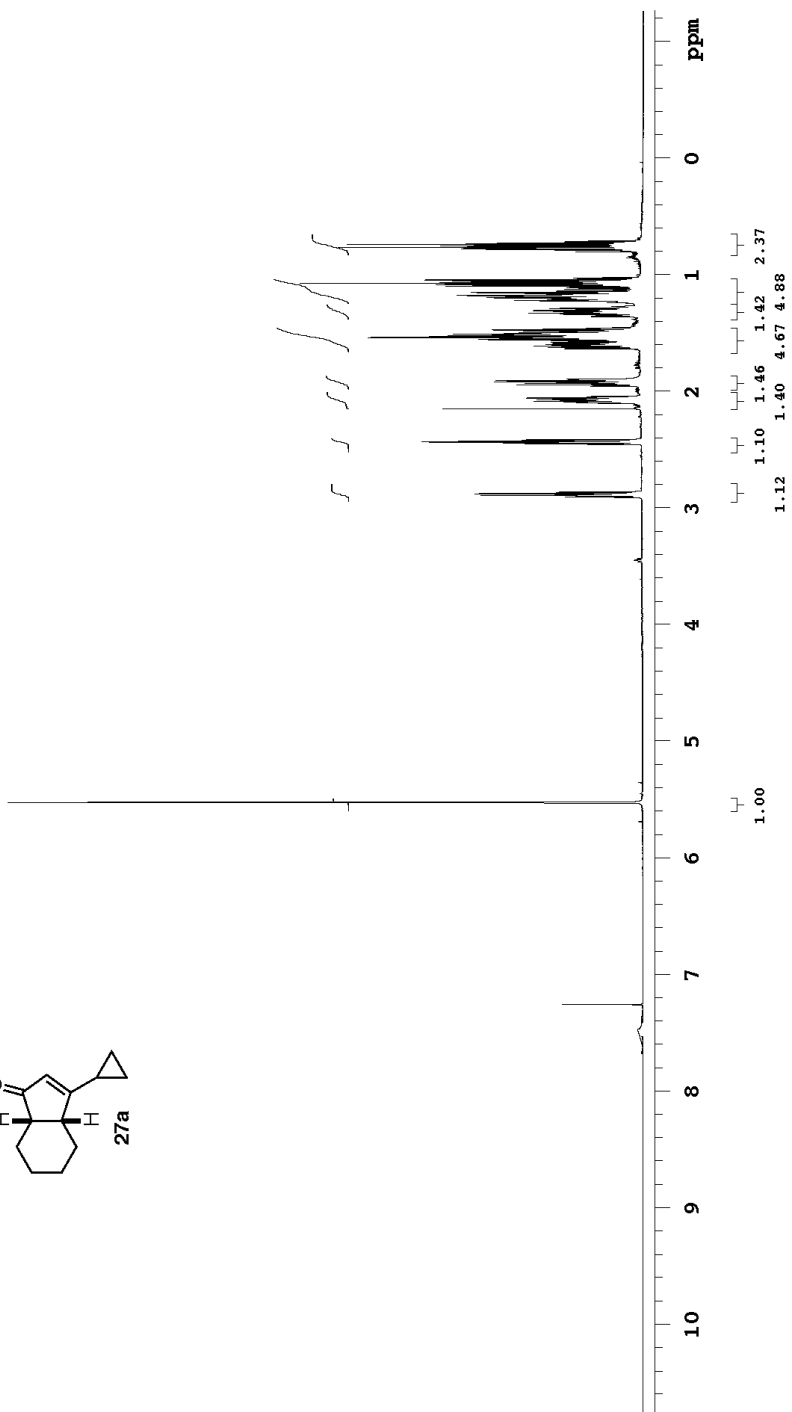
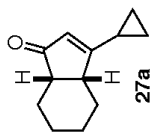


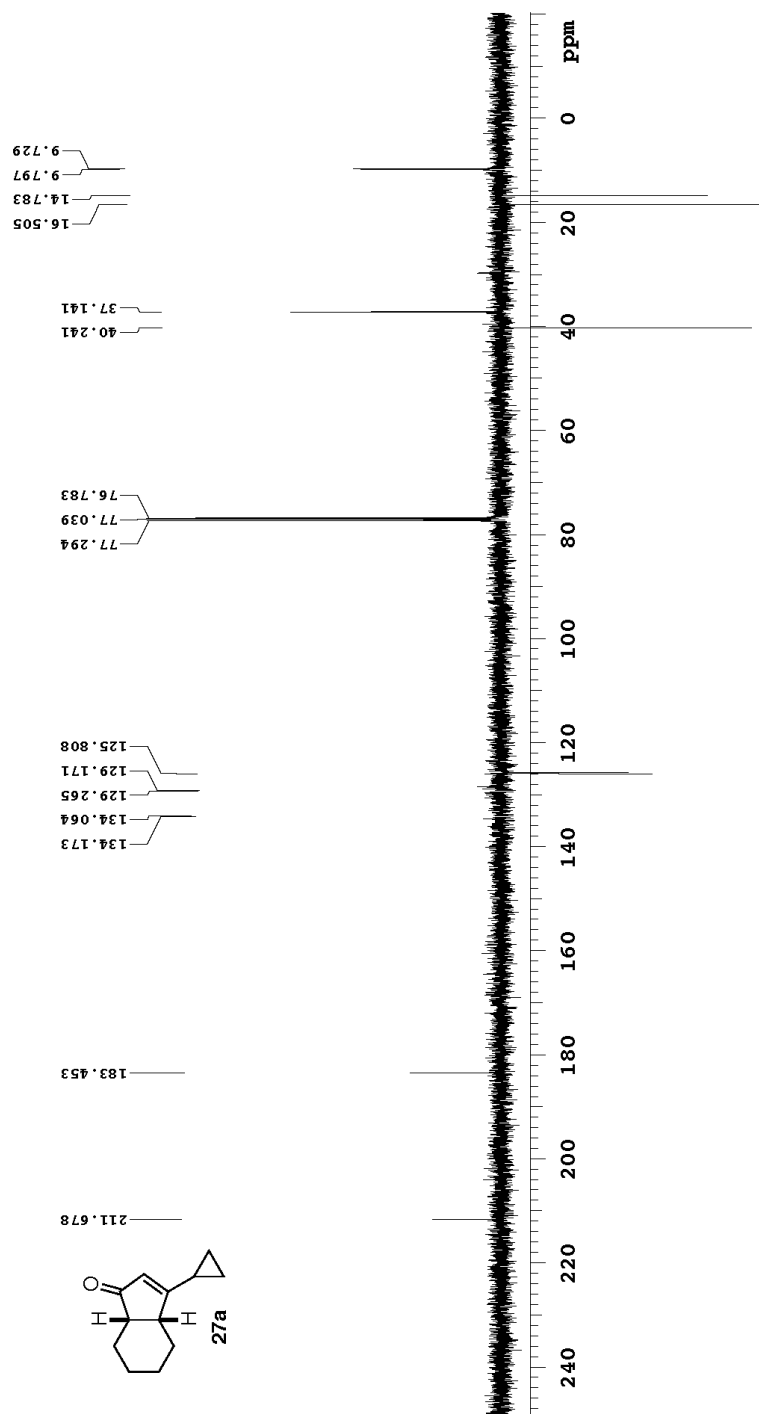


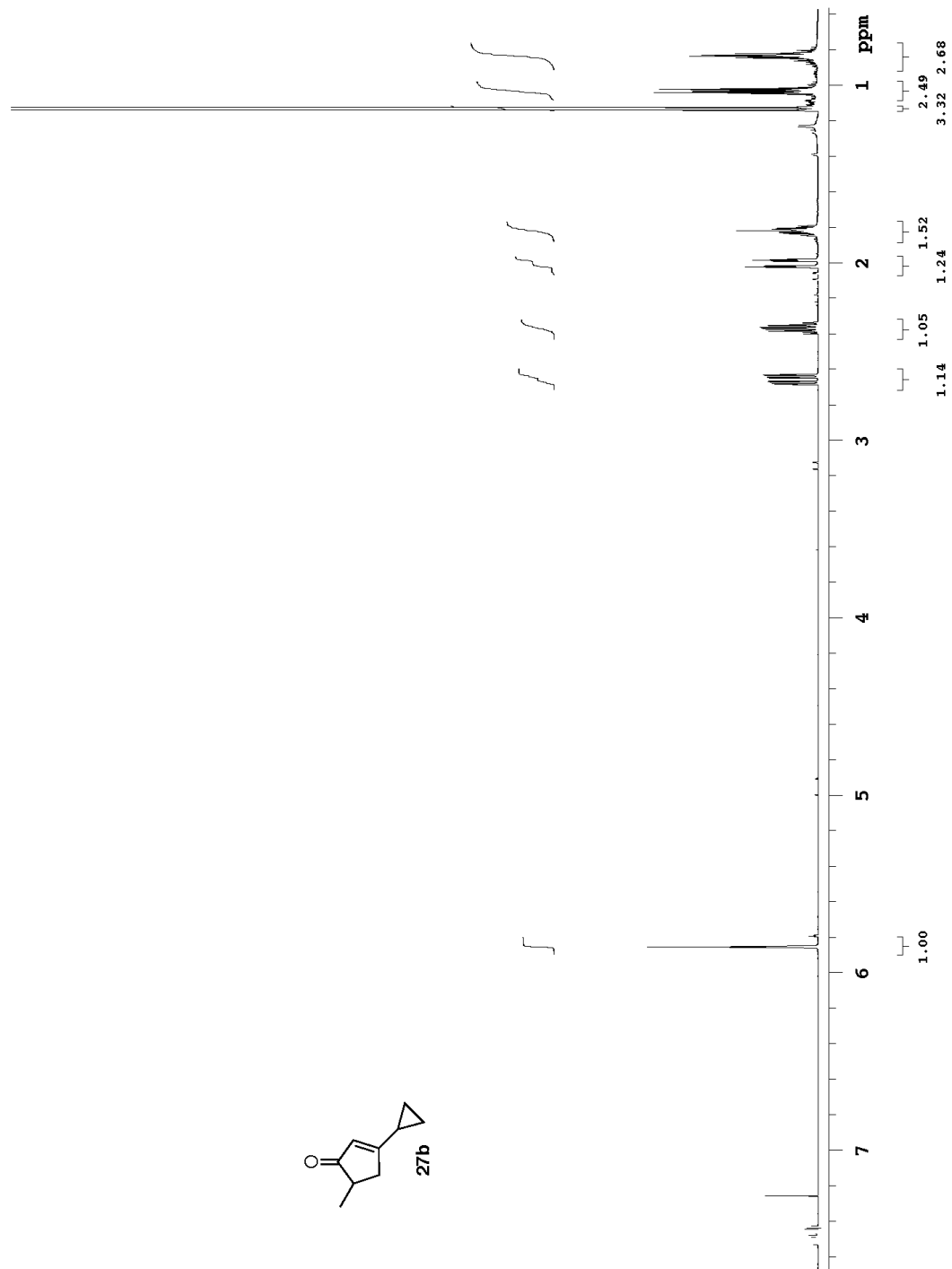
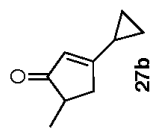


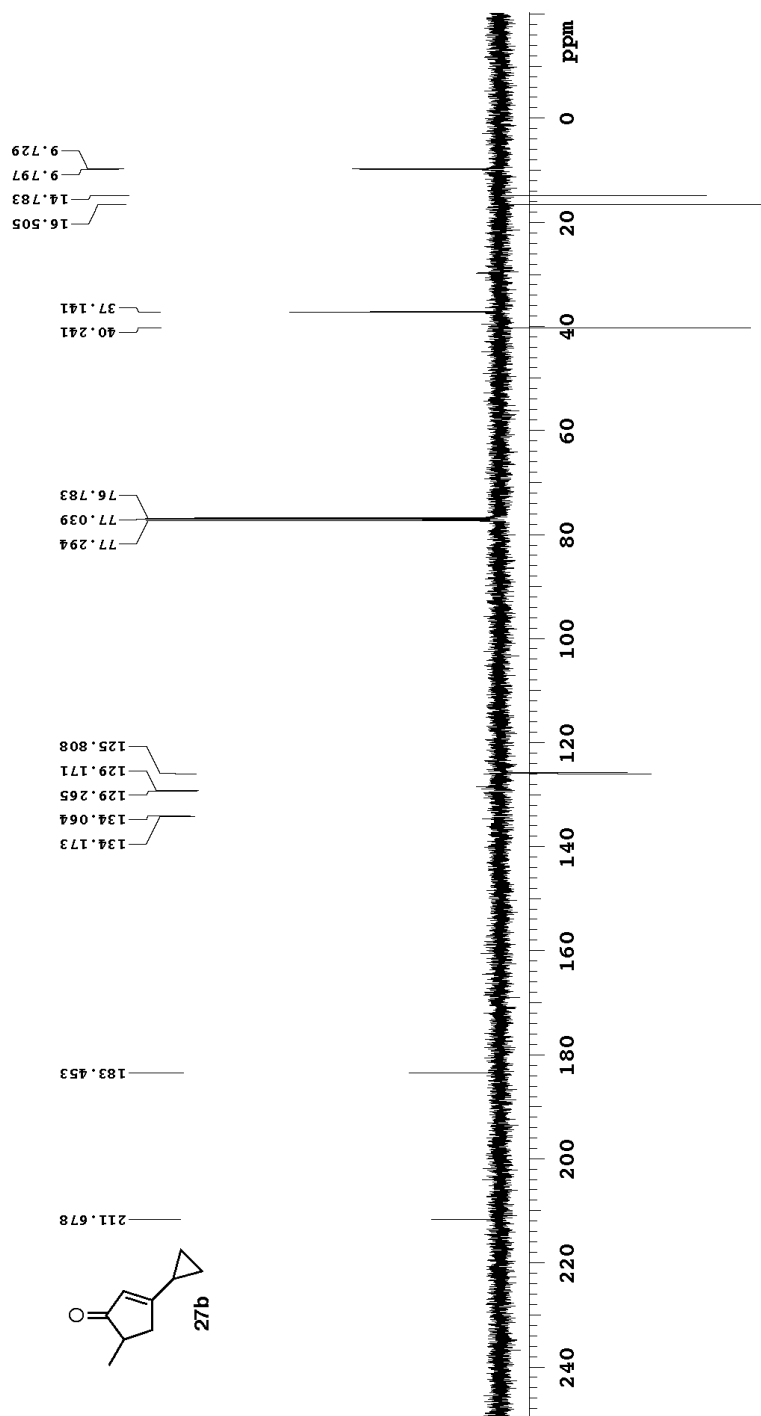






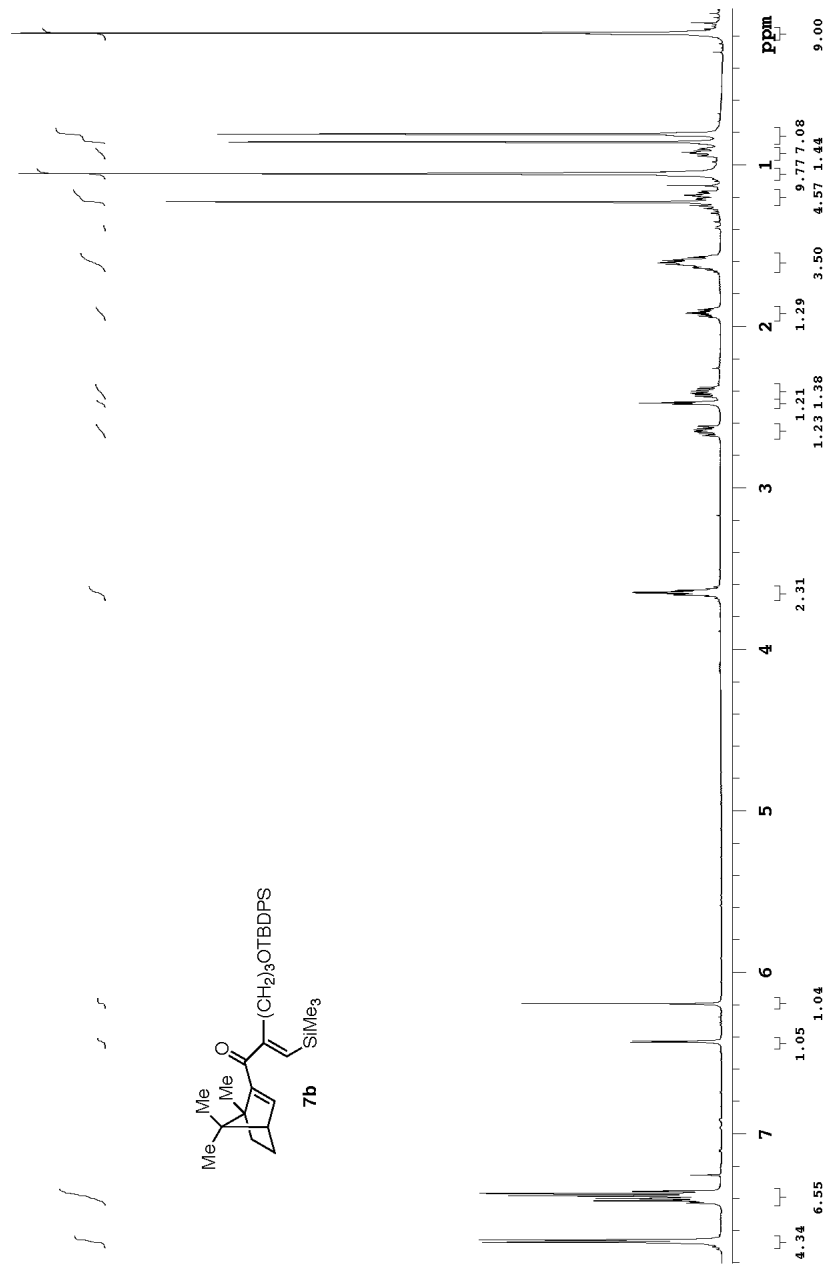


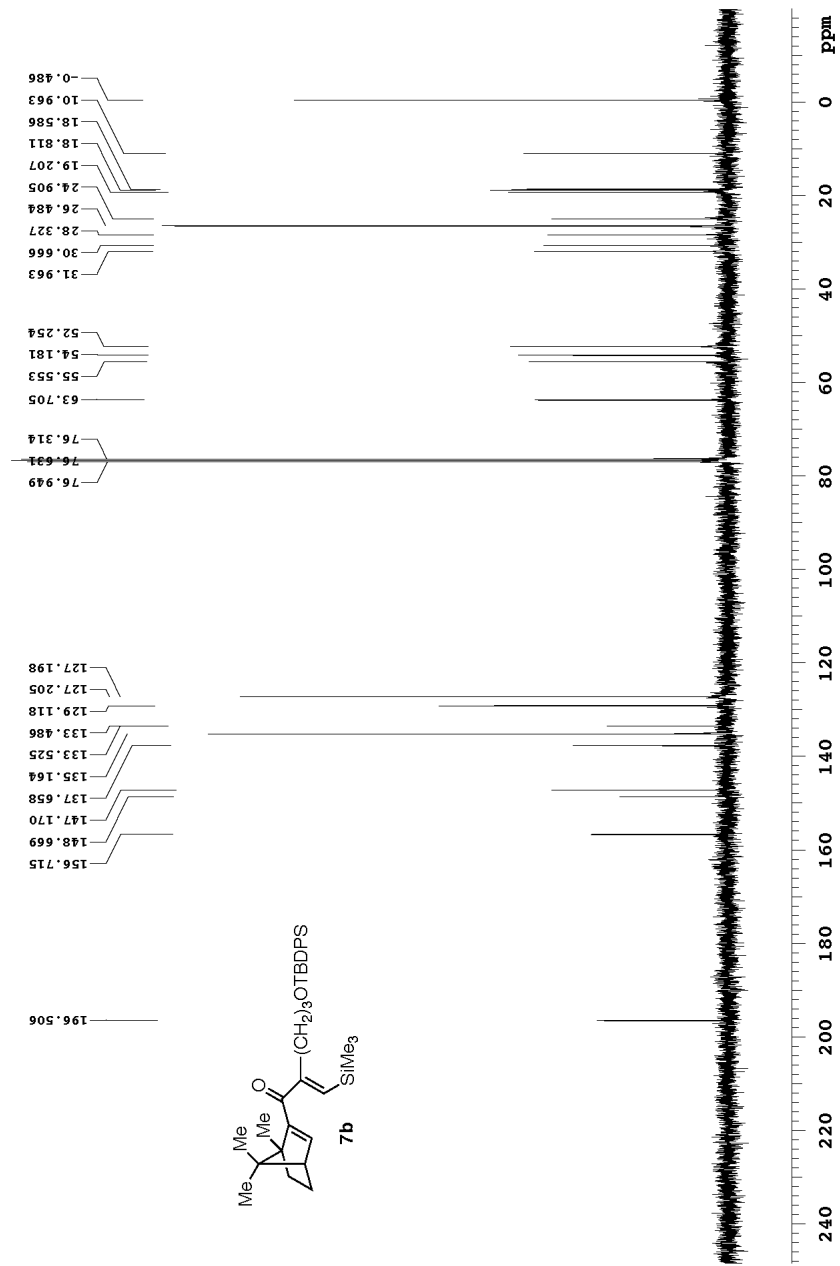


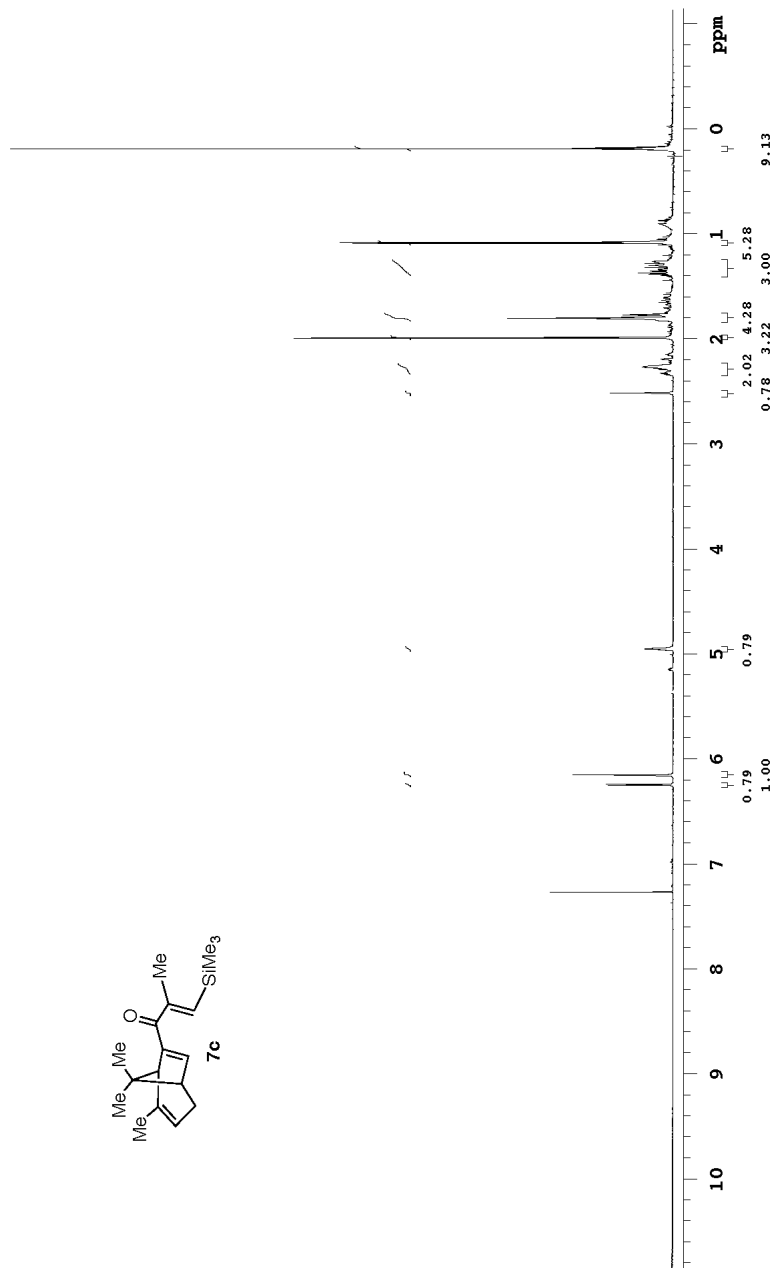
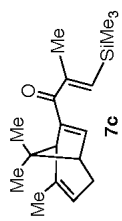


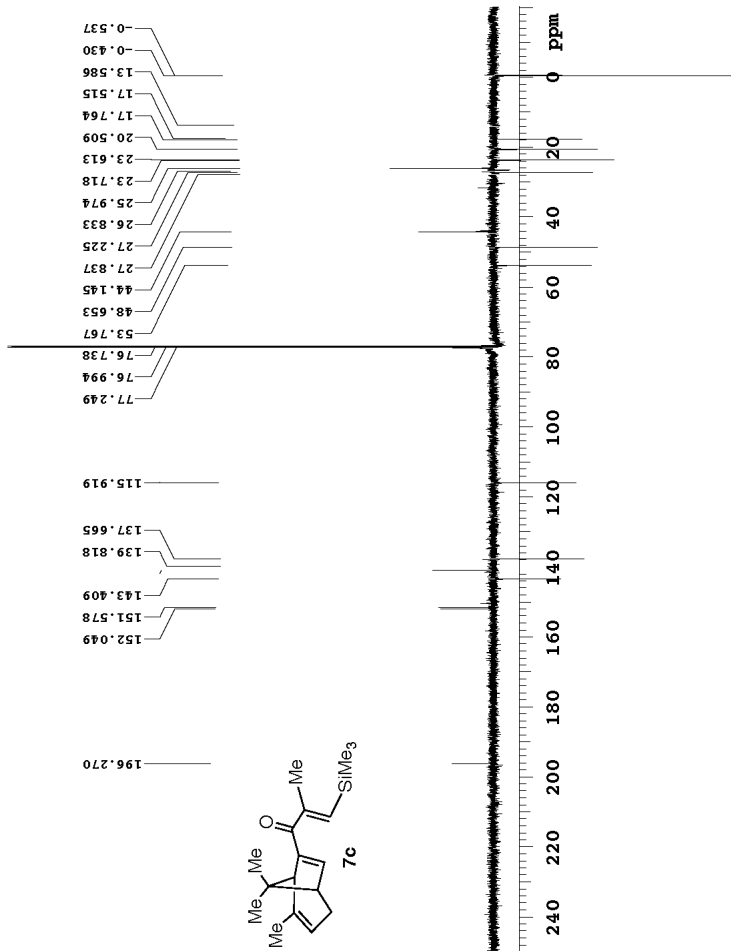
Appendix II (Selected NMR Spectra)

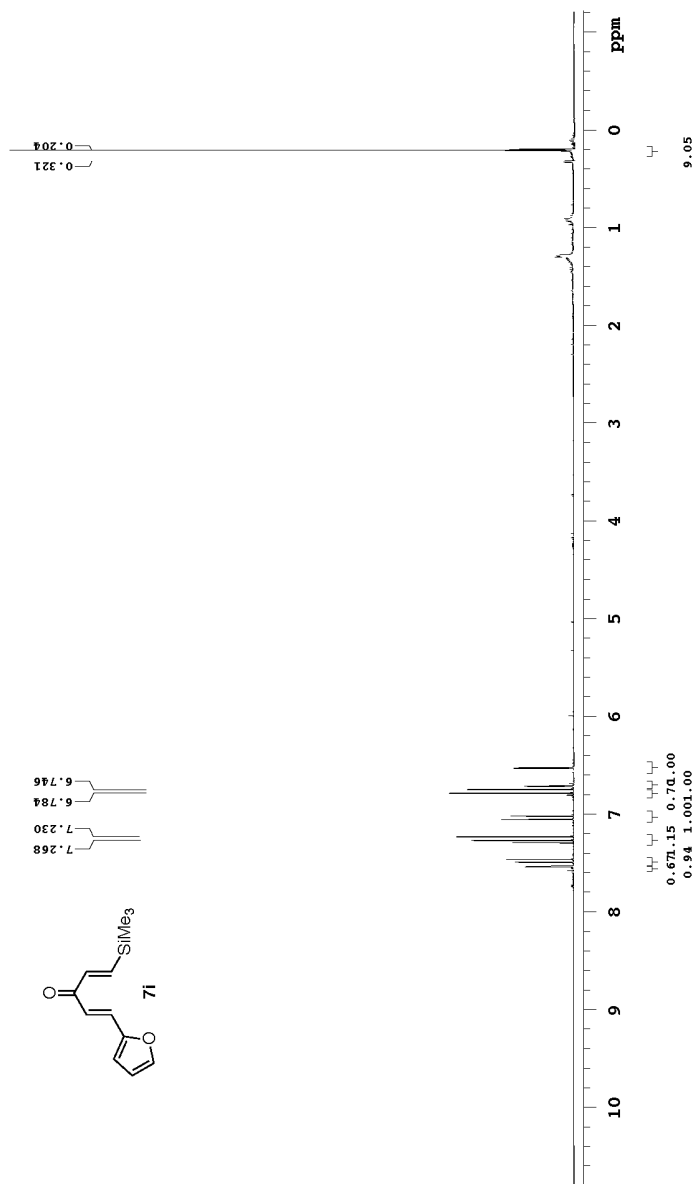
Chapter 3

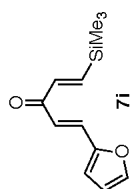
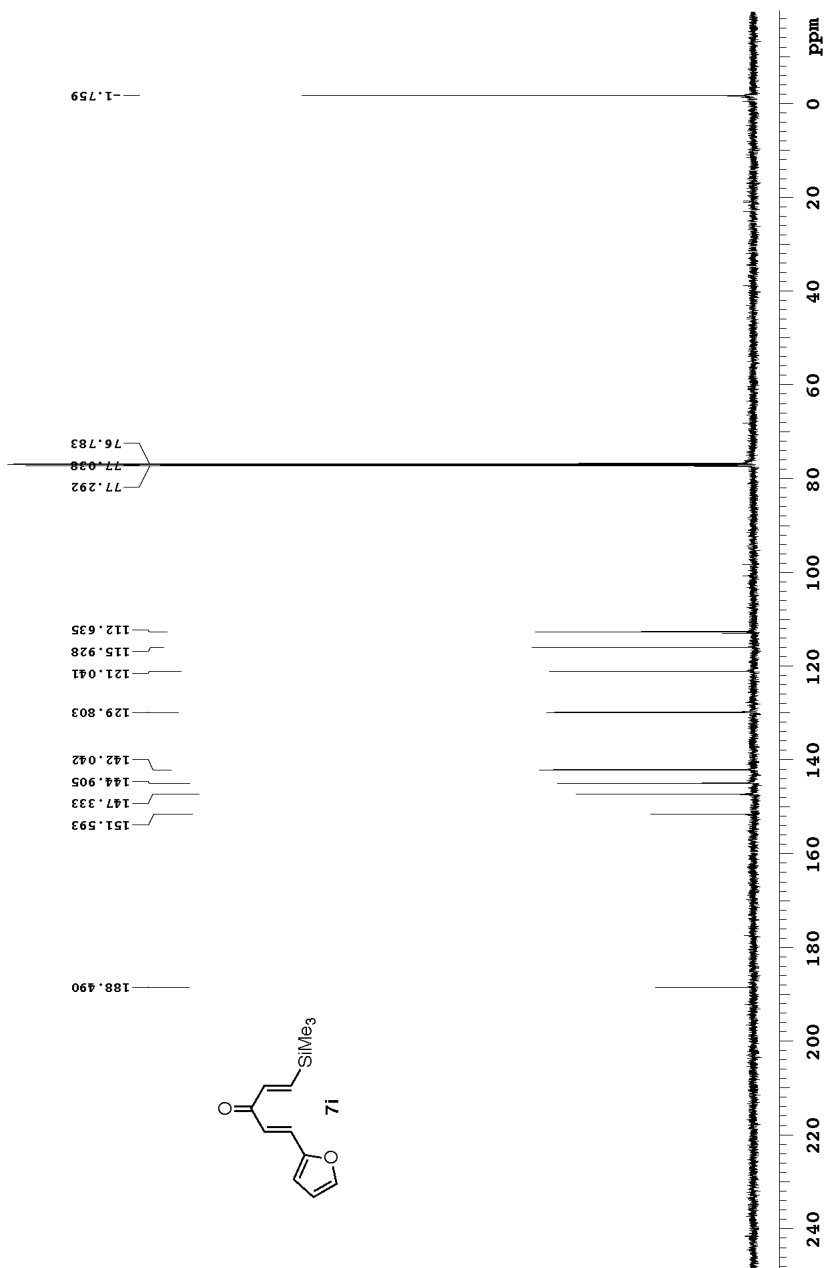


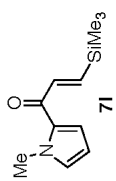
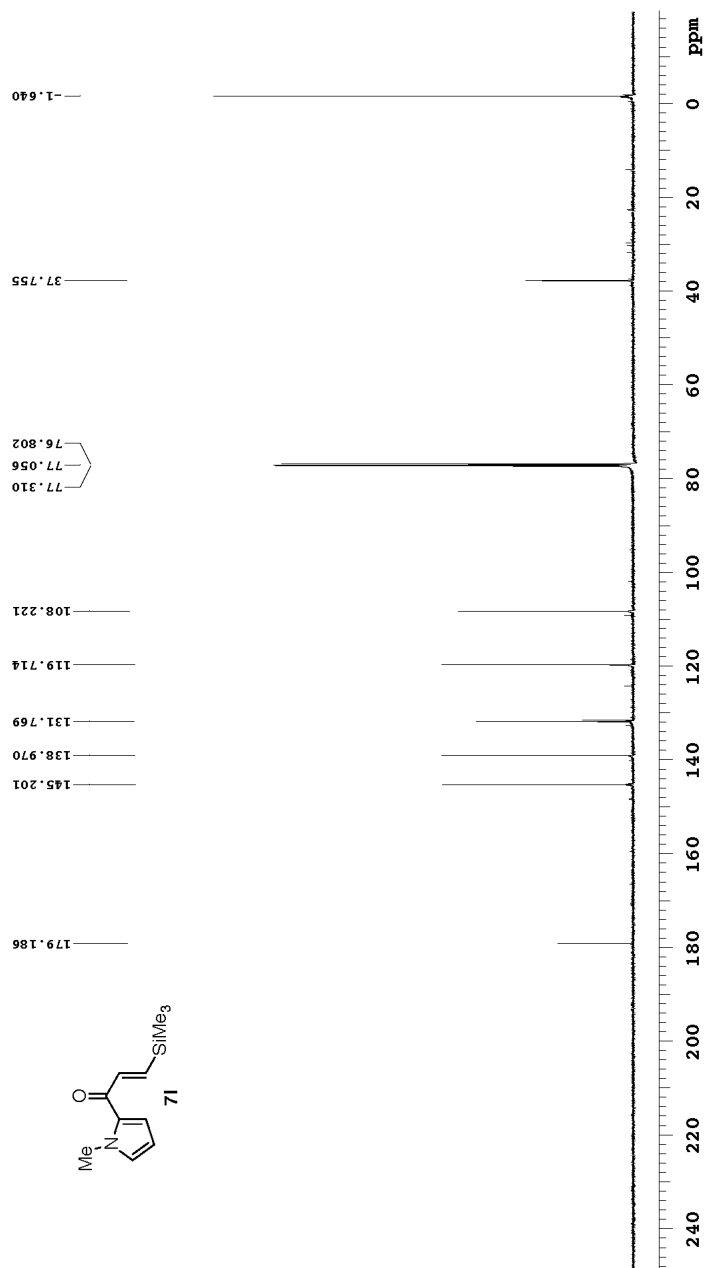


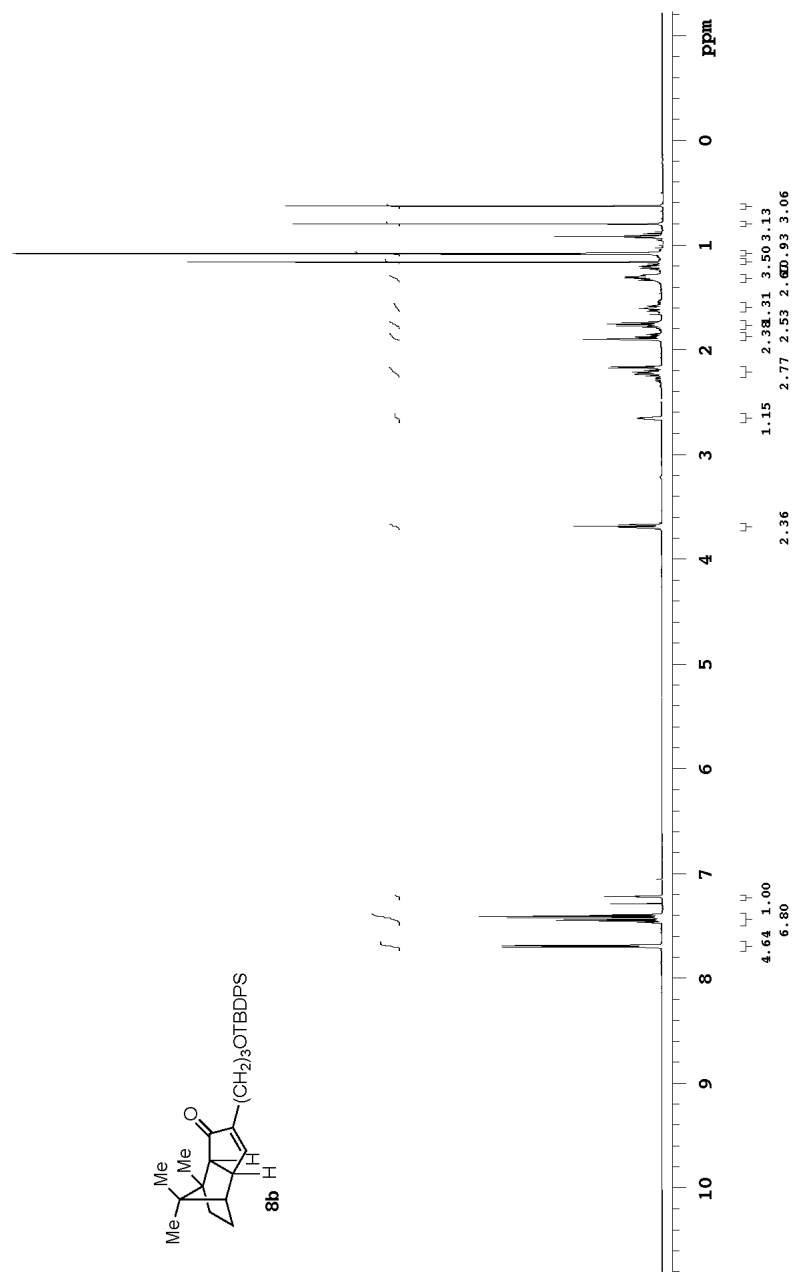
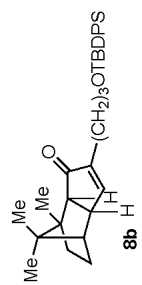


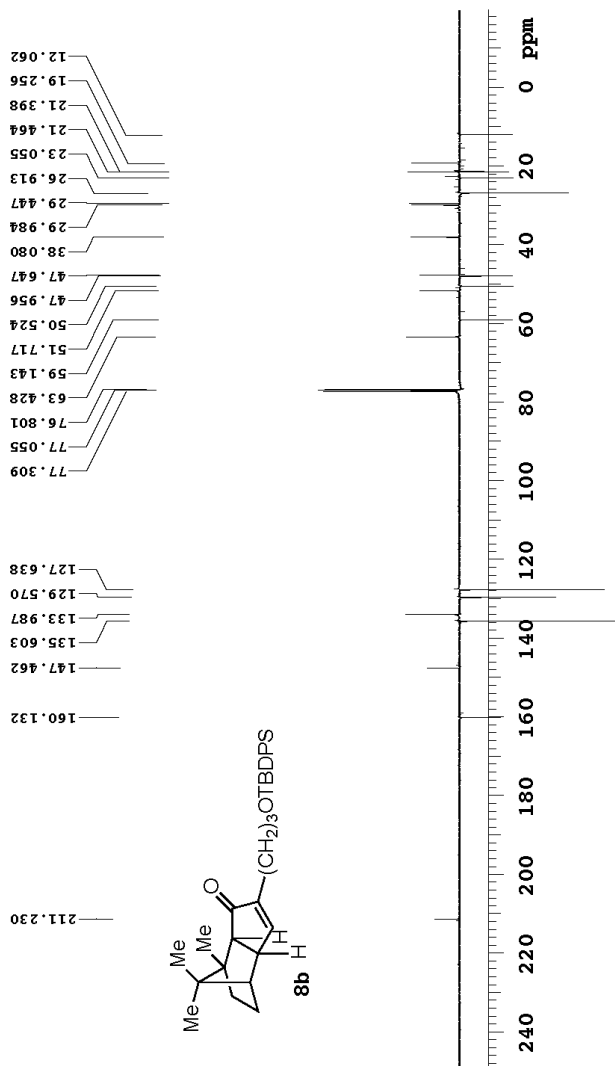


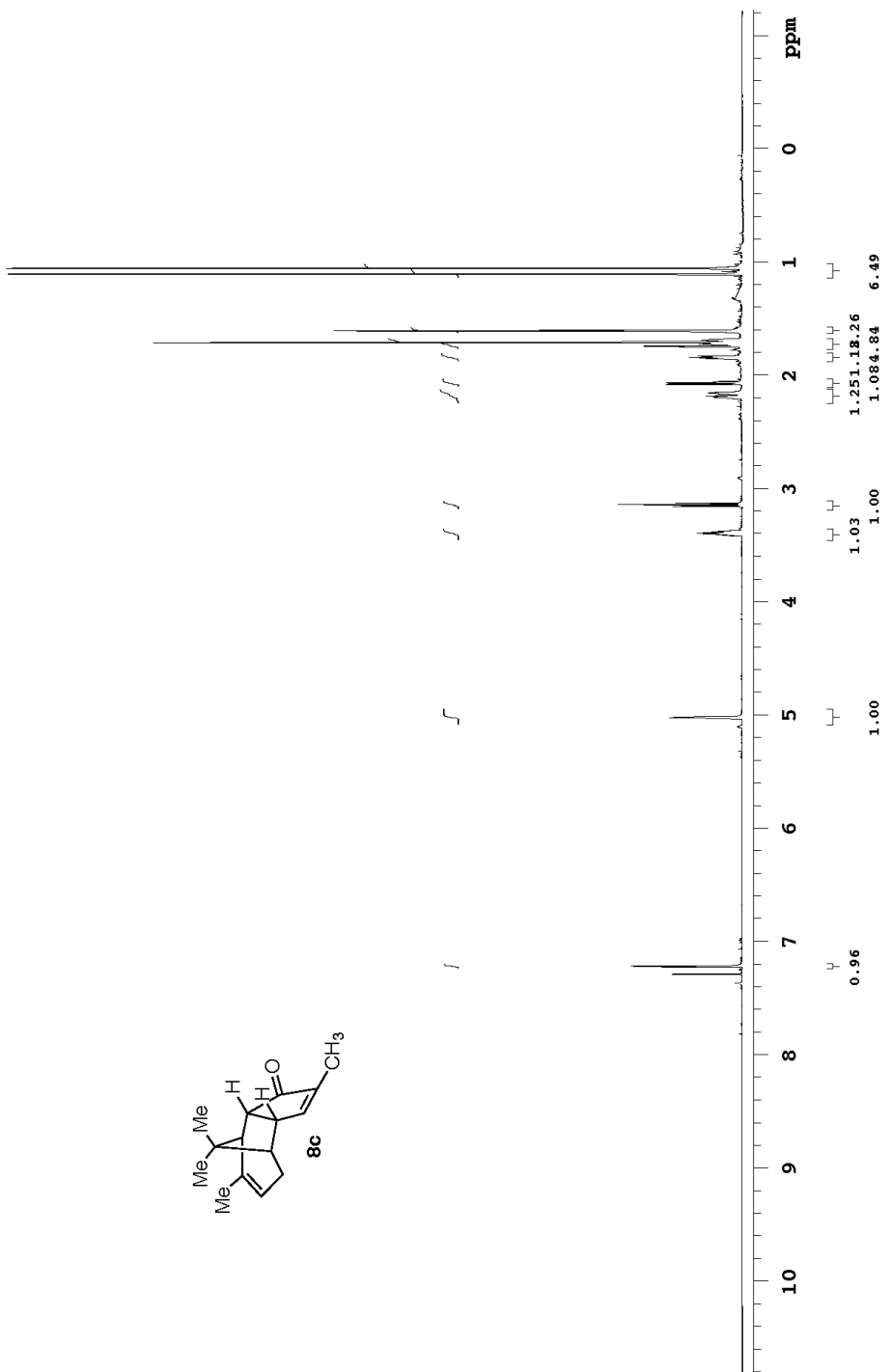
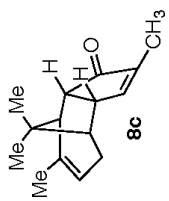


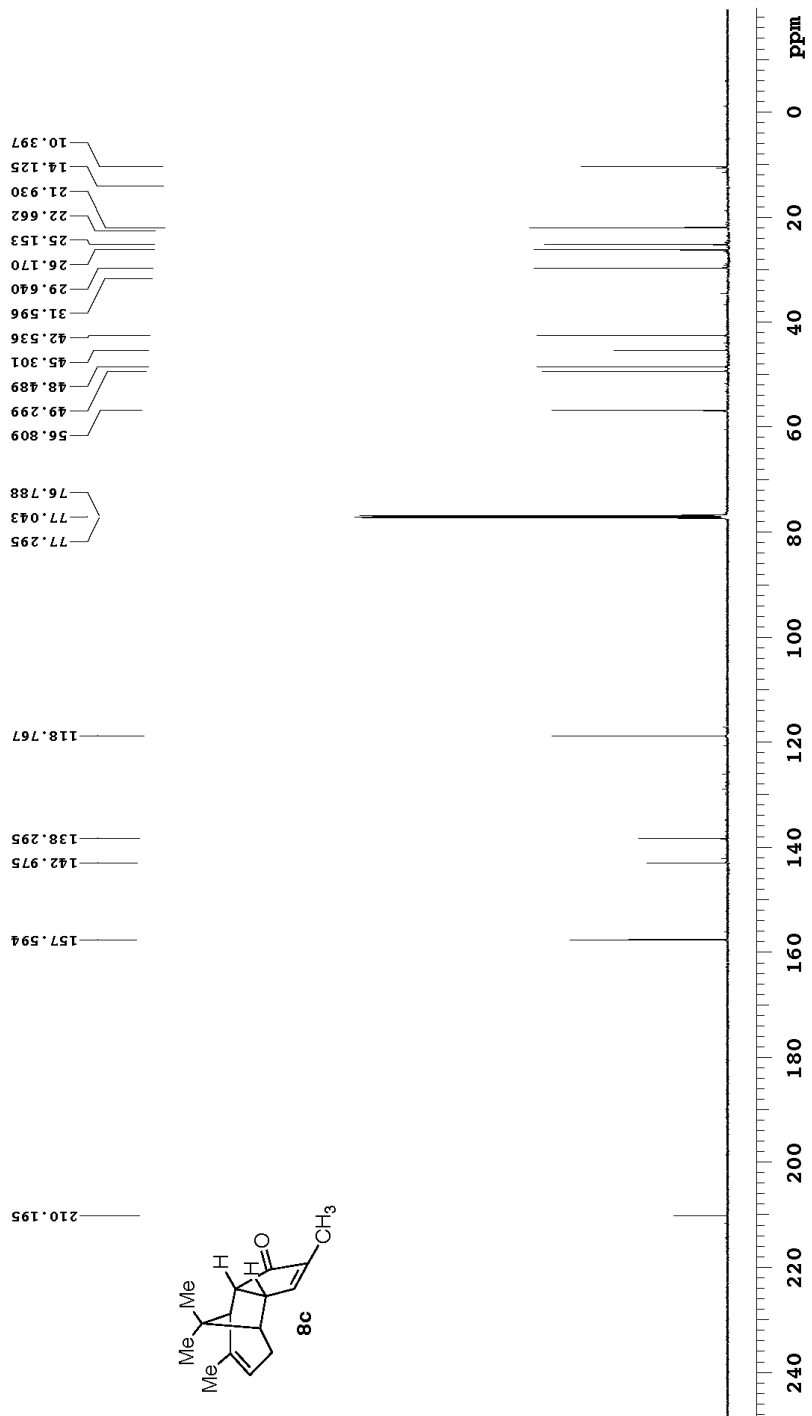


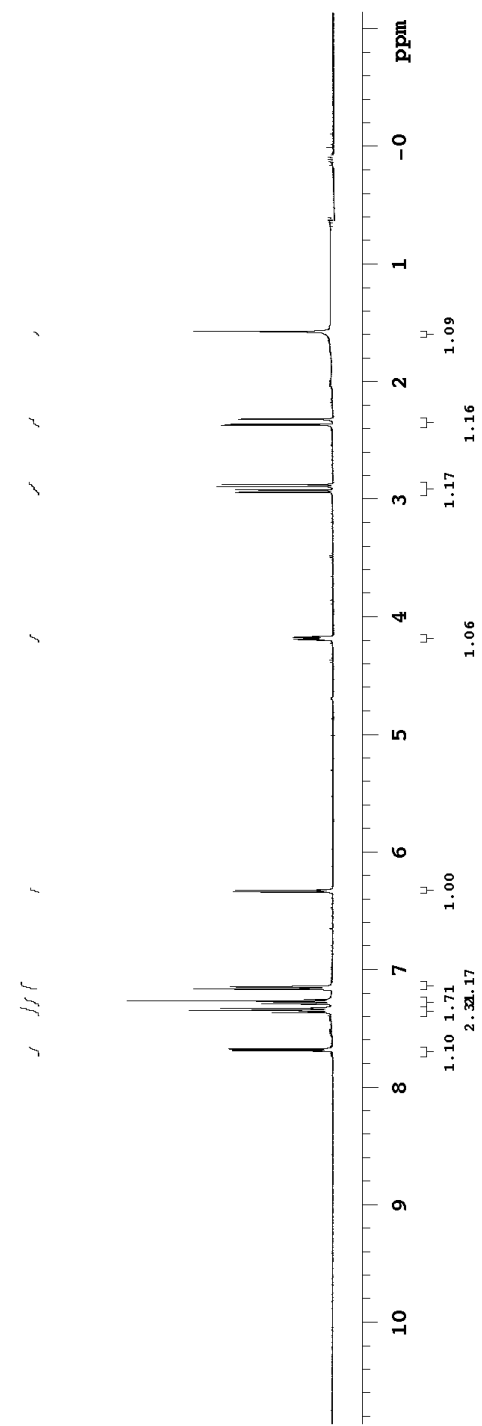
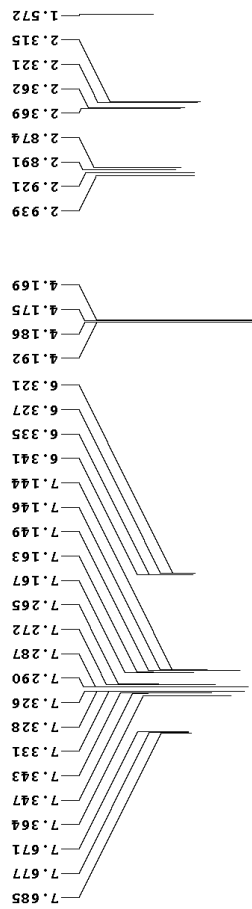
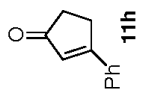


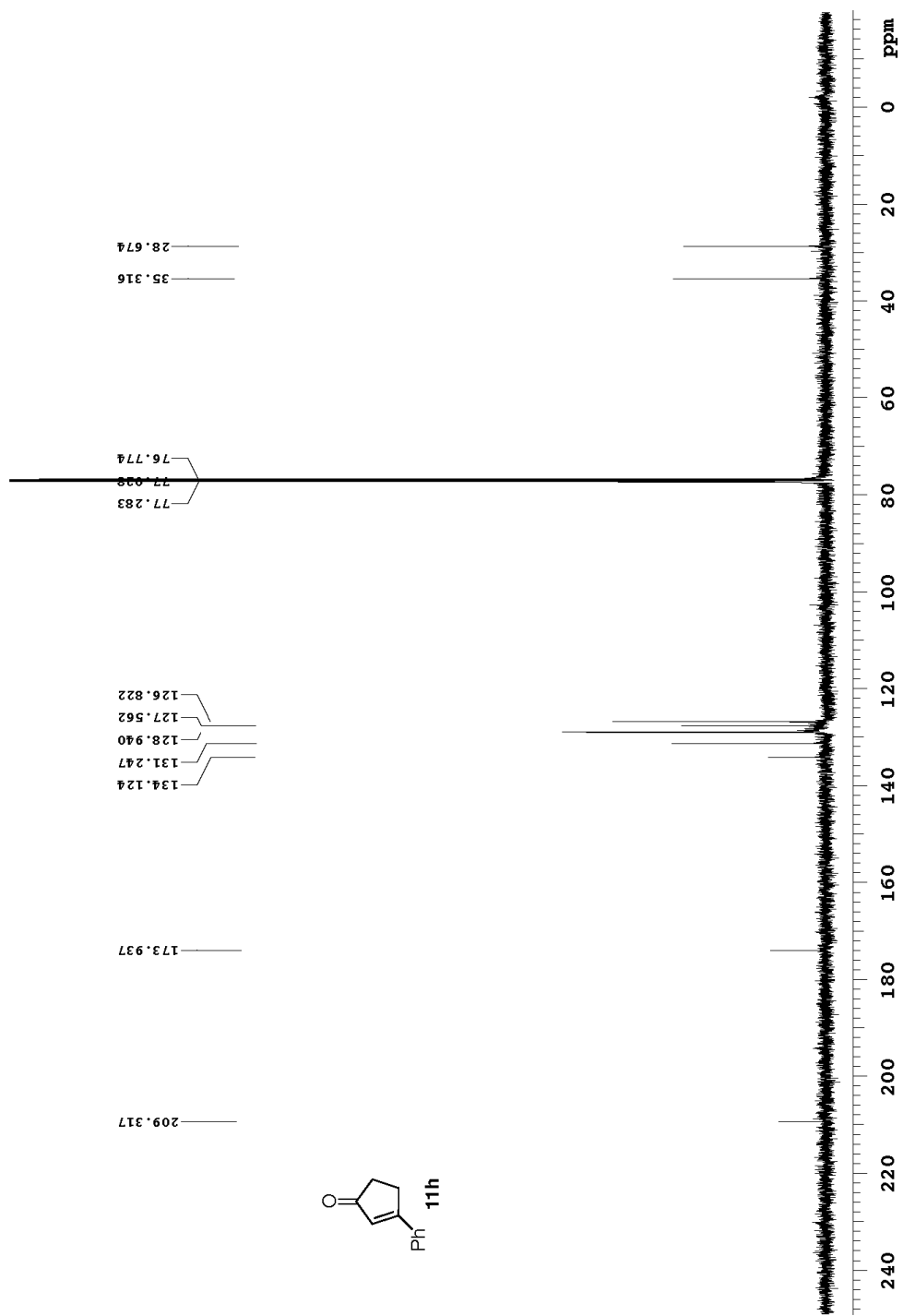


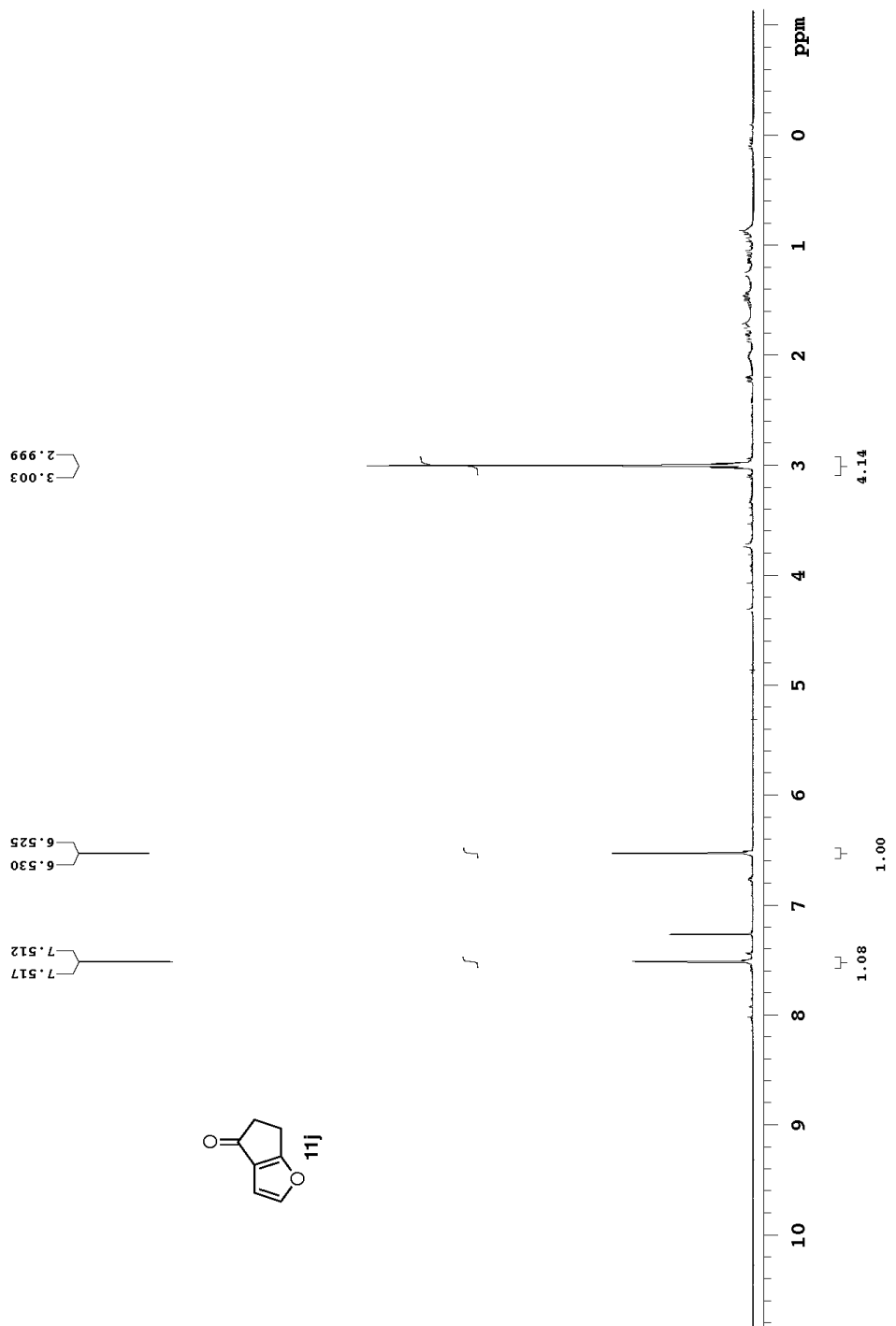


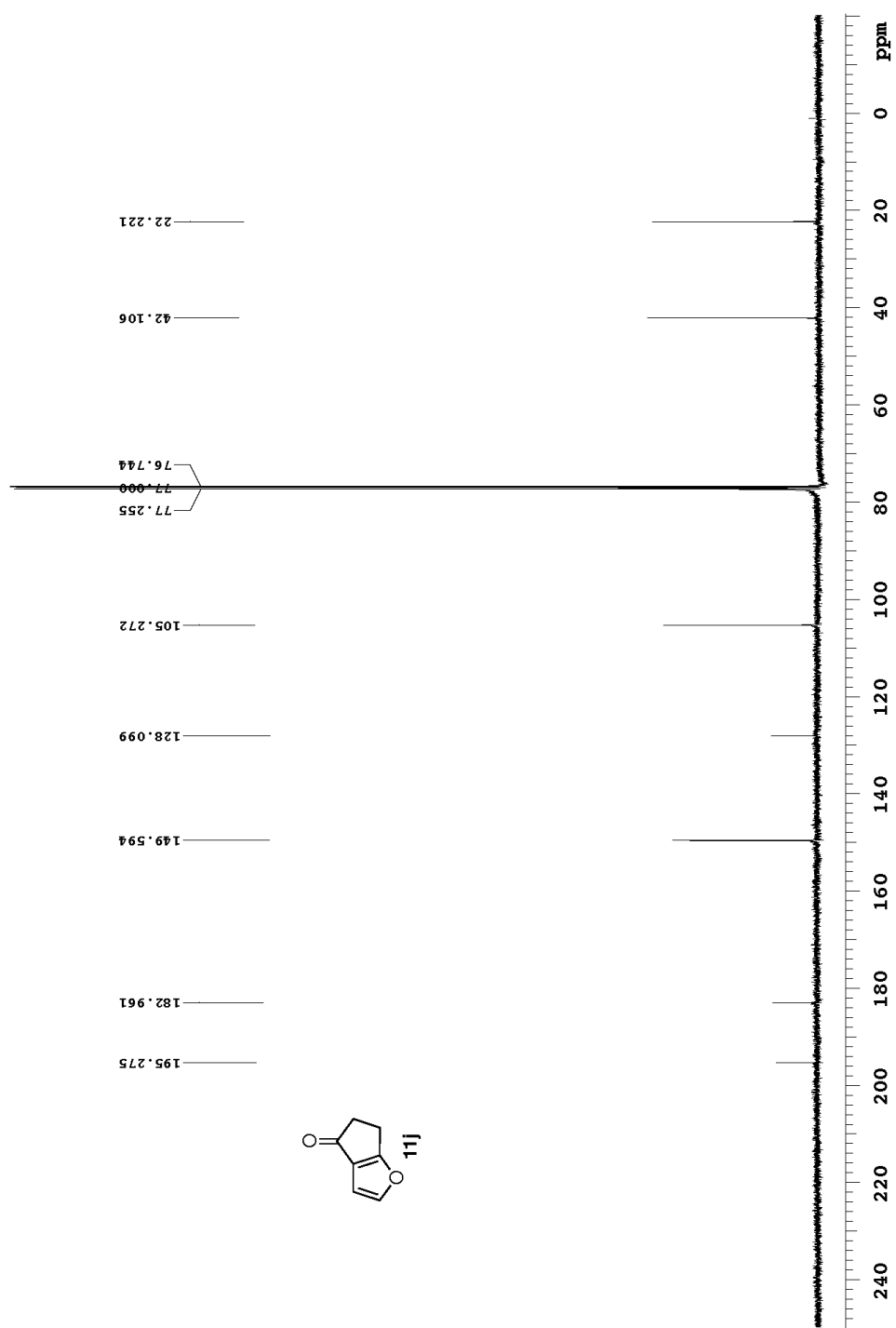


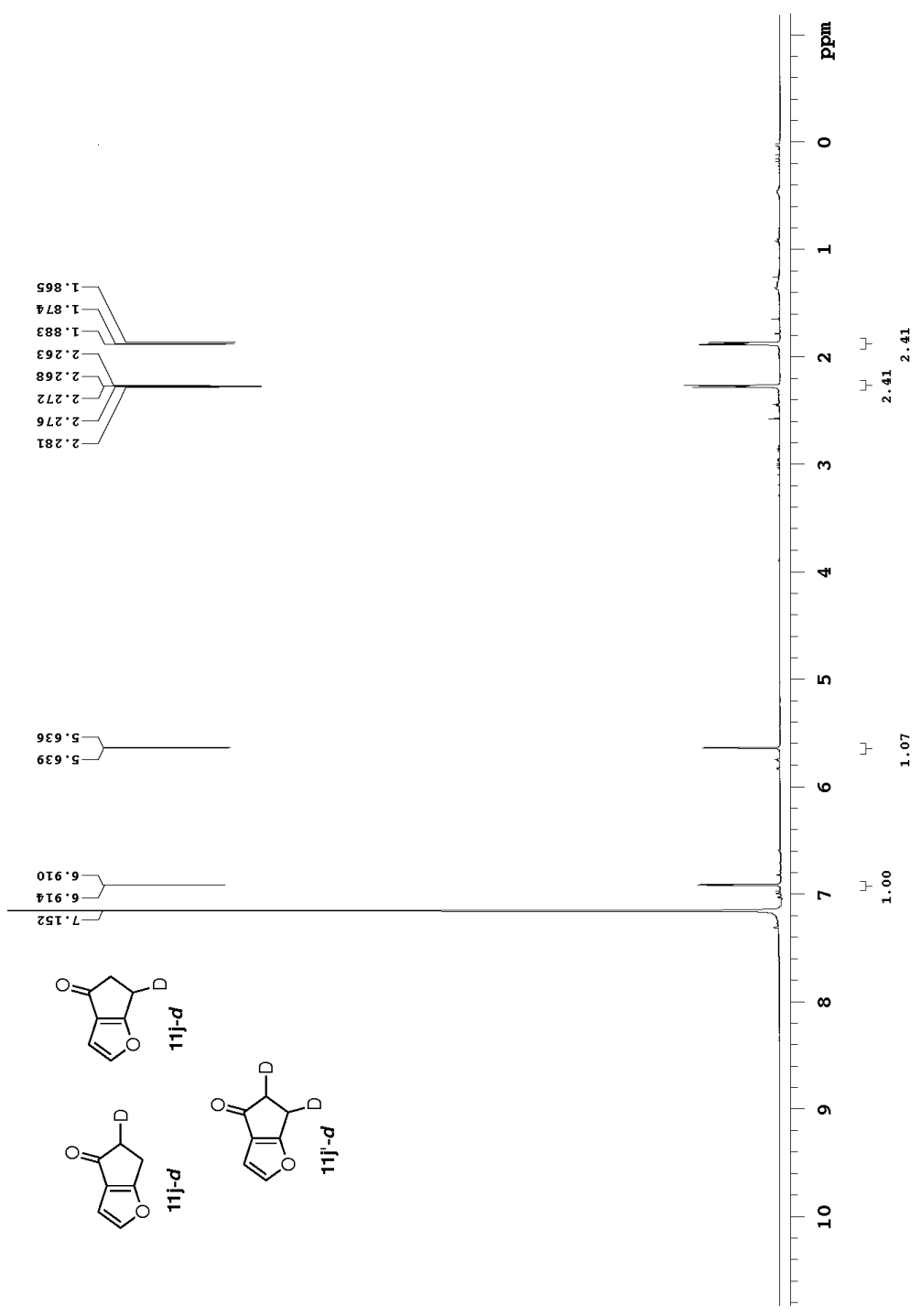


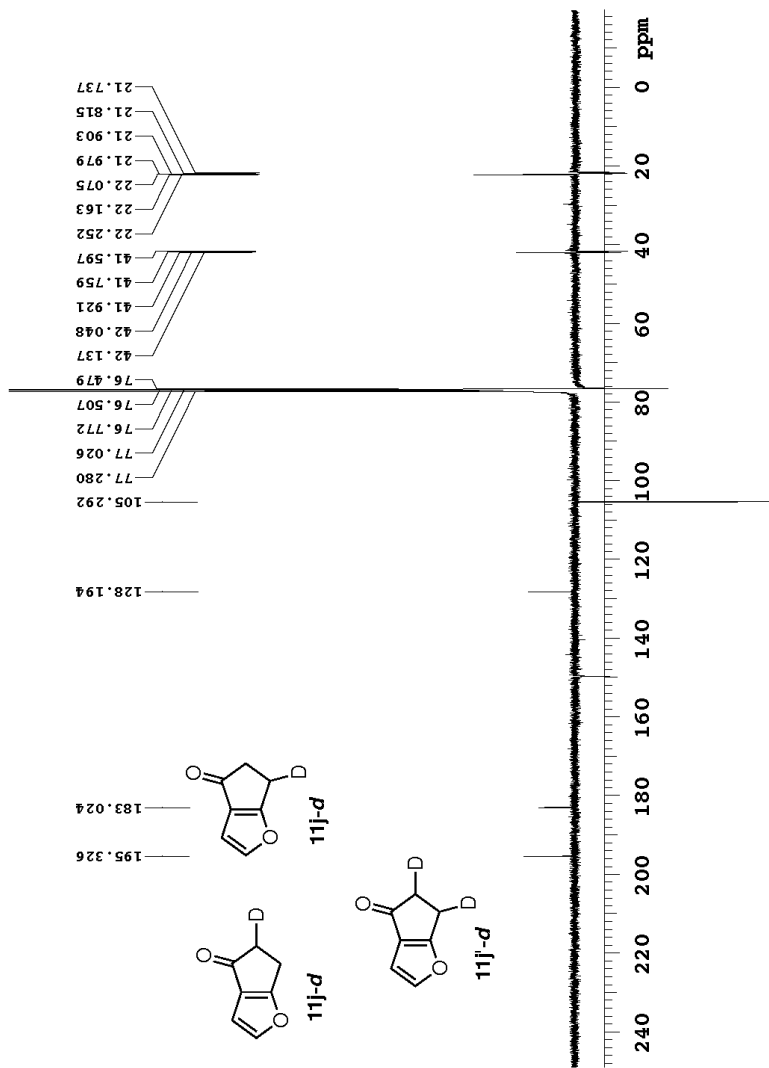


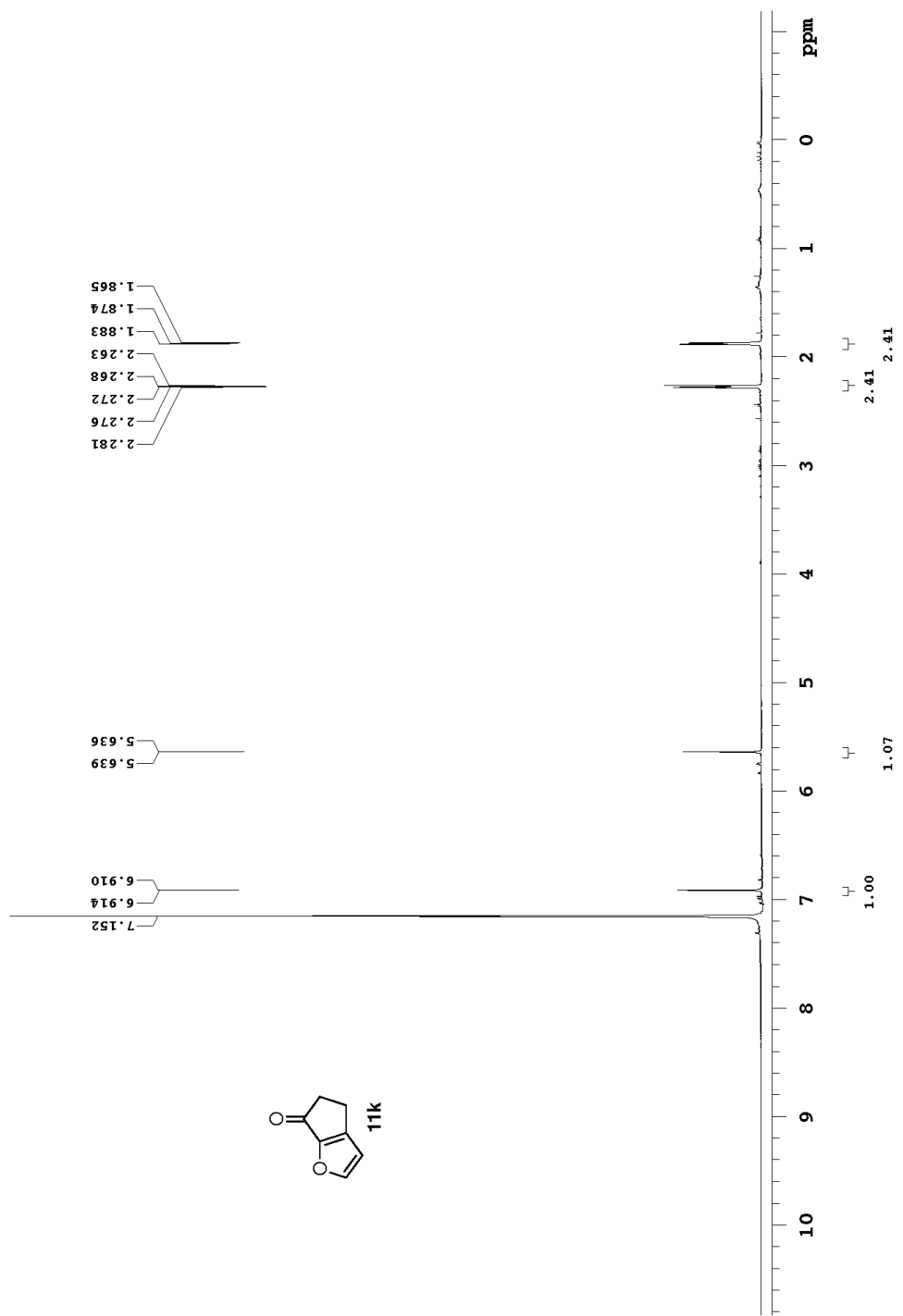


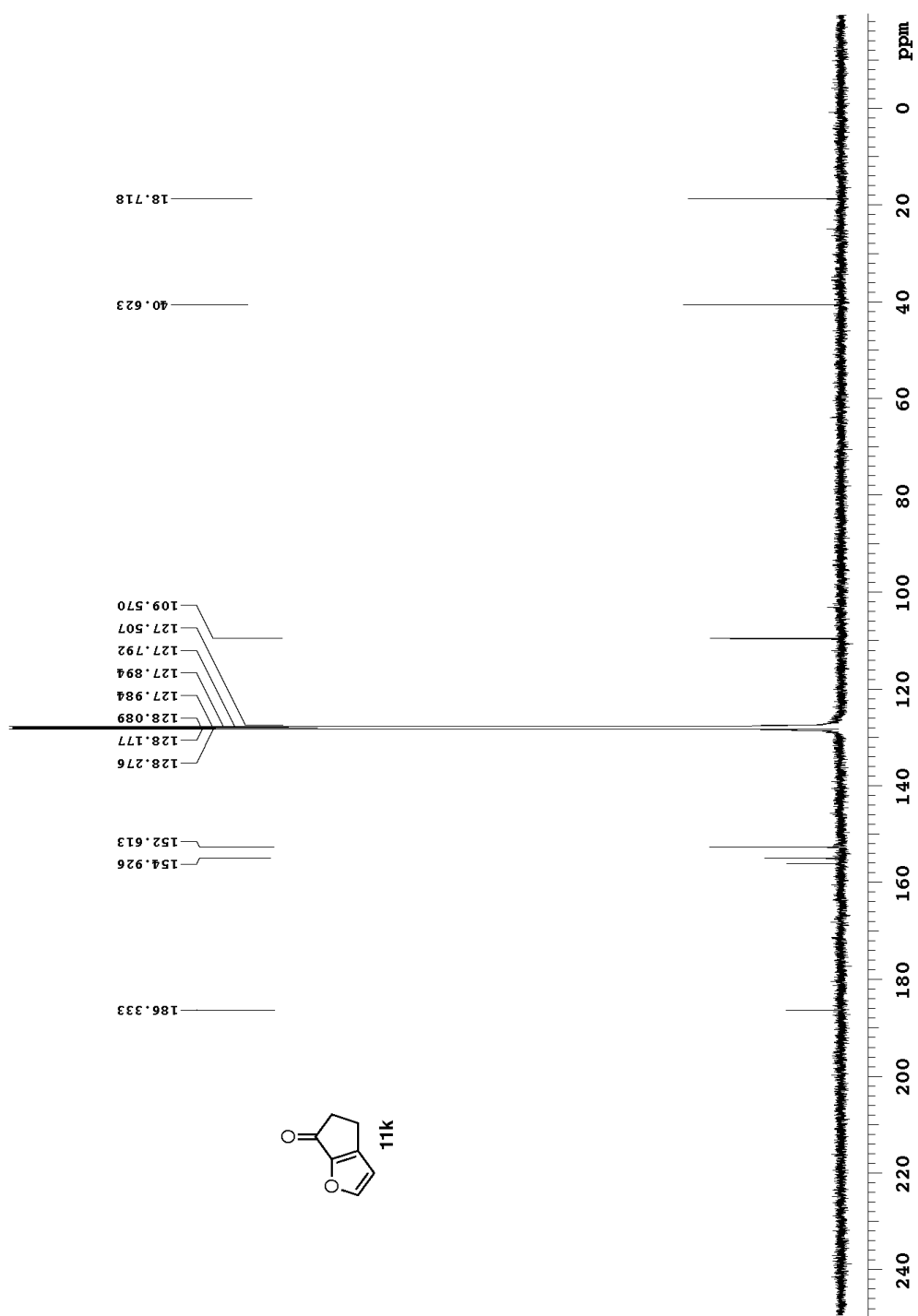


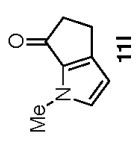
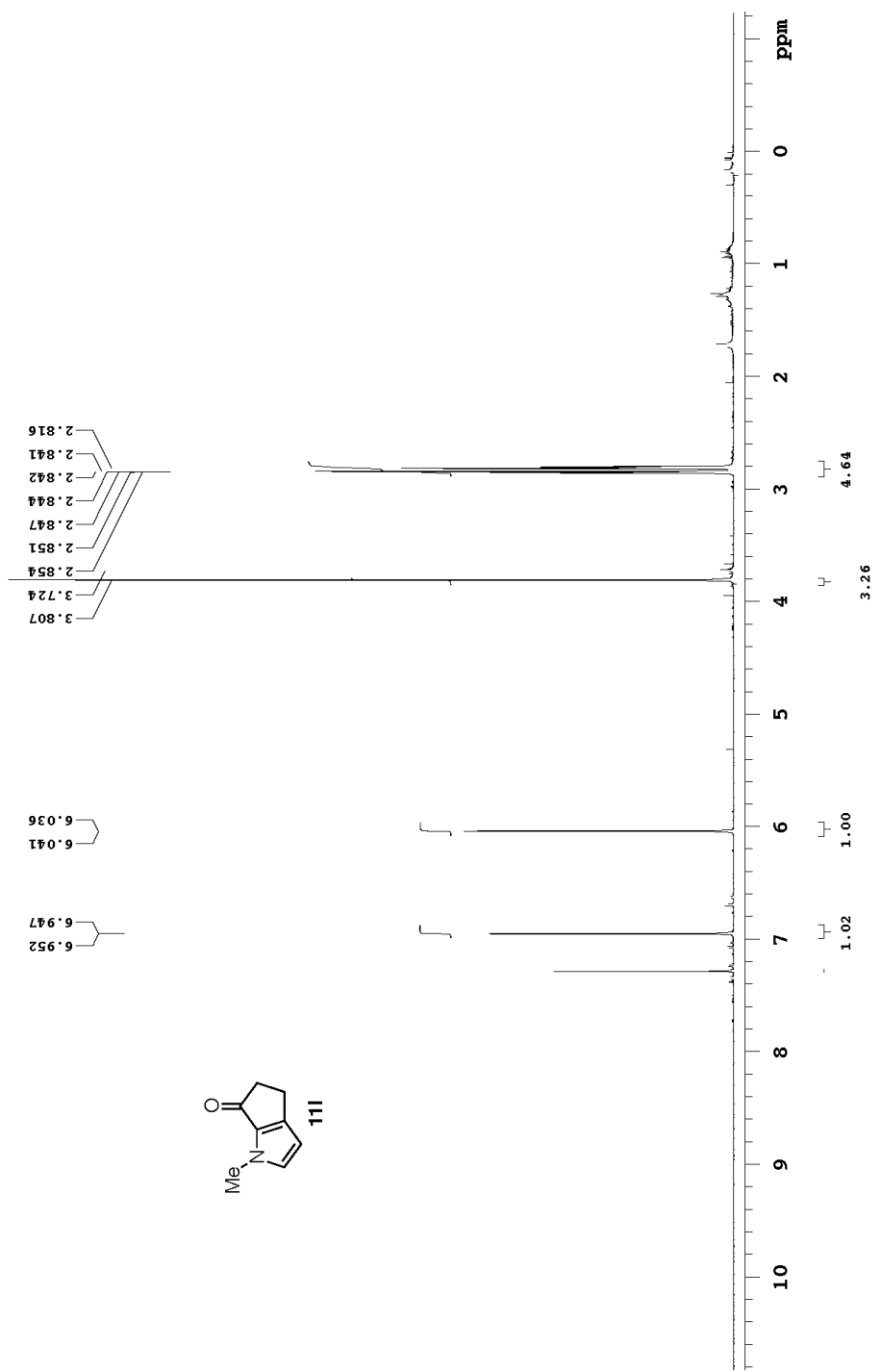


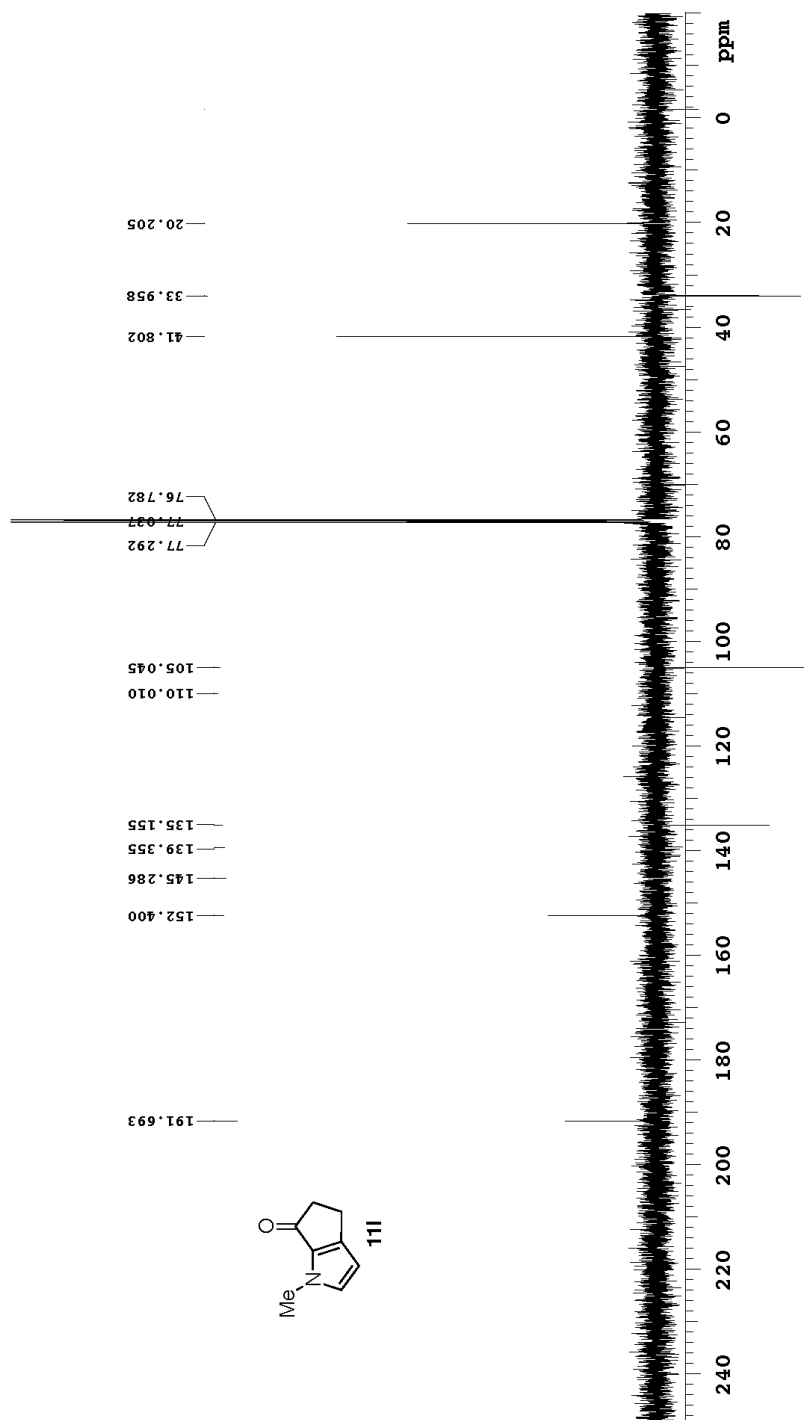






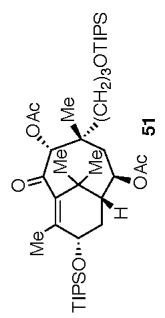
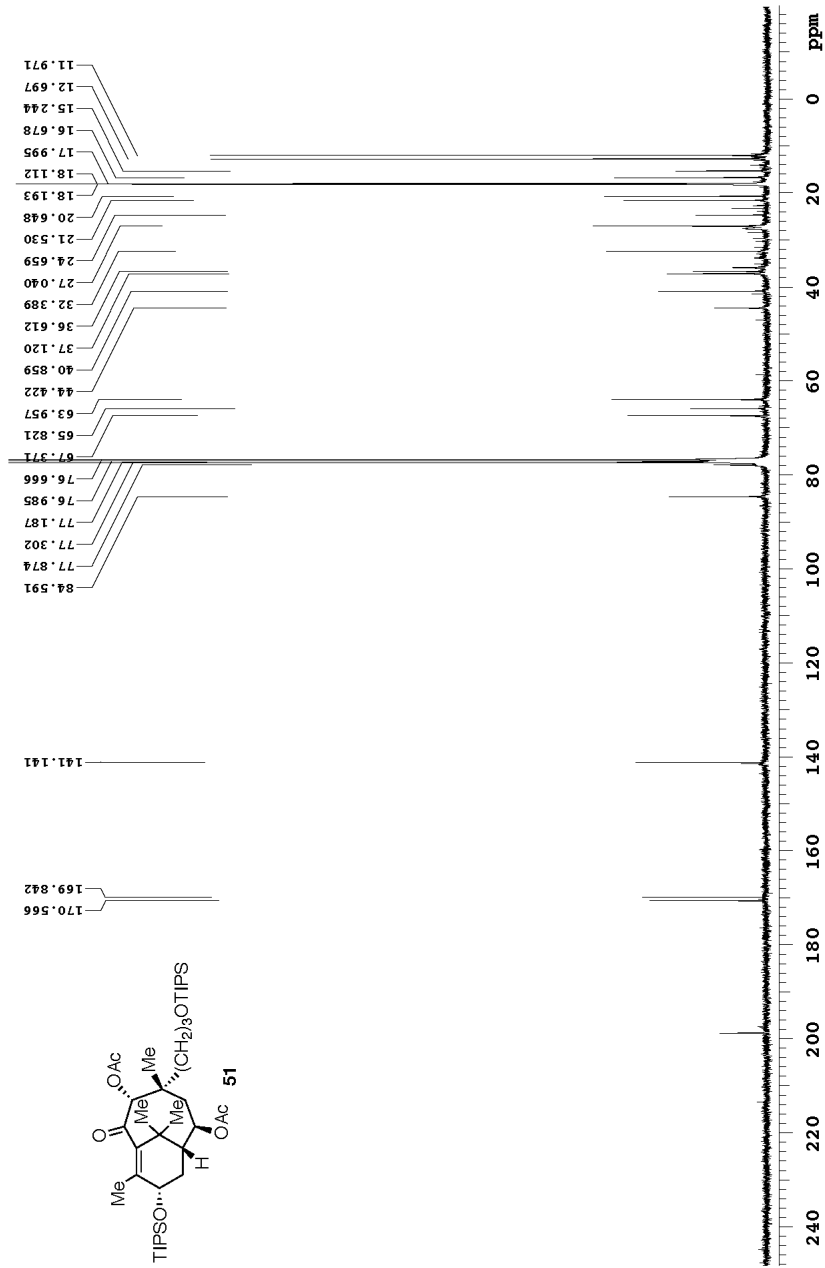


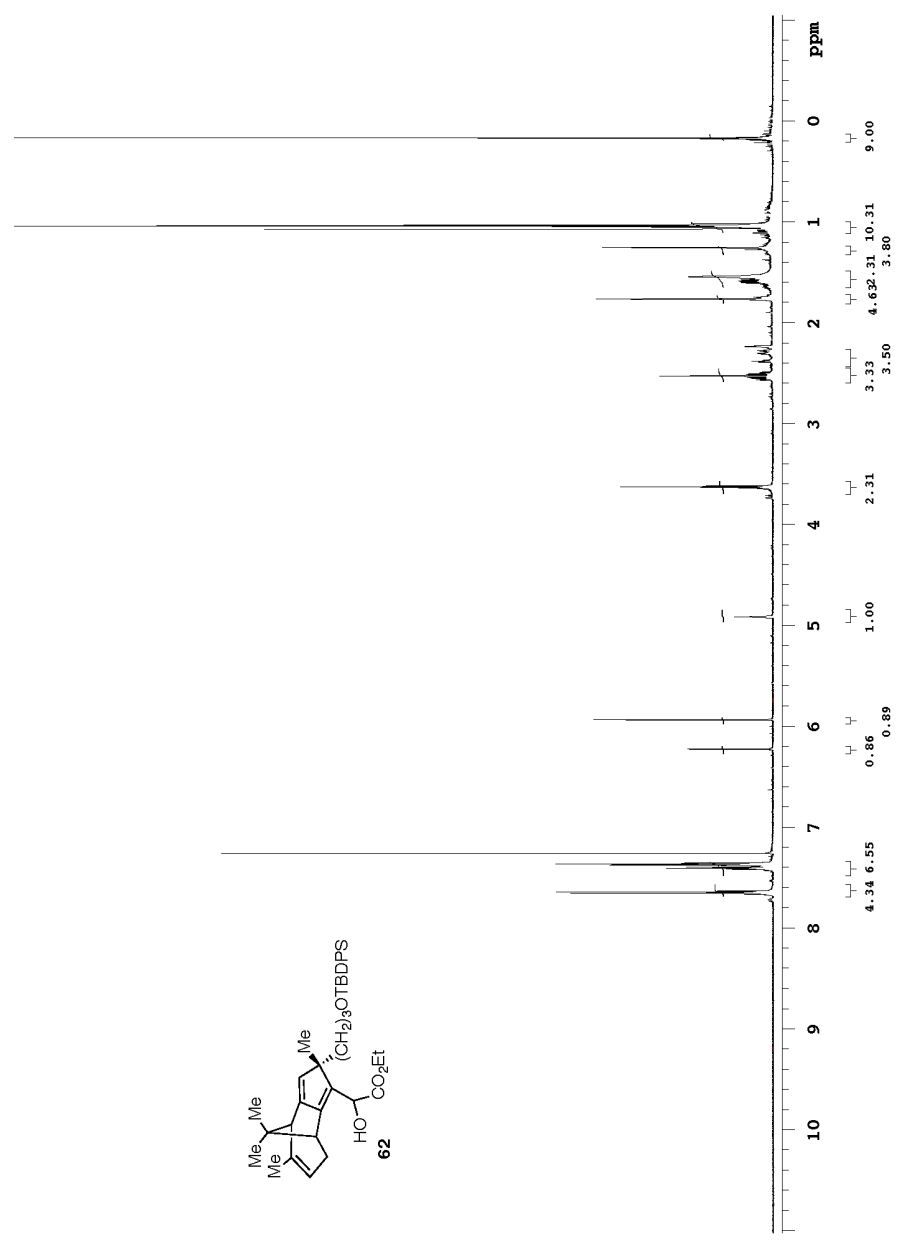
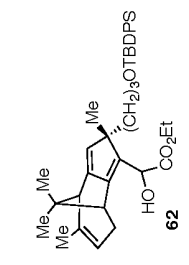


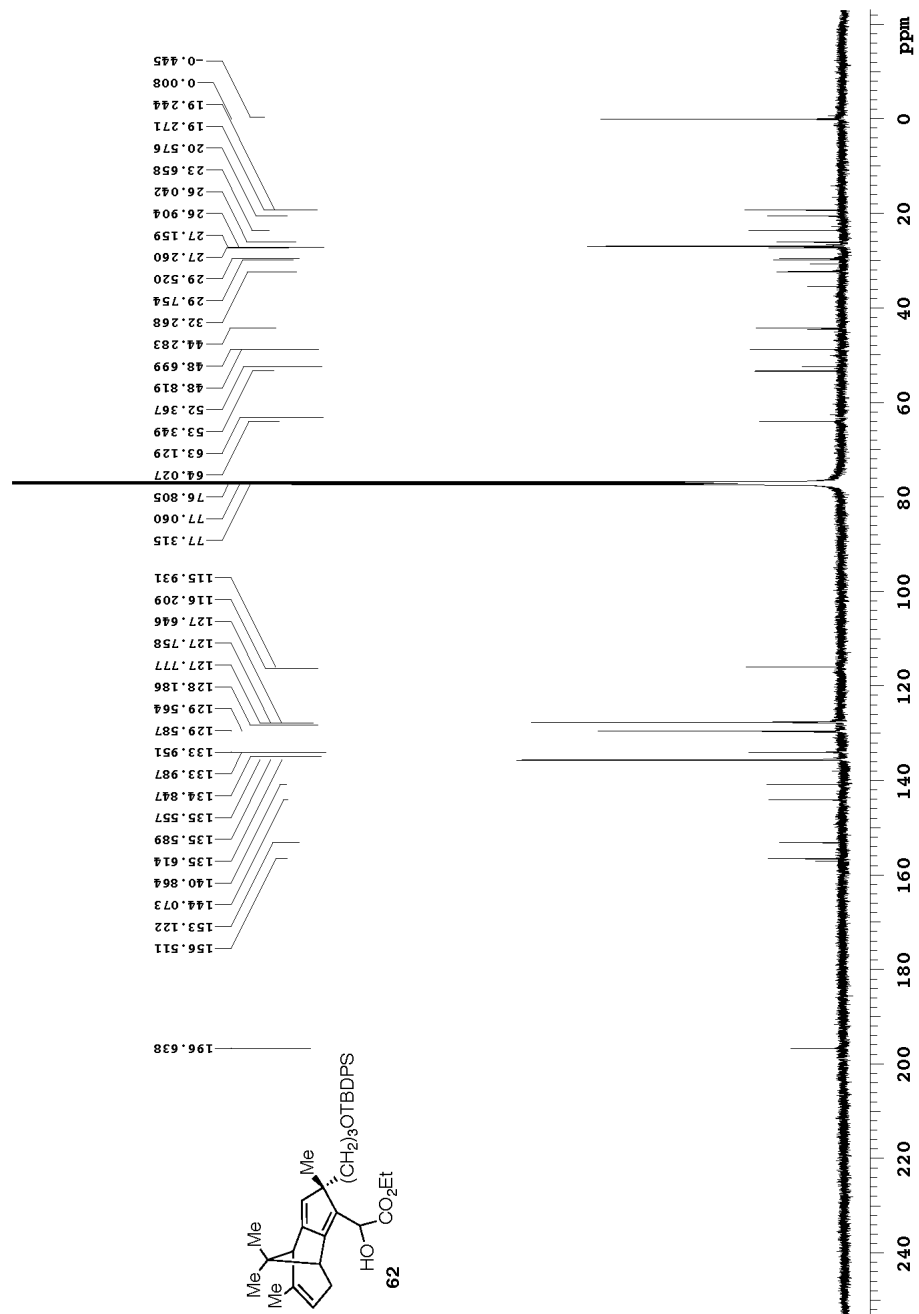


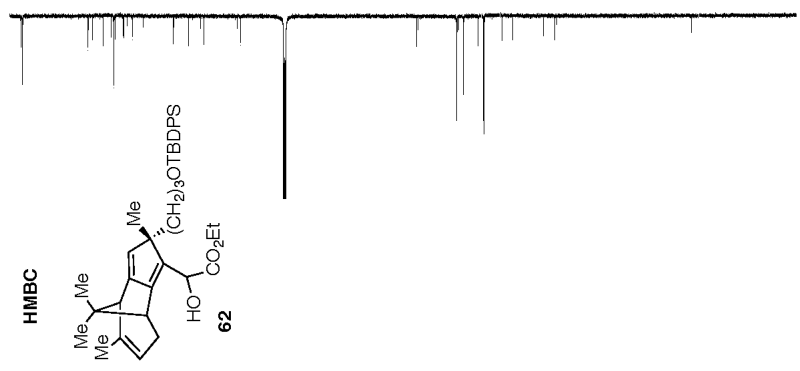
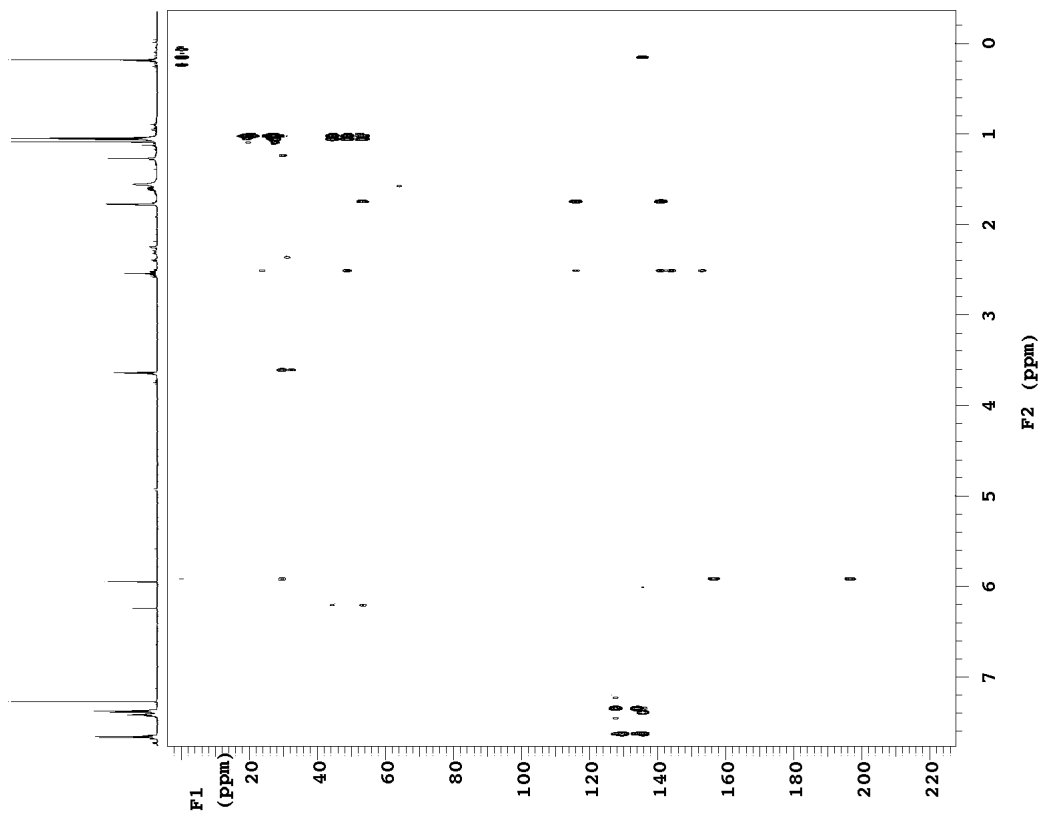
Appendix III (Selected NMR Spectra)

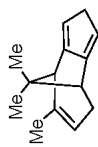
Chapter 4



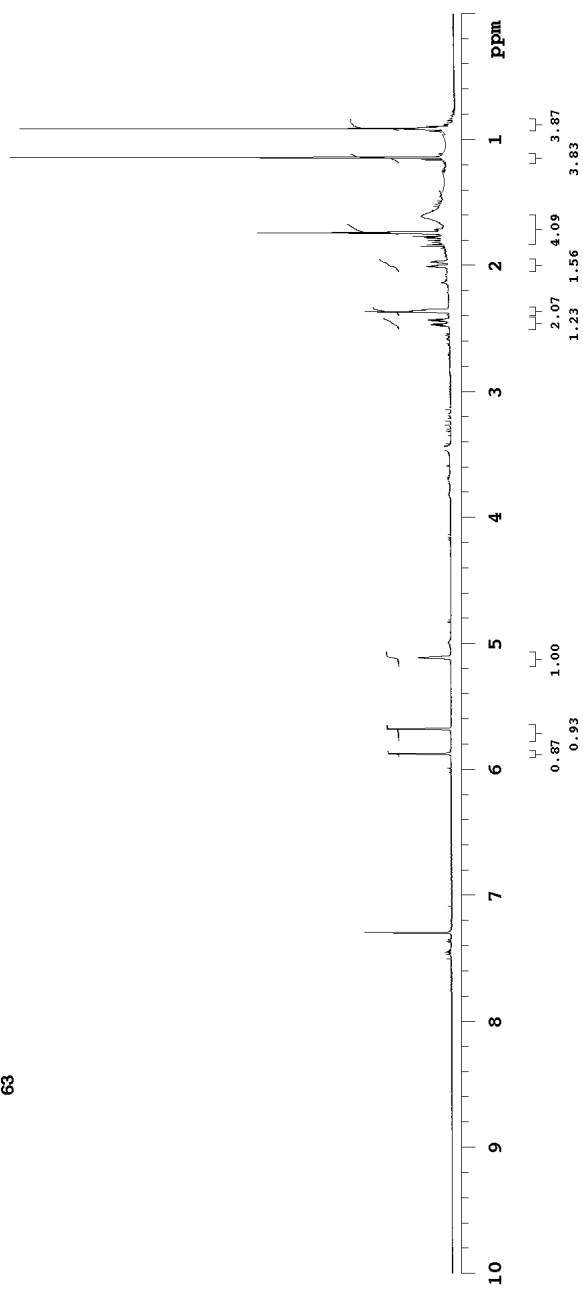


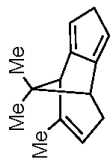
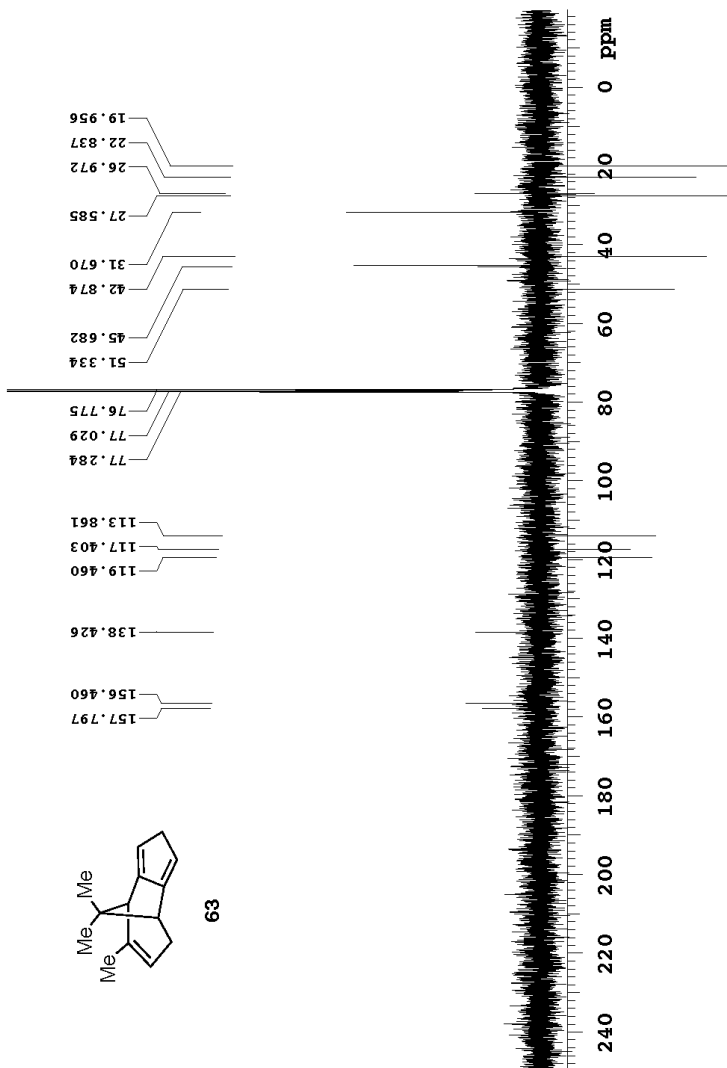




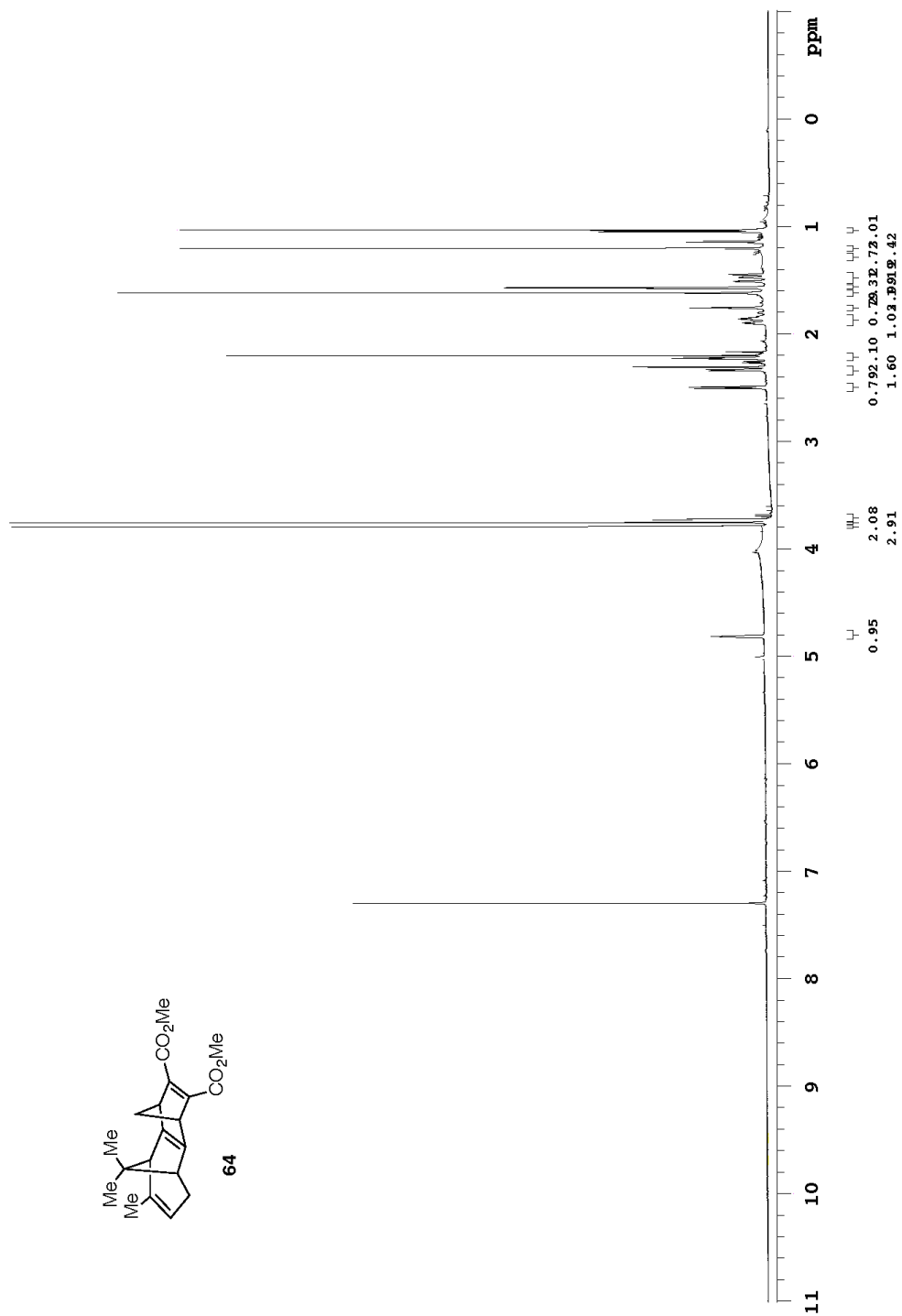
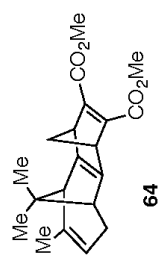


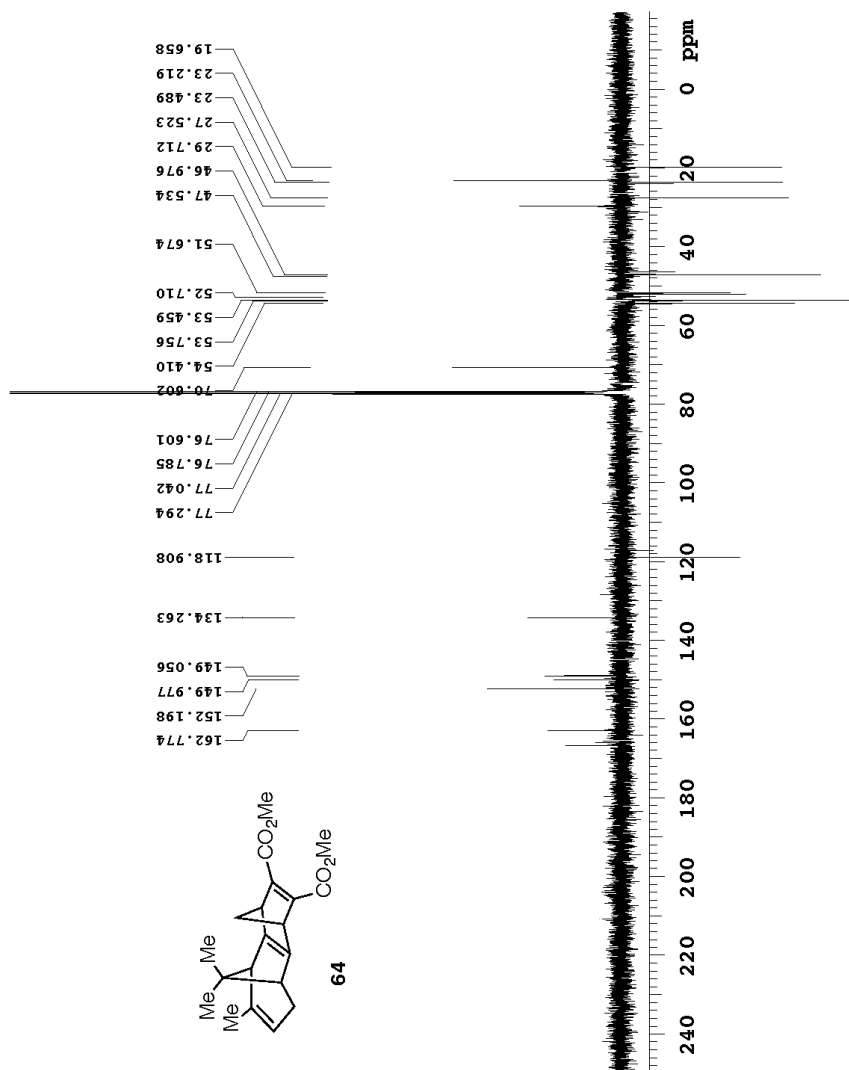
63

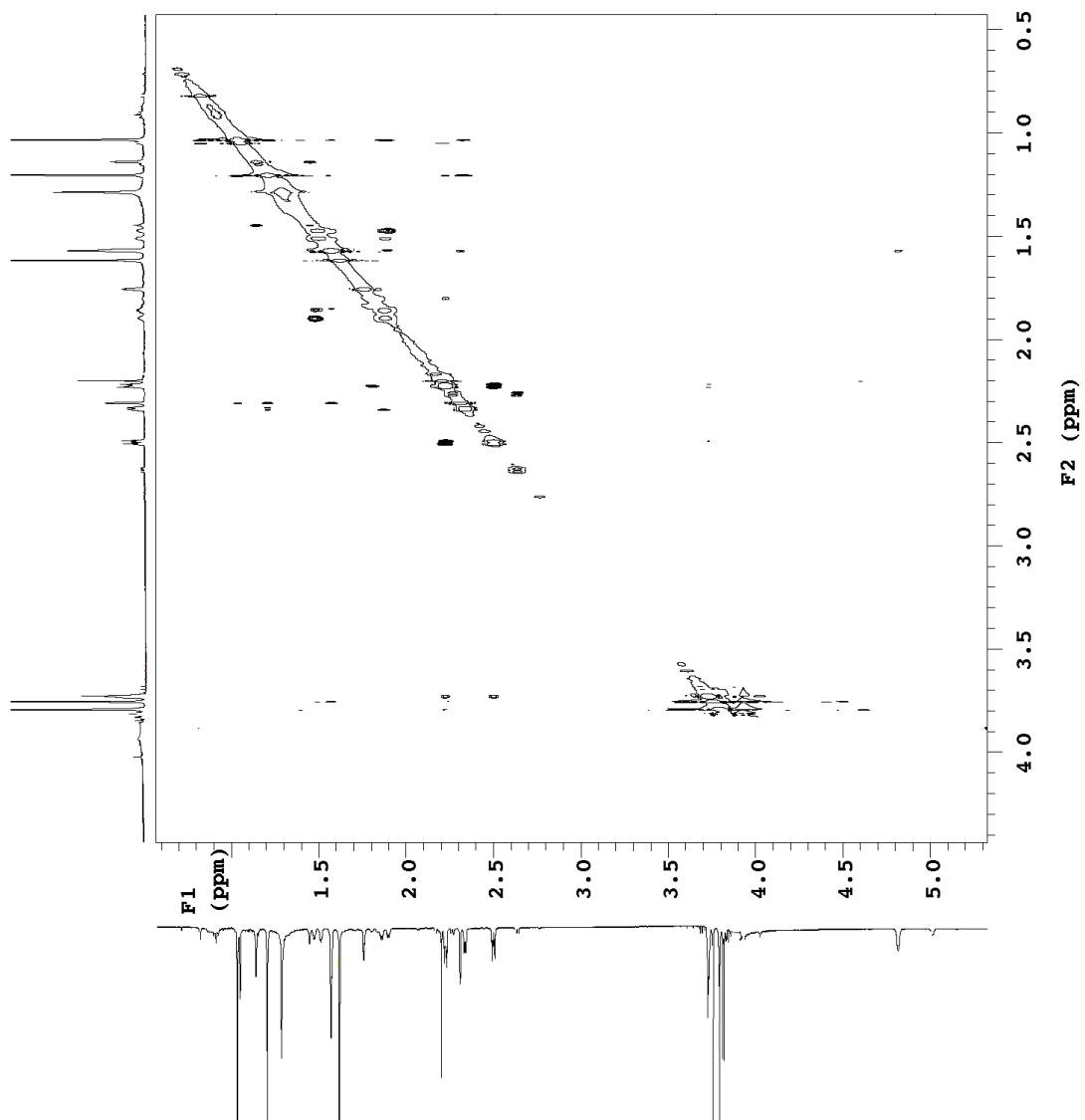
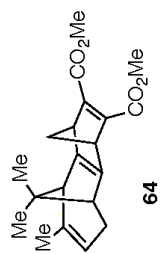


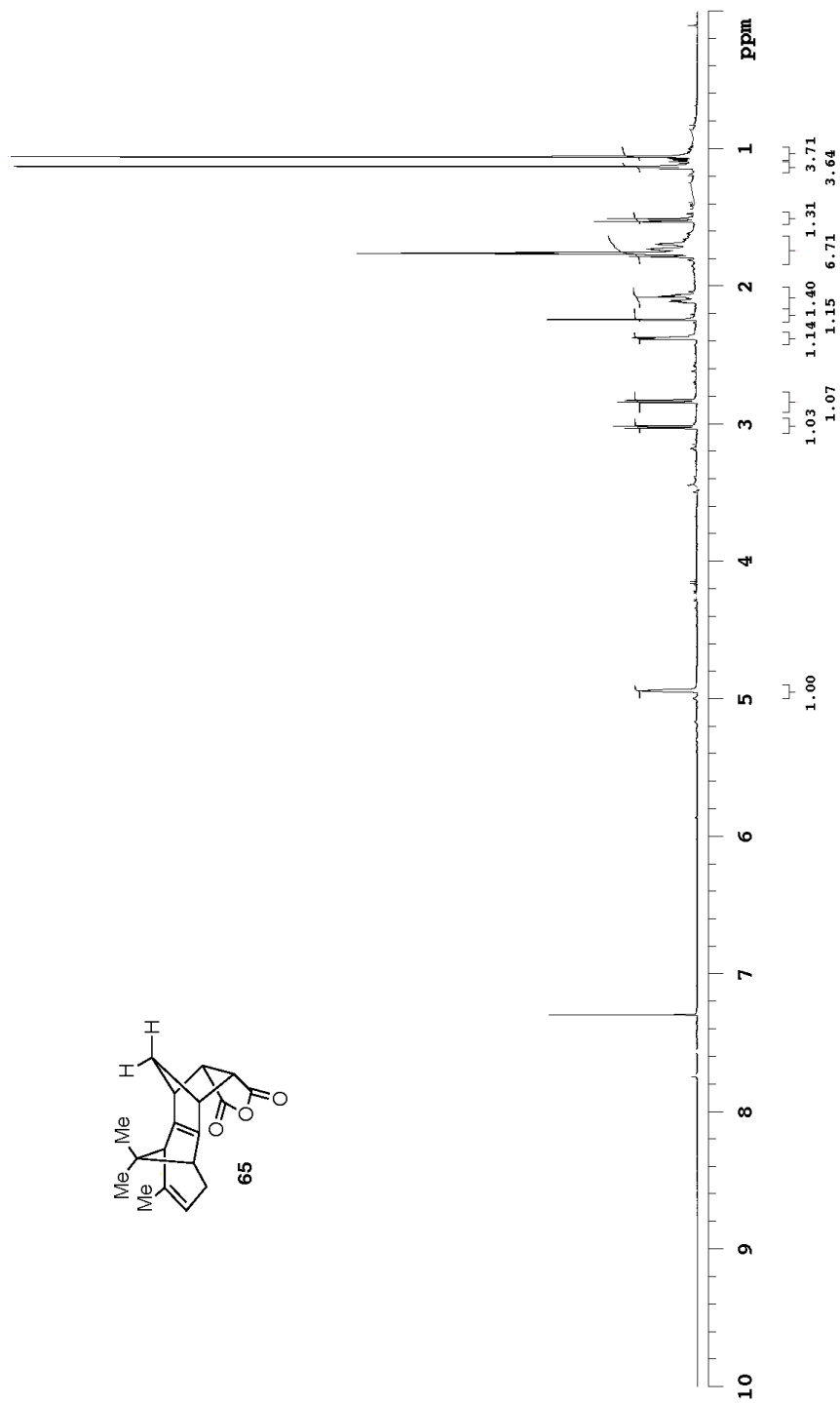
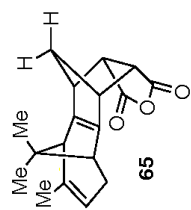


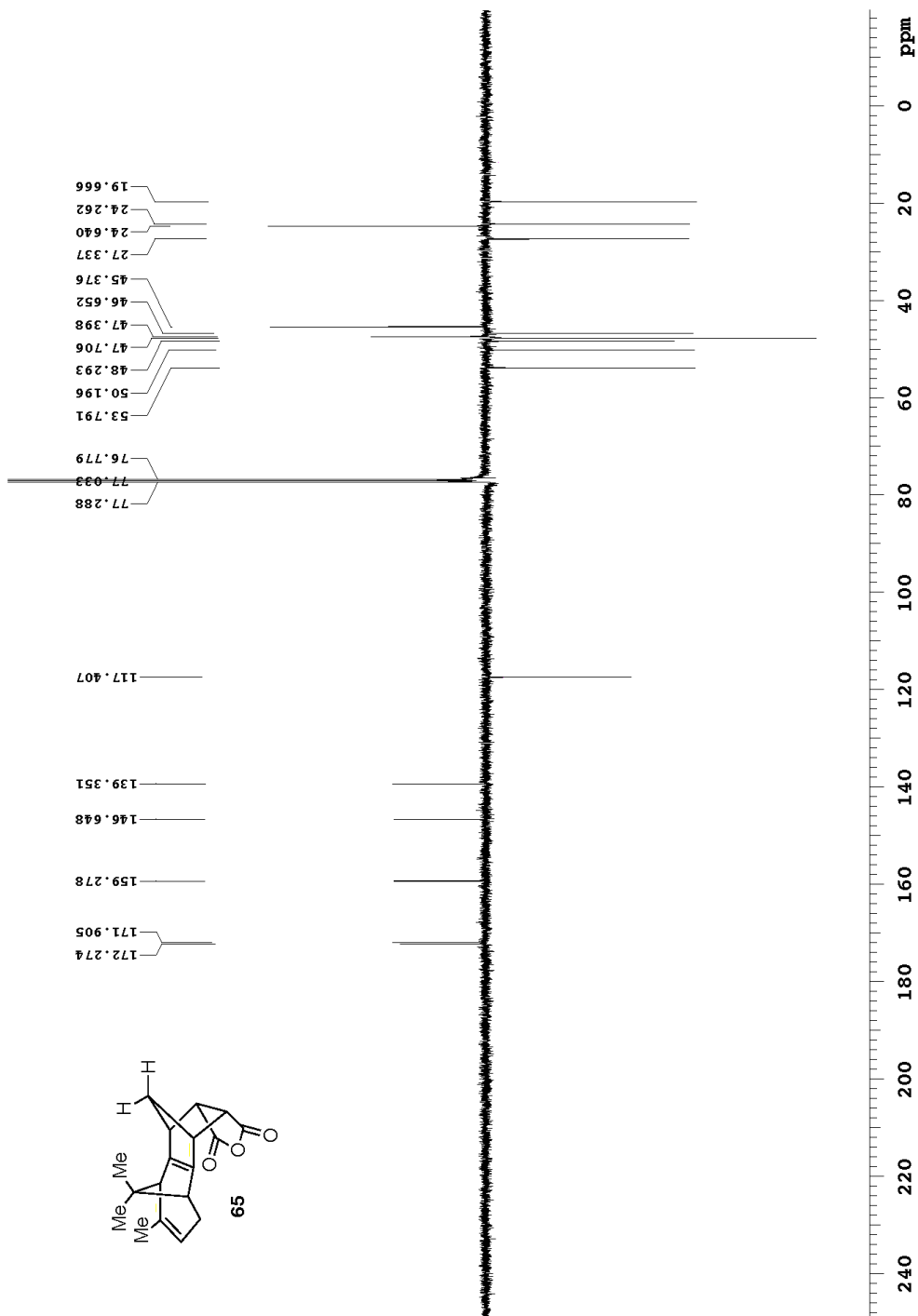
63

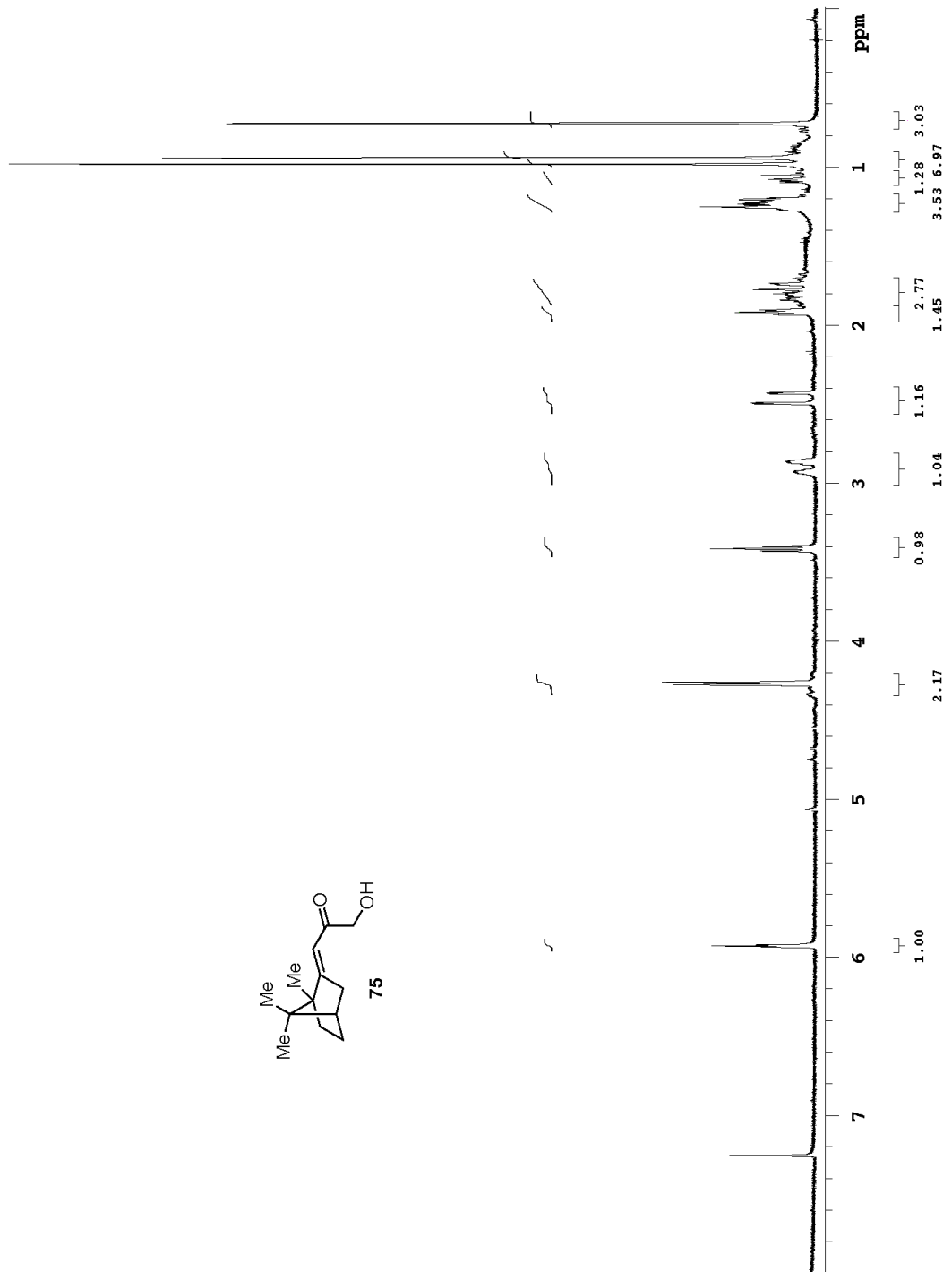
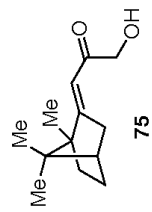


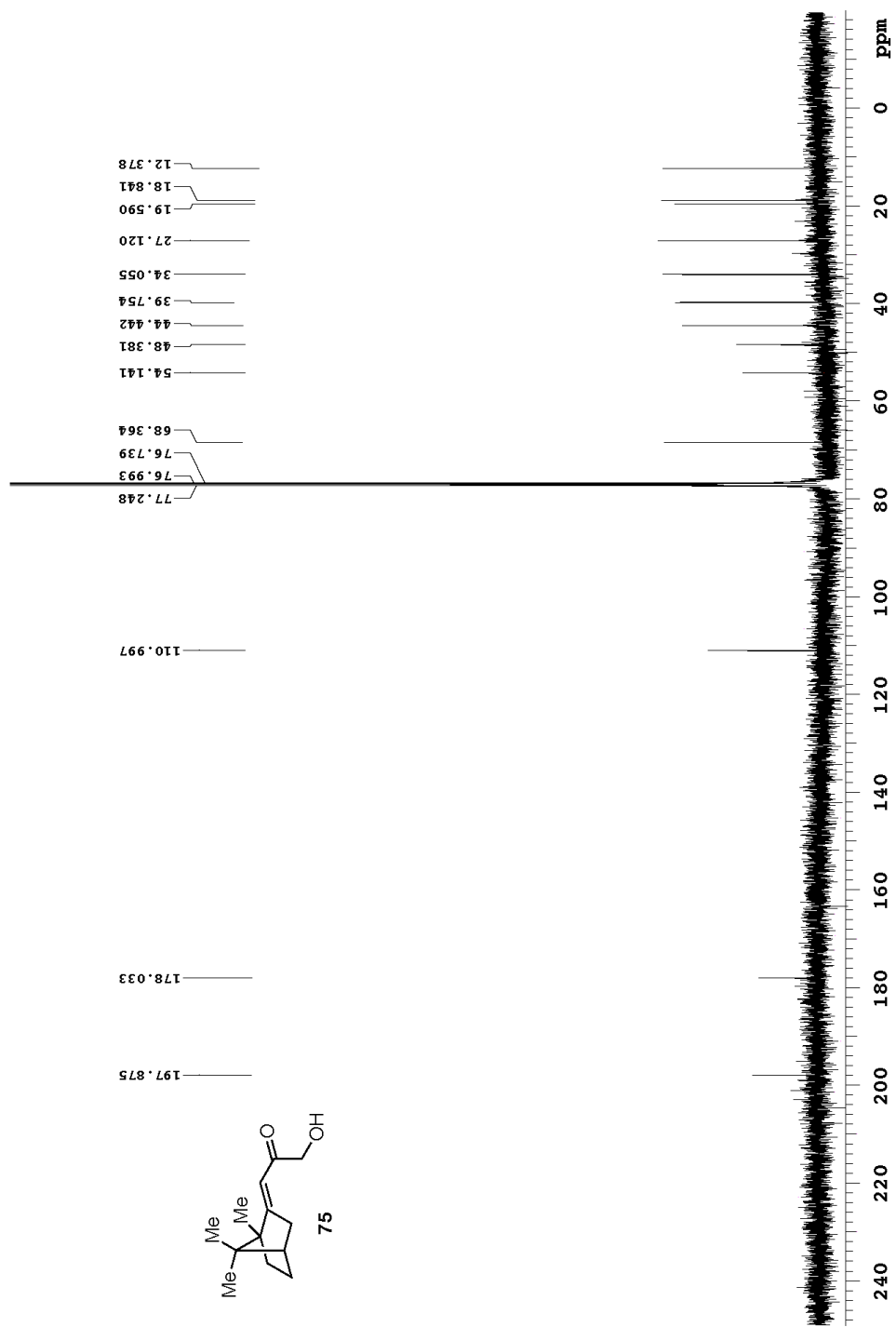












Appendix IV (Selected NMR Spectra)

Chapter 5

